2016

Stratigraphy, Sedimentology and Reservoir Modeling of the Late Devonian Berea Sandstone/Siltstone in northeastern Kentucky and southeastern Ohio

Forrest Christopher Mattox
mattox6@marshall.edu

STRATIGRAPHY, SEDIMENTOLOGY AND RESERVOIR MODELING OF THE LATE DEVONIAN BEREA SANDSTONE/SILTSTONE IN NORTHEASTERN KENTUCKY AND SOUTHEASTERN OHIO

A thesis submitted to
The Graduate College of
Marshall University
In partial fulfillment of
The requirements for the degree of
Masters of Science
in
Applied and Physical Science
by
Forrest Christopher Mattox
Approved by
Dr. Ronald Martino Committee Chairperson
Dr. Aley El-Shazly
Dr. William Niemann
Dr. Mitchell Scharman

Marshall University
December 2016

APPROVAL OF THESIS

We, the faculty supervising the work of Forrest Christopher Mattox, affirm that the thesis, *Stratigraphy, Sedimentology and Reservoir Modeling of the Late Devonian Berea Sandstone in northeastern Kentucky and southeastern Ohio,* meets the high academic standards for original scholarship and creative work established by the Applied and Phsycial Science Program and the College of Science. The work also conforms to the editorial standards of our discipline and the Graduate College of Marshall University. With our signatures, we approve the manuscript for publication.

Dr. Ronald Martino, Department of Geology Committee Chairperson — Date 1/9/17

Dr. William Niemann, Department of Geology Committee Member — Date 01/05/2017

Dr. Aley El-Shazly, Department of Geology Committee Member — Date 1/9/2017

Dr. Mitchell Scharman, Department of Geology Committee Member — Date 1/9/2017

Acknowledgments

The author would like to thank: Dr. Ronald Martino, who served as thesis advisor during the planning, preparation and completion of this study; without his patience, expertise and encouragement, this work would not have been possible; Mr. Ed Rothman for serving as a stand-in advisor during Dr. Martino's sabbatical; and Dr. Mitch Scharman for helping with field photography, poster assembly, and Gigapan photos.

The author would also like to express his gratitude to the geology students and faculty of Marshall University for their help with fieldwork and many helpful suggestions and comments throughout this process. In addition, I wish to thank my parents, Mr. Chris Mattox and Mrs. Karrie Mattox, for their patience, moral support, and financial assistance.

CONTENTS

LIST OF FIGURES ix

LIST OF TABLES AND CHARTS xiv

ABSTRACT xiv

CHAPTER 1 1

INTRODUCTION 1

OBJECTIVES 2

CHAPTER 2 4

PREVIOUS WORK 4

STRATIGRAPHIC FRAMEWORK 4

Regional Overview 4

Local Overview 4

Ohio Shale 5

Bedford Shale 5

Berea Sandstone 6

Sunbury Shale 6

PALEOECOLOGY/PALEOCLIMATE 7

STRUCTURE 8

SUBSURFACE STUDIES 9

DEPOSITIONAL ENVIRONMENT 10
OIL AND GAS HISTORY 12
PETROGRAPHY 12
CHAPTER 3 14
METHODS 14
Field Data 14
Laboratory 15
CHAPTER 4 17
RESULTS 17
Facies Description and Interpretation 17
Lower Lithofacies 17
Sedimentary Facies A 17
Description 17
Interpretation 18
Sedimentary Facies B 20
Description 20
Interpretation 21
Upper Lithofacies 22
Sedimentary Facies C 22

Description 22

Interpretation 22

Sedimentary Facies D 24

Description 24

Interpretation 25

Sedimentary Facies E 26

Description 26

Interpretation 27

Sedimentary Facies F 28

Description 28

Interpretation 28

Sedimentary Facies G 29

Description 29

Interpretation 30

Sedimentary Facies H 31

Description 31

Interpretation 31

Sedimentary Facies I 31

Description 31

Interpretation 32

Sedimentary Facies J 33

Description 33

Interpretation 34

Sedimentary Facies K 34

Description 34

Interpretation 35

Paleoecology 37

Trace Fossil Interpretation 38

CHAPTER 5 43

DISCUSSION 43

Depositional Model 43

Outcrop to Subsurface Correlation 48

Sequence Stratigraphy 49

Sequence Model for Northeastern Kentucky 49

Reservoir Modeling 54

Structural Trends 54

Thickness Trends 54

Reservoir Analysis 56

CHAPTER 6 60

SUMMARY AND CONCLUSION 60

FIGURES 65

CHARTS AND TABLES 136

STRATIGRAPHIC COLUMNS 143

REFERENCES 166

APPENDIX I IRB LETTER 177

APPENDIX II RIPPLE INDEX 178

Bedford-Berea Ripple Index 178

APPENDIX III PALEOCURRENTS 180

Wave Ripple Crest Measurements 180

Current Measurements 182

Cross-beds Tener Mountain Location 13 184

APPENDIX IV MEASURED SECTIONS 185

APPENDIX V TRACE FOSSILS 234

Epirelief Traces 234

Hyporelief Traces 235

Appendix VI Log List 236

Kentucky Well List 236

Ohio Well List 239

LIST OF FIGURES

Figure 1. Location of outcrops and well locations included in this study.................................... 65

Figure 2. Location of outcrops in northeastern Kentucky and southeastern Ohio. 66

Figure 3. Upper Devonian-Lower Mississippian stratigraphic framework in eastern Kentucky (from Harris, 2014)... 67

Figure 4. Paleogeography during the Late Devonian during deposition of the Berea Sandstone (modified from Pepper et al., 1954). 68

Figure 5. Paleogeography for the Bedford-Berea sequence in and near the study area (from Pashin and Ettensohn, 1995). 69

Figure 6. Major tectonic structures in the Appalachian Basin that affected deposition on the Bedford-Berea sequence (modified Pashin and Ettensohn, 1995)……………………………………..70

Figure 7. Isopach map of the Bedford-Berea interval in eastern and south-central Kentucky (Elam, 1981). 71

Figure 8. Isopach map of the Berea sandstone in Athens County, Ohio (Riley and Baranoski, 1988).. 72

Figure 9. The interpreted depositional model for the Bedford-Berea sequence in and around the study area (from Pashin and Ettensohn, 1995). 73

Figure 10. QFL and Qm-F-L plots of the Bedford-Berea sequence (Pashin and Ettensohn, 1995).. 74

Figure 11. Locality 12 near Garrison, Kentucky, illustrating the separation of the lower and upper lithofacies.. 75

Figure 12. Location of outcrops used for a south-north outcrop correlation. 76

Figure 13. South-North trending outcrop cross-section.. 77

Figure 14. Selected photos of facies A and facies B from locality 2 near Garrison, Kentucky. 78

Figure 15. Facies A and B at locality 12 near Garrison, Kentucky.. 79

Figure 16. Typical facies sequence (Ta -Te) produced by purely waning flow (modified from Bouma, 1962) in an ignitive turbidite. 80

Figure 17. Generalized architecture in Bedford-Berea siltstone beds (Pashin and Ettensohn, 1995). 81

Figure 18. A) Cross-section of classical turbidite flow (Intrabasinal) vs. hyperpycnal flows (Mutti et al., 1999; Zavala et al., 2011a). 82

Figure 19. Selected photos showing bed architecture present in facies assemblage A-B.. 83

Figure 20. Selected photos of facies C-I at locality 2. 84

Figure 21. Common facies found at locality 22. 85

Figure 22. Photos of facies within the Bedford-Berea sequence. 86

Figure 23. Facies associated with hyperpycnal flows (Zavala et al., 2011a). 87

Figure 24. Bed architecture of facies C-I in a single Bedford-Berea bed. 88

Figure 25. Selected bed architecture photos that show flow variation within one bed in the Upper Berea Lithofacies. 89

Figure 26. Line drawings of common beds within the Bedford-Berea sequence.. 90

Figure 27. Flow velocity and sediment concentration variations during a single long-lived hyperpycnal discharge (Zavala et al., 2011b). 91

Figure 28. Paleocurrent rose diagrams from outcrops in northeastern Kentucky. 92

Figure 29. Paleocurrent rose diagrams from outcrops in southeastern Ohio. 93

Figure 30. Spoke diagram illustrating asymmetric paleocurrent orientations throughout the Bedford-Berea sequence in northeastern Kentucky and southeastern Ohio. 94

Figure 31. Composite paleocurrent rose diagram for all locations. 95

Figure 32. Typical sequence of sedimentary structures and flow patterns from a wave-modified turbidite with purely waning flow (Myrow et al., 2002). 96

Figure 33. Selected images of facies I. 97

Figure 34. The evolution of a hyperpycnal discharge (Zavala et al., 2011a). 98

Figure 35. Selected photos of facies J. 99

Figure 36. Schematic of the typical sedimentary structure sequences in coarse-grained and fine-grained storm beds (Cheel and Leckie, 1992). 100

Figure 37. Selected photos of facies K. 101

Figure 38. Cross sectional sketch of internal structures present at locality 3 in facies K. 102

Figure 39. Typical bedding in submarine channel and fan facies in both proximal and distal settings (Kendall, 2012; modified from Bouma, 1997 and DeVay et al., 2000)……………………… 103

Figure 40. Selected trace fossil photographs from the lower Lithofacies.. 104

Figure 41. Trace fossil photos from samples of the lower lithofacies. 105

Figure 42. Heavy bioturbation in the upper 30cm at locailty 2 and 23. 106

Figure 43. Selected trace fossil photographs from the upper lithofacies. 107

Figure 44. Selected trace fossils from the upper lithofacies. 108

Figure 45. Eustatic sea level curve and conodont zones during the Devonian age (Modified from Morrow and Sandberg, 2008). 109

Figure 46. Biostratigraphy around the Famennian-Tournaisian boundary (Kaiser et al., 2015).. 110

Figure 47. Fossil groups affected by the Hangenberg Crisis (Kaiser et al., 2015)..**Error! Bookmark not defined.** 111

Figure 48. Regional depositional model for Bedford-Berea sequence (from Pashin and Ettensohn, 1995).. 112

Figure 49. Predicted depositional environment of hyperpycnal beds within the Bedford-Berea sequence in northeastern Kentucky and southeastern Ohio (Modified from Zavala et al., 2011b)... 112

Figure 50. Typical Bedford-Berea stratigraphic column compared (A) compared to a general storm-wave influenced delta stratigraphic column (B) and a depositional model (C).. 113

Figure 51. Depositional model during the lowstand system tract near the beginning of Bedford-Berea deposition.. 114

Figure 52. Map depicting the location of outcrops and nearby geophysical logs used in the correlation of outcrops to geophysical logs. 115

Figure 53. Stratigraphic column of outcrop 20 in southeastern Ohio correlated to a geophysical log (OH 34079202530000) illustrating how Bedford-Berea facies are represented in the subsurface (Figure 46 shows location). 116

Figure 54. Stratigraphic column of outcrop 1 in northeastern Kentucky correlated to a nearby geophysical log (KGS 9704) illustrating how Bedford-Berea facies are represented in the subsurface.. 117

Figure 55. System tracts model within gamma-ray logs (Rider, 1996; Plint and Nummedal, 2000; Catuneanu, 2002)... 118

Figure 56. Sequence stratigraphy of the Bedford-Berea sequence in northeastern Kentucky and southern Ohio.. 119

Figure 57. Outcrop to well log correlation of systems tracts within the Bedford-Berea sequence. 120

Figure 58. Location of geophysical logs and GQ map points (red squares) examined in this study.. 121

Figure 59. Structure contour map constructed for the top of the Berea sandstone in northeastern Kentucky and southeastern Ohio.. 122

Figure 60. Bedford-Berea isopach map in northeastern Kentucky and southeastern Ohio.. 123

Figure 61. Net Berea isopach map using a gamma-ray cutoff of 101 API units which Floyd (2015) interpreted to be a best-fit signature for sand in log-to-core comparisons. 124

Figure 62. Location of large Bedford-Berea sequence oil and gas fields.................................. 125

Figure 63. Geophysical log highlighting the Bedford-Berea reservoir in Lawrence County, Kentucky in the Beech Farm Consolidated Field.. 126

Figure 64. Geophysical log highlighting the Bedford-Berea reservoir in Greenup County, Kentucky in a new horizontal field.. 127

Figure 65. Geophysical log highlighting the Bedford-Berea reservoir in Hocking County, Ohio in the Old Gore gas field 128

Figure 66. Locations of outcrops and wells used for the outcrop and geophsyical log correlations. 129

Figure 67. Correlation of KY-1 to nearby geophysical logs going from West-East. 130

Figure 68. Illustrates the outcrop to subsurface correlation of outcrop OH-22 to nearby geophysical wells in southeastern Ohio. 131

Figure 69. Net pay sand map within the Bedford-Berea sequence.. 132

Figure 70. Location map of cross section through the Ashland Gas Field in Boyd County, Kentucky.. 133

Figure 71. Cross section of the Ashland Gas Field in Boyd County, Kentucky. 134

Figure 72. Schematic cross sectional illustration of facies and diagenetic changes cause the accumulation of hydrocarbons in the Ashland Gas Field. 135

LIST OF TABLES AND CHARTS

Chart 1. Ripple index values of oscillatory ripples in the Lower Bedford/Berea Lithofacies…. 136

Chart 2: Ripple index values of oscillatory ripples in the Upper Berea Lithofacies……… 136

Table 1: Identifies and describes sedimentary facies and facies assemblages present within the lower and upper lithofacies………………………………………………………………………………………. 137 - 139

Table 2: Description of ethology, toponomy, and ichnogenera of tracemakers within the lower lithofacies of the Bedford-Berea sequence using Chaplin (1980) classification techniques.. 140

Table 3: Description of ethology, toponomy, and ichnogenera of tracemakers within the upper lithofacies of the Bedford-Berea sequence using Chaplin (1980) classification techniques.... 141

Table 4: Description of ethology, toponomy, and ichnogenera of tracemakers in the Bedford-Berea sequence compared to tracemakers of the Cowbell Member………………………………….. 142

ABSTRACT

The Berea Sandstone is a Late Devonian unit that interfingers with and overlies the Bedford Shale. In the study area, the Bedford-Berea sequence averages 120 feet thick based on geophysical logs. The Bedford Shale makes up roughly 45 feet of the interval and the Berea Sandstone makes up the remaining 75 feet. Horizontal drilling and hydraulic fracturing have caused the Berea to become one of the largest oil producing formations in Kentucky to date. Depositional models proposed for the Bedford-Berea sequence fail to explain the vertical successions of sedimentary structures observed in outcrop and thickness patterns within the subsurface. Thus, an integrated outcrop and subsurface analysis of the Bedford-Berea sequence was conducted using 22 outcrops and 148 gamma ray/density logs in northeastern Kentucky and southeastern Ohio. Recent research into extrabasinal turbidites (hyperpycnites) has shown that similar vertical successions of sedimentary structures were produced by fluctuating flows. These vertical successions of sedimentary structures are observed in the Bedford-Berea sequence in outcrop and suggest hyperpycnal influence. Thus, the Bedford-Berea sequence represents wave influenced hyperpycnal and tempestites deposits, which were deposited in a prodelta to distal delta front setting where sediment was being derived from a northern fluvial/deltaic source.

A better understanding of sediment dispersal, depositional conditions, and facies will help the oil and gas industry create more accurate reservoir maps within the study area. Furthermore, the presence of hyperpycnal facies within the Bedford-Berea sequence may explain sedimentary structures within other shallow marine deposits in southern Ohio and northeastern Kentucky.

CHAPTER 1

INTRODUCTION

The Bedford-Berea sequence is a major oil and gas producing unit in eastern Kentucky, southeastern Ohio, western and central West Virginia and southwestern Virginia. The Berea Sandstone is an Upper Devonian siliciclastic sequence that is quickly becoming the highest oil-producing unit in Kentucky despite its low permeability as a reservoir. Horizontal drilling combined with hydraulic fracturing has allowed industry to overcome the low permeability, making the Bedford-Berea a profitable play. The focus area of this study is northeastern Kentucky and southeastern Ohio. Recent road construction in this area has exposed Bedford-Berea outcrops that have not previously been comprehensively studied (Figures 1 and 2).

Early paleoenvironmental models in the study area suggested that Bedford-Berea sediments were deposited along a shoreline in western West Virginia where they were reworked by wave and storm currents before being transported further onto the shelf to modern day northeastern Kentucky and southeastern Ohio (Pepper, De Witt, and Demarest, 1954). Pepper et al. (1954) suggested that deltas prograded into central Ohio during Bedford deposition, which is represented by a tongue of red Bedford shale in central Ohio. Subsequent studies built off Pepper et al.'s (1954) work and suggested that the Bedford-Berea sequence was deposited on a marine shelf between fair-weather and storm-weather wave base (Rothman, 1978; Potter, DeReamer, Jackson, and Maynard, 1983; Pashin and Ettensohn, 1987; Pashin, 1990; Pashin and Ettensohn, 1992). However, the most recent studies interpret the Bedford-Berea sequence as being composed of ignitive turbidites and tempestite deposits, which accumulated in a shelf/slope setting (Pashin and Ettensohn, 1995). Several ideas regarding the sediment source area for Bedford-Berea sequence in the study area have been proposed. Past studies suggested that sediment was derived from the east, through the Gay-fink and Cabin Creek Trend and from the north through the Bedford Delta (Pepper et al., 1954), while recent studies suggest that sediment was derived solely from the east through the Gay-Fink and Cabin Creek fluvial trends (Pashin and Ettensohn, 1995). Although previous studies are very thorough, none incorporate trace fossils and sequence stratigraphy in their detailed sedimentological analysis of outcrops.

Ichnofacies are groups of trace fossils that provide important depositional information such as salinity, oxygenation, sedimentation rates, turbidity, and water depth (MacEachern and Bann, 2008). Furthermore, ichnofacies help identify transgressive-regressive cycles, sequence boundaries, and flooding surfaces. Paleogeographic models developed for the Bedford-Berea sequence involved regional studies that encompass the entire extent of the Bedford-Berea sequence. As a result, comprehensive stratigraphic and paleoenvironmental analysis for the study area is lacking. A detailed examination of outcrops was used to develop a more accurate and complete reconstruction of the paleogeography and depositional systems during accumulation of the Bedford-Berea sequence. Also, a better understanding of sediment dispersal systems and facies architecture may benefit future exploration for oil and gas.

OBJECTIVES

The goals of this study are to: 1) identify the type of currents (storm, density, tidal) that affected deposition and explain N-S oriented thickness trend in northeastern Kentucky; 2) explain why linear thickness trends are perpendicular to the interpreted paleoslope if the paleoenvironment is a wave-dominated shelf; 3) determine if the Berea Sandstone could be a wave dominated, nondeltaic shelf deposit (instead of a deltaic one), where sediment was derived from the shoreface and being reworked; 4) identify potential deltaic influence on the Bedford-Berea sequence (e.g. fluvial distributary channels, mouth bars, deltaic depocenter); 5) explain the cause of coarsening- upward sequences within the Bedford-Berea sequence; 6) determine if there is evidence of barrier islands within the Bedford-Berea sequence which are common to other Devonian sequences in Pennsylvania and West Virginia; 7) determine the origin of the "massive" channel- form siltstone facies outcrop on Highway 59 in northeastern Kentucky; 8) correlate Bedford-Berea facies in outcrop into the subsurface to help test paleoenvironmental interpretations; 9) identify trace fossil ichnogenera and ichnofacies that are present in the Bedford-Berea sequence, and what information about water depth, salinity and deposition rate can be determined from them; and 10) create a better understanding of sediment dispersal systems and source areas for the Bedford-Berea sequence.

CHAPTER 2

PREVIOUS WORK

STRATIGRAPHIC FRAMEWORK

Regional Overview

Regionally, the Bedford-Berea sequence is comprised of the Bedford Shale, the Berea Sandstone, and in eastern most Ohio, the Cussewago-Second Berea Sandstone. The Bedford-Berea sequence is a thin interval that separates the Catskill and Pocono clastic wedges, which were derived from the Acadian Orogen (Ettensohn and Barron, 1981; Ettensohn and Elam, 1985; Pashin and Ettensohn, 1995). The Bedford-Berea sequence is a widespread unit throughout the northwestern part of the Appalachian Basin (Pashin and Ettensohn, 1995) and is described as the sequence that lies between the Cleveland Shale and the Sunbury Shale (Figure 3; Elam, 1981; Harris, 2014).

Local Overview

The Sunbury Shale is an easily recognizable black shale that lies directly above the Berea Sandstone. Therefore, the Sunbury Shale was used as a “marker” bed in the field to distinguish Bedford-Berea outcrops. The basal contact between the Berea Sandstone and Bedford Shale is often hard to distinguish due to its thinly interbedded nature. The thickest Bedford-Berea sequence measured in outcrop of this study occurs in northeastern Kentucky and is 26 meters thick, whereas the Sunbury had a maximum thickness of four meters. No outcrops contained an entire Bedford-Berea section from the base of the Sunbury Shale to the top of the Cleveland Member. Geophysical logs show that the Bedford-Berea sequence is significantly thicker in the study area, than in surrounding areas (Pepper et al., 1954; Floyd, 2015).

Ohio Shale

The Ohio Shale is described as a carbonaceous black shale unit that conformably overlies the Olentangy Shale (Shaler, 1877; Figure 3) and various thicknesses have been reported in Ohio and Kentucky (Pepper et al., 1954). The Ohio Shale is thickest in north central Ohio (500 feet) and thins southward to 291 feet in northeastern Kentucky (Potter et al., 1983). Two black shale members are within the Ohio Shale: the Huron Member near the base and the Cleveland Member at the top, with three non-organic, greenish-gray shale beds called the “Three Lick Bed” separating the two units (Potter et al., 1983). The contact between the Bedford Shale and Cleveland Member of the Ohio Shale is sharp in Kentucky and transitional in southeastern Ohio (Pepper et al., 1954).

Bedford Shale

The Bedford Shale is a gray to greenish-gray, and locally red silty shale that contains thin interbedded sandstone and siltstone beds, pyritic nodules and calcareous concretions (McDowell, 1986). The Bedford Shale lies conformably above the Cleveland Member (Elam, 1981; Pashin and Ettensohn, 1987, 1995; Ettensohn et al., 1988; De Witt, Roen, and Wallace, 1993; Figure 3). The Bedford Shale is present throughout eastern Ohio, eastern Kentucky, northwestern Pennsylvania, Virginia, the Michigan Basin and locally in western West Virginia (Pepper et al., 1954; Pashin, 1990). Regionally, the Bedford Shale has varying thicknesses and compositions. In the study area, geophysical logs show that the Bedford Shale is up to 45 feet thick and pinches out to the west. In the study area, the Bedford Shale is mapped together with the Berea Sandstone as an indistinguishable Bedford-Berea sequence (Ettensohn and Elam, 1985; Floyd, 2015).

The Bedford Shale is known for two major colors. The first of these is a gray shale facies containing thin beds of siltstone and is the most widespread phase. In northeastern Ohio, this facies contains two siltstone bodies called the “Euclid” and “Sagamore Members” (Prosser, 1912; De Witt, 1951). These members are similar to Second Berea Sandstone of southeastern Ohio. The second facies is the red shale facies that occurs in a belt extending from north-central Ohio into northeastern Kentucky and western West Virginia (Pepper et al., 1954).

Berea Sandstone

Geophysical logs show that the Berea Sandstone averages 75 feet thick in the study area. The Berea Sandstone consists of a light gray siltstone to very fine sandstone that interfingers and overlies the Bedford Shale (Elam, 1981; Pashin and Ettensohn, 1987, 1995; Ettensohn et al., 1988; De Witt et al., 1993; Figure 3). The Berea Sandstone is found throughout eastern Ohio, eastern Kentucky, northwestern Pennsylvania, western and central West Virginia, and southwestern Virginia (Pepper et al., 1954, De Witt et al., 1993; Pashin and Ettensohn, 1995). In Lewis County, Kentucky, the Bedford Shale splits the Berea Sandstone into an upper and lower tongue (Morris and Pierce, 1967; McDowell, 1986; Pashin and Ettensohn, 1987). In outcrop near Vanceburg, Kentucky the lower tongue of the Berea Sandstone has been interpreted as a channel sand with a southwest orientation (Morris and Pierce, 1967). Morris and Pierce (1967) also noted the Berea Sandstone quickly pinched out laterally to the west and south of Vanceburg, Kentucky.

Sunbury Shale

The Sunbury Shale has a sharp unconformable boundary with the Berea Sandstone in the study area (Figure 3). To the west in central Kentucky, the Bedford-Berea sequence is reported to thin and pinch out (Pepper et al., 1954; De Witt et al., 1993), placing the Sunbury Shale directly on the Cleveland Member. The Sunbury Shale is made of black, organic rich, fissile shale. Near Morehead, Kentucky where the Berea Sandstone is absent, the Sunbury shale has a pyritic basal lag zone, which represents an unconformity (Ettensohn, 1994; Ettensohn, Lierman, and Mason, 2009). The Sunbury Shale's maximum thickness in the study area is 30 feet. The presence of the conodont *Siphonodella sulcate* at the base of the Sunbury suggests the basal portion of the Sunbury Shale represents the base of the Mississippian system (De Witt, 1970).

PALEOECOLOGY/PALEOCLIMATE

The Late Devonian was a time of significant global events such as sea-level variations, extinctions and extensive black shale deposition (Myrow et al., 2011). During this time, the paleolatitude of the Catskill Delta complex falls within the monsoonal climatic belt between 15° and 10°S (Woodrow, Fletcher, and Ahrnsbrak, 1973; Dennison, 1996). The Acadian Orogen is located East of the study area, running parallel to the interpreted epicontinental sea and represents a potential source area for siliciclastic material (Pepper et al., 1954). Recently, Kaiser, Steuber, Becker, and Joachimski (2006) used δ^{18} values of conodont apatite to suggest that following deposition of the Cleveland Member a glaciation episode occurred during the Late Devonian. Furthermore, Ettensohn, et al. (2009) described an ice rafted boulder in the top of the Cleveland Member near Morehead, Kentucky which suggests that glaciation was occurring near the end of deposition of the Cleveland Member. Furthermore, Dennison (1985) suggested that the glaciation of Gondwanaland occurred in several events causing multiple fluctuations in eustatic sea level during the Late Devonian. Glaciation during the Late Devonian supports the hypothesis that the Bedford-Berea sequence was produced by a forced regression (Pashin and Ettensohn, 1995).

Pepper et al. (1954) reconstructed the paleogeography during the Late Devonian and Early Mississippian (Figure 4). The eastern side of the Appalachian Basin was covered with an epicontinental sea, the Acadian Orogen was just east and parallel to the sea and the western extent of the sea was bounded by the Cincinnati Arch (Pepper et al., 1954). The Gay-Fink and Cabin Creek channels fed sediment into the Epicontinental Sea from the east while the Bedford-Berea delta supplied sediment from the north and the Virginia-Carolina Delta supplied sediment in the southeast (Pepper et al., 1954).

Pashin and Ettensohn (1995) suggested a two phase paleogeographic model, where phase one represented basin filling and phase two was delta destruction (Figure 5). During basin filling a regressive event caused incision into the Catskill Clastic Wedge and caused progradation of deltas into the basin. The second phase was delta destruction, in which deposits in the western part of the basin were reworked by marine currents, causing deposition of a widespread siltstone on the shelf.

STRUCTURE

The study area lies within the Appalachian Plateau physiographic province. Strata in this area are flat-lying to gently dipping synclines and anticlines (Tankard, 1986). The Rome Trough is also located within the study area and formed during the Late Cambrian due to rifting of the North American Continent (Harris, 1975). In eastern Kentucky, the Rome Trough is bounded by the Kentucky River Fault Zone (north), the Warfield and Rockcastle River Fault Zones (south), and the Lexington Fault System (west) (McGuire and Howell, 1963; Harris, 1975; Ammerman and Keller, 1979; Floyd, 2015). The Kentucky River Fault Zone is made of a system of normal faults, with displacement varying from 500 to 3,000 feet (Harris et al., 2004; Figure 6).

SUBSURFACE STUDIES

Elam (1981) constructed an isopach map of Bedford-Berea sequences based on 9,400 geophysical logs from Kentucky. Elam (1981) noted that the thickest interval of Bedford-Berea sediments had a north-south trend in eastern Kentucky (Figure 7). In addition, it was noted that the increased thickness of the Bedford-Berea sequence was related to an added thickness in sandstone and siltstone compared to shale (Elam, 1981). Elam (1981) used gamma signatures to present evidence that the Bedford-Berea sequence represents a regressive clastic wedge which prograded into a sediment deficient basin.

Riley and Baranoski (1988) studied well logs from Lawrence County, Ohio. Their isopach map of the Berea Sandstone showed NE-SW oriented elongate sand bodies (Figure 8) which, in some areas, thin sheets of silty sand connected. Riley and Baranoski (1988) reported that silty marine shale prevails where these thin sand sheets are absent, especially in southern Lawrence County, Ohio. Baranoski and Riley (1988) interpreted the elongate sand bodies to represent offshore silty sand bars based upon the findings of Pepper et al. (1954).

Floyd (2015) evaluated 555 geophysical logs in Kentucky and used two methods for differentiating the Bedford Shale from the Berea Sandstone. Floyd (2015) determined that a 101 API unit gamma-ray cutoff was a best fit of log-to-core comparisons for the Berea Sandstone. Floyd (2015) recognized a north-south thickness trend in the Bedford-Berea sequence, which supports thickness trends previously proposed by Pepper et al. (1954) and Elam (1981). Surprisingly, Floyd (2015) noted thicker Bedford-Berea sequences containing coarser material on structural highs, while thinner intervals dominated shales occurred on structural lows.

DEPOSITIONAL ENVIRONMENT

The Bedford-Berea sequence has many regional interpretations including fluvial-deltaic, coastal, and marine sandstones, with deltas to the east in West Virginia and to the north in northern Ohio and Pennsylvania (Pepper et al., 1954; Tomastik, 1996). Several depositional models have been suggested for the Bedford-Berea sequence in northeastern Kentucky and southeastern Ohio. Pepper et al. (1954) concluded the Bedford-Berea sequence in the study area was initially deposited along a shoreline in western West Virginia, with sediment influx coming from an eastern source. The sediment was winnowed by both wave and storm currents and carried further onto the shelf to modern day northeastern Kentucky and southern Ohio. Pepper et al. (1954) also noted the southwest trend of paleocurrents within the Bedford-Berea sequence and suggested that they reflected longshore currents that flowed parallel to paleoshoreline. Rothman (1978) built upon these findings and described two facies in the Bedford-Berea sequence: a lower facies containing thin-bedded siltstones and shales, with common ripple marks; and an upper facies with thick-bedded siltstones that alternated with thin-bedded siltstones and shales. Based upon these facies, Rothman (1978) proposed a regressive shallow marine shelf depositional model for the Bedford-Berea sequence.

Pashin and Ettensohn (1987, 1992, 1995) described several lithofacies in northeastern Kentucky and southeastern Ohio, the most widespread being a siltstone lithofacies containing unrippled siltstone and rippled siltstone beds that represent shelf tempestite deposits and ignitive turbidite deposits. The second lithofacies is a gray shale, which is present throughout much of the study area and is represented by the section of the Bedford-Berea sequence composed of “greater than 67% gray shale and thin-bedded siltstone” (Pashin and Ettensohn, 1995). Pashin and Ettensohn (1995) proposed that active faulting created over steepened slopes and seismic vibrations, which contributed to turbidite deposition. Thus, Pashin and Ettensohn (1995) suggested that the Bedford-Berea sequence was composed of ignitive turbidites and tempestite deposits, deposited in a shelf/slope setting with sediment being derived from the Gay Fink and Cabin Creek fluvial/deltaic systems to the east (Figure 5 and Figure 9).

Floyd (2015) hypothesized that the Berea Sandstone was deposited in storm-dominated shelves on two distinct structural highs. Coarser grained material was deposited on structural highs, while finer grained material was deposited in structural lows. The development of shelves on structural highs suggests basement faults potentially influenced lithofacies distribution within the north-south depositional trend (Floyd, 2015).

Eustasy was a controlling factor of deposition of the Bedford-Berea sequence. Kaiser, Aretz, and Becker (2015) describe a carbon isotope excursion of up to -21% $\delta^{13}C_{org}$ in carbonates and sedimentary organic matter of the Hangenberg Black Shale, which is dated as middle *Fammenian*. The isotope excursion is in conjunction with a high content of sedimentary organic carbon (Kaiser et al., 2006). The elevated organic carbon burial rates during deposition of the Hangenberg Black Shale may have resulted in lowering of atmospheric pCO_2 causing climatic cooling (Kaiser et al., 2006). Kuypers, Schouten, and Sinninghe Damste (1998) suggested as much as a 50-90% decrease in atmospheric CO_2 levels during the Latest Devonian.

OIL AND GAS HISTORY

In Lawrence County, Kentucky there are two major oil and gas fields called the Cordell Consolidated and the Beech Farms Consolidated (Tomastik, 1996). In 1988, the discovery of the Big Laurel Schools and Road Fork (Tomastik, 1996) plays caused an increased interest in the Berea Sandstone in Kentucky. All the major Berea oil and gas fields found in Kentucky are located in the far eastern part of the state. The locality of these fields is due to the Berea Sandstone coarsening eastward where sediment was originating in a deltaic environment and limited extent of Berea Sandstone in Kentucky (Tomastik, 1996). The more proximal location to fluvial trends creates an increase in porosity and permeability creating good reservoirs characteristics (Tomastik, 1996). Recently, new technologies such as hydraulic fracturing have allowed the Berea Sandstone to become an economical play throughout eastern Kentucky despite its low porosity and permeability.

In the study area, hydrocarbon accumulation in the Bedford-Berea sequence appears to be primarily stratigraphic. However, some fields contain combination traps due to localized structural features (Larese, 1974; Coogan and Wells, 1992; Cox, 1992; Nolde and Milici, 1993), which potentially enhance the fracture porosity within the fields (Nolde and Milici, 1993). Hydrocarbons are believed to have been derived from the Ohio Shale or Sunbury Shale (Cole, Drozd, Sedivy, and Halpern 1987).

PETROGRAPHY

Rothman (1978) studied the petrography of the Berea sandstone by analyzing thin sections taken from outcrops in the area of this study. He noted that the Berea Sandstone was predominately-coarse silt, with grain sizes averaging from very fine sand to medium silt. In stratigraphic section, the grain size had a coarsening upward trend suggesting a regressive sequence. Rothman (1978) noted that samples taken near the transition zone between the Bedford and Berea contained small patches of spary calcite or massive spar cement with floating quartz grains in the spar. He classified the majority of Berea samples as sublitharenites according to Pettijohn's (1975) classification system.

Jackson (1985) performed a petrographic analysis of the Berea Sandstone in Ashland County, Ohio. Jackson (1985) found three diagenetic associations based on cementation in samples. The first association is a patchy dolomite and minor quartz; this zone had the highest average porosity of around 15%. The second association contains siderite cement that replaced patchy dolomite cement, with an average porosity of around 13.1%. The third association contains tightly packed quartz cemented sandstones with patchy dolomite cement and small amounts of quartz cement and had the lowest average porosity of approximately 12.5%.

Pashin and Ettensohn (1995) plotted the framework grain composition of samples from the Berea Sandstone on QFL and Qm-F-Lt diagrams of Dickinson et al. (1983; Figure 10). The QFL plots suggest that the Berea sandstone was derived from a recycled orogen. However, the majority of samples plot on the boundary of Craton Interior and Recycled Orogen provenances, indicating the potential for both sources. The Qm-F-Lt diagram places the Berea Sandstone within the Quartzose Recycled Orogen with several samples plotting in the Craton Interior.

CHAPTER 3

METHODS

Field Data

Outcrops at 22 locations from Lewis County, Kentucky to Pike County, Ohio were examined (Figure 1). Outcrops along Kentucky State Highway 9 and 10 (AA Highway) in the Garrison and Vanceburg Quadrangles were located using USGS 7.5 geologic quadrangle maps, while outcrops in other areas were identified using Google Earth and previous studies. The outcrops along the Kentucky State Highway 9 are relatively new and have not been studied in detail. Potter et al. (1983) previously described outcrops on Kentucky State Highway 10 in the study area. Individual sections were measured using a Jacob's staff that was 1.5 meters in height. Each section was analyzed for lithology, sedimentary structures, trace fossils, biogenic structures, faunal assemblages, vertical and lateral extent, facies geometry, and where possible, paleocurrent directions. Directional data for paleocurrent analysis were measured using a Brunton Compass (Figures 12, 13, 14, and Appendix II and III). The elevation at the base of outcrops was determined using an American Paulin System MICRO model M-1 altimeter and then compared to a Garmin Astro GPS for accuracy. Occasionally, Google Earth was used to obtain pre-field excursion base elevations and location coordinates; these elevations were then checked using the two methods mentioned previously. Samples were collected for each facies within each outcrop.

Since biogenic features are sparse in the Bedford-Berea sequence, representative samples were collected when available. The locations of these samples were noted within the stratigraphic column. The bedding plane bioturbation index (1-6) was determined by visual comparison with Miller and Smail (1997), classification system, which state: 1) no bedding plane bioturbation recorded; only disruption is caused by physical or chemical processes; 2) discrete, isolated trace fossils; up to 10% of original bedding disturbed; 3) approximately 10 to 40% of bioturbation, local zones of disruption. Burrows are generally isolated, but locally overlap; 4) approximately 40 to 60% disturbed, zones of generalized disruption; and 5) approximately 60-100% disruption, up to 100% of bedding plane surface has been disrupted.

Laboratory

The field-generated stratigraphic columns were manually inputted into Adobe Illustrator CS6 and cross-sections were created to compare stratigraphic columns to observe facies thickness changes over distance. Bulk samples were examined for both trace and body fossils using a Leica 30-x stereomicroscope and photographs were obtained using an Iphone 6. A total of 148 gamma ray/density logs were analyzed to create net sand isopach maps and identify distinctive gamma ray/density signatures of which 107 logs in Kentucky and 41 logs in Ohio were examined. These logs were downloaded from the Ohio Geological Survey and the Kentucky Geological Survey. Log signatures were used to correlate outcrop facies into the subsurface and to search for more proximal channel systems implied by paleogeographic models. The logs were processed using Petra version 3.8.3, which is a subsurface modeling software that allows for detailed analysis and mapping of structures and stratigraphic units within the subsurface. Correlation was performed using the base of the Sunbury Shale and top of the Cleveland Shale, which are organic-rich shales with a high gamma ray response that bound the Bedford-Berea sequence. Floyd (2015) compared Bedford-Berea cores with geophysical logs and determined that the appropriate sand-silt/shale cutoff was 101 gamma-ray units. Thus, this study used 101 gamma-ray units as the sand-silt/shale cutoff for the net isopach of the Berea Sandstone-siltstone in both northeastern Kentucky and southeastern Ohio. Any alteration or enhancement of the geophysical logs was performed using Adobe Illustrator CS6, including highlighting specific facies or creating well-to-well cross-sections.

In northeastern Kentucky and southern Ohio, well spacing is sparse and limited to areas east of the outcrop area. In order to supplement thickness data west of the outcrop area, geologic quadrangle maps were used including: Charters quadrangle (Morris, 1965a), the Stricklett quadrangle (Morris, 1965b), the Buena Vista quadrangle (Morris, 1966), the Vanceburg quadrangle (Morris and Pierce, 1967) and the Garrison quadrangle (Chaplin and Mason, 1978) to calculate the thickness of the Bedford-Berea sequence and the Berea Sandstone. The calculation was performed by finding intersection points of structure contours placed at the base of the Sunbury Shale with the elevation of mapped contacts of the base of the Bedford Shale and Berea Sandstone. Utilizing this, thicknesses for the Berea Sandstone and the Bedford-Berea Sequence could be calculated by identifying the contour at the base of the Bedford Shale and subtracting it from the structural contour of the Sunbury Shale.

CHAPTER 4

RESULTS

Facies Description and Interpretation

The Bedford-Berea sequence contains two lithofacies, the lower lithofacies and an upper lithofacies (Figure 11) within the study area. The lower lithofacies contains medium-bedded siltstones and interlaminated siltstones and shales with lenticular and wavy ripple bedding. The upper lithofacies contains medium to thick-bedded siltstone and very fine-grained sandstones with thin shales separating thicker beds. Sedimentary facies within both lithofacies were distinguished primarily by sedimentary structures, and to a lesser extent by: a) lithology, b) trace fossils, and c) facies geometry. Eleven facies are identified within the Bedford-Berea sequence, which are summarized in Table 1 and facies assemblages correlated in figures 12 and 13.

Lower Lithofacies

Sedimentary Facies A

Description

Facies A varies in thickness from 20 cm to 1.5 meters and is present throughout much of the study area, being best exposed at localities KY-2 and KY-12 (Figures 14 and 15). Facies A contains unrippled medium-bedded siltstones with sparse current ripple cross-laminations, parallel laminations and hummocky cross-stratification, with common ball and pillow structures. Paleocurrent measurements within this facies have a south/southwest trend (210-225). Bedding plane bioturbation is rare, with horizontal burrows occurring on bedding surfaces and beds having a bedding plane bioturbation index of 1-2. Trace fossils include *Planolites,* *Palaeophycus, Nereites, Scalarituba* and *Neonereites*. Siltstone beds have a tabular geometry and are persistent laterally (1000+ feet). Large ball and pillow structures are common within this facies but do not persist laterally.

Pashin and Ettensohn (1995) described similar beds in their “gray shale lithofacies” noting unrippled beds were graded and contained successions resembling the Bouma T_{cde} sequences (Figure 18), lacked grading, and contained asymmetrical ripple bedforms that were commonly overlain by wave rippled siltstone.

Interpretation

Although sparse, the presence of current ripple cross-laminations to the southwest suggests deposition with a unidirectional flow that moved down paleoslope. The majority of sedimentary structures found within this facies are produced under combined flow conditions, such as hummocky cross-stratification and parallel laminations, which suggest both oscillatory currents and unidirectional currents affected deposition. Aerobic conditions were present during deposition, with the best evidence being the common wave ripples as previously reported by Pashin and Ettensohn (1995). Pashin and Ettensohn (1995) classified beds within facies A as thin to medium-bedded unrippled beds formed by intrabasinal (ignitive) turbidites that follow the Bouma model (Figure 16 and 17).

There are two types of turbidite deposits, ignitive turbidite deposits and hyperpycnal turbidite deposits. Ignitive turbidites, also known as “intrabasinal turbidites,” (Zavala, Arcuri, Gamero Diaz, Contreras, and Di Meglio 2011a) are derived from purely waning flows. These turbidites are made up of vertical changes in grain size and structures that are indicative of decreasing flow velocity and follow the (Bouma, 1962) sequence. The maximum speed of an ignitive turbidite flow is developed at the flow head and velocity declines towards the body and tail of the flow (Figure 20A; Zavala, Arcuri, Di Meglio, and Zorzano 2016). Intrabasinal turbidite flows are triggered when slope instability occurs from over-steepened slopes or other disturbances, which create a sediment flow that moves down slope due to gravitational forces.

In contrast, hyperpycnal deposits also known as “extrabasinal turbidites,” are associated with flows having a slow moving head and the occurrence of both inverse and normal grading in thick sandstone beds produced from fluctuating flows (Zavala et al., 2011a). Hyperpycnal deposits are directly linked to fluvial sources and have been reported to reach 100’s of kilometers into the basin (Zavala et al., 2011a; Zavala, Marcano, Carvjal, and Delgado 2011b). A recent study of 150 rivers discharging into the oceans concluded that 71% of these rivers could produce an extrabasinal turbidite with an event interval of one event every year to one event every 100 years (Zavala et. al., 2016). Unlike ignitive turbidites, extrabasinal turbidites deposit wax-wane beds, which are directly linked to the rising and falling discharge of a flooding river (Myrow, Lamb, Lukens, Houck, and Strauss 2008). In order to produce a hyperpycnal flow, a delta must have sediment laden and/or cold fresh water, which causes the fresh water to become denser than the seawater (Figure 18, Zavala et. al., 2016). Zavala et al. (2011a) provided the first in depth sedimentary descriptions of extrabasinal turbidite beds.

The association of facies A with other facies that are similar to extrabasinal turbidite (hyperpycnal) facies suggests that facies A was deposited from storm-generated combined flows, and subordinate hyperpycnal flows and represents distal storm deposits and minor hyperpycnal deposits in a prodelta setting to distal delta front setting. The presence of both wave and combined flow ripples and minor unidirectional flow structures in some beds within facies A c (Figures 14 and 15) support this theory. The sparse bedding plane bioturbation on upper and lower bedding surfaces suggests that deposition occurred rapidly with fluctuating turbidity and salinity. These factors coupled with Late Devonian mass extinction events created stressful conditions for tracemakers during deposition.

Howard and Lohrengel (1969) identified three (3) requirements needed for the formation of ball-and-pillow structures: 1) coarser clastics deposited over finer sediments; 2) unconsolidated sediments; and 3) sediments deposited in shallow, subaqueous environments. Although several theories on the formation of ball-and-pillow structures have been suggested, vertical movement of dense sand into less dense mud has become the most widely accepted hypothesis (Single, 1956; Kuenen, 1958, 1965; Sorauf, 1965; Howard and Lohrengel, 1969; McBride, Weidie, and Wolleben 1975; Brenchley and Newall, 1977).

Sedimentary Facies B

Description

Facies B is limited to outcrops of the lower lithofacies near the Bedford-Berea contact. Localities KY-2, KY-12, OH-7 and OH-8 have great exposures of facies B. Facies B is composed of wavy (50%) and lenticular (50%), ripple-bedded, interlaminated siltstone and shale with siltstones ranging from .5 cm to 5 cm in thickness (Figures 14 and 15). Occasional thin discontinuous beds of siltstone are present but rarely exceed two feet in length. Micro-hummocky cross-stratification, parallel lamination, ripple cross-lamination, asymmetric, and symmetric ripples are abundant within this facies (Figures 14, 15 and 19). Paleocurrents within this facies are consistent with other Bedford-Berea facies, with ripple crest orientations having a consistent strike to the northwest (305) and unidirectional paleocurrents structures such as ripple cross-laminations dipping toward the southwest (210-225). Facies B has a tabular and occasional discontinuous geometry and is moderately bioturbated with bedding plane bioturbation indices ranging from 1-3. Horizontal burrows are dominated by the *Planolites, Palaeophycus, Nereites, Neonereites,* and *Scalarituba*.

Interpretation

Facies B was deposited under similar depositional conditions as facies A. However, the abundance of wave-generated ripples within this facies indicates more frequent storm influence and even less hyperpycnal flows, and is supported by the abundance of combined flow structures found within this facies such as hummocky cross-stratification (Zavala et al., 2016). The low amount of bedding plane bioturbation indicates that harsh depositional conditions coupled with fluctuating flows drastically affected tracemakers during deposition. Facies B was deposited between fair weather and storm wave base in aerobic conditions as suggested by the abundance of wave ripples capping beds. Thus, facies B represents tempestites that were deposited in a distal delta front to prodelta setting near fair weather wave base and above storm wave base, which allowed storm wave generated currents to affect deposition.

This facies is similar to the rippled gray shale lithofacies of Pashin and Ettensohn (1995). In Pashin and Ettensohn (1995) bed architecture, (Figure 17) the rippled gray shale lithofacies begins at the hummocky strata portion of the thick bedded deposits, and follows the vertical sequence of the bed architecture. The rippled “gray shale lithofacies” has been interpreted as being distal storm deposits that accumulated in an upper slope environment in northeastern Kentucky and southeastern Ohio (Pashin and Ettensohn, 1995).

Upper Lithofacies

Sedimentary Facies C

Description

Facies C consists of thick successions of very fine-grained sandstones and siltstones with beds ranging from 30 cm up to 4 meters thick with no visible internal structures (Figs. 20, 21, and 22). Beds are tabular and persist laterally over long distances up to 2,000 feet at some localities. Facies C is the most abundant facies in outcrop. Bedding plane bioturbation in this facies is mostly rare; nevertheless, some bedding plane bioturbation is present at locality 1 in the form of sparse horizontal burrows, which include *Planolites, Palaeophycus, Chondrites*, *Lophoctenium, Nereites, Neonereites,* and *Scalarituba.* Small, reworked brachiopods and other possible invertebrates (Crinoids?) can be locally found within the Berea Sandstone near its contact with the Sunbury Shale at locality OH-22 (found by Dr. Martino). Unlike other outcrops, at locality 2 near the contact with the Sunbury Shale the Berea Sandstone has a high bioturbation index of 4-5. Large Ball and pillow structures are common at the base of this facies but are not persistent laterally. Thickness of sandstone beds varies from a few centimeters up to half a meter. Wave and combined flow ripples are sometimes present at the top of this facies and are very well preserved.

Interpretation

This facies is similar in some respects to the T_a facies at the base of the Bouma sequence (Figure 18), that is described as a massive and graded sandstone (Bouma, 1962). However, this facies is more comparable to the S1 facies of Zavala et al., (2011a) which is associated with hyperpycnal flows (Figure 23). Both facies are very similar and are only differentiated based on the vertical succession of structures that follow. If facies C was deposited from a purely waning flow (ignitive turbidite), it is expected that vertical sequences will follow the Bouma facies sequence with facies C (T_a) (Figure 16), followed by parallel lamination (T_b), overlain by cross-laminated sands (T_c), then laminated silts (T_d) and finally pelagic and hemipelagic mud (T_e). In contrast, if facies C was deposited by hyperpycnal flows the vertical sequences will transition from facies C (S_1) - facies D (S_2) - back to facies C (S_1) which supports fluctuating flow (Figure 24, 25, and 26). The irregular transitions between facies suggests that deposition occurred through long-lived currents associated with extrabasinal turbidites lasting from weeks to months with fluctuating flows (Figure 27) instead of short-lived currents associated with ignitive turbidites. Furthermore, Woodrow et al., (1973) and Dennison, (1996) suggested that during the Late Devonian the paleogeography was within the monsoonal climatic belt. The monsoonal climatic belt is associated with rainy and dry seasons, which optimize conditions for sediment transport and storm-floods that optimize conditions for hyperpycnal events.

Sparse bedding plane bioturbation indicates generally inhospitable environmental conditions. Favorable conditions occurred for only short intervals. In addition, salinity fluctuations were common during deposition due to hyperpycnal systems bringing influxes of fresh water into the basin causing marine conditions to become brackish during deposition and only returning to open marine conditions between hyperpycnal events. These events coupled with extinction events during the Late Devonian caused increased stress on tracemakers. The presence of reworked and size sorted brachiopods, other invertebrates, and a high bioturbation index near the top of the Berea Sandstone in facies C indicate an extended period of slow or non-deposition.

Previous researchers (Pashin, 1990; Pashin and Ettensohn, 1995) described lithofacies similar to facies C as being part of the Bouma sequence (Bouma, 1962). However, the tendency of facies C to transition vertically to structures that are not produced by purely waning flows (Figure 24, 25 and 26) suggests that this facies is not part of the Bouma sequence but part of the hyperpycnal sequence described by Zavala et al. (2011a) where waning-waxing-waning flows are prominent.

Similar facies in hyperpycnal deposits have been described to have formed by vertical aggradation from long-lived sediment laiden flows (Sanders, 1965; Kneller and Branney, 1995; Camacho, Busby, and Kneeler 2002; and Zavala et al., 2011a). Arnott and Hand (1989) and Sumner, Amy, and Talling (2008) have performed experiments to determine that facies C can originate from a turbidity flow that has fall out rates in excess of 0.44 mm/s; any lower fall out rates result in the formation of parallel lamination. Thus, facies C was deposited by a hyperpycnal flow within a delta front setting in water depths between fair weather and storm wave base and is supported by wave and combined flow ripples that are sometimes present on top of the facies, which indicate storm modification of sediment.

Sedimentary Facies D

Description

This facies is composed of light gray, fine-grained sandstone/siltstone having parallel laminations with a transitional or sharp boundary with vertically adjacent facies and lacks bedding plane bioturbation (Figures 20 and 21). Facies D is present throughout the study area, ranges from a few centimeters up to 20 cm thick, and is abundant in outcrop, second to only facies C. Laminations in this facies are millimeter thick and sometimes contain low angle diverging laminations (hummocky-like laminations). Facies D is commonly present in the upper portion of Berea beds with facies C beneath it. Facies D has a tabular geometry and is persistent laterally.

Interpretation

This facies is similar to the T_b facies of the Bouma sequence for ignitive turbidites and other researchers have interpreted it as the T_b facies (Pepper et al., 1954; Rothman, 1978; Potter et al., 1983; Pashin and Ettensohn, 1995). However, this facies better fits the hyperpycnal S2 facies of Zavala et al. (2011a) due to facies transitions vertically which are not explained by purely waning flows, but rather fluctuating flows.

Previous studies suggest that parallel laminations of the T_b facies formed under unidirectional flows in the upper flow regime (Arnott and Hand, 1989). However, more recent experiments suggest that parallel laminations can also form under combined flow, where the unidirectional component is at a low ratio compared to the oscillatory component (Plint, 2010). Thus, parallel laminations can form due to a small unidirectional flow despite the presence of a larger oscillatory flow. The Plint (2010) hypothesis is supported by the transitioning of parallel laminations into numerous combined flow sedimentary structures including micro-hummocky cross-stratification, swaley cross-stratification and hummocky cross-stratification within the Bedford-Berea sequence. Furthermore, this type of facies transition is a diagnostic characteristic of long-lived turbulent flows, such as hyperpycnal flows, where facies transitions (facies C-D-I-C-D) support fluctuating flows rather than waning flows of typical turbidite sequences (Facies C-D-E). The lack of bedding plane bioturbation suggests Late Devonian extinctions, coupled with uninhabitable environmental conditions for organisms due to high energy, rapid deposition, high turbidity rates and brackish conditions, drastically affected tracemakers during deposition. Thus, facies D was deposited by hyperpycnal flows in a delta front setting with water depths between fair weather and storm wave base.

Sedimentary Facies E

Description

Facies E is composed of wave rippled and combined flow rippled siltstone, very fine-grained sandstone, climbing ripple cross-laminated siltstone, and very fine grained sandstones with shale present between siltstone and sandstone beds. Facies E commonly grades upward to facies C and D (Figures 20, 21, and 22). Facies E is present throughout the majority of the study area and has a bedding plane bioturbation index of 1-3. Bed thicknesses range from 5 cm to 20 cm with a tabular to irregular geometry. Paleocurrent directions from this facies are oriented to the southwest (210-225) and are consistent with paleocurrent measurements throughout the Bedford-Berea sequence. Both symmetrical and combined flow ripples occur on top of beds and are well exposed in the study area.

Ripple marks show an average wavelength of 8 cm and a height of .57 cm with sharp crest-lines and nearly symmetrical profiles. Ripple marks appear to be symmetric in the field. However, upon closer examination some ripples do have a steeper lee slope than stoss slope, making them slightly asymmetric with steeper, shorter side to the southwest. Pepper et al. (1954) and Rothman (1978) also found ripple marks in the Berea outcrops to be slightly asymmetrical to the southwest. Paleocurrent measurements throughout the Bedford-Berea sequence in northeastern Kentucky and southeastern Ohio have a vector mean azimuth of 225.28^{o} and a vector magnitude of 91.6 percent (Figures 28, 29, 30 and 31), which is similar to other studies that described paleocurrents within the study area (Hyde, 1911; Pepper et al., 1954; Rothman, 1978; Potter et al., 1983). The only exception of this finding was cross-beds at the Tener Mountain locality that had a mean direction of N 53^{o} E; only three of these cross-beds were noted in the outcrop.

Interpretation

Facies E is similar to the S3 and S3w facies of Zavala et al. (2011a). The S3 facies is composed of fine-grained sandstone with climbing ripples, while the S3w facies is composed of fine-grained sandstone with symmetric ripple bedding and is associated with shallow water environments affected by combined flows and wave-formed structures (Zavala et al., 2016). Both facies are represented within the Bedford-Berea sequence by facies E with the S3w facies being the more dominant in outcrop. Experimental studies suggest that oscillatory currents with a velocity between 20-50 cm/s and a small unidirectional or asymmetric oscillatory flow create combined flow ripples (Plint, 2010). Sparse bedding plane bioturbation indicates large stresses affected tracemakers during deposition and include: (i) high turbidity rates; (ii) salinity fluctuations; (iii) rapid deposition; and (iv) Late Devonian mass extinctions. Facies D commonly grades upward into the facies E suggesting a transition from higher to lower velocity down section. Zavala et al. (2011a) suggested that gradual changes in flow velocity (transition from facies D to facies E) and in the rate of sediment fallout (shifts between facies C and facies D) are suggestive of long-lived turbulent flows being deposited by energy fluctuations, characteristic of a hyperpycnal system.

Ripple indices of wave and combined flow ripples were collected for both lithofacies with the majority of all ripple indices plotting within the current ripple category and some plotting within the wave ripple category (Tables 1 and 2). Three ripple indices plotted outside of these categories; this was caused by erosion of the ripple crests, which skewed the classification. The abundance of wave formed structures such as symmetrical ripples occurring at the top of sandstone beds indicates wave influence. These wave ripples and the abundance of hummocky cross-stratification in outcrop suggest river floods occurred during major storms, which created "storm floods" where storms enlarged river discharge and coastal areas (Wheatcroft, 2000; Mutti, Tinterri, Benevelli, di Biase, and Cavanna 2003). The presence of facies S3W that is created by combined flows associated with wave currents suggests that facies E represents wave modified hyperpycnites deposited in a delta front environment between fair weather and storm weather wave base.

Sedimentary Facies F

Description

Facies F is found throughout the study area and is composed of tabular beds of hummocky cross-stratified siltstone and very fine-grained sandstones that are medium bedded, lack bedding plane bioturbation and are commonly wave ripple capped (Figure 22). Facies F is often present in the lower portion of a sandstone/siltstone bed and ranges from several centimeters to 15 cm in thickness, transitioning vertically to facies D and facies E, indicating fluctuating flow velocity. An irregular geometry can sometimes be associated with this facies as a result of its tendency to transition to other facies laterally.

Interpretation

Plint (2010) suggested that the presence of hummocky cross-stratification is a result of deposition above storm wave base under combined flows, where currents have a strong oscillatory component and weak unidirectional component, with large depositional rates to preserve hummocks. Dumas and Arnott (2006) suggest hummocky cross-stratification forms in water depths ranging from 13 to 50 meters. Fair weather wave base has been suggested to be around 10 meters, and storm wave base can extend to 70 meters (Pashin, 1990). Water depths between fair weather and storm wave base have previously been interpreted for the Bedford-Berea sequence by Pashin (1990) and Pashin and Ettensohn (1995). The presence of hummocky stratification and common wave ripple capped beds suggest that facies F represents wave modified hyperpycnite deposits similar to those previously described by Myrow, Fischer, and Goodge (2002) (Figure 32). Furthermore, the lack of bedding plane bioturbation within this facies suggests that benthic conditions were inhospitable.

Sedimentary Facies G

Description

Facies G is present throughout the study area, is common in the mid-upper portion of the upper lithofacies and is well exposed at localities 2 and 12 near Garrison, Kentucky (Figure 22). Facies G is comprised of sharp based, very fine-grained sandstone and siltstone that are swaley cross-stratified, lack bedding plane bioturbation, commonly capped by wave ripples, and have a thickness of several centimeters to 15 cm. Facies G commonly grades upward to facies D and facies E. Facies G occasionally exhibits ball-and-pillow structures; however, these structures are not persistent laterally.

Interpretation

Swaley cross-stratification forms in similar hydraulic conditions as hummocky cross-stratification. Experimental studies by Dumas and Arnott (2006) suggest that swaley stratification forms in an oscillatory-dominant, combined-flow condition. Swaley cross-stratification occurs in shallow water where sedimentation rates are low causing scouring producing swales over hummocks (Dumas and Arnott, 2006). Swaley cross-stratification is associated with more proximal settings such as the lower shoreface within storm-wave influenced deltaic models (Bhattacharya, 2011).

Facies G was deposited close to the maximum regression in shallower water than the other facies within the Bedford-Berea sequence. The increased occurrence of erosive events caused scouring of hummocks and preserved only the swaley portion of the bedforms. The lack of bedding plane bioturbation suggests rapid deposition, salinity fluctuations, Late Devonian mass extinctions, or other stresses affected tracemakers. Pashin (1985) and Pashin and Ettensohn (1987) described a similar facies and suggested an outer marine shelf edge as the interpreted depositional environment for their "Swaley sandstone" lithofacies. Facies G represents storm deposits (tempestites) that formed in a proximal delta front environment. The presence of swaley stratification in sharp-based siltstone and very fine sandstones topped by wave ripples is typical of tempestites deposits (Cheel and Leckie, 1992). Deposition of this facies occurred in a more proximal setting with water depths ranging just deeper than fair weather wave base allowing frequent storm currents to affect sediment.

Sedimentary Facies H

Description

Facies H is present throughout the study area but is not as abundant as facies C through G. Facies H is comprised of very fine-grained sandstones and siltstones that have convolute laminations, ball and pillow structures and load structures that typically occur in the lower portion of the bed. Facies H commonly grades both vertically and laterally to facies E and F (Figure 20), has a thickness range between 5 cm and 1 meter, lacks bedding plane bioturbation and has an irregular geometry. Ball and pillow structures represent the upper extent of the thickness range (20 cm – 1 meter), while convolute laminations represent the lower extent (5-10 cm).

Interpretation

Convolute laminations result from soft sediment deformation and form when complex folding of a bedding occurs soon after deposition and indicates rapid deposition (Boggs, 2006). Bhattacharya (2011) has reported large soft-sediment deformation structures in river-dominated deltas and prodelta facies similar to the Bedford-Berea sequence. In this environment, prodelta muds are beneath heavier sands causing movement of the overlying sand resulting in soft-sediment deformation structures (Bhattacharya, 2011).

Sedimentary Facies I

Description

Facies I consists of thin couplets of alternating siltstone and clay that have abundant intercalations of plant debris and micas (Figure 33). Facies I is often associated with facies C but can also be associated with facies E and D. Individual silt layers have a thickness from 1 mm up to 1 cm and are separated by thin laminae of fine, sand-sized carbonaceous detritus. Facies I has a tabular geometry, but is easily weathered away and can sometimes be very hard to distinguish from other facies. Bedding plane bioturbation in this facies is sparse, with an index of 0-1. Burrows include *Planolites* and *Palaeophycus*.

Interpretation

Facies I is directly associated with hyperpycnal deposits and represents the finest materials transported by a hyperpycnal event (Zavala, Carvajal, Marcano, and Delgado 2008; Figure 34 from Zavala et al., 2011a). Facies I was deposited when less dense fresh water mixed with marine water was lofted allowing the finest fraction of sediment to accumulate from normal settling (Spark et al., 1993). The presence of facies I and its transition with facies C, which is linked to long-lived turbidity currents produced by hyperpycnal events, illustrate flow fluctuations over time (Zavala et al., 2011a; Figure 40). The sparse bedding plane bioturbation is linked to harsh depositional conditions and Late Devonian mass extinctions which negatively affected tracemakers during deposition.

In some beds, this facies may also represent tidal influence upon delta front settings. The rhythmic layering of this facies is suggestive of tidal deposits. Presumably, flood and ebb tides directly affected river discharge. During high tide, river discharge slowed causing sediment accumulation to decrease and during low tide, river discharge increased causing sediment accumulation to increase. Bhattacharya (2011) has suggested that heterolithic strata with tidal bundles, rhythmites, double mud drapes and bimodal cross-stratification are characteristic of tidally influenced delta front deposits. In some beds of the Bedford-Berea sequence, rhythmic layering in horizontal laminations resembling tidal rhythmites appear to be preserved (Figure

33). Tidal rhythmites are horizontal laminations consisting of alternating sandy/silty and muddy material that show cyclic changes in layer thickness due to neap-spring disparities in tidal current (Dalrymple, 2009). Previously, Bhattacharya (2011) has noted tidal features throughout deltaic deposits, such as wavy-bedded mudstones, tidal rhythmites and rippled sandstones that indicate significant tidal influence of river discharge. Similar rippled sandstones and wavy-bedded mudstones are present in the delta front sands of the mid to upper Berea Sandstone.

Sedimentary Facies J

Description

Facies J is composed of thin bedded, interbedded siltstone, and shale with beds ranging between 5 and 10 cm in thickness. Sedimentary structures within this facies include micro-hummocky cross-stratification, parallel laminations, ripple cross-lamination, and wavy and lenticular ripple bedding, which includes symmetric and combined flow ripples (Figure 35). Facies J occurs within the upper lithofacies and separates medium to thick-bedded extrabasinal turbidite siltstones/sandstones. Wave ripple crests strike northwest (305) and unimodal paleocurrent indicators such as ripple cross-lamination dip azimuths are oriented southwest (210-225). Facies J has a tabular geometry and persists laterally. The bedding plane bioturbation index ranges from 1 to 3, with all bioturbation occurring on bedding surfaces and containing the horizontal burrows of *Planolites, Palaeophycus, Thallasinoides, Lophoctenium,* sparse *Chondrites, Nereites, Neonereites,* and *Scalarituba*. Small ball and pillow structures are common within this facies and occur on the base of thin-bedded siltstones that are underlain by shale.

Interpretation

Facies J is comparable to facies B and closely resembles current models of shallow-marine storm beds, where individual beds have basal parallel lamination followed by hummocky cross-stratification and capped with symmetrical ripples. However, combined flow ripples often cap the sequence, suggesting deposition occurred with a strong oscillatory flow component and a subordinate unidirectional component. The abundance of combined-flow structures and combined-flow ripples suggests that facies J was deposited by storm currents and represents intervals of deposition between hyperpycnal events. Similar to other facies within the Bedford-Berea sequence the low bedding plane bioturbation index is due to harsh depositional conditions and mass extinction events during the Late Devonian. Facies J represent storm deposits (Figure 36) and minor hyperpycnal deposits deposited in a delta front setting. Facies J is similar to facies B, but is a more proximal deposit based on the abundance of wavy ripple bedding (70%) over lenticular bedding (30%).

Sedimentary Facies K

Description

Facies K is restricted to locality 3 and consists of a large paleochannel, filled with bioturbated siltstone. A matrix-supported intraformational conglomerate occurs at the base of the channel fill and has sub-angular clasts of shale and siltstone up to 3 cm in diameter. The channel trend is reported to be oriented southwest from outcrop KY-3 to Holly Cemetery, with an azimuth of 225° (Morris and Pierce, 1967). The facies is up to 6.8 m thick and is at least 96 m wide. The boundaries of the channel-fill are not exposed. However, erosive sands at the contact between the Cleveland and Bedford/Berea have been reported in Quadrangles west of locality

3 (Morris and Pierce, 1967). Facies K contains a variety of sedimentary structures not mentioned by previous workers (Figures 37 and 38). The base of this facies rests uncomformably above the Cleveland Shale Member and contains abundant shale rip-ups (presumably from the underlying Ohio Shale), and pyrite nodules. Convolute bedding is also present in the lower portion of this facies. Compound cross-stratification composed of large-scale foresets (60-70 cm) and internal trough cross-stratification (5-10 cm) is present. Bedding plane bioturbation occurs at the base of the facies and has an index of 1-2, consisting of horizontal burrows of *Planolites* and *Palaeophycus*. Bedding plane bioturbation is present in localized zones within the facies and traces are poorly preserved.

Interpretation

Large shale rip-up clasts represent erosion of the underlying Cleveland Member. The matrix supported intraformational conglomerate is similar to previously described debris flow deposits in other formations associated with submarine channels (Arnott, 2010). Convolute laminations indicate rapid deposition, which caused alteration of semi liquefied sediment soon after deposition (Boggs, 2006). Compound cross-stratification consisting of large-scale foresets were produced by unidirectional currents directed down paleoslope, while trough subsets are produced by 3-D dunes moved by currents (Harms, Southard, Spearing, and Walker 1975). Arnott (2010) has suggested that compound cross-stratification may be related to lateral accretion deposits (LADs) formed on the inner-bend levee of a horizontally migrating, highly confined submarine channel. Also, the presence of dune-sized bedforms suggests grain sizes are coarser than silt and are in the very fine sand range (Boggs, 2006).

There are two possible origins for facies K. The first is that deposition may have occurred in the upper portion of a submarine channel near the upper/middle fan where erosion was taking place similar to figure 39 from Kendall, (2012); Bouma, (1997); and Devay, Risch, Scott, and Thomas (2000). The submarine channel would have been located on the slope edge and feed sediment to deeper portions of the basin. Pashin (1990) described the outcrop at location 3 as being feeder channel deposits composed of “massive siltstone.” Submarine channels can be erosional, aggradational, or both (Normark, 1970). Harris and Whiteway (2011) classified submarine canyons into three types: 1) shelf-incising canyons, connected to a major fluvial or estuarine source, but do not incise onto land; 2) shelf-incising canyons with no distinct fluvial or estuarine source; and 3) slope-incising blind canyons, confined to the continental slope. Considering previous evidence of fluvial-deltaic channels in geophysical logs in southern Ohio from Tomastik (1996) within 70 miles up dip, this feeder channel would likely represent a submarine channel that is connected to a major fluvial source from the north.

The second hypothesis for the deposition of facies K is that an incised valley fill (IVF) formed during a falling stage system tract due to glacioeustasy and was then backfilled under marine influence during a subsequent transgression. Fluvial-deltaic channels are described in northern Ohio where Berea channels down cut into the red Bedford shale and Bedford channels down cut into the Cleveland shale (Pepper et al., 1954). The problem with facies J representing an IVF is the lack of basal-fluvial lag overlain by estuarine deposits, which are typical of IVF deposits that are backfilled during a transgressive event (Dyson and Christopher, 1994).

Floyd (2015) suggested the presence of three channels in the subsurface of northeastern Kentucky. The log patterns were bell-shaped, fining upward signatures (Cant, 1992) that are typical of submarine channel facies and were located near the base of the Bedford-Berea sequence. Submarine channels described by Floyd (2015) were 30-40 ft thick, occurred near the base of the Bedford-Berea sequence, and incised into the Cleveland Shale Member. Also, highly confined, leveed submarine channels described by Arnott (2010) have channel widths and depths of tens of meters to several hundred meters and would be difficult to map in northeastern Kentucky due to inadequate well spacing.

Paleoecology

The lower lithofacies is comprised of facies A and B, with both containing impoverished ichnofauna. The lower lithofacies has an average bedding plane bioturbation index of 1-3 with all traces occurring on bedding surfaces. Trace fossils are not very abundant in this lithofacies and are diminutive in size, ranging from .1 to 1.3 cm in diameter with lengths ranging from 0.3 to 7 cm. The same ichnogenera are found throughout the lower lithofacies, and include *Planolites, Palaeophycus, Thalassinoides,* sparse *Chondrites,* and horizontal burrows (*Nereites, Scalarituba, and Neonereites*; Figures 40 and 41; Table 2). The horizontal burrows are small and preserved in short segments making them nearly impossible to distinguish between *Scalarituba, Nereites,* and *Neonereites*; however, these traces represent the same burrow preserved in different ways due to contrasting preservation (Ekdale, Bromley, and Promberton 1984). Sparse, circular traces up to 2 cm in diameter are preserved on bedding surfaces and appear to be vertically oriented resembling *Skolithos.* However, these traces are shallow, are not seen in full relief, and rarely penetrate further than 0.5 cm into the bed.

The upper lithofacies contains facies C through K and all contain impoverished fauna. The average bedding plane bioturbation index for the upper lithofacies is 1 to 3. Similar to the lower lithofacies traces are limited to bedding planes. The only exception to this occurs at the Berea-Sunbury contact where the upper 30 cm of the Berea Sandstone is highly bioturbated with a bioturbation index of 4-6 (Figure 41). Only two facies, facies E and facies J, contain significant amounts of trace fossils. As in the lower lithofacies, trace fossils in the upper lithofacies are diminutive in size. Ichnogenera in the upper lithofacies include *Planolites, Palaeophycus, Lophoctenium, Thalassinoides,* horizontal burrows, (*Nereites, Scalarituba, and Neonereites*) and *sparse Chondrites* (Figures 42, 43 and 44; see Table 3). Circular traces on bedding planes that appear to be vertical also appear in the upper lithofacies. Similar to the lower lithofacies these traces do not penetrate more than .5 cm within the bed and are not seen in full relief view.

Trace Fossil Interpretation

Ichnodiversity within the Bedford-Berea sequence is low when compared to ichnodiversity described in Early Mississippian members deposited under similar depositional conditions (Chaplin, 1980). The Cowbell Member of the Borden Formation is Early Mississippian in age and like the Berea Sandstone was deposited in a delta front environment (Kepferle, 1971). Furthermore, the Cowbell Member is interpreted as being deposited in aerobic conditions (Kepferle, 1971) at similar water depth ranges as the Berea Sandstone (Pashin and Ettensohn, 1992). Utilizing Chaplin's (1980) list of ichnogenera in the Cowbell Member, a comparison of Bedford-Berea ichnogenera has been made in Table 4.

The basal portion of the Bedford Shale has been interpreted to be a dysaerobic deposit based on the presence of thin-shelled, brachiopod mollusc-dominated fauna; whereas, the rest of the Bedford Shale was deposited under aerobic conditions indicated by wave ripples, which are typically produced by shallow-water processes (Pashin and Ettensohn 1992). Pashin and Ettensohn (1992) describe intertounguing of black shale and fossiliferous gray shale at the Cleveland-Bedford contact in northeastern Kentucky and suggest ignitive turbidite mud created livable conditions for tracemakers for a narrow amount of time. Unfortunately, the dysaerobic basal section of the Bedford Shale was not exposed in outcrops of this study.

The sparse distribution and low amount of bedding plane bioturbation in both lithofacies indicates that sediment was deposited rapidly during inhospitable conditions. Bedding plane bioturbation in the Bedford-Berea sequence represents times between hyperpycnal events when normal salinity and slow sedimentation conditions prevailed (Bhattacharya, 2006). The medium-bedded siltstones and very fine-grained sandstones from facies A of the lower lithofacies were deposited under higher sedimentation rates and harsher conditions than facies B of the lower lithofacies, based on the lower bedding plane bioturbation index in facies A, thicker beds in facies A and sedimentary structures within the facies.

The upper lithofacies was deposited in a more proximal setting than the lower lithofacies. Conditions in the upper lithofacies were also harsh, with medium to high sedimentation rates and salinity fluctuations commonly occurring due to hyperpycnal and storm events.

Traces within both lithofacies contain: 1) low diversity ichnogenera; 2) simple biogenic structures; 3) suites dominated by a single ichnogenus; 4) diminished size and 5) horizontal ichnofossils that resemble common ichnogenera in the *Cruziana* ichnofacies. These characteristics resemble brackish water assemblages described by Pemberton and Wightman (1992). Thus, the Bedford-Berea sequence contains an impoverished *Cruziana* ichnofacies in the study area. The *Cruziana* ichnofacies is typically found in shallow, marginal marine, moderately oxygenated, sandy substrates.

The Late Devonian period is associated with a series of mass extinction events, which occurred near the Frasnian-Famennian boundary (Kellwasser Event) and Late Famennian (Hangenberg Event); (Morrow and Hasiotis, 2007; Kaiser et al., 2015). Due to the dating of the Alamo impact, the early Frasnian Stage is associated with a series of comet showers (Morrow and Hasiotis, 2007). These comet showers caused late Frasnian mass extinction and induced global cooling during the Famennian (Sandberg, Morrow, and Zieglar 2002). Global cooling during the late Frasnian caused sea level fluctuations which created increased stress on fauna and helped spark the Kellwasser event (Sandberg et al., 2002).

The Kellwasser event is characterized by stepped extinction (Cooper, 2002), which is supported by evidence of the loss of nearly all marine tropical and subtropical species, deterioration of low-latitude reef ecosystems, and a sudden negative shift in global biomass just below the Frasnian-Famennian boundary (McGhee, 1996**;** Morrow and Hasiotis, 2007). Morrow and Hasiotis, (2007) suggested a negative feedback/response for ichnogenera following the Kellwasser event. Nearly all diagnostic characteristics of ichnogenera were greatly reduced during the extinction and recovery phase (Morrow and Hasiotis, 2007). Following the extinction event Gutschick and Rodriguez, (1977, 1979) noted that ichnodiversity remained low until the middle Famennian (*Marginifera* Zone). Thus, fauna may have been recovering as long as 1-3 million years after the event (Morrow and Hasiotis, 2007). Morrow and Sandberg (2008) constructed a detailed breakdown the late Devonian eustatic sea level curve using condonts zones (Figure 45) and showed drastic sea level fluctuations during the latest Devonian.

The Hangenberg crisis occurred during the middle *praesulcata* zone to the middle *sulcata* zone (Figure 46; Kaiser et al., 2015). The event lasted several thousand years as represented by extinctions of different fauna during different times (Kaiser et al., 2015). Kaiser et al., (2015) suggested that the main extinction took place during deposition of the Hangenberg Black Shale, while small extinction events occurred later in the Famennian/Tournaisian (Figure 47). Multiple hypotheses attempt to explain the late Famennian and early Tournaisian environmental changes, which caused the Hangenberg crisis. However, the asteroid impact hypothesis has the most merit based on Bai, Ning, and Orth (1986), Bai, Bai, Ma, Wang, and Sun (1994), and Bai and Ning's (1989) identification of iridium and nickel spikes in Hangenberg sandstone equivalents in south China. In addition, the Woodleigh impact in Western Australia correlates almost perfectly with the Hangenberg Crisis (Glikson, et al., 2005; Kaiser et al., 2015). Overall, the Hangenberg crisis and the Kellwasser event acted together to decimate tracemakers during the Late Devonian and explain the limited diversity and diminutive size of tracemakers in the Bedford-Berea sequence.

Open marine environments are commonly colonized by stenohaline organisms that are sensitive to minimal fluctuations in salinity (Angulo and Buatois, 2011). Since Bedford-Berea sediment was influenced by hyperpycnal events which transport large amounts of sediment and fresh water into the basin (Zavala et al., 2016), salinity and turbidity were frequently fluctuating, increasing stress on organisms. In modern rivers, hyperpycnal events can occur with a frequency of one event every year to one event every 100 years (Zavala et al., 2016). Sedimentation rates during these events are high, limiting the time organisms have to rework the sediment. In addition, the presence of ichnogenera that have been described by Pemberton and Wightman (1992) as being tolerant of brackish-water conditions such as *Palaeophycus*, *Planolites*, and *Thalassinoides*, further support brackish conditions during deposition of the Bedford-Berea sequence.

The lower-middle Mississippian-aged Cowbell Member of the Borden Formation in northeastern Kentucky has been described as a series of delta front deposits comprised largely of distal bar and storm deposits (Kearby, 1971; Mason and Chaplin, 1979; Lierman, Mason, Pashin, and Ettensohn 1992). Despite having a similar depositional environment as the Bedford-Berea sequence, the Cowbell Member displays a vastly more diverse ichnofacies and traces are significantly larger (Table 4). *Planolites* is common in both the Bedford-Berea sequence and the Cowbell Member; however, the diminutive average size of *Planolites* (3.18 mm) in diameter in the Bedford-Berea sequence compared to photos of *Planolites* measuring 1 cm in the Cowbell Member (Chaplin, 1980) illustrates the increased stresses on tracemakers during Bedford-Berea deposition. The vast difference in ichnodiversity and size may reflect the limited recovery of tracemakers from the extinction events taking place during the Frasnian and Fammenian, coupled with salinity fluctuations and high sedimentation rates which created generally inhospitable conditions for tracemakers during Bedford-Berea deposition.

CHAPTER 5

DISCUSSION

Depositional Model

There have been several models proposed for the deposition of the Bedford-Berea sequence in the study area. Pepper et al. (1954) proposed that sediment was initially deposited on shoreline near the West Virginia and Kentucky border; sediment was then reworked by wave and storm currents and transported further onto the shelf to modern day northeastern Kentucky. On the other hand, Rothman (1978) and Potter et al. (1983) suggested that deposition occurred on a shallow marine shelf during a regression. Whereas, Pashin, (1990) and Pashin and Ettensohn, (1995) suggested deposition as ignitive turbidites and tempestite deposits in a shelf/slope setting (Figure 7 and 48). However, the complex sequence of sedimentary structures within the Bedford-Berea unit is not adequately explained by the most recent model. Many beds contain structures that show deposition occurred from long, sustained, fluctuating flows typical of hyperpycnal flows (Figures 25 and 26), rather than purely waning flow typical of ignitive turbidites.

Recently, new research into turbidites, specifically extrabasinal turbidites, has allowed for the distinction between extrabasinal turbidites (hyperpycnal flows) and intrabasinal turbidites based on vertical successions of sedimentary structures (Zavala et al., 2008; Zavala et al., 2011a). Upon close examination the vertical succession of sedimentary structures within the Bedford-Berea sequence are indicative of extrabasinal turbidites. Furthermore, sedimentary structures and sequences within the Bedford-Berea sequence are similar to extrabasinal turbidite deposits of the Merecure Formation in Venezuela, which were deposited in a delta front and prodelta setting described by Zavala et al. (2011b; Figure 49). These similarities indicate that proposed depositional models, even the most recent, do not accurately explain deposition of the Bedford-Berea sequence in the study area. Thus, this study proposes that the Bedford-Berea sequence is made up of wave modified extrabasinal turbidites and tempestites, which were deposited in a prodelta to delta front setting (Figure 50 and 51).

In the Bedford-Berea sequence, the lower lithofacies comprises the lower portion of the sequence and represents the more distal member. As mentioned previously, this lithofacies is composed of interlaminated siltstones and shales and minor medium-bedded siltstones (Figure 10). The lower lithofacies was deposited in a distal delta front to prodelta setting where both extrabasinal turbidite and storm deposition was common. Deposition of very fine-grained sandstone and siltstone occurred above storm-weather wave base where storm currents directly affected deposition. Swift, Han, and Vincent (1986) reported that storm winds are responsible for two main currents on the shelf; the first is a slow-moving unidirectional current, which is a coast-parallel geostrophic flow that results from wind stress on the sea surface, and the second being an oscillatory flow due to wave motion. Geostrophic flows and wave-induced oscillatory flows have been shown to operate together during storms and are identified as the most important currents in sediment transport (Swift et al., 1986; Duke, 1990; Nittrouer and Wright, 1994). In addition, prodelta deposits similar to the Bedford-Berea sequence have shown highly variable levels of bioturbation, depending on sedimentation rates and the influence of brackish water associated with hyperpycnal flows (Bhattacharya, 2006). Thus, the low amount of bedding plane bioturbation within the Bedford-Berea sequence, SSW unidirectional currents and hyperpycnal facies suggest hyperpycnal flows were present. Also, aerobic conditions were present during deposition, which is supported by the presence of wave ripples and shallow water sedimentary structures (Pashin and Ettensohn, 1995). As the general regression continued, the depositional environment shifted to more proximal settings causing more frequent deposition of medium-bedded siltstones (Figure 11).

The upper lithofacies represents the more proximal deposits of the Bedford-Berea sequence and is composed of thick-medium bedded siltstone and sandstones that are commonly separated by thin-bedded siltstone and shales (Figure 11). The upper lithofacies was deposited in a delta front setting. Medium to thick bedded siltstone/sandstones represent extrabasinal turbidites (hyperpycnal flows) while thin bedded siltstone/sandstones and shale beds represent storm deposits during breaks in hyperpycnal events. The hyperpycnal model is supported by the vertical sequences of sedimentary structures, which show wax-wane sequences and eliminate the possibility of Bedford-Berea sediment being deposited on a wave-dominated shoreline where sediment is being reworked from the shoreface. Deposition of this lithofacies occurred in similar, but slightly shallower water depths than the lower lithofacies, occurring between fair-weather and storm-weather wave base. The sparse amount of bioturbation on bedding surfaces indicates rapid deposition and harsh environmental conditions during deposition and the effect of Late Devonian extinctions. The more proximal position of this lithofacies suggests the continuation of a forced regression. However, the top two (2) meters of this lithofacies contain massive sandstone, which may represent a transgressive sand. The upper section is heavily bioturbated (Figure 42), which is unusual in the Bedford-Berea sequence, indicating a long period of non-deposition and contains exotic brachiopods and other invertebrates. Directly above this transgressive sand is the black, anoxic

Sunbury Shale that has a sharp boundary with the Berea Sandstone. The presence of this highly bioturbated zone suggests that near the end of Berea deposition, the regression stopped and gave way to a transgression, allowing prolonged exposure of Berea sands to tracemakers and continuation of the transgression resulted in the deposition of the Sunbury Shale.

The fluvial-deltaic origin of hyperpycnal flows in the Bedford-Berea sequence is supported by fluvial-deltaic deposits in central Ohio, which are within 35 miles of the study area (Tomastik, 1996). Tomastik (1996) identified subsurface fluvial-deltaic channels in a geophysical log (API 3416320883) as far south as Vinton County, Ohio, indicating that fluvial-deltaic systems in Ohio during the Late Devonian may have advanced much further south than previously thought. Coupling this information with paleocurrent information and the knowledge that extrabasinal turbidites can travel hundreds of kilometers as long as discharges are maintained for weeks or months (Zavala et al., 2011a) suggests that Bedford-Berea sediment originated from fluvial-deltaic systems to the north. Furthermore, wave ripple crest orientation (NW-SE) support a northwest-southeast trending paleoshoreline in the study area. The presence of Bedford fluvial/deltaic channels eroding the Cleveland Shale in central Ohio reported by Pepper et al. (1954) suggests a major regressive event took place during Bedford deposition. During this regressive event these fluvial/deltaic systems prograded into the basin and fed submarine channels which were backfilled during the following transgression, explaining the occurrence of Bedford channels which down cut into the Cleveland Shale south of Vanceburg. The presence of fluvial-deltaic channels in central Ohio and southwest oriented paleocurrents suggest that the origin of hyperpycnal flows originated from a northern source.

Delta front environments are often tidal influenced (Bhattacharya, 2006). In the Bedford-Berea sequence, horizontal laminations resembling tidal rhythmites in facies I are sometimes present near the tops of siltstone/sandstone beds (Figure 33B). The presence of potential tidal rhythmites suggests tidal influence on deposition. Even if tidal influence was miniscule, tidal influence has never before been noted within the Bedford-Berea sequence. Furthermore, tides can affect the discharge of rivers. During high tide, river discharge will decrease due to the backing up of the river, and during low tide, river discharge will increase (Bhattacharya, 2006). Since the Bedford-Berea sequence is composed of hyperpycnal events that are directly linked to rivers, tidal sequences could have affected deposition daily and caused fluctuations in discharge. The idea of tidal influence on extrabasinal turbidites (hyperpycnal flows) is relatively new and requires experimental and field research to corroborate it.

In West Virginia, barrier island deposits are common in other Late Devonian sequences. However, the presence of hyperpycnite deposits in the Bedford-Berea sequence suggests that barrier islands were not present at least during hyperpycnite deposition. Furthermore, shoreline and offshore facies associated with barrier island deposits would have had optimal conditions for tracemakers and more ichnodiversity would have have been expected. Barrier islands are also associated with glauconite and shell debris (Selley, 1998) which are not found within the Bedford-Berea sequence.

The Bedford-Berea sequence represents a period of approximately three million years based on biostratigraphy (Gutschick and Sandberg, 1991). Extrabasinal deposits in the Bedford-Berea sequence could represent 10,000-year floods or seasonal deposits that accumulated during rainy seasons which created long-lived discharges. The paleoclimate during deposition of the Bedford-Berea sequence falls within the monsoonal climatic belt (Woodrow et al., 1973; Dennison, 1996) which would favor seasonal deposits. Bhattacharya (2006) reported that the signature of progradation of a delta is a coarsening-upward facies succession. The Bedford-Berea sequence has a coarsening-upward facies succession and shows a transition from a muddier prodelta facies to a sandier delta front facies. Either progradation stopped due to rising sea level causing a transgressive sand to be deposited, or coastal ravinenment occurred during the transgression, which eroded delta plain deposits.

Outcrop to Subsurface Correlation

The correlation subsurface data with outcrops allows for the predicition of lithofacies. In southeastern Ohio, outcrop OH-22 was correlated to Ohio API: 34079202530000 which was the closest well to the outcrop location (Figure 52 and 53). Unfortunately, there are no geophysical well logs in Scioto County, Ohio, which is the county in which OH-22 is located. The lower lithofacies is characterized by an average gamma ray reading of 100 API units and has a serrate well log pattern that is produced by the interbedding of shales and siltstones. In Ohio, API: 34079202530000 the lower lithofacies is approximately 32 feet thick and in outcrop OH-20 it has a thickness of 21 feet.

In Ohio API: 34079202530000 the upper lithofacies is characterized by a relative low gamma ray reading (around 60-75) with a bell-shaped or occasionally funnel-shaped well log pattern at the top of the Bedford-Berea sequence. Below the bell-shaped or funnel funnel-shape pattern, the upper lithofacies has a serrate well log pattern where medium bedded (usually <40cm) sands are separated by siltstones/shales. In southeastern Ohio the resevoir sand is restrictied to the upper 19.7 feet of the Bedford-Berea sequence. The top portion of the upper lithofacies represents the best reservoir rock within the Bedford-Berea sequence. Directly under the upper lithofacies is the lower lithofacies.

In northeastern Kentucky, outcrop 1 and the closest well (KGS record number 9704) were used for an outcrop to well log correlation (Figure 54). The lower lithofacies is characterized by a serrate well log pattern that ranges between 80 and 100 API gamma units and is around 50 feet thick suggesting that only a portion (18ft) of the lower lithofacies is exposed in outcrop 1.

The upper lithofacies is much thicker both in outcrop and subsurface in northeastern Kentucky than in southeastern Ohio. Outcrop 1 contains around 52 feet of the upper lithofacies and KGS record number 9704 which is just to the east of the outcrop contains approximately 50 feet. Similar to southern Ohio, the best reservoir rock is concentrated at the top of the upper lithofacies; however other pay zones are also common throughout the upper and middle section of the Bedford-Berea sequence. The upper lithofacies is dominated by a serrate well log pattern; however, bell-shaped patterns up to 12 feet thick are present in logs (Figure 54, blue arrow). Furthermore, the distribution of the reservoir sand produces multiple pay zones that may be hydraulically isolated.

Sequence Stratigraphy

Sequence Model for Northeastern Kentucky

In geophysical logs, system tracts can be identified based upon log signatures (Figure 55; Rider, 1996; Plint and Nummedal, 2000; Catuneanu, 2002). Conodont zones were used to precisely determine the timing of deposition of the Bedford-Berea sequence. Conodonts identified by Streel and Traverse (1978) from the basal section of the Bedford Shale near Cleveland, Ohio include *Branmehla fissilis, Branmehla culminidirectus, Bispathodus aculeatus anteposicornis,* and possibly a broken fragment of *Siphonodella praesulcata*. Gutschick and Sandberg (1991) suggested that the fauna is comparable to conodonts in the upper zone of the Saverton Shale or basal portion of the Louisiana Limestone in southern Illinois, which is dated as upper *expansa* or lower *praesulcata* Zone (Figure 45). Moreover, correlation of the Bedford-Berea sequence suggests that accumulation occurred during the IIf cycle within the Devonian sea-level curve (Figure 45) (Johnson, Klapper, and Sandberg 1985**;** Johnson, Klapper, Murphy, and Trojan 1986**;** and Johnson and Sandberg, 1989). The eustatic sea level curve shows a eustatic sea level rise in the Upper *expansa* zone and a eustatic fall which coincides with the Hangenberg Event (Kaiser et al., 2015) in the middle *praesulcata* Zone (Sandberg, 1988). Thus, the Bedford Shale falls within the Upper *expansa* to Lower *praesulcata* Zone and the Berea sandstone in the middle to Upper *praesulcata* Zone (Gutschick and Sandberg, 1991). The deposition of the Sunbury Shale marks the beginning of the Mississippian and a transgressive system tract.

In the study area, it is possible to identify two cyclic episodes of transgression and regression within the Bedford-Berea sequence. One autocyclic regression in the Upper *expansa* zone was produced by local influences on sea level and is not represented in the eustatic sea level curve for the Late Devonian. The second regression within the Bedford-Berea sequence appears to be a third order cycle. Plint (2010) suggested that third order cycles represent relatively short-term sea-level changes (1 m to 10 million years) that are produced by several events: (i) continental ice sheets; (ii) tectonism and volcanism; and (iii) spreading and subduction. Bedford-Berea deposition occurred in approximately three million years. The forced regression inferred for the Bedford-Berea sequence by Pashin and Ettensohn (1995) requires a rapid fall in eustatic sea level. Recent evidence suggests that the forcing mechanism of the Bedford-Berea lowstand was glaciation related to a series of comet showers and impacts occurring near the Frasnian-Famennian boundary that induced global cooling (Sandberg et al., 2002). Furthermore, Caputo, de Melo, Streel, and Isbell (2008) presented evidence for Late Devonian glaciation in South America and suggested that these events were large enough to result in eustatic sea level fluctuations. Moreover, Ettensohn et al. (2009) identified a dropstone at the top of the Cleveland Shale near Morehead, Kentucky suggesting that a eustatic fall in sea level from glaciation was occurring near the end or directly following deposition of the Cleveland Shale. Using combined data collected from trace fossils and facies architecture it is possible to tentatively define depositional sequences within the Bedford-Berea stratigraphic section.

The geophysical logs combined with outcrop data from northeastern Kentucky appear to show two regressions, one associated with local sea level changes $FSST_1$ and one eustatic event $FSST_2$ (Figure 56 and Figure 57). A maximum flooding surface occurs at the top of the anoxic Cleveland Shale and indicates the boundary between the transgressive systems tract TST_1 and the highstand systems tract HST_1. The basal portion of the Bedford Formation has been interpreted as being deposited in dysaerobic conditions due to the presence of thin-shelled, brachiopod-molluscs (Pashin and Ettensohn, 1992). The absence of these brachiopods past the basal portion of the Bedford Formation indicate shallowing during the highstand systems tract. The falling-stage system tract $FSST_1$ reflects the onset of a forced regression caused by glaciation. Forced regression is supported by a rapid transition from dysaerobic conditions to aerobic conditions suggested by abundant wave ripples in northeastern Kentucky. The lowstand system tract LST_1 directly overlies the $FSST_1$. The lowstand system tract LST_1 is associated with fluvial/deltaic channels in the Red Bedford Delta associated with the Ontario River (Figure 4) in Ohio, which created a complex network of channels in the region described by Pepper et al. (1954) and could explain the channel facies at location 3. Fluvial-deltaic channels in central Ohio advanced as far south as Vinton County (Tomastik, 1996). Thus, the channel facies may represent a submarine channel event, which caused incision of submarine channels SB_1 associated with a shelf edge delta of the Ontario River to form in the study area due to increased proximity to fluvial-deltaic channels (Figure 4). The submarine channels were then backfilled during the late lowstand systems tract LST_2 (Figure 56).

Following the lowstand systems tract, the peak of the transgressive systems tract TST_2 is represented by an increased gamma ray reading marking the maximum flooding surface and the top of the transgressive systems tract. In gamma ray logs, this surface is traceable in northeastern Kentucky. However, the maximum flooding surface gamma ray kick can be subtle or removed due to the erosion of this layer during the advance of submarine channels during a subsequent episode of incision. The maximum flooding surface represents the maximum water depth at the beginning of sea level highstand and highest organic content of the shale. Unfortunately, this event is not recognized in the outcrops of this study. The highstand system tract HST_2 is placed directly above the maximum flooding surface and is associated with a regression, as supported by shallowing upward facies and coarsening upward grain size.

A falling-stage system tract $FSST_2$ directly overlies the highstand system tract is suggested regionally by a system of sand-filled Berea channels SB_2 in northern Ohio that lie above Bedford channel sands and in some places are separated by red shale described by Pepper et al. (1954). In the study area, the falling-stage system tract $FSST_2$ is masked; this is caused by the more basinward position; sea level did not drop enough to create fluvial-deltaic channels typical of a falling-stage system tract in the study area.

Finally, a transgressive systems tract TST_3 deposited the upper 30-40 cm of the Berea Sandstone which represents a transgressive sand and the black, anoxic, Sunbury Shale directly on top of the regressive Berea Sandstone. In outcrop, the top 30-40 cm of Berea Sandstone is dominated by medium to thick-bedded massive sandstones, and at locality 2 (Garrison, Kentucky) the Berea sandstone is heavily bioturbated 30 cm below the Sunbury (Figure 42). The intense bioturbation suggests a period of prolonged non-deposition which allowed tracemakers to heavily rework sediment. At locality 22 (near Friendship, Ohio) brachiopods are present at the top of the Berea Sandstone (discovered by Dr. Martino) at its contact with the Sunbury Shale. The brachiopods are size-sorted and reworked indicating they were not related to the depositional environment of the Berea Sandstone, but were exotic.

This sequence stratigraphy model is based upon outcrop observations, gamma ray logs and eustatic sea level curves during the Late Devonian, which show two regressions separated by a transgressive event (Figs. 45 and 57). The regressive hypothesis supports Pepper et al. (1954) and Pashin and Ettensohn's (1995) theories of two episodes of regression in Bedford-Berea sequence regionally in northern Ohio, based on erosion of the Chagrin Shale and Cleveland Member by the Second Berea fluvial system in northern Ohio. In outcrop, the upper lithofacies is composed of thicker beds and sedimentary structures, such as swaley cross-stratification and scours, which suggest the second regression was more substantial than the first regression and is supported by eustatic sea level curves for the Late Devonian (Figure 45).

Reservoir Modeling

Structural Trends

There are several faults within the study area, the most significant being the Kentucky River Fault (Figure 58). The structure countour map of the Bedford-Berea interval shows a regional southeast dip direction in northern Kentucky and southeastern Ohio (Figure 59). In southwestern Lawrence county, Kentucky, one limb of the Hood Creek Anticline (red arrow) can be recognized which is associated with the Paint Creek Uplift (red circle). The Hood Creek anticline continues into southeastern Morgan and northwestern Johnson Counties (Hudnall and Browning, 1924; Drahovzal and Noger, 1995). However, due to parts of the structure lying outside of the study area a portion of this structure is masked in Morgan and Johnson Counties in figure 56. The Hood Creek anticline is an eastward pluning fold, which has locally contributed to oil and gas accumulation in the area. It is important to note that well spacing of this study is constrained enough for regional structure interpretation; however, does not allow for local structure interpretation.

Thickness Trends

The Bedford-Berea isopach map shows a defined north-south oriented trend in northeastern Kentucky; however, in southern Ohio the thickness trend appears to be northeast-southwest oriented (Figure 60). Geologic quadrangle maps were used in northeastern Kentucky to further supplement subsurface information where well data were limited. The additional data points are indicated by red squares. The isopach map is similar to that of Pepper et al. (1954), which shows a north-south trend of maximum thickness for the Bedford-Berea section in northeastern Kentucky and southeastern Ohio. Pepper et al. (1954) also noted a thick Bedford-Berea sequence in Scioto County, Ohio. The Bedford-Berea sequence in Scioto County is likely similar in thickness to surrounding counties but is not as thickened as the extrapolated isopach maps suggests. Limited well control in Scioto County causes extrapolation and the Bedford-Berea sequence isopach may not accurately represent its true thickness in the county.

The Bedford-Berea isopach map shows a north-south, linear thickness trend in northeastern Kentucky, that extends from Lewis County, Kentucky to Morgan County, Kentucky. Floyd (2015) further mapped the Bedford-Berea sequence from Lewis County, Kentucky to Pike and Letcher Counties and suggested the north-south thickness trend extends to Pike and Letcher Counties. The thickest Berea net sand occurs in the northeastern part of Kentucky in Lewis, Greenup, and Carter Counties with net sands ranging from 80-110 feet thick. Moving off of the flanks of the north-south thickness trend the net sand interval thins from 50 feet to 25 feet (Figure 60).

A net Berea sand iospach map was constructed using a gamma-ray cutoff of 101 API units (Figure 61). Unfortunately, the 101 API cut-off for net sand within the Bedford-Berea sequence was not accurate in southern Ohio, as a majority of logs chosen for this study showed gamma-ray values lower than 101 API units for the entire Bedford-Berea sequence. In northeastern Kentucky the Bedford Shale is distinguished by a gamma ray reading greater than 101 API units; however, the Bedford Shale in southeastern Ohio typically has a gamma ray reading less than 101. Thus, the classification method for the differentiation of the Bedford-Berea in northeastern Kentucky is not consistent with that used in southeastern Ohio.

The Bedford-Berea sequence is thickest in northeastern Kentucky, north of the Kentucky River Fault system, in Lewis and Greenup Counties. Floyd (2015) reported that the thickest Bedford-Berea sequence occurs on a structural high and the Bedford-Berea sequence is locally thin in the structural low above the Rome Trough. Floyd (2015) suggested two explanations for a thickened Bedford-Berea sequence on structural highs: 1) post-depositional compaction of intervals shale in the structural lows relative to siltstones and sandstone on structural highs; and 2) decreasing sedimentation from the north to the south due to greater distance from a northern source and local increase in thickness to the south due to an eastern sediment source. However, the latter explanation does not account for the Bedford-Berea sequence thickness anomaly, due to paleocurrents (which are oriented southwest) and sequences of sedimentary structures that suggest sediment was being derived from a northern source through hyperpycnal flows and storm deposits (at least for the outcrop belt). Furthermore, there is no evidence (paleocurrents, etc.) of an eastern source contributing sediment to northeastern Kentucky or southeastern Ohio in outcrop.

Reservoir Analysis

Locations of Bedford-Berea oil and gas fields within the study area are shown in figure 62. In northeastern Kentucky and southeastern Ohio, the Bedford-Berea sequence commonly contains multiple pay intervals. The most prolific zones occur at the top of the Berea Sandstone where pay sands are thicker (8-16 feet) and have porosity ranges of 8-14% and a relatively low permeability of around .01 millidarcies (Figs. 63, 64 and 65). The pay zones in the middle and lower part of the Bedford-Berea sequence are rarely targeted due to the limited thicknesses. Reservoir sands in the Bedford-Berea sequence are often affected by large soft sediment deformation structures within the upper lithofacies; however, these structures do not persist over large lateral distances (500 ft) and are not associated with one bed in particular (Figure 11, red arrows).

The Bedford-Berea sequence is dominated by three well logs patterns: (i) a serrate pattern associated with interbedded siltstones and sandstones; (ii) a bell-shaped pattern; and (iii) a funnel pattern. Both bell-shaped and funnel patterns are associated with reservoirs within the Bedford-Berea sequence. Outcrop to well log correlations suggest that serrate well log patterns are usually composed of facies J, and facies assemblages A-B and C-I where beds do not exceed 40 cm thick (Figs. 66, 67 and 68). Bell-shaped patterns, which are associated with submarine channels usually occur at the bottom of the Bedford-Berea sequence (Figure 64) and are up to 30 feet thick. Smaller 3 to 6 foot bell-shaped signatures occur within the middle of the sequence and may represent small submarine channels (Figure 64).

The Bedford-Berea reservoir package in central Ohio only contains a single reservoir sand, which in some cases is almost 25 feet thick and has a funnel shaped gamma ray pattern (Figure 65). The single reservoir sand is unlike reservoirs in northeastern Kentucky, which typically have multiple pay zones. Although this pay zone is thick, the overall gross pay within the Bedford-Berea sequence is thinner in central Ohio than in southernmost Ohio and northeastern Kentucky due to the absence of multiple zones. Based on geophysical logs in this study, the pay sand averages around 20 feet thick, has a porosity ranging from 8-14 percent and has the classic low permeability that is common with Berea reservoirs.

The net pay sand map (Figure 69) is based on sandstone and siltstone within the Bedford-Berea sequence which has porosity greater than 8 percent. The low porosity limit was selected due to horizontal drilling and hydraulic fracturing techniques that allow for oil extraction from this unit. The thickest pay sand in northeastern Kentucky (60 ft) occurs in Greenup County. Just north of Greenup County the pay sand thins, until eastern Vinton County, Ohio where a dramatic thickness increase occurs due to the presence of a fluvial/deltaic channel within the Bedford-Berea sequence (Tomastik, 1996). The pay sand, which has greater than 8% porosity, exceeds 150 feet in thickness. In northeastern Kentucky, the net pay sand thins southward and is thinnest within the study area in southern Lawrence County, Kentucky.

Based on geophysical logs, the Bedford-Berea sequence is on average 120 feet thick within the study area, reaching a maximum thickness of 160 feet in northeastern Kentucky. Facies assemblage C-I within the upper lithofacies has the best reservoir potential based on its medium to thick-bedded siltstone/very-fine sandstone composition. Thin shale beds separating thicker siltstone/sandstone beds are common throughout the upper and lower lithofacies and compartmentalize reservoirs (Olariu, Streel, and Petter 2010). Lateral changes in the form of both facies and diagenetic changes capture hydrocarbons in the Berea Sandstone; however, the majority of lateral changes are related to diagenetic changes and the formation of secondary porosity. Thus, the primary trapping mechanism in the Bedford-Berea play is stratigraphic as previously suggested by Larese (1974), Warner (1978), Mele (1981), Cox (1992) and Tomastik (1996). However, both depositional and structural features influence hydrocarbon accumulation due to local combination traps (Larese, 1974; Coogan and Wells, 1992; Cox, 1992; Nolde and Milici, 1993; Tomastik, 1996) and is evident in figure 56, where the presence of a local anticlinal feature enhances the accumulation of oil and gas and represents a combination trap.

The Ashland Gas Field is located in Boyd County, Kentucky (Tomastik, 1996). The driving mechanism for hydrocarbon accumulation in this field is a stratigraphic trap. The consistency of gamma ray signatures both inside and outside of the field suggests diagenetic changes altered porosity and permeability within reservoir rock. Thus, lateral diagenetic changes caused the accumulation of gas within this field (Tomastik, 1996; Figs. 70, 71 and 72). However, other oil and gas fields in the Berea Sandstone may be driven by facies changes, or a combination of facies and diagenetic changes. The uppermost pay (most prolific pay) within the Berea Sandstone does thin laterally, moving away from the Ashland Gas Field. Tomastik (1996) suggested a diagenetic stratigraphic trap produces accumulation of hydrocarbons in the Ashland Gas Field, where porosity and permeability are lost laterally. Currently, operators are targeting the edges of these fields with hydraulic fracturing, and horizontal drilling techniques are successfully producing commercial quantities of oil and gas.

CHAPTER 6

SUMMARY AND CONCLUSION

1) The Bedford-Berea units in northeastern Kentucky and southeastern Ohio represents a wave dominated prograding prodelta and delta front sequence, with two overall coarsening-upward facies successions that show a transition from muddier facies of the prodelta to sandier facies of the delta front. The coarsening-upward sequences within the Bedford-Berea sequence represent two regressive episodes. The first transgressive-regressive cycle during the deposition of the Bedford Shale represents an autocyclic event that is not represented in the eustatic sea level curve. The second cycle represents an allocylic event that was caused due to Southern Hemisphere glacial-interglacial episodes (Matchen and Kammer, 2006).
2) The Bedford-Berea sequence is composed of hyperpycnal and storm deposits. The presence of facies I, which corresponds to the "lofting facies" of Zavala et al. (2011a) and associated hyperpycnal facies, suggests that long-lived turbulent flows were present during the deposition of the Bedford-Berea sequence. Many beds within the Bedford-Berea sequence contain sedimentary structures created by wane-wax-wane flows associated with hyperpycnal flows (Zavala et al., 2008). Paleocurrent measurements throughout the Bedford-Berea sequence were unidirectional (SSW) parallel to paleoslope indicating formation as extrabasinal turbidites supporting a hyperpycnal model. The presence of wave ripple crests on the top of hyperpycnal beds suggests that wave modification of beds took place following initial deposition. Wave ripple crests are oriented NW-SE suggesting a NW-SE oriented paleoshoreline

which is perpendicular to the previously interpreted NE-SW oriented paleoshoreline of Pepper et al. (1954) and Pashin and Ettensohn (1995) in the study area. The abundance of siltstone and very fine grained sandstone with combined flow structures, such as hummocky cross-stratification, combined flow ripples, wave ripple crests and swaley cross-stratification represent tempestite deposits.

3) Unidirectional paleocurrents are dominated by a SSW trend, suggesting that fluvial and deltaic channels brought sediment from the NNE into the basin. The presence of fluvial and deltaic channels in southeastern Ohio and southwest-trending paleocurrents coupled with south-southwest directed paleoslope controls on hyperpycnal flows explains the general north-south/northeast-southwest thickness trend within the Bedford-Berea sequence in northeastern Kentucky and southeastern Ohio.

4) Two hypotheses have been presented for deposition of facies K at locality 3 (Channel Outcrop): 1) facies K represents a submarine channel deposit that was deposited in the upper fan on the edge of the transition zone between the shelf and slope. However, an issue with this idea is that coarse sand and gravel typical of the lower portion of an erosional submarine channel fill are absent. The second hypothesis is that facies K represents an incised valley fill (IVF) which was backfilled under marine influence during a transgressive event. The issue with this explanation is that basal-fluvial and estuarine deposits, which are typical of transgressive backfilled IVF deposits, are absent.

5) Ichnodiversity within the Bedford-Berea sequence is relatively low, but higher than previously thought. Traces within the sequence are small, ranging from 5 mm-1 cm in diameter and only occasionally exceed 1 cm in size. The low bedding plane bioturbation index (1-3) throughout the majority of the Bedford-Berea sequence in the study area indicates a stressed environment during deposition. Traces such as *Planolites, Palaeophycus, Lophoctenium, Thalassinoides,* and horizontal burrows (*Nereites, Neonereites, and Scalarituba)* and sparse *Chondrites* in the Bedford-Berea sequence represent an impoverished *Cruziana* ichnofacies. The trace fossil assemblage found in the Bedford-Berea sequence is consistent with deposition in a brackish water environment and resembles brackish assemblages described by Pemberton and Wightman (1992). The low bedding plane bioturbation prevails with the exception of the upper one meter of Berea Sandstone, which has a high bioturbation index at locality KY-2 and indicates slow depositional rates and better ecological conditions associated with the Sunbury transgression and may represent a transgressive sand.
6) The diminutive size and limited ichnodiversity of ichnofacies within the Bedford-Berea sequence is due to two factors, (i) a negative feedback response following the Kellwasser and Hangenberg mass extinction events in the study area, and (ii) brackish water conditions and high turbidity rates during deposition of hyperpycnal flows. Brackish water conditions and high turbidity rates were local stressors while the Hangenberg and Kellwasser events were global stressors.

7) The Bedford-Berea sequence was deposited by two forced regressions due to Late Devonian. The two forced regressions are supported by Bedford fluvial/deltaic channels present in central Ohio that incise into the Cleveland Shale and Berea fluvial/deltaic channels which are incised into the Bedford and are sometimes separated by the Red Bedford Shale (Pepper et al., 1954). In northeastern Kentucky and southeastern Ohio, which was more basinward than central Ohio, submarine channels were cut and filled in the falling stage/lowstand system tracts near the base of the Bedford-Berea sequence. These channels were then backfilled during the early (Transgressive systems tract TST) that followed and are recognized in the subsurface of northeastern Kentucky.

8) One limb of the Hood Creek Anticline is recognizable in southern Lawrence County, Kentucky. The Hood Creek Anticline has locally contributed to the accumulation of hydrocarbons in the area within the Bedford-Berea sequence. A north-south Bedford-Berea thickness trend dominates in northeastern Kentucky; however, in southern Ohio, a thickness trend is less apparent and maybe more NE-SW oriented.

9) Facies assemblage C-I within the upper lithofacies of the Bedford-Berea sequence represents the best reservoir sands in both northeastern Kentucky and southeastern Ohio. In northeastern Kentucky, the distribution of facies assemblage C-I and facies J produces multiple pay zones that are separated by thin shales acting as flow barriers. In Kentucky, stratigraphic traps are the main accumulators of hydrocarbons; however structural traps influence accumulation locally. In southeastern Ohio, a single pay zone is present at the top of the Bedford-Berea

sequence with the occasional presence of a second pay zone near the bottom of the sequence.

FIGURES

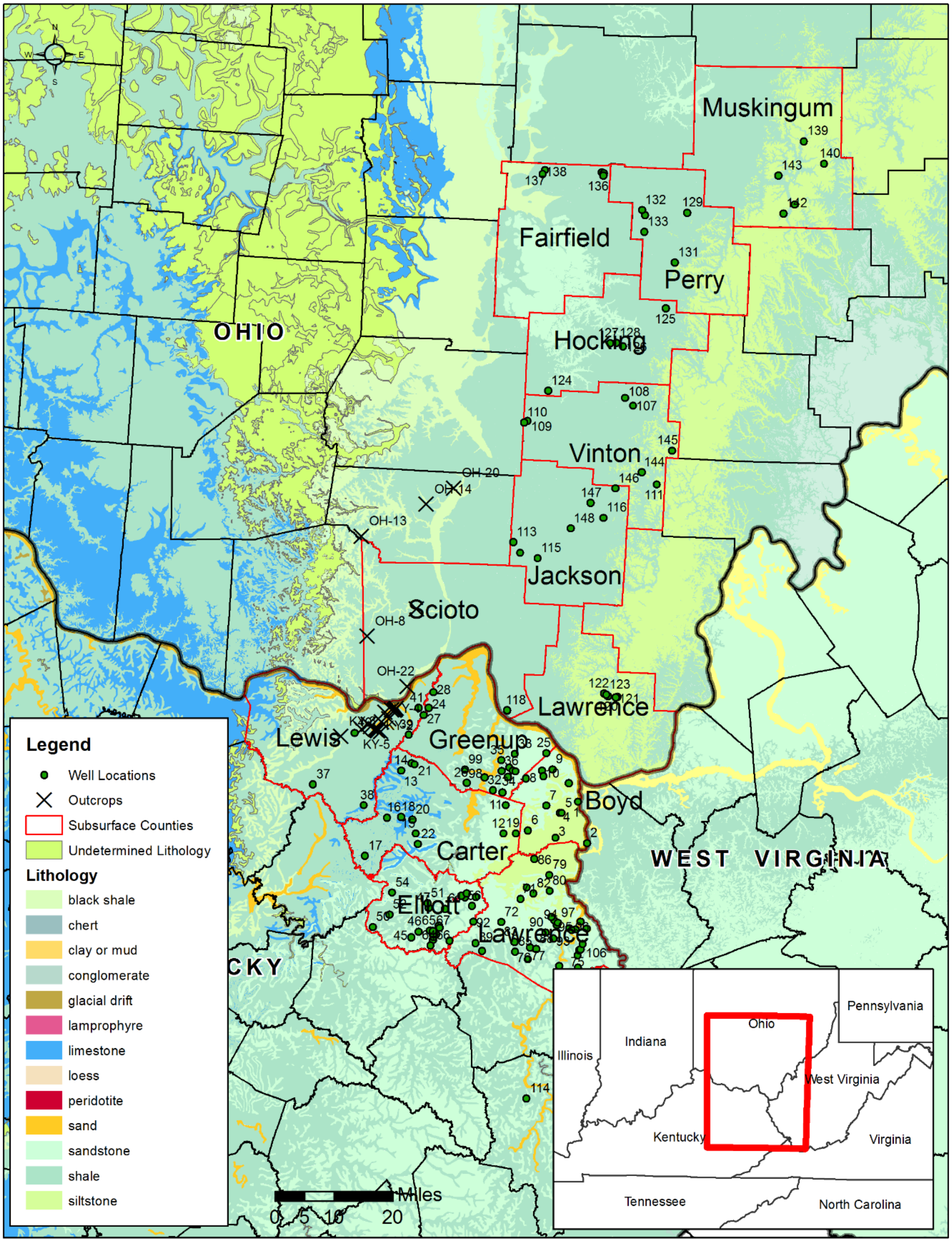

Figure 1. Location of outcrops and well locations included in this study.

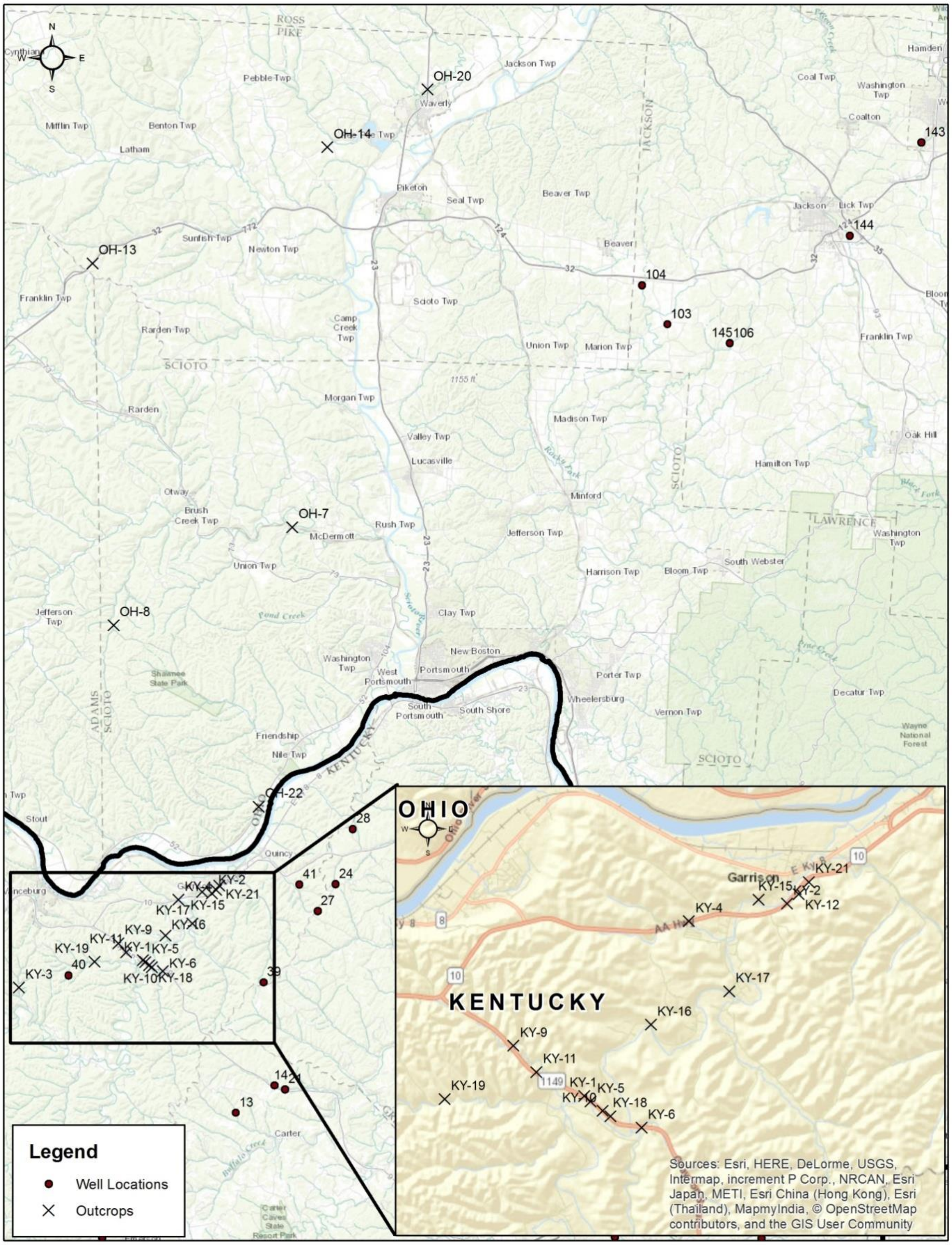

Figure 2. Location of outcrops in northeastern Kentucky and southeastern Ohio.

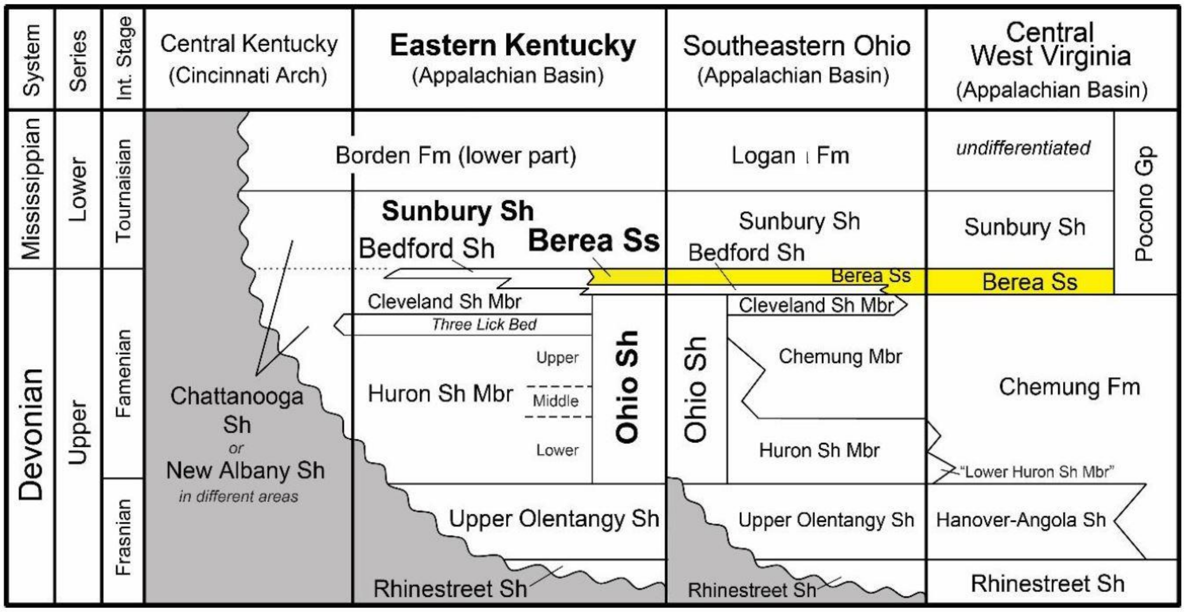

Figure 3. Upper Devonian-Lower Mississippian stratigraphic framework in eastern Kentucky (from Harris, 2014).

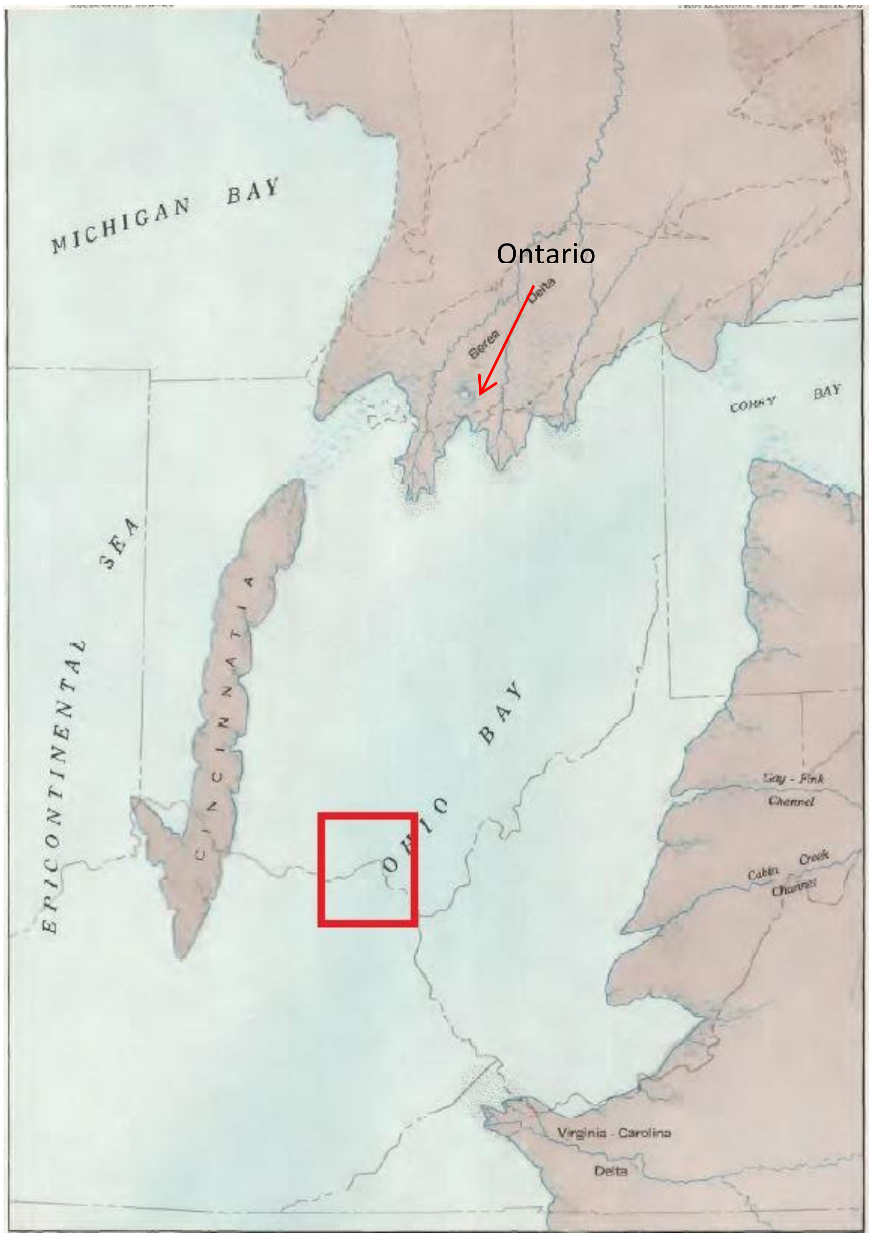

Figure 4. Paleogeography during the Late Devonian during deposition of the Berea Sandstone (modified from Pepper et al., 1954). The red box indicates the outcrop study area and the red arrow indicates the flow of the Ontario River (Pepper et al., 1954).

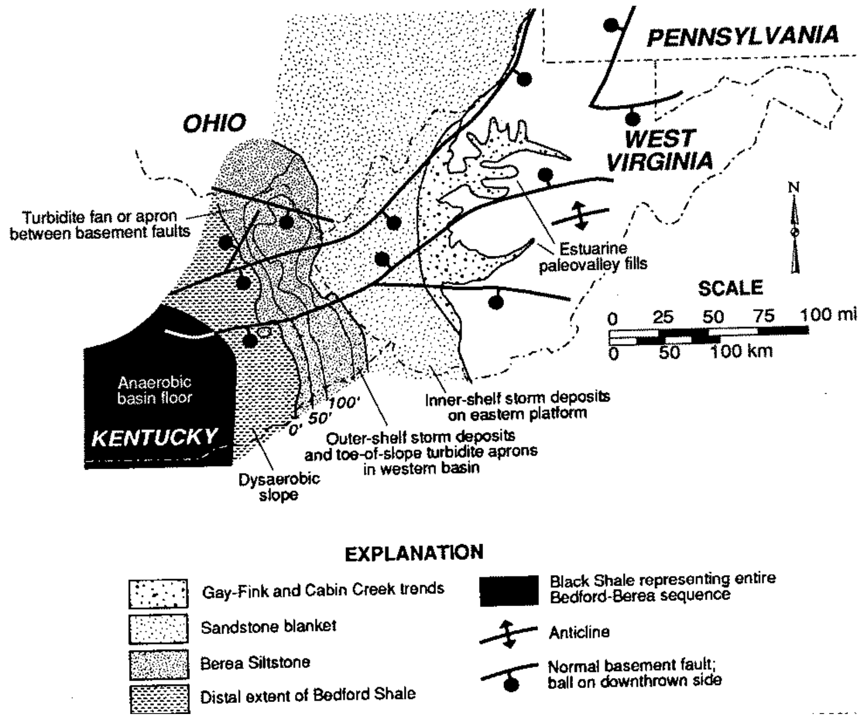

Figure 5. Paleogeography for the Bedford-Berea sequence in and near the study area (from Pashin and Ettensohn, 1995).

Bedford-Berea sequence in Ohio and adjacent states 15

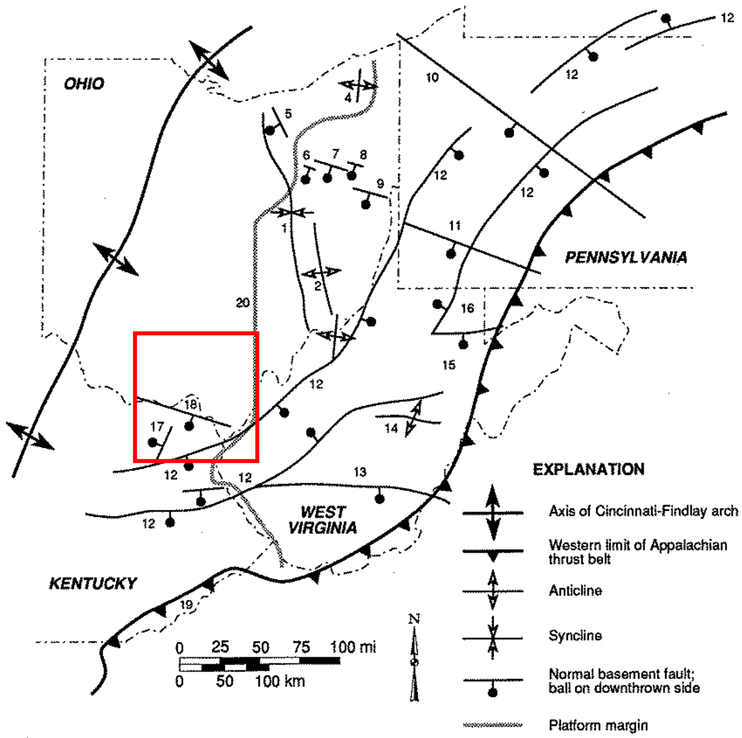

STRUCTURES OF THE NORTHERN APPALACHIAN BASIN			
1	Parkersburg-Lorain syncline	11	Transylvania fault
2	Cambridge arch	12	Rome Trough basement-fault systems
3	Burning Springs anticline	13	Warfield fault
4	Ashtabula anticline	14	West Virginia dome
5	Middleburg fault	15	Cross-over rift
6	Akron fault	16	Tri-state block
7	Suffield fault	17	Waverly arch basement fault
8	Smith Township fault	18	Vanceburg-Ironton fault
9	Highlandtown fault	19	Pine Mountain thrust
10	Tyrone-Mount Union lineament	20	Bedford-Berea platform margin

Figure 6. Major tectonic structures in the Appalachian Basin that affected deposition on the Bedford-Berea sequence (modified Pashin and Ettensohn, 1995).

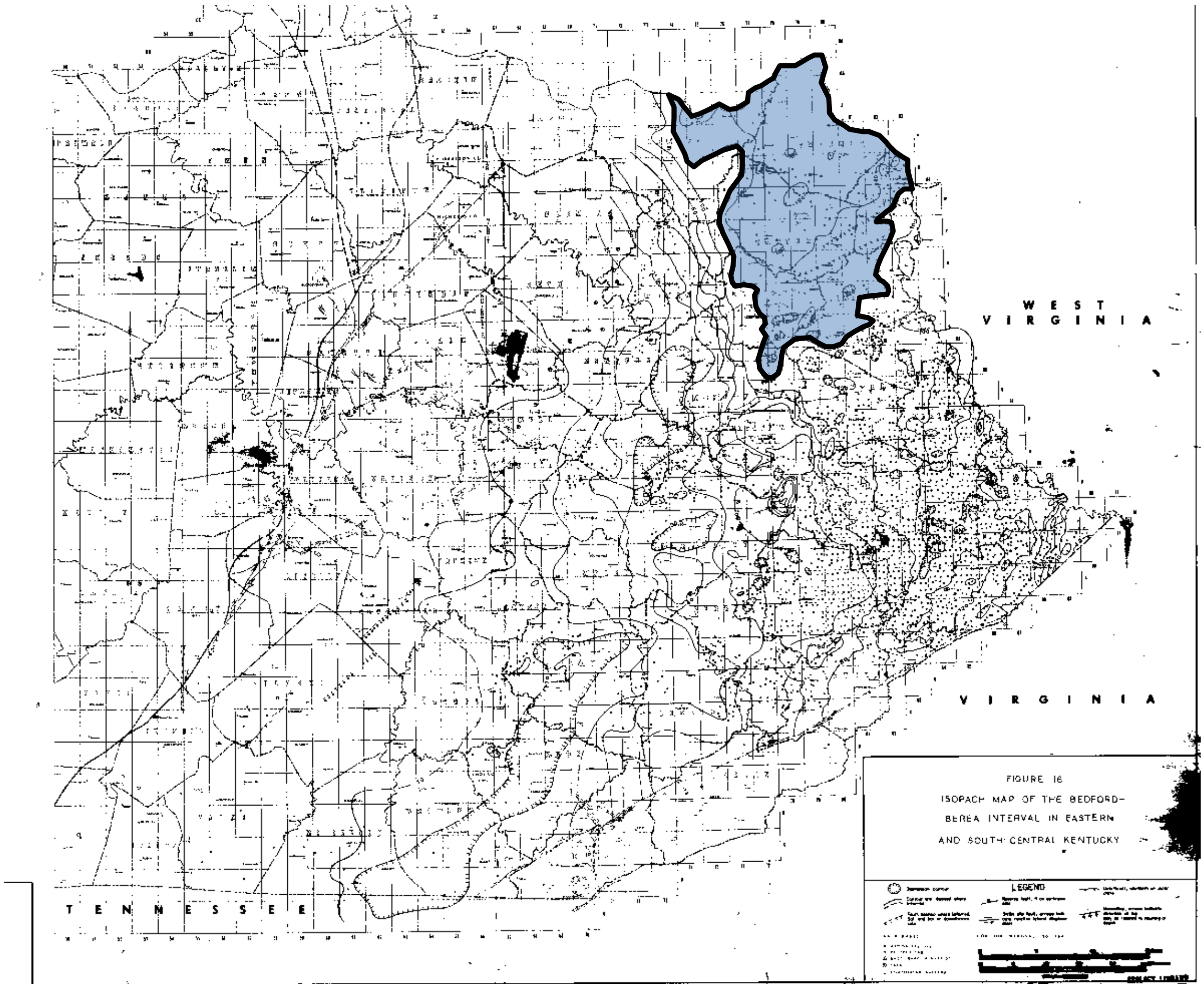

Figure 7. Isopach map of the Bedford-Berea interval in eastern and south-central Kentucky (Elam, 1981). A thickened Bedford-Berea sequence has a north-south trend and is bounded by areas of thin clastics to the east and west (Elam, 1981). The black line represents the 120 foot isopach line for the Bedford-Berea sequence and the blue polygon represents thickness in excess of 120 foot.

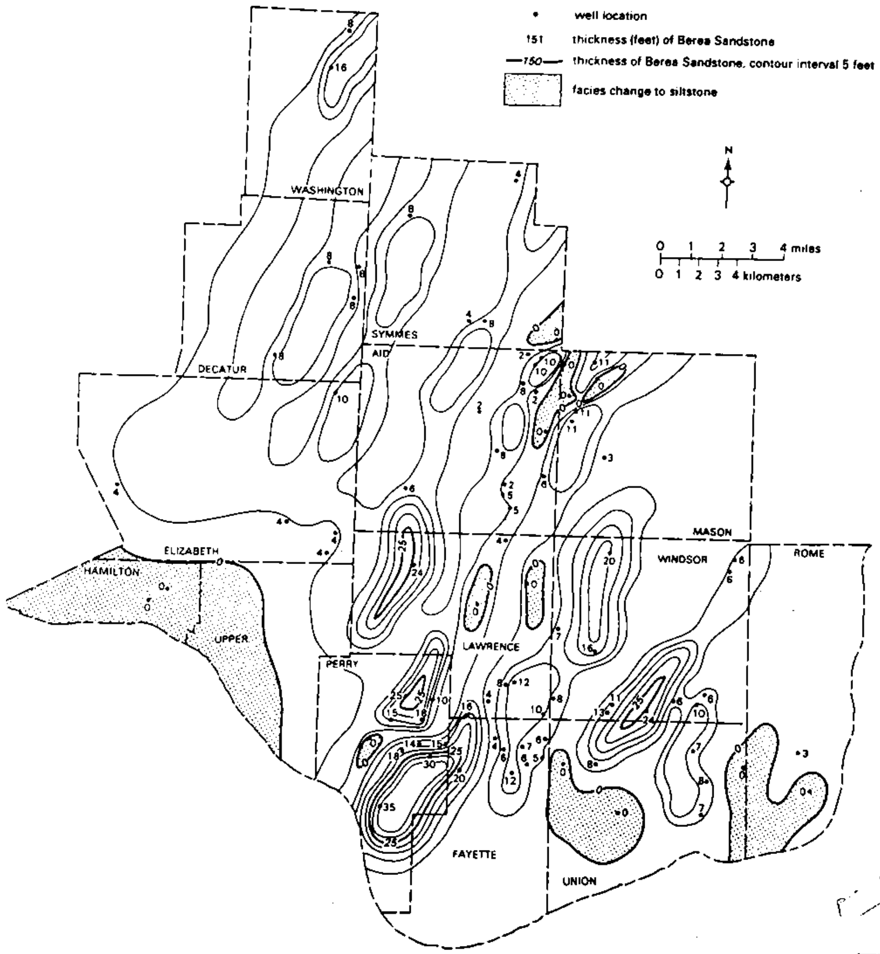

Figure 8. Isopach map of the Berea sandstone in Athens County, Ohio (Riley and Baranoski, 1988). Northeast-southwest elongate sand bodies were interpreted as offshore silty sand bars (Riley and Baranoski, 1988).

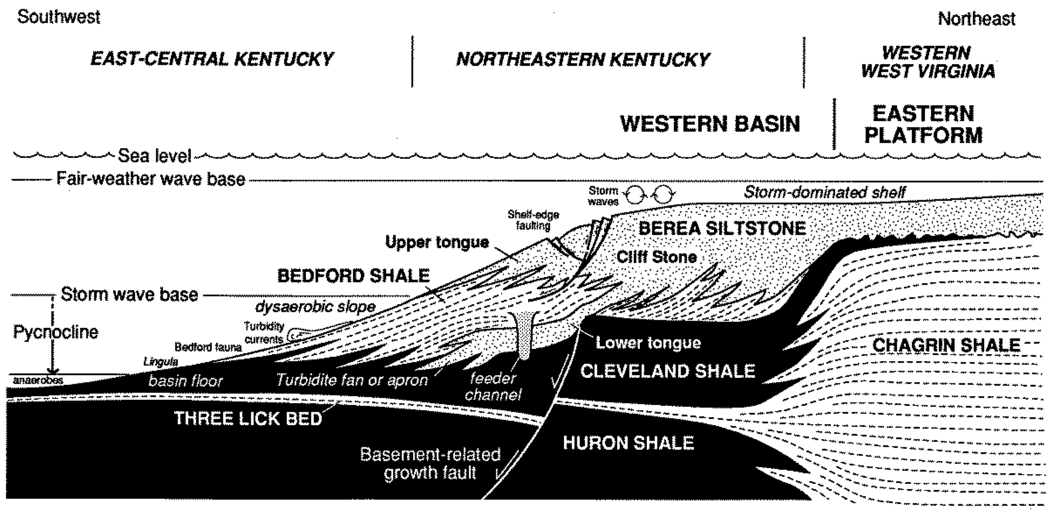

Figure 9. The interpreted depositional model for the Bedford-Berea sequence in and around the study area (from Pashin and Ettensohn, 1995).

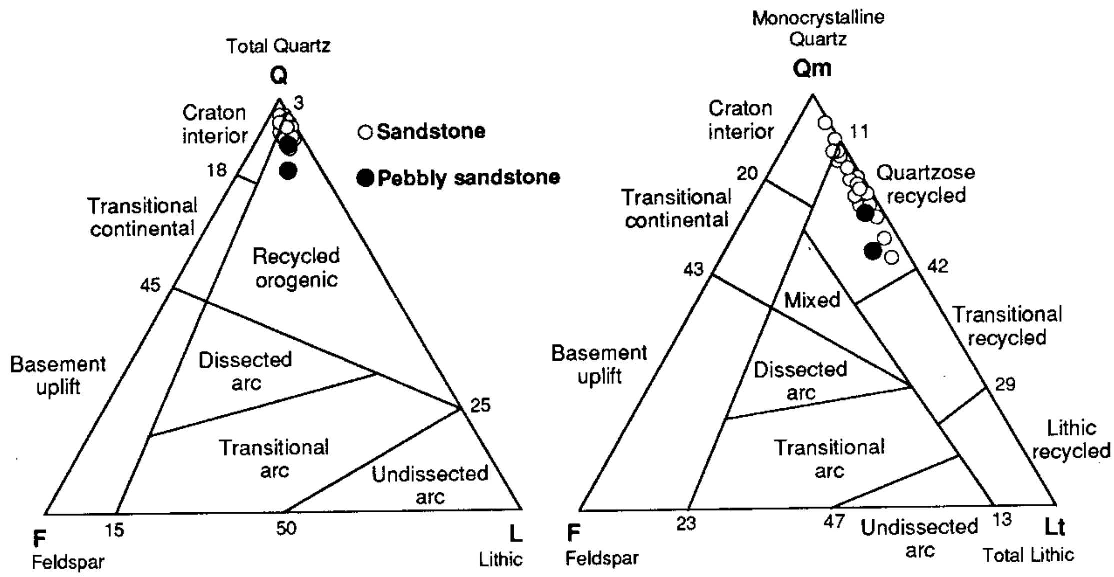

Figure 10. QFL and Qm-F-L plots of the Bedford-Berea sequence (Pashin and Ettensohn, 1995). The QFL plots on the boundary of craton interior and recycled orogen provenances and the Qm-F-L plots on the border of craton interior and quartzose recycled orogen provenance and could be due to the Ontario River deriving sediments from both sources.

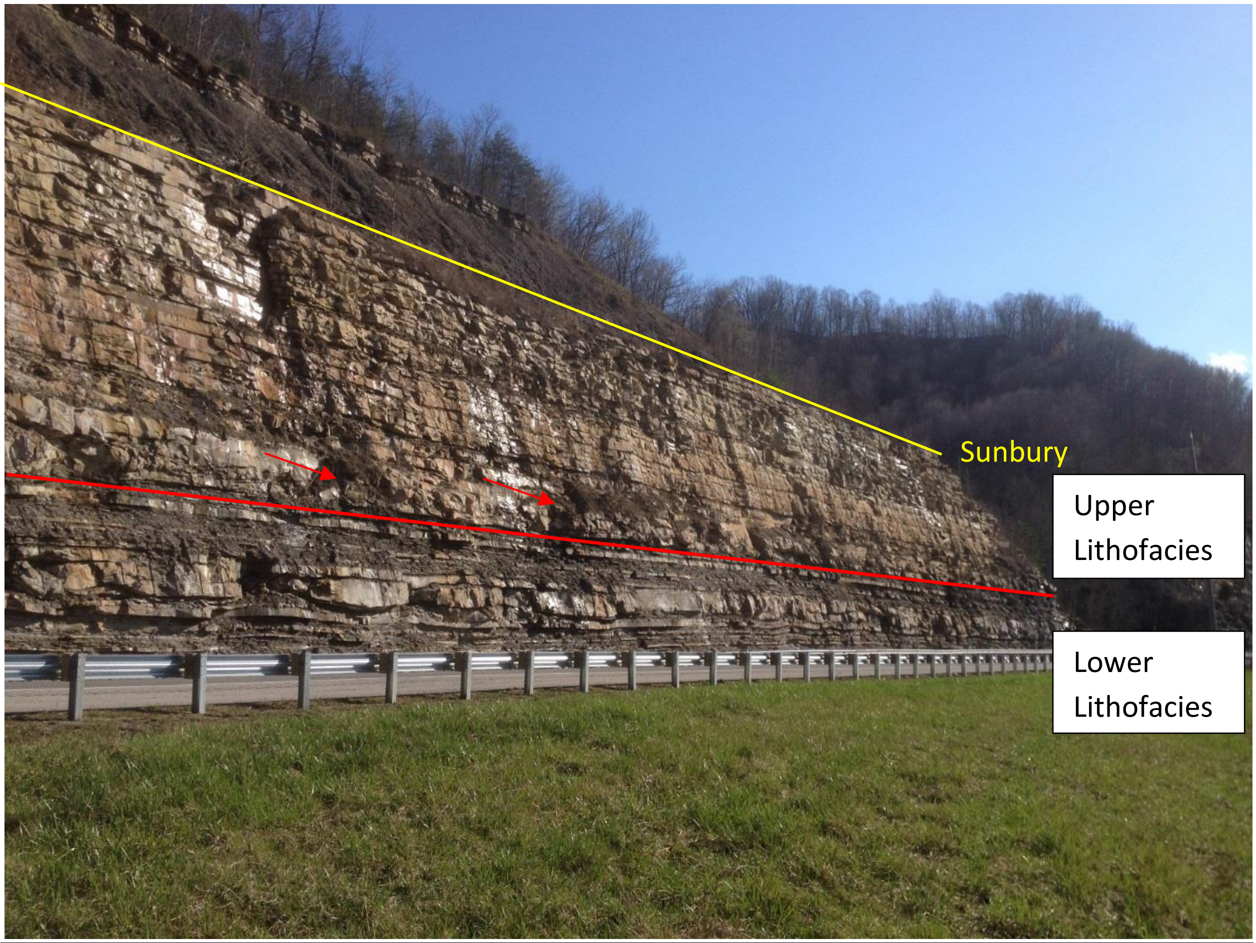

Figure 11. Locality 12 near Garrison, Kentucky, illustrating the separation of the lower and upper lithofacies. The lower lithofacies is dominated by interlaminated siltstones and shales and subordinate medium-bedded siltstones. The upper lithofacies is dominated by medium-thick bedded siltstones and sandstones. The red line indicates the separation of the lower and upper lithofacies and the red arrow indicates soft sediment deformation structures within the upper lithofacies where shale has been upwelled. The yellow line indicates the boundary between the Sunbury Shale and the Berea Sandstone.

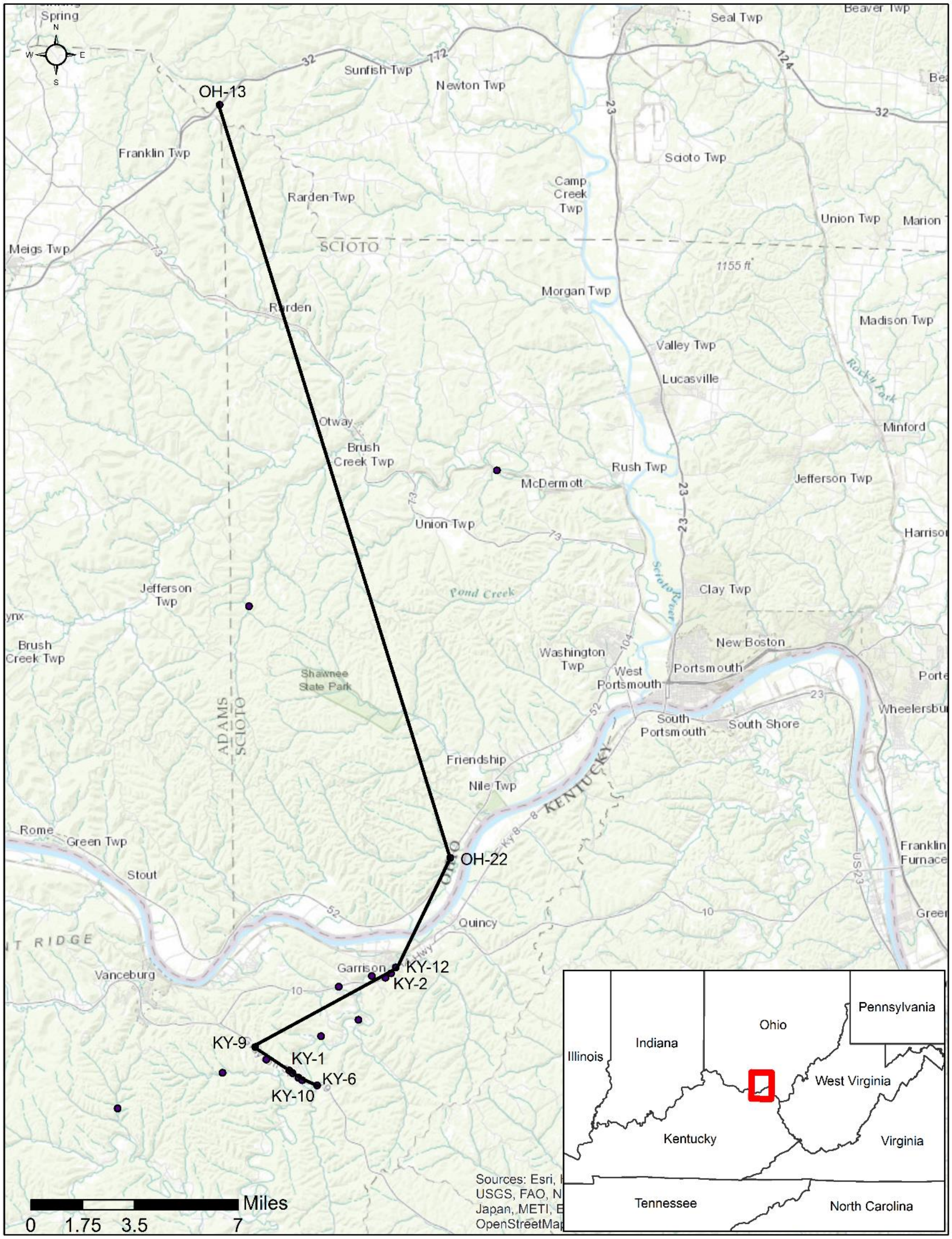

Figure 12. Location of outcrops used for a south-north outcrop correlation. Only outcrops that had exposures of the Sunbury Shale were selected. The Sunbury was used as the hanging formation for correlation.

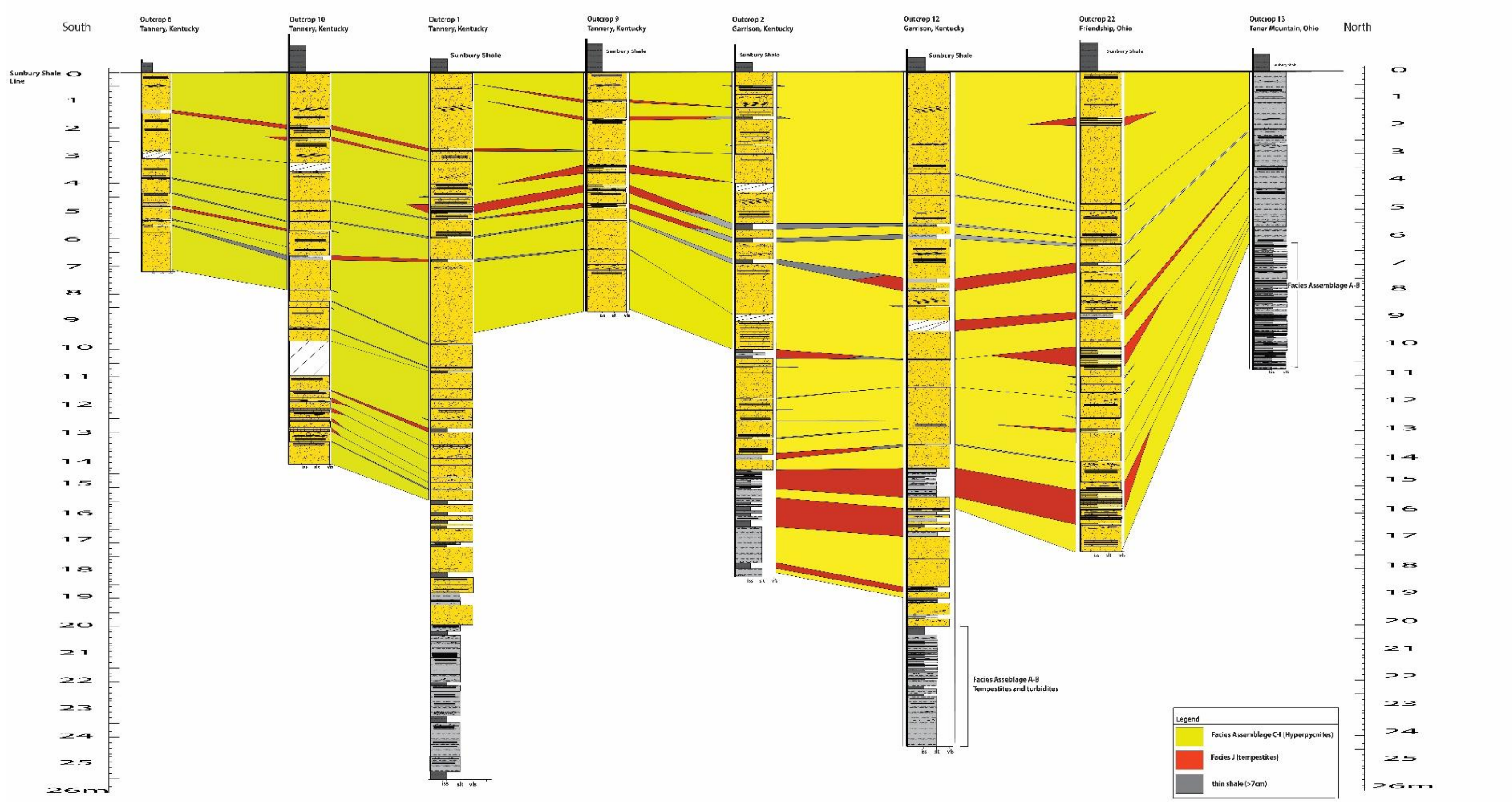

Figure 13. South-North trending outcrop cross-section. Outcrops in northeastern Kentucky are dominated by a thick succession of facies assemblage C-I. Thinning of this unit occurs moving north into southern Ohio which is evident at outcrop 13 at Tener Mountain, Ohio. Outcrop 13 is southwest of a suggested fluvial-deltaic channel (Tomastik, 1996) interpreted in a geophysical log in Vinton County, Ohio. Furthermore, outcrop 13 in Ohio is west of the North-South oriented thickness trend within the Bedford-Berea sequence. The thickness trend can be explained by hyperpycnal flows parallel to paleoslope from fluvial systems to the north in central Ohio. Inactive tectonics in the region could have limited accommodation space during deposition of the Bedford-Berea sequence; tectonic activity has previously been linked to irregular thickness patterns within the sequence (Pashin, 1990; Pashin and Ettensohn, 1995; Floyd, 2015).

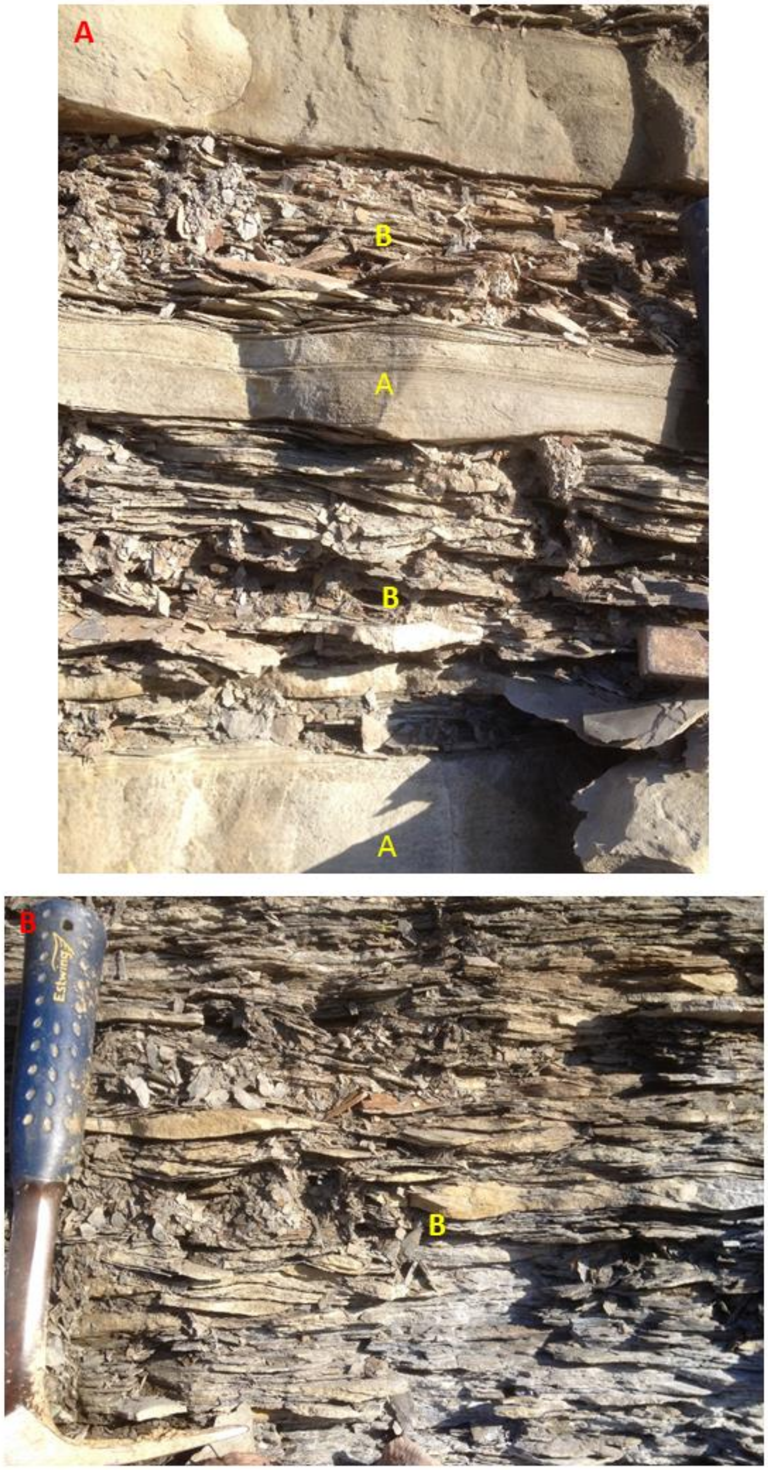

Figure 14. Selected photos of facies A and facies B from locality 2 near Garrison, Kentucky. A) Lenticular bedding that is common in facies B and shows a bed of facies A with micro-hummocky stratification and ripple cross-lamination near the top. B) Slightly asymmetric lenticular ripples within facies B.

Figure 15. Facies A and B at locality 12 near Garrison, Kentucky. A) Large section of facies B primarily made of lenticular ripple bedding with subordinate wavy bedding. B) Shows ripple cross-lamination in facies A and micro-hummocky cross-stratification. Facies B is mainly made of lenticular ripple bedding.

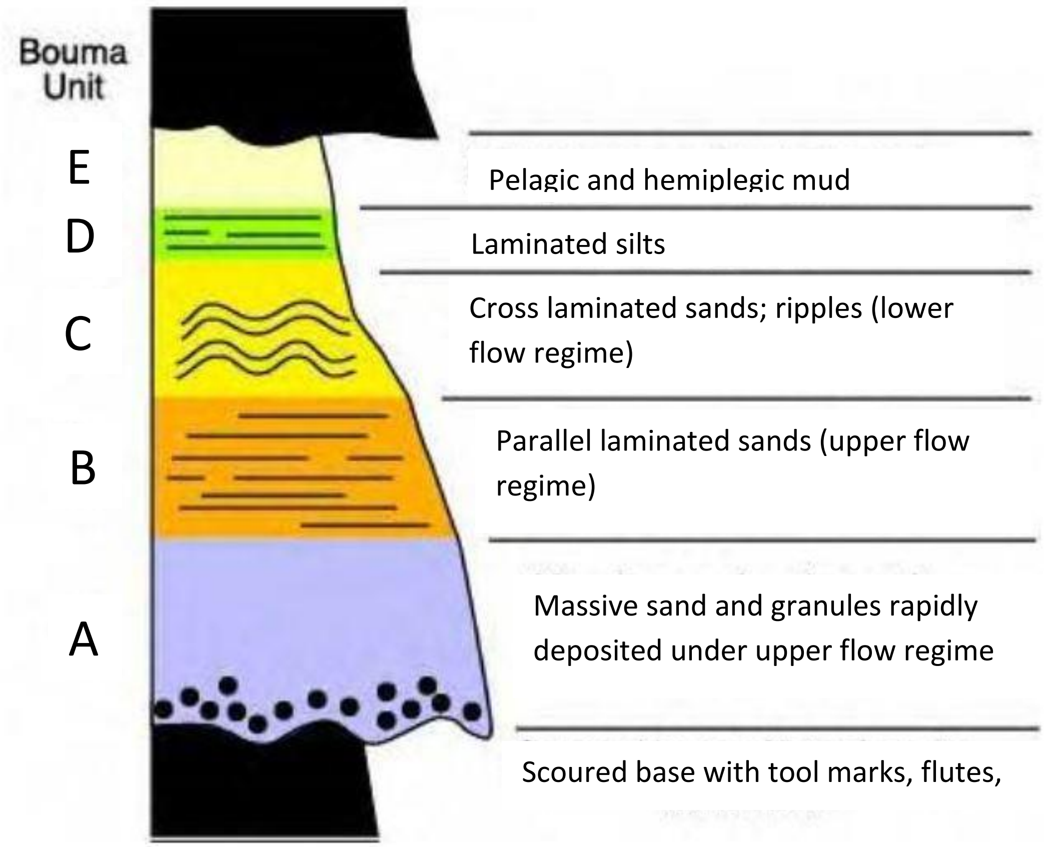

Figure 16. Typical facies sequence (T_a -T_e) produced by purely waning flow (modified from Bouma, 1962) in an ignitive turbidite.

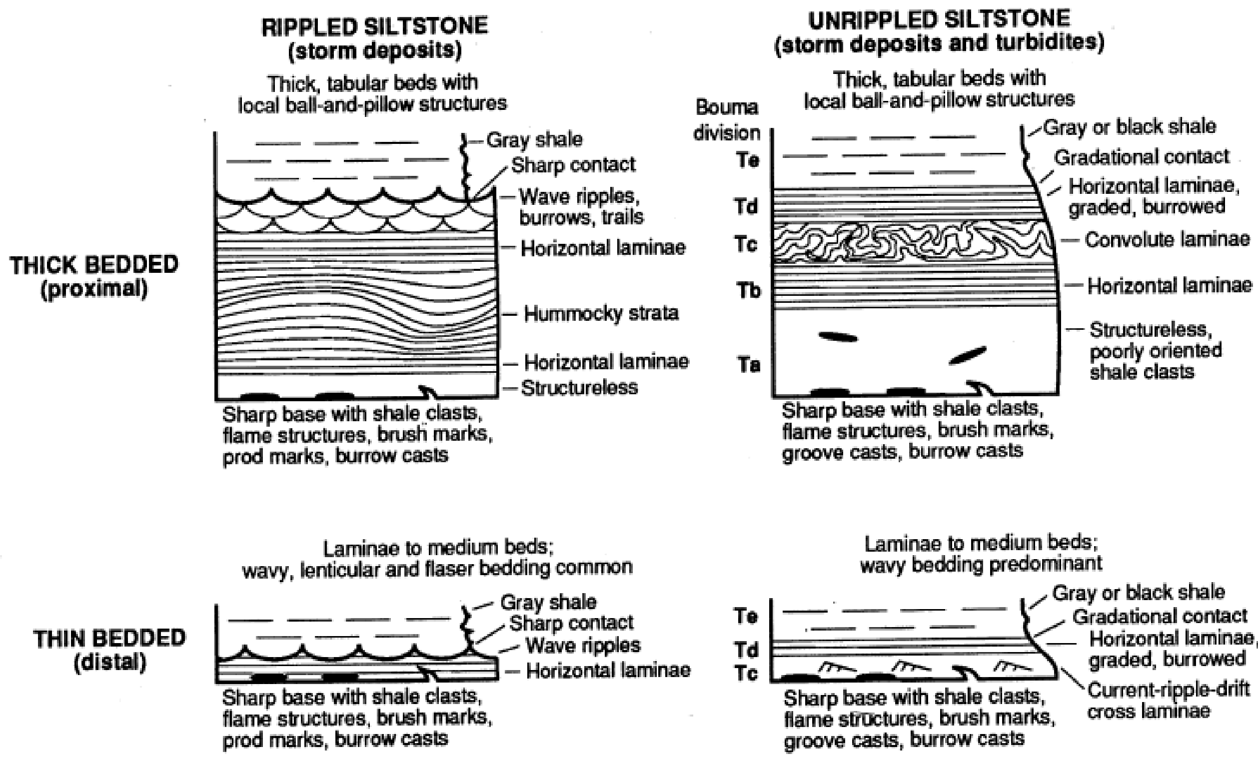

Figure 17. Generalized architecture in Bedford-Berea siltstone beds (Pashin and Ettensohn, 1995).

Surge Turbidity Flow

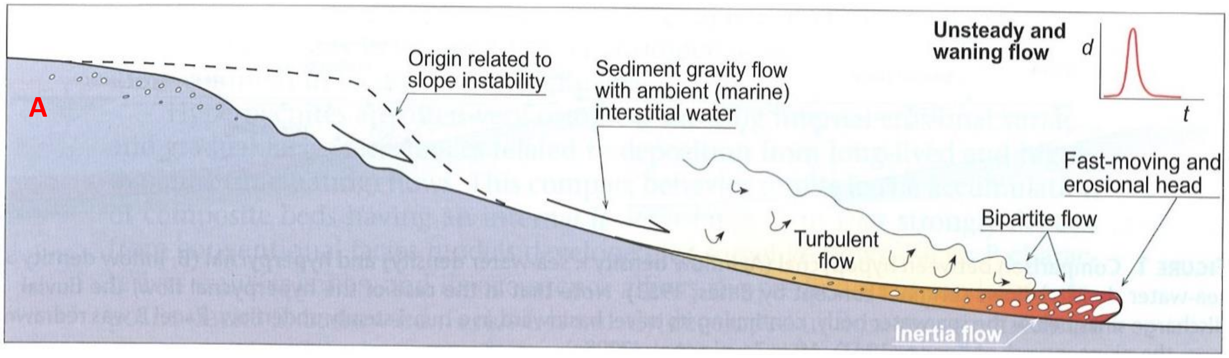

Sustained Hyperpycnal Flow

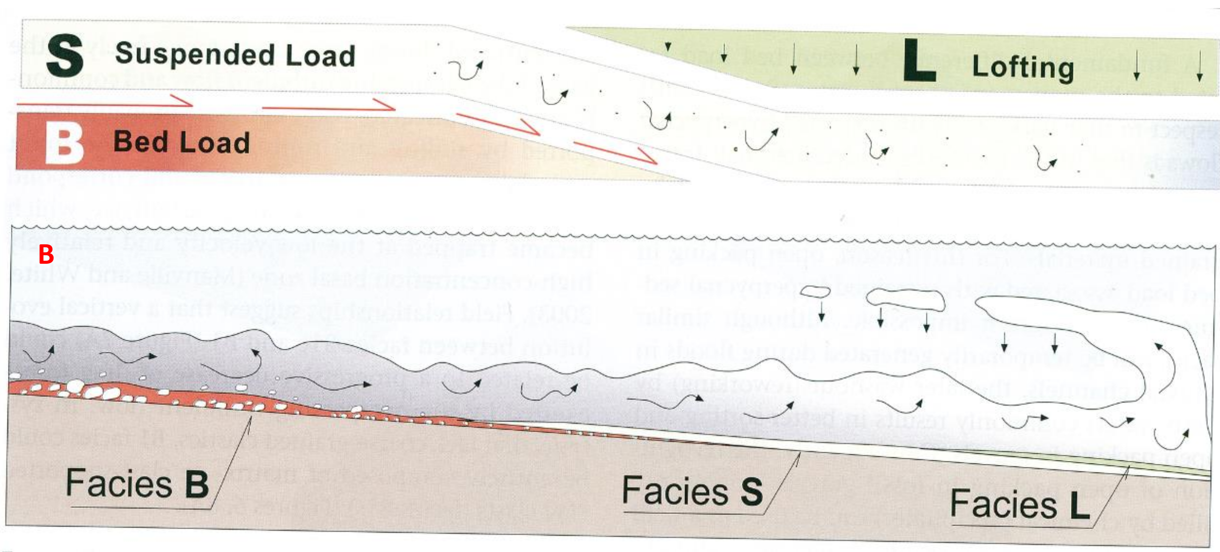

Figure 18. Cross-section of classical turbidite flow (Intrabasinal) vs. hyperpycnal flows. A) Cross-section of classical turbidite flow (Intrabasinal), with a waning flow that originates from slope instability (Mutti et al., 1999; Zavala et al., 2011a). B) Cross section illustrating the origin of the Zavala et al. (2011a) facies sequence. Facies B represents the bed-load facies that is deposited from over passing turbulent flows. Facies S is sand/silts transported by suspension. Facies L is derived from the lofting of fresh water due to density differences (Zavala et al., 2011a).

Figure 19. Selected photos showing bed architecture present in facies assemblage A-B. A) Thin bedded siltstone bed with micro-hummocky cross-stratification overlain by lenticular-bedded shale and siltstone, B) Thin bedded siltstone beds with parallel lamination and micro-hummocky cross-stratification that contain thin couplets of laminated carbonaceous detritus and silt (facies I), which is associated with hyperpycnal turbidites, suggesting these beds are hyperpycnal turbidites that are wave modified. C) Siltstone bed with parallel lamination transitioning to micro-hummocky cross-stratification.

Figure 20. Selected photos of facies C-I at locality 2. A) Facies C is present near the bottom of the bed and transitions vertically to facies D, which then transitions to facies E that is typical of a waning flow. Then facies E transitions to D, which implies a waxing flow, followed by a waning flow, which produces facies E.B) Bedford-Berea bed that resulted from a mainly waning flow.

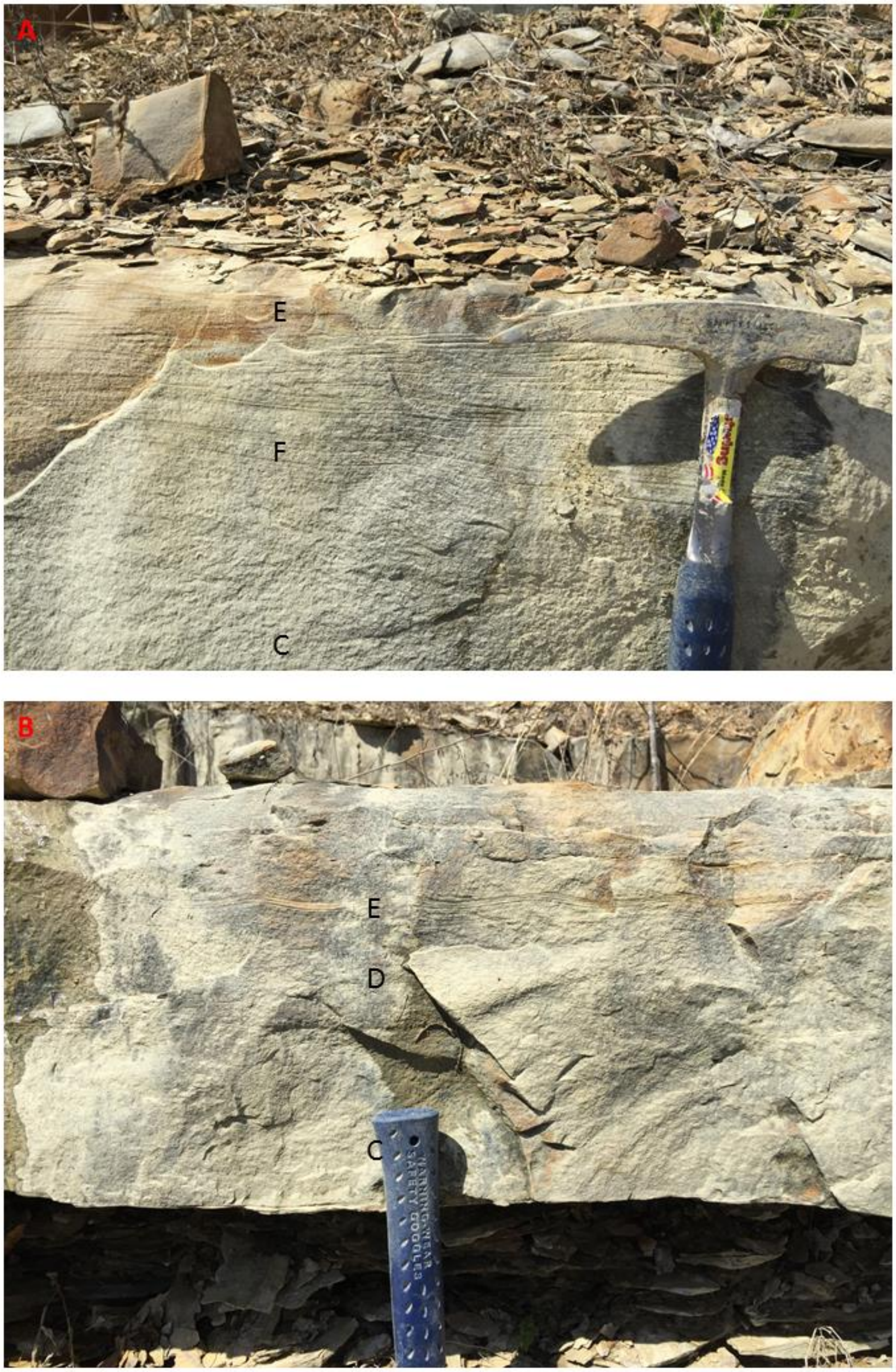

Figure 21. Common facies found at locality 22. A) Shows facies C, which is a massive very fine-grained sandstone facies, facies F that is hummocky cross-stratified sandstone facies and facies E that is a climbing ripple cross-laminated sandstone facies. B) This bed is similar to the bed in image A; however, facies D replaces facies F within this fine grained sandstone bed.

Figure 22. Photos of facies within the Bedford-Berea sequence. A) Facies C and facies F at locality KY-5. B) Facies C which transitions to facies H at locality KY-2. C) Facies C which transitions into facies D and facies G at locality KY-12. D) Facies E on top of a hyperpycnal bed at locality KY-5 near Garrison, KY.

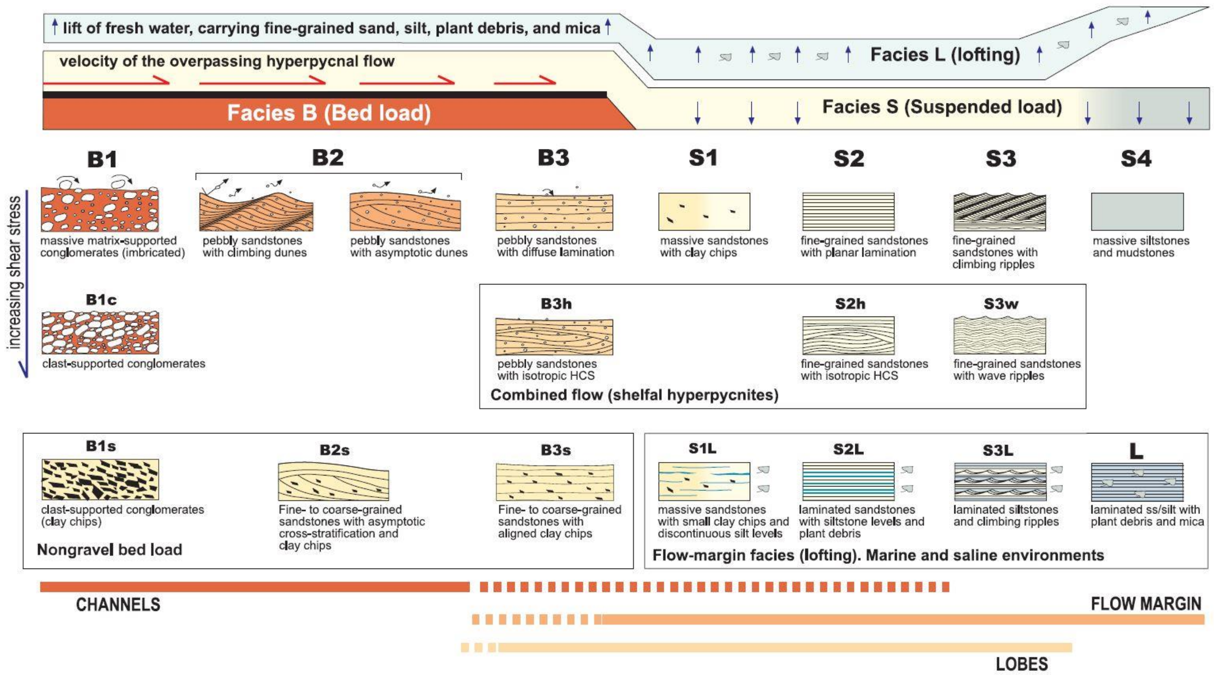

Figure 23. Facies associated with hyperpycnal flows (Zavala et al., 2011a). The presence of the lofting facies, carbonaceous detritus, and structure sequences suggesting flow fluctuations, are key elements in distinguishing hyperpycnal deposits from standard intrabasinal turbidites (Zavala et al., 2011a).

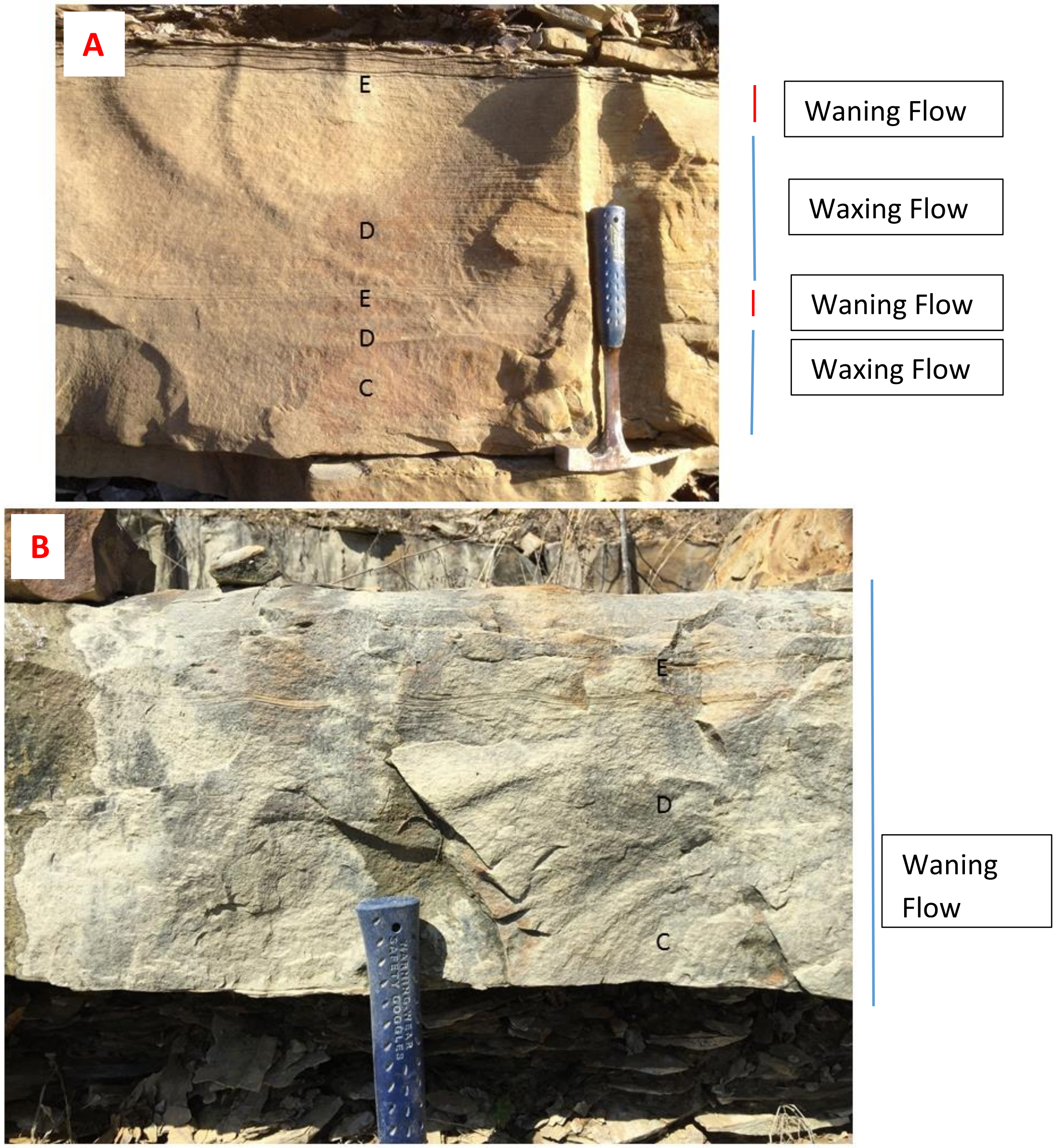

Figure 24. Bed architecture of facies C-I in a single Bedford-Berea bed. A) Berea bed photo from outcrop 2 in the Upper-Berea lithofacies that illustrate common sedimentary sequences in waning-waxing-waning flow conditions; waning flow is indicated by blue lines while waxing flow is identified as red lines. In this sequence the waning portion is illustrated by the massive sandstone (C) facies, then the parallel laminated (D) facies, followed by the climbing ripple cross-lamination facies (E) which is then overlain by the (D) facies and the (E) facies. B) Typical facies sequence in waning flow conditions. Massive sandstone (C), transitioning to parallel laminated sandstone (D), followed by climbing ripple cross-laminated sandstone (E) and rippled top from locality 22.

Figure 25. Selected bed architecture photos that show flow variation within one bed in the Upper Berea Lithofacies. A) Shows waning-waxing-waning cycles. B) Shows Facies I, which is composed of bundles of sandstone/siltstone separated by carbonaceous detritus and provides direct evidence of long-lived turbulent flows in Bedford-Berea sediment.

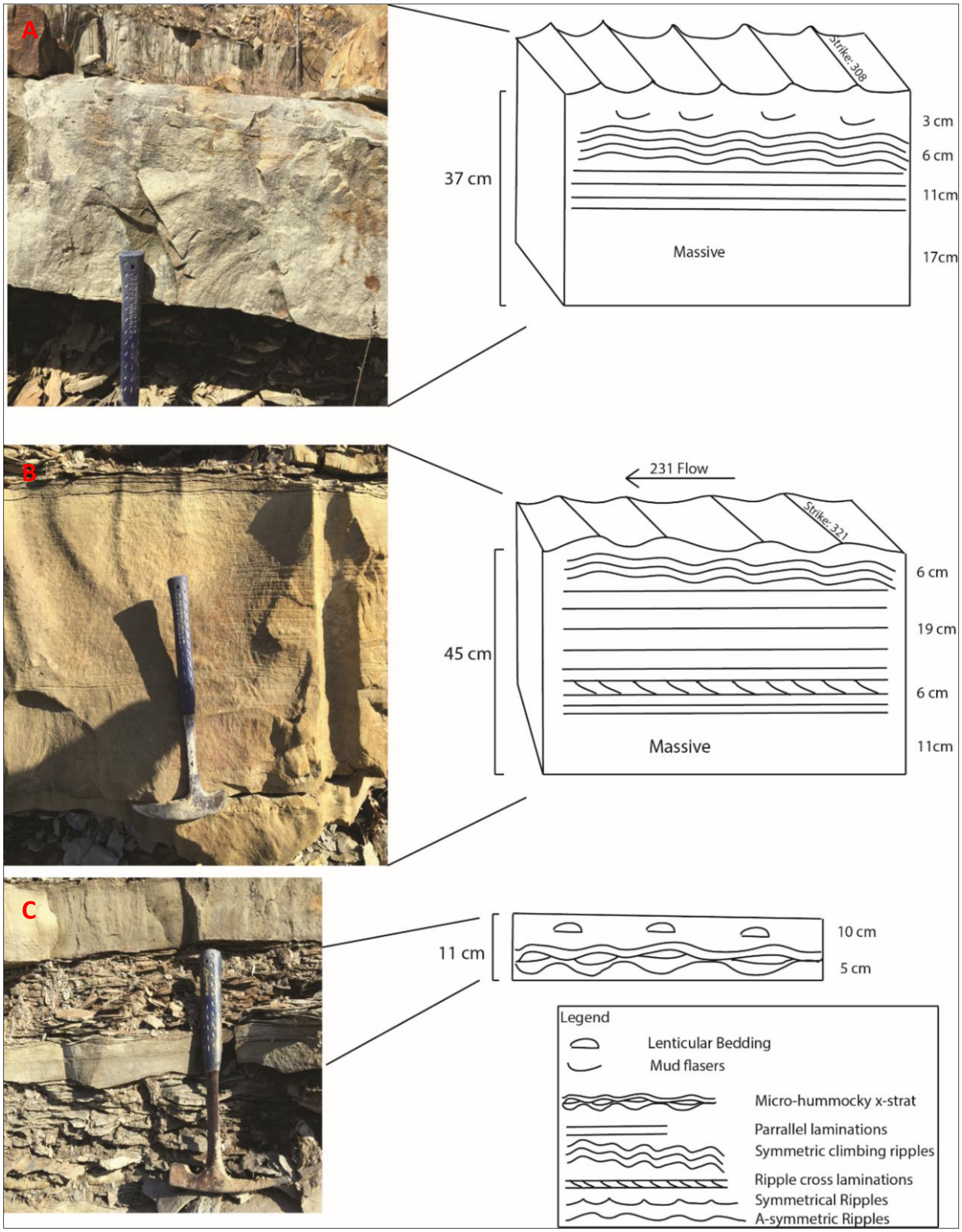

Figure 26. Line drawings of common beds within the Bedford-Berea sequence. Medium-bedded sandstones (image A and B) are composed of facies assemblage C-I, while thin and interbedded siltstone and shales (image C) are made up of facies assemblage A-B in the lower lithofacies and thin-bedded siltstone and shales belong to Facies J in the upper lithofacies.

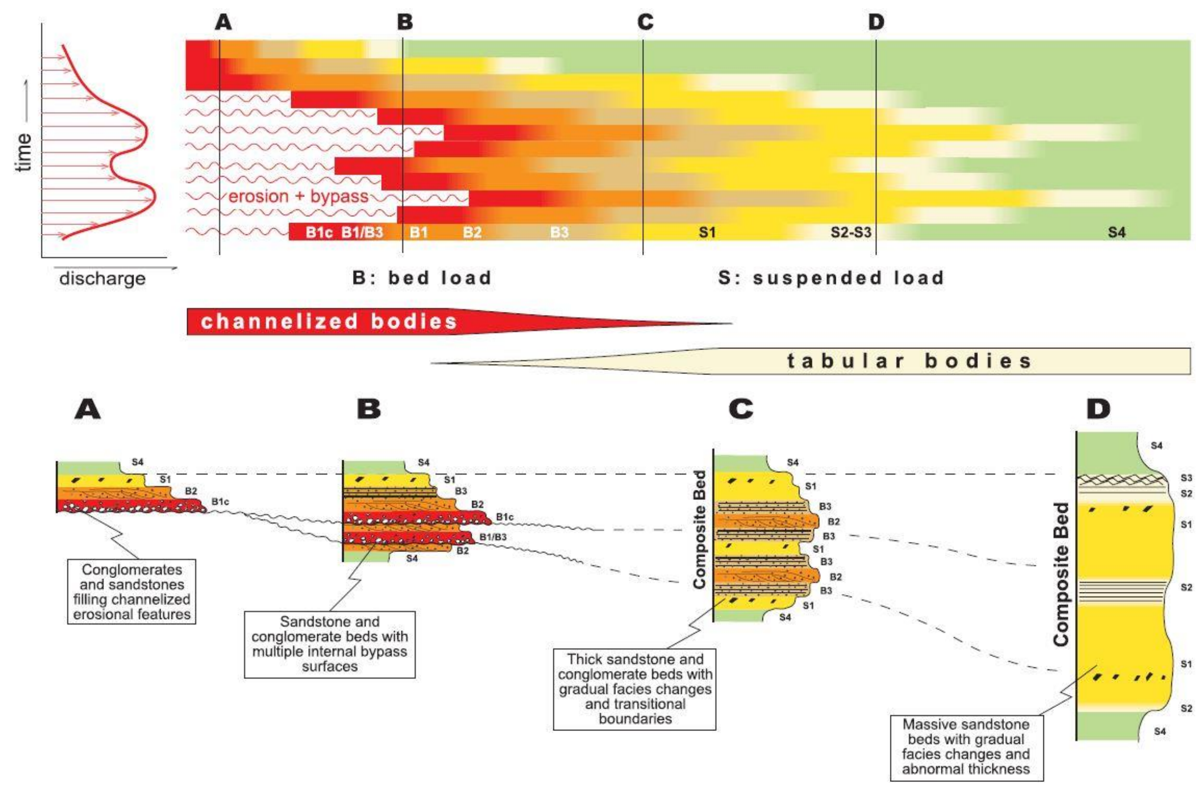

Figure 27. Flow velocity and sediment concentration variations during a single long-lived hyperpycnal discharge (Zavala et al., 2011b). Increased discharge is associated with the massive sandstone facies where long-lived bottom flows having high-suspended loads prevented the formation of primary structures.

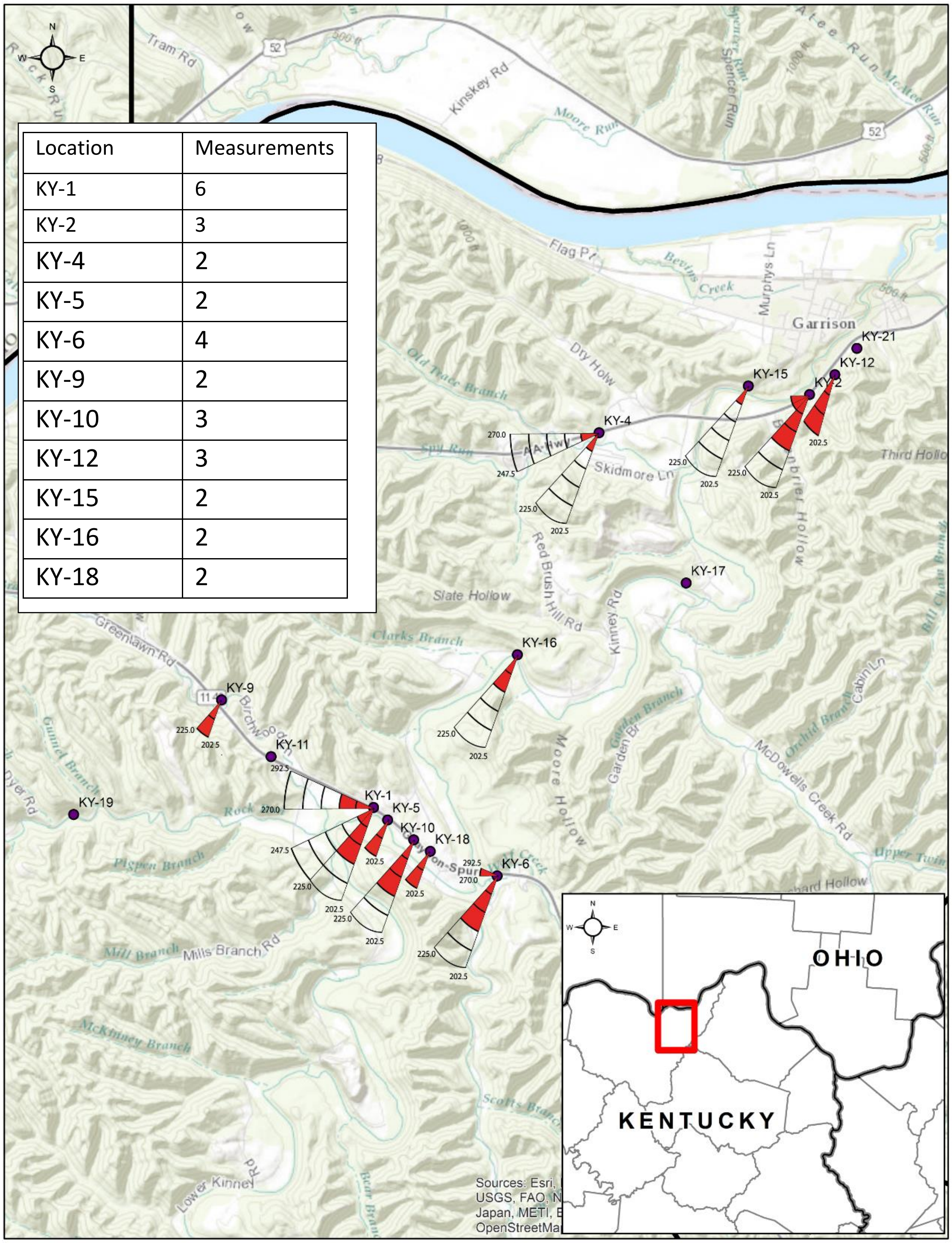

Location	Measurements
KY-1	6
KY-2	3
KY-4	2
KY-5	2
KY-6	4
KY-9	2
KY-10	3
KY-12	3
KY-15	2
KY-16	2
KY-18	2

Figure 28. Paleocurrent rose diagrams from outcrops in northeastern Kentucky. Any empty portion of a rose diagram was not included. Paleocurrent measurements within northeastern Kentucky support prior measurement by Rothman (1978) and Pashin and Ettensohn (1995).

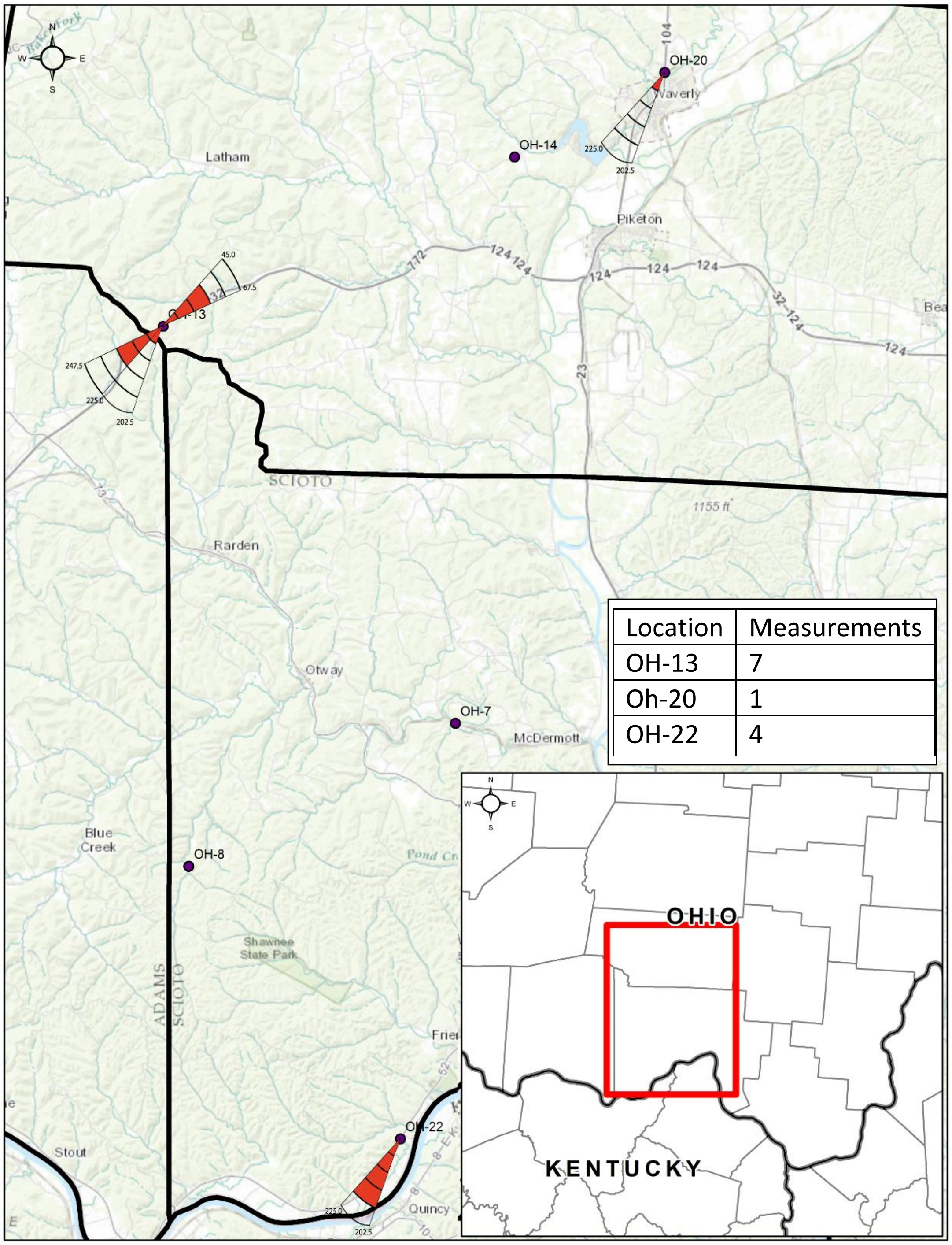

Location	Measurements
OH-13	7
Oh-20	1
OH-22	4

Figure 29. Paleocurrent rose diagrams from outcrops in southeastern Ohio. Outcrops 7, 8 and 14 are old outcrops which are now poorly exposed and in the case of outcrop 7 relatively inaccessible. Paleocurrents were not measured on these outcrops. However, paleocurrent measurements have been taken at these outcrops and measurements are consistent with paleocurrent measurements from surrounding outcrops (Rothman, 1978; Pashin and Ettensohn, 1995).

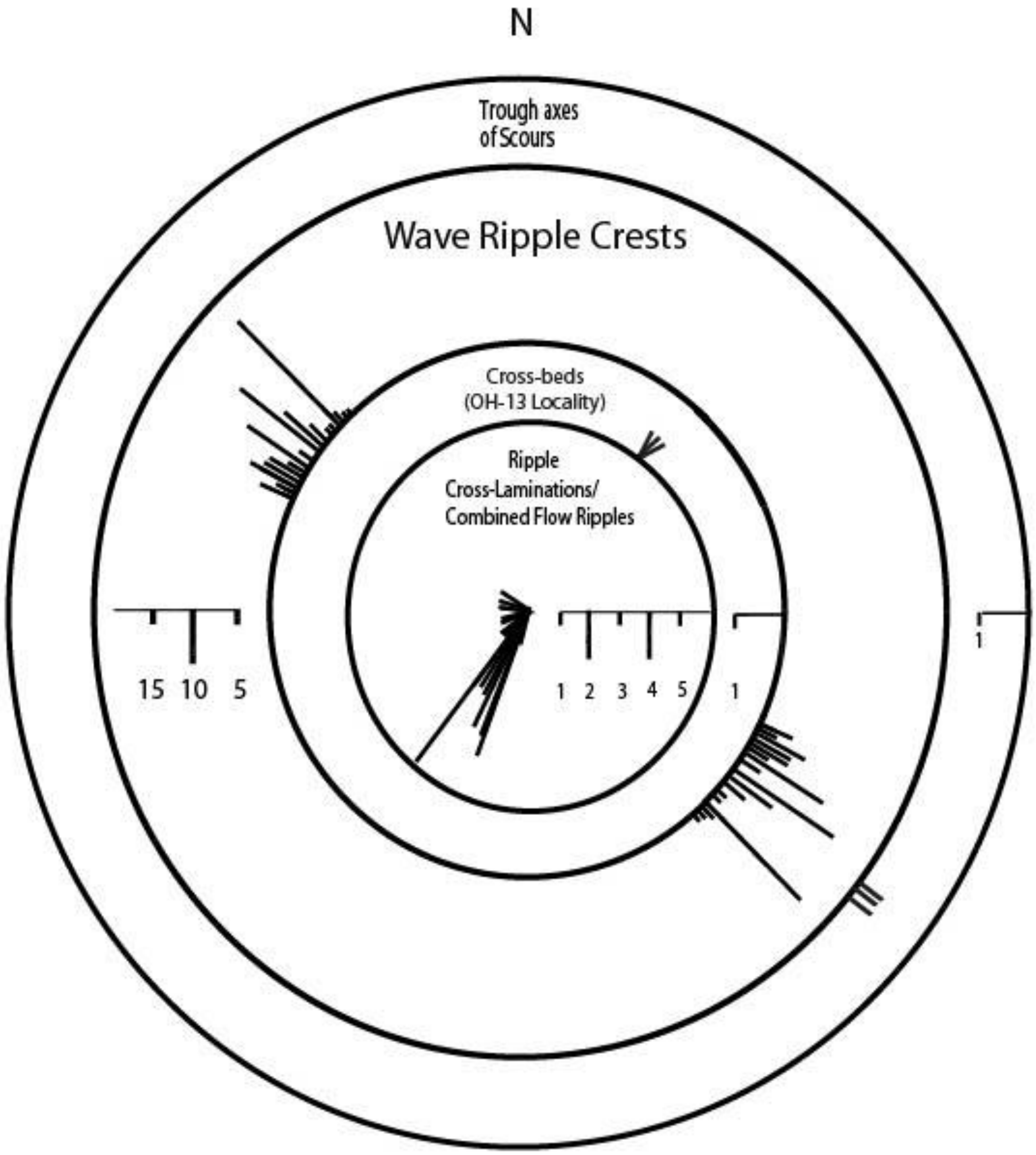

Figure 30. Spoke diagram illustrating asymmetric paleocurrent orientations throughout the Bedford-Berea sequence in northeastern Kentucky and southeastern Ohio (see Appendix I and II for statistics). The mean average for unidirectional flow was S32W and the mean strike of ripple crests was N38W. A total of 68 ripple crests, 41 ripple cross-laminations/combined flow ripples and 3 cross-beds were measured.

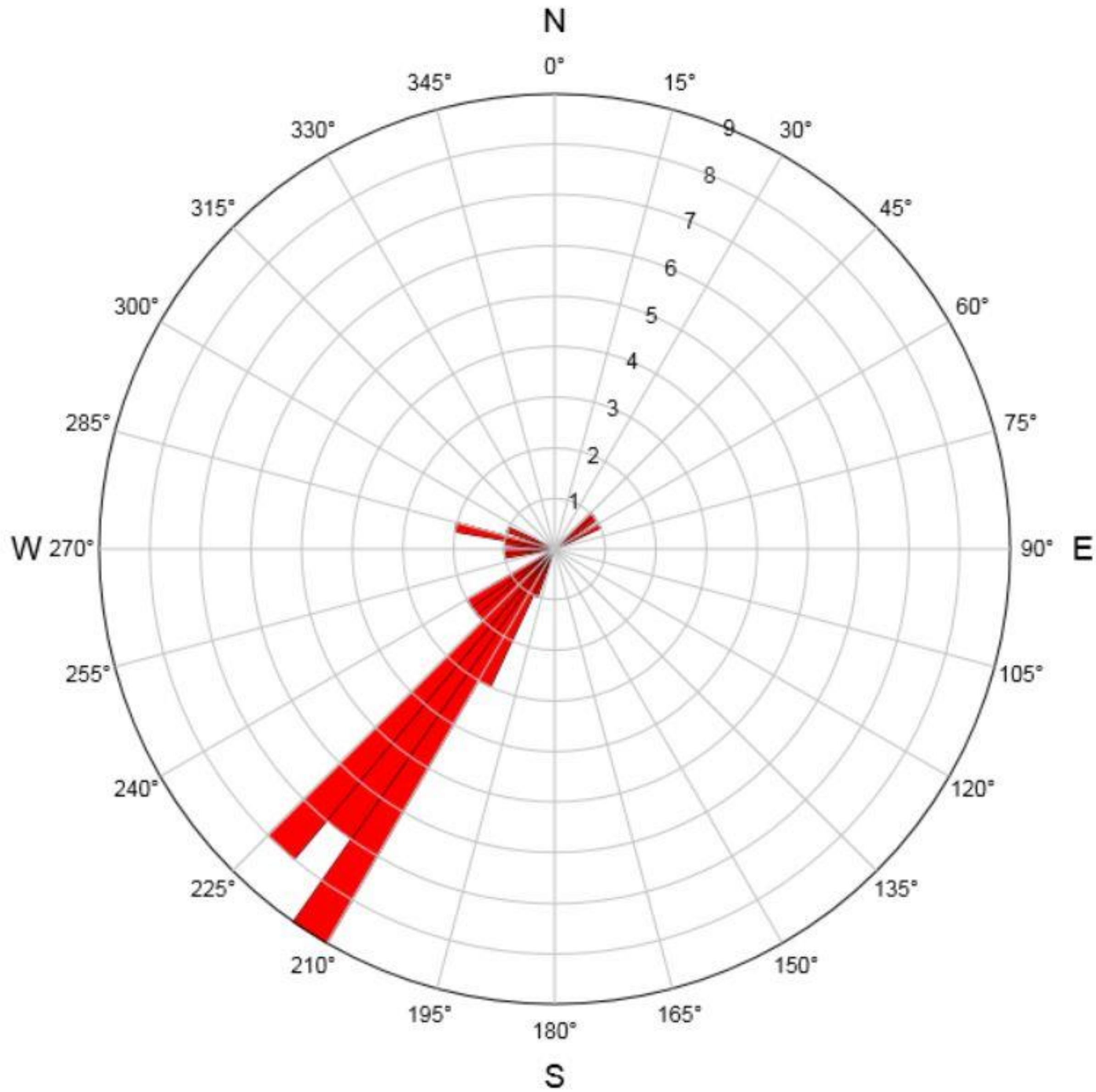

Figure 31. Composite paleocurrent rose diagram for all locations. Forty current measurements were measured; the vector mean of these currents was 226.57° and the vector magnitude was 91.6 percent. The high vector magnitude indicates the low dispersion of paleocurrents in the Bedford-Berea sequence.

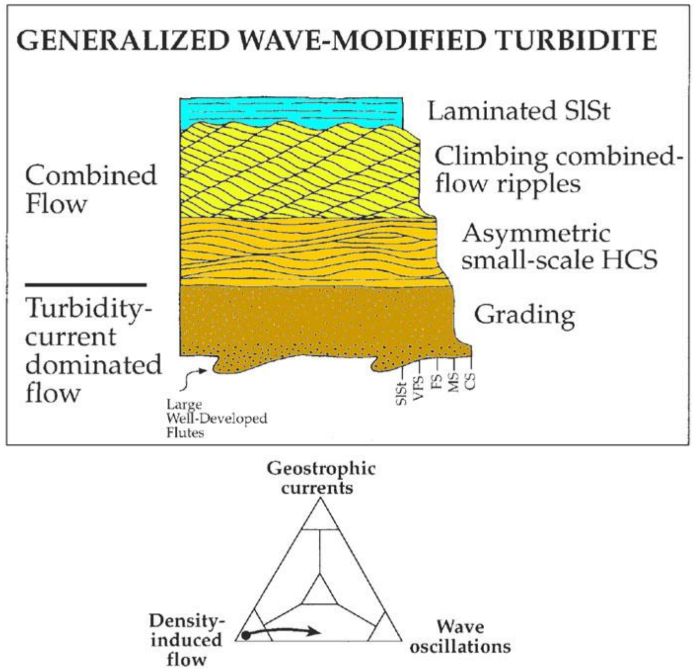

Figure 32. Typical sequence of sedimentary structures and flow patterns from a wave-modified turbidite with purely waning flow (Myrow et al., 2002).

Figure 33. Selected images of facies I. A) Thin couplets of carbonaceous detritus and silt that are mm thick with small soft sediment deformation. B) Thin couplets of darker material and siltstone/vfs (light material) which resemble tidal rhythmites but could be facies I; a thin section is needed to differentiate.

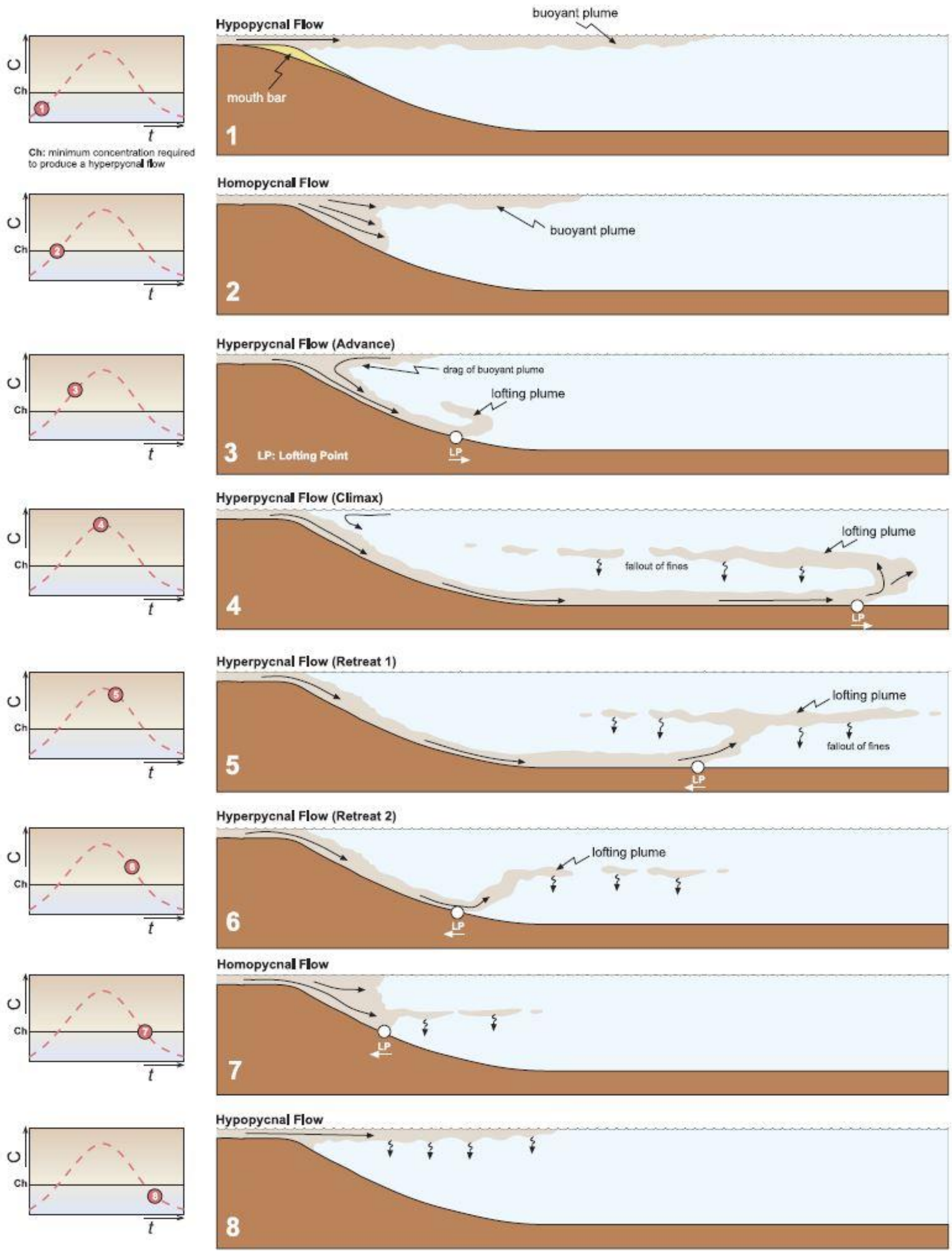

Figure 34. The evolution of a hyperpycnal discharge (Zavala et al., 2011a). Stages 3-6 illustrate the different depositional scenarios that create the lofting facies (LF).

Figure 35. Selected photos of facies J. A) Facies J and C, at locality 12, wavy ripple bedding predominates and beds are thinly interbedded as opposed to mainly lenticular ripple bedded and interlaminated in facies. B) Micro-hummocky cross-stratification in wavy ripple bedded siltstone within facies J and locality 4. C) Wavy ripple bedding and lenticular ripple bedding in facies J; wavy ripple beds commonly exhibit micro-hummocky cross-stratification.

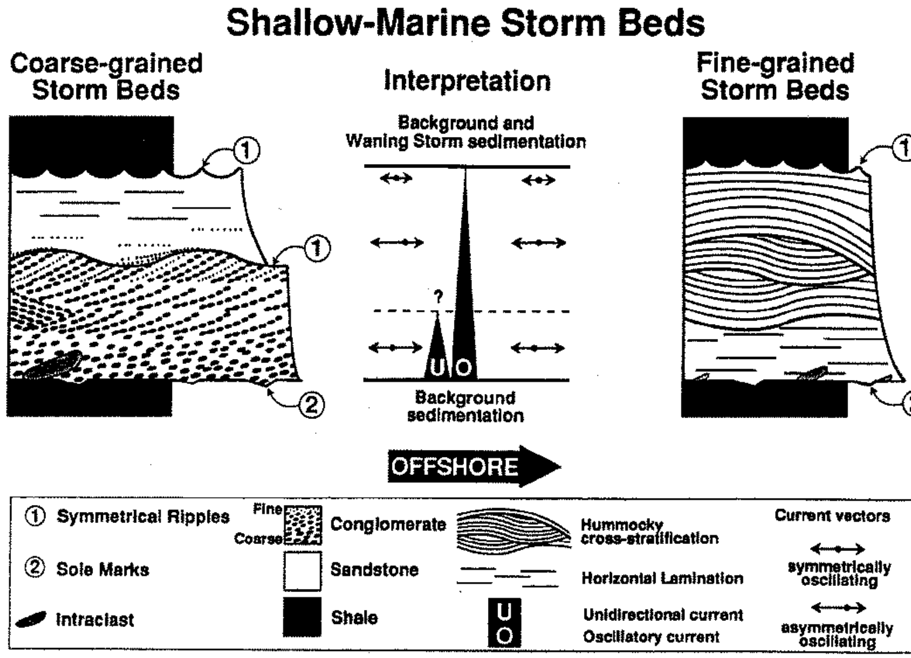

Figure 36. Schematic of the typical sedimentary structure sequences in coarse-grained and fine-grained storm beds (Cheel and Leckie, 1992). Fine-grained storm beds are present within the Bedford-Berea sequence and occur in thin-bedded siltstone beds in both the upper and lower lithofacies.

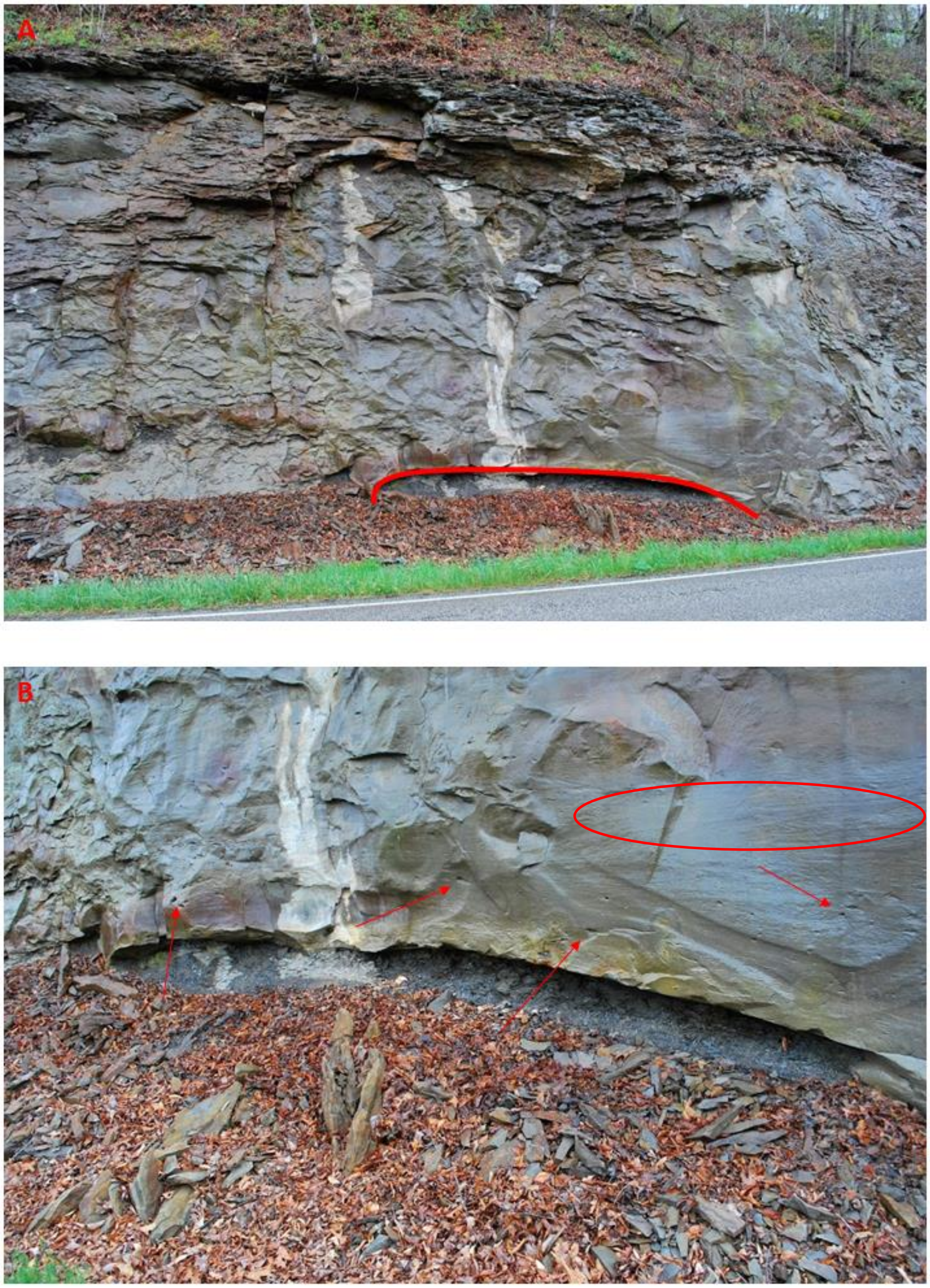

Figure 37. Selected photos of facies K. A) The red line indicates the sharp contact between the Berea Formation and the Cleveland Member of the Ohio Shale. The Cleveland Member likely represents relief along the base of a channel. B) Close up view of the contact of the Berea and Cleveland Member, showing large rip-up clasts (red arrows) and trough cross-beds (red ellipse).

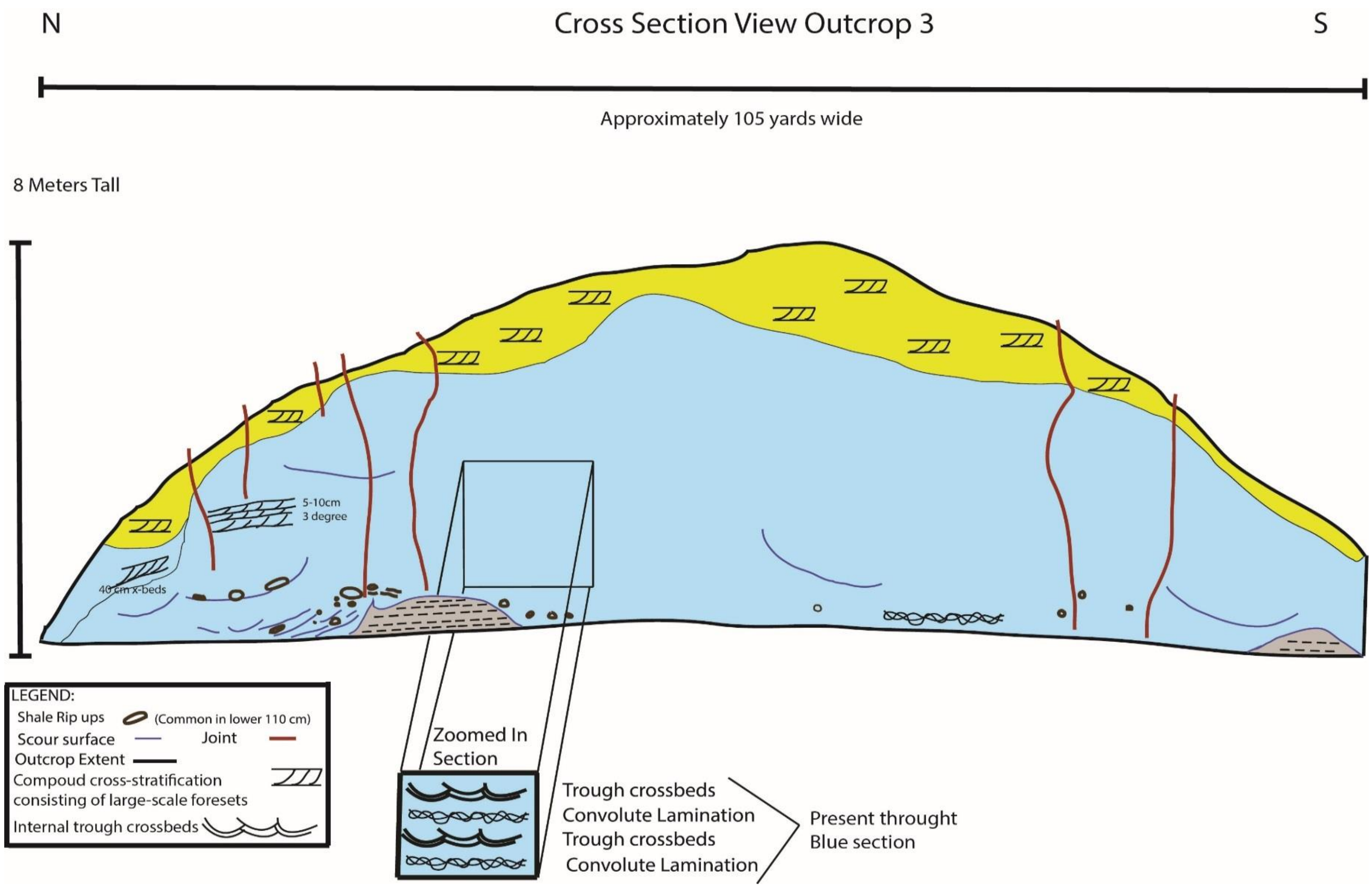

Figure 38. Cross sectional sketch of internal structures present at locality 3 in facies K. Shale rip ups are common in the lower 110cm of the outcrop. Trough cross-beds and convolute laminations are present throughout the outcrop, except for the upper two meters which contain medium bedded foreset cross-beds. One set of large scale cross-beds is present on the left flank of the outcrop.

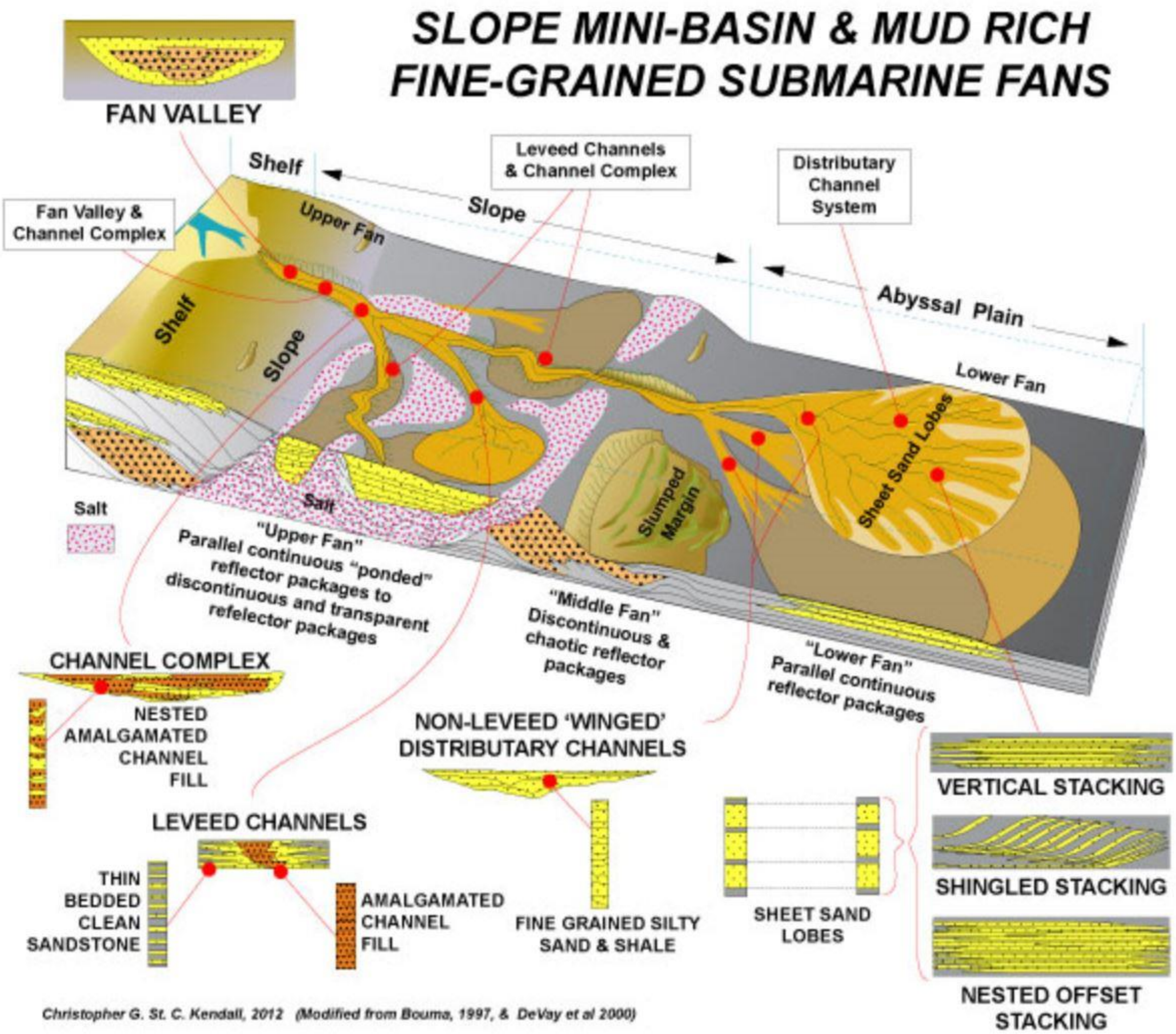

Figure 39. Typical bedding in submarine channel and fan facies in both proximal and distal settings (Kendall, 2012; modified from Bouma, 1997 and DeVay, Risch, Scott, Thomas 2000).

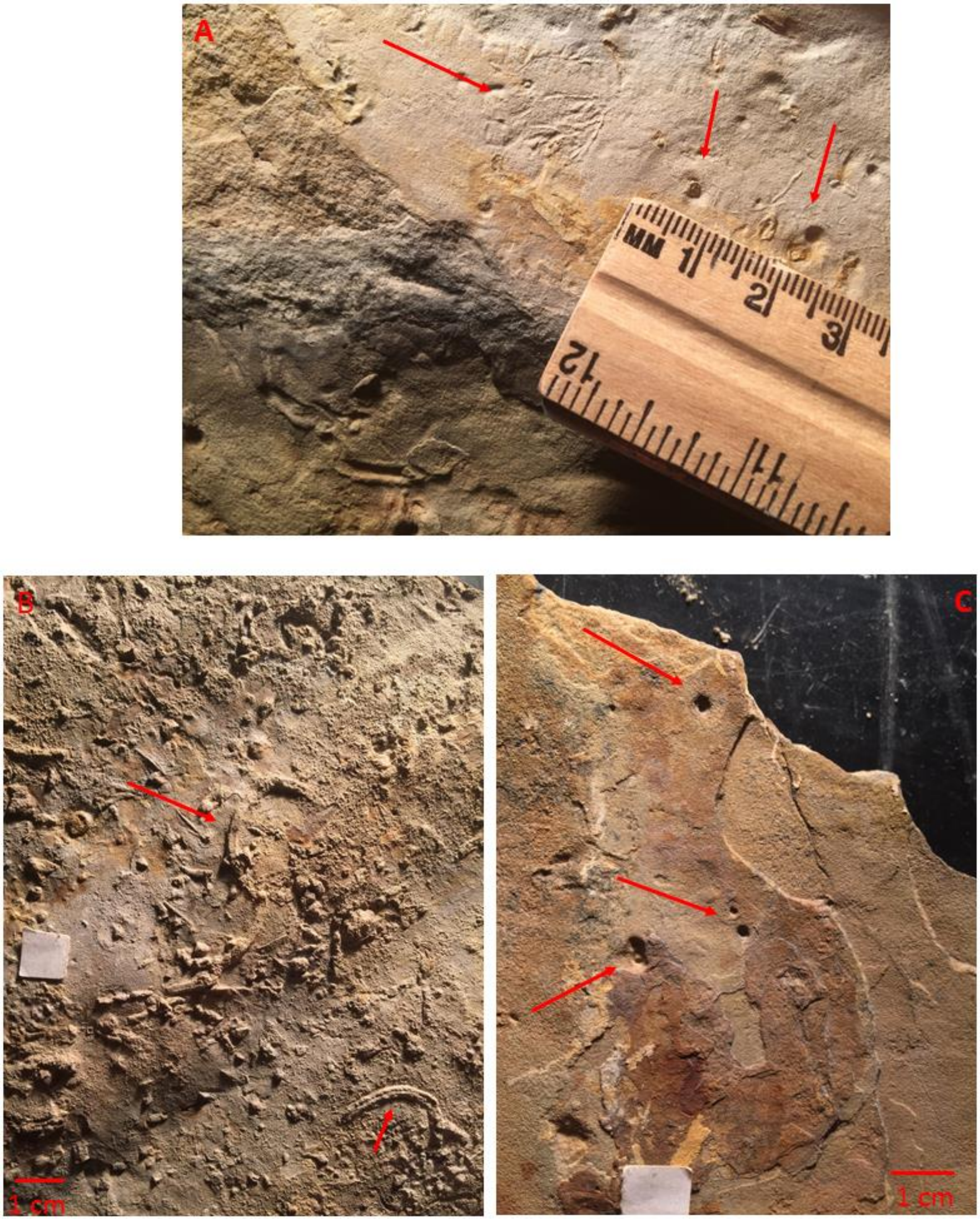

Figure 40. Selected trace fossil photographs from the lower Lithofacies. A) Epirelief views of *Chondrites* (top left arrow), taken from locality 2 near Garrison, Kentucky. B) Hyporelief views of *Planolites*, a simple unbranched horizontal burrow taken from locality 12 near Garrison, Kentucky. C) Epirelief views of circular vertical traces that are not preserved in full relief (arrows), taken from locality 12 near Garrison, Kentucky.

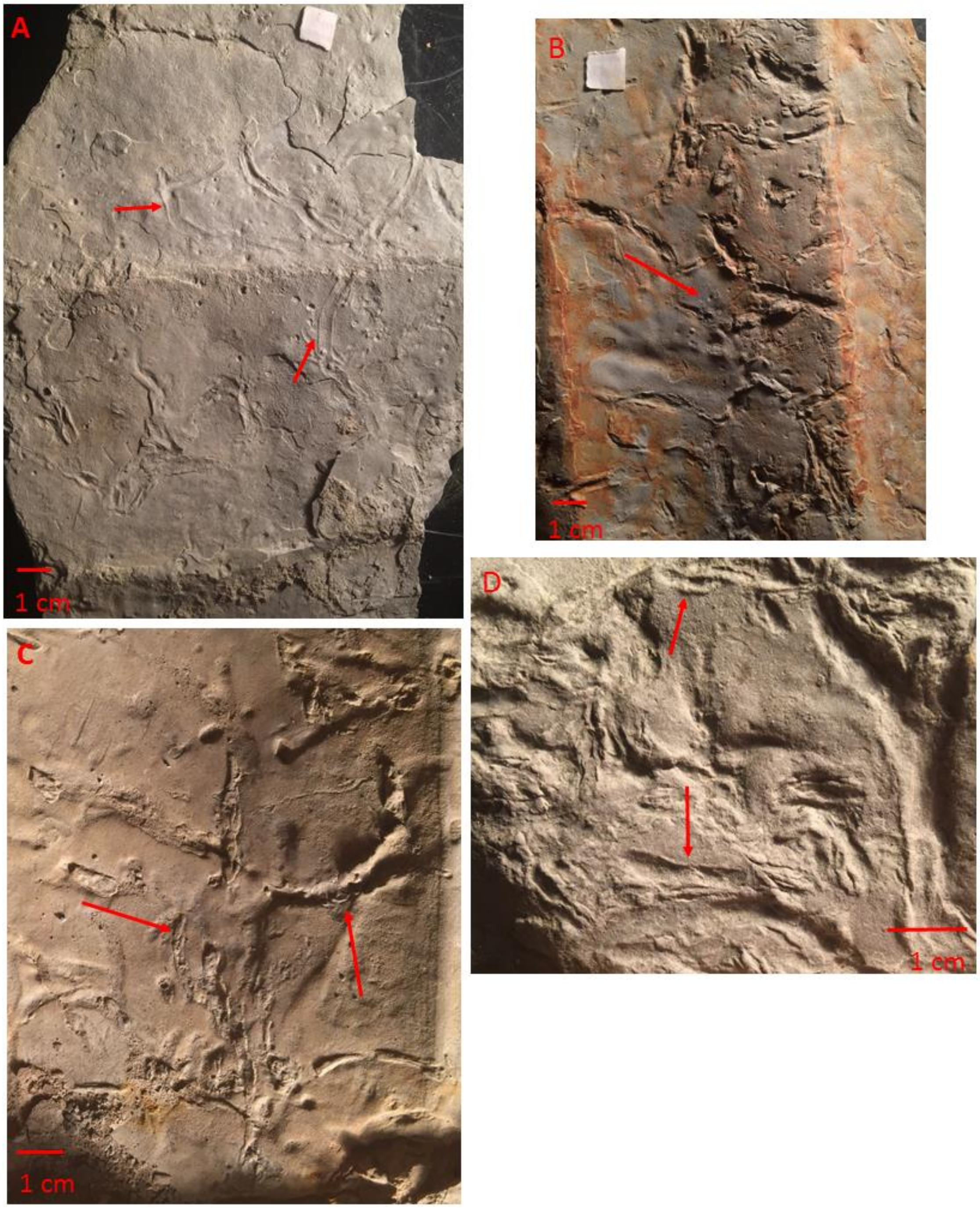

Figure 41. Trace fossil photos from samples of the lower lithofacies. A) Epirelief view of Sample 14 taken at locality 12 near Garrison, Kentucky with *Skolithos?* (arrows) and concave rarely branching, sinuous horizontal burrows. B) *Skolithos* (arrow), and concave rarely branching sinuous horizontal burrows in Epirelief view taken from locality 7 near McDermott, Ohio. C) Epirelief view of Sample 13 taken from locality 2 near Garrison, Kentucky with *Skolithos?* (arrow), and concave small sinuous horizontal burrows. D) Small sinuous horizontal burrows in Epirelief view taken from locality 1 near Tannery, Kentucky.

Figure 42. Heavy bioturbation in the upper 30cm at locality 2 and 23. A) Pyritized brachiopod at the top of the Berea Sandstone at locality 23. B) Close-up view of brachiopod at locality 23 in southeastern Ohio. C) Heavy bioturbation index of four to six (4-6) in the upper 20cm of the Berea Sandstone below the Berea-Sunbury contact at locality 2 near Garrison, Kentucky.

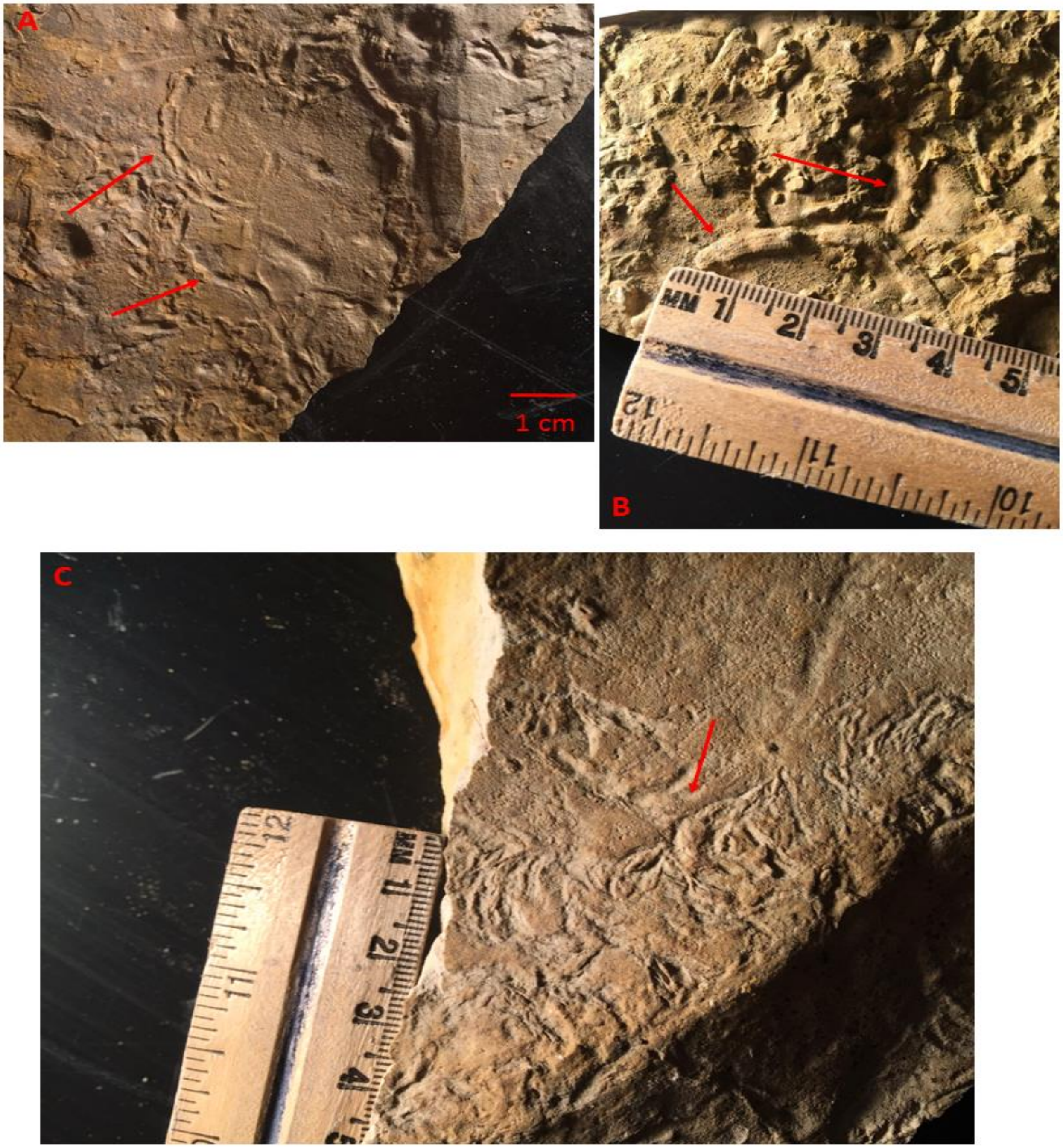

Figure 43. Selected trace fossil photographs from the upper lithofacies. (A) Epirelief, views of *Nereites*? which are concave meandering horizontal burrows that are finely striated flanked with circular lobes taken at locality 2, Garrison, Kentucky. (B) Hyporelief, views of *Planolites*, convex simple unlined, unbranched horizontal to slightly inclined burrows taken at locality 14 near Lake White, Ohio. (C) Epirelief, views of *Lophoctenium* that are concave with closely spaced bunches of inwardly bent grooves with comb like branches taken at locality 1 Tannery, Kentucky.

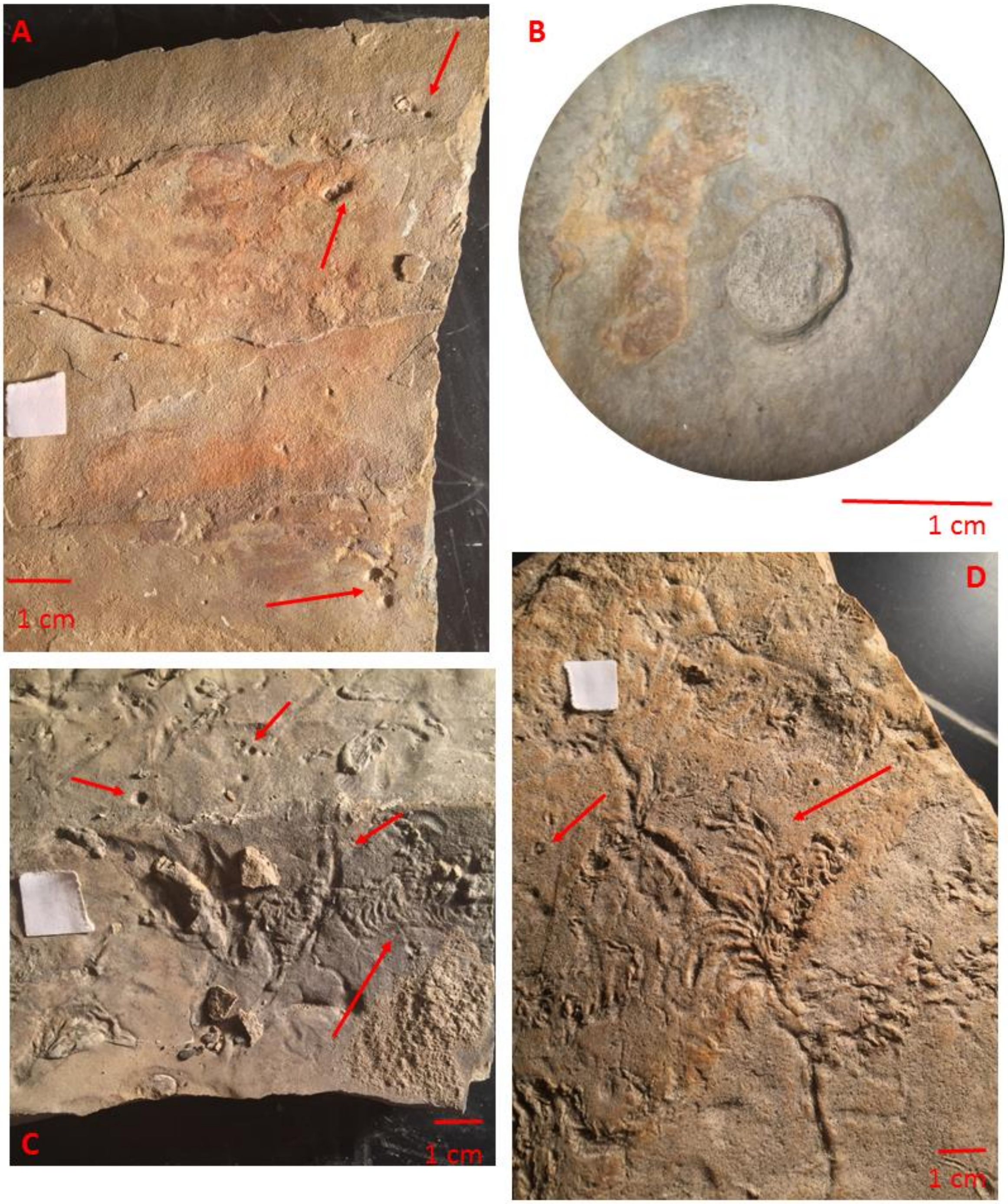

Figure 44. Selected trace fossils from the upper lithofacies. A) Epirelief view of circular traces that resemble Skolithos; however, are not seen in full relief at locality 12 near Garrison, Kentucky. B) Microscope view of lined vertical burrow in Epirelief view, taken at locality 13 near Tener Mountain, Ohio. C) Epirelief view of Lophoctenium (bottom right), and horizontal burrow (middle) taken at locality 12 near Garrison, Kentucky. D) Epirelief view of Lophoctenium (right arrow) and circular traces that are not preserved in full relief (left arrow) taken at locality 5 near Tannery, Kentucky.

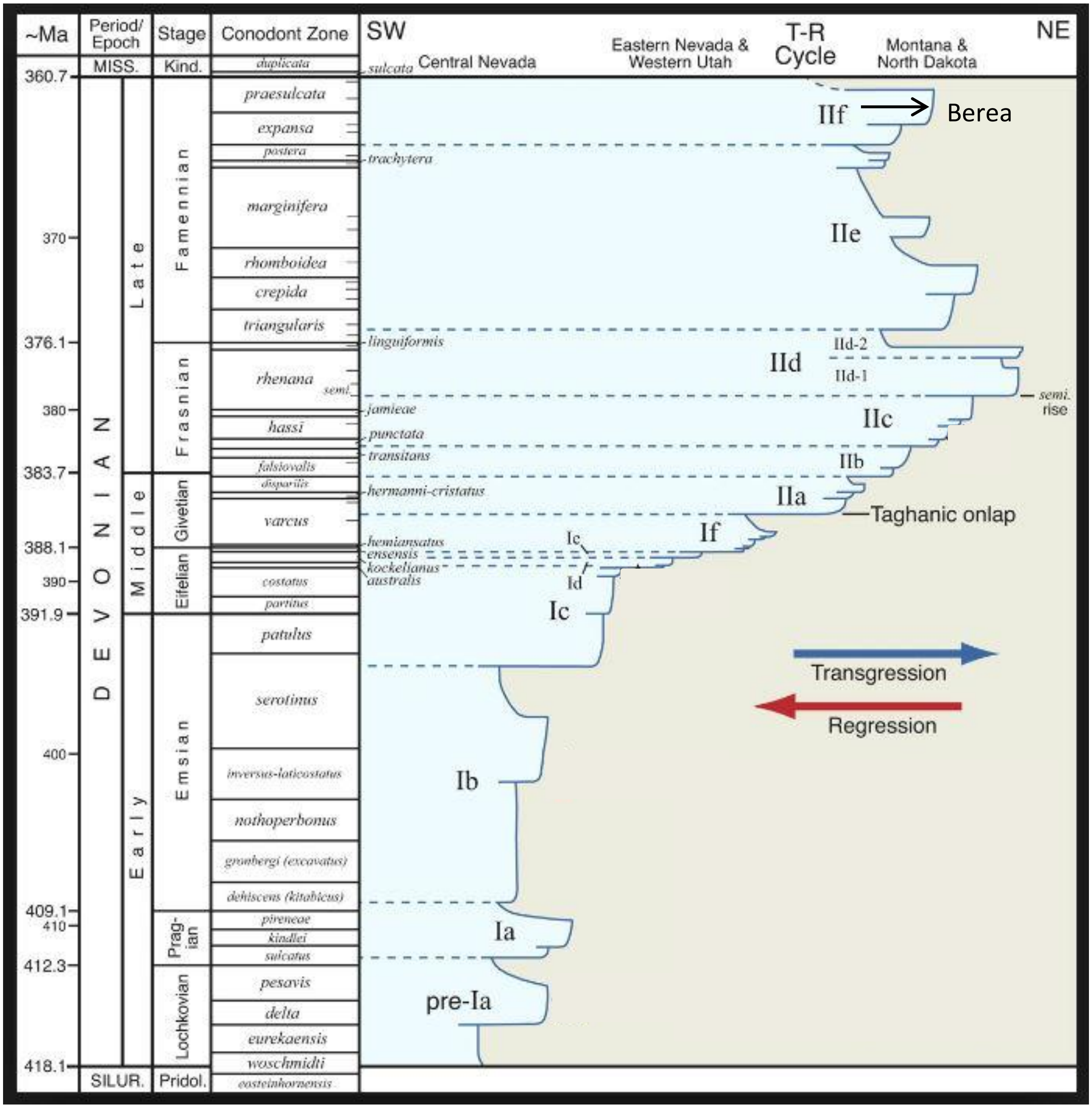

Figure 45. Eustatic sea level curve and conodont zones during the Devonian age (Modified from Morrow and Sandberg, 2008). The Bedford has been placed in the Upper expansa to Lower praesulcata Zone with the Berea being deposited in the Middle to Upper praesulcata Zone (Gutschick and Sandberg, 1991).

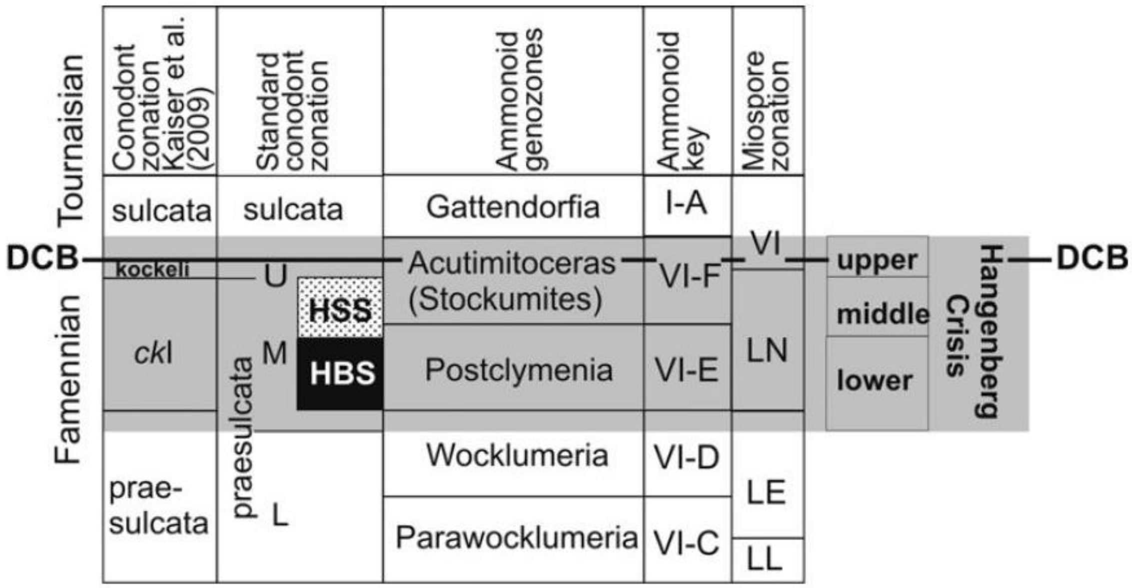

Figure 46. Biostratigraphy around the Famennian-Tournaisian boundary (Kaiser et al., 2015).

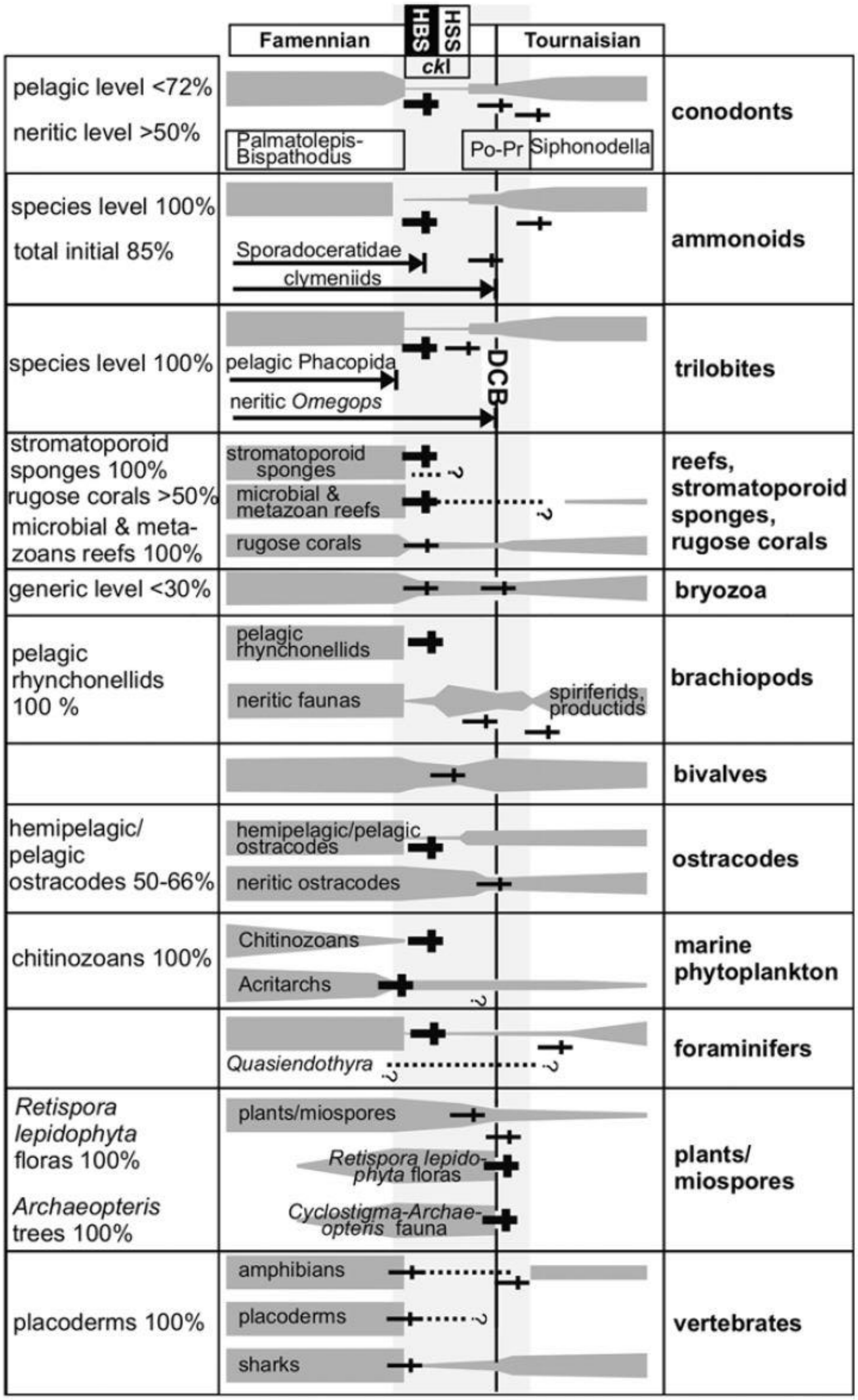

Figure 47. Fossil groups affected by the Hangenberg Crisis (gray). Gray bars represent radiations, extinctions and diversity changes, while crosses represent extinctions (Kaiser et al., 2015).

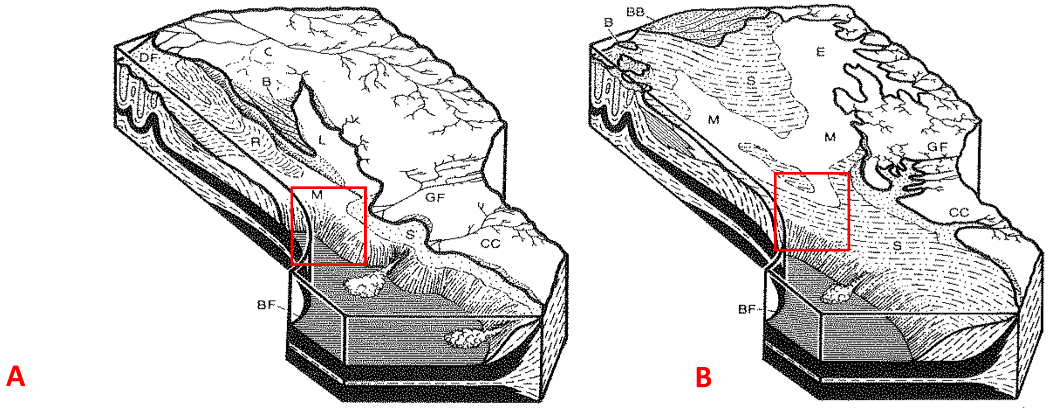

Figure 48. Regional depositional model for Bedford-Berea sequence (from Pashin and Ettensohn, 1995). A) Represents basin filling time, where fluvial systems down cut the Catskill wedge and provided sediment to the shelf. B) Depicts delta destruction time, where delta front deposits in the west were uplifted and redeposited. Red boxes indicate the general location of the study area.

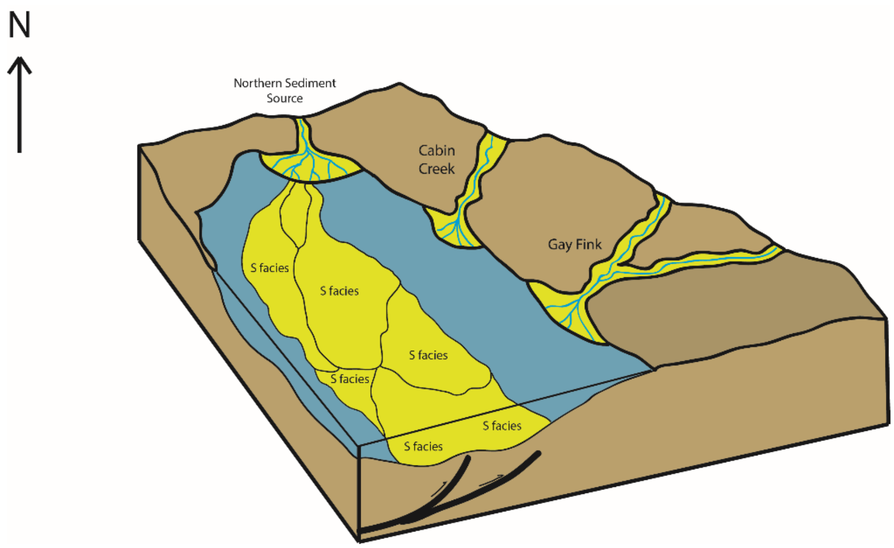

Figure 49. Predicted depositional environment of hyperpycnal beds within the Bedford-Berea sequence in northeastern Kentucky and southeastern Ohio (Modified from Zavala et al., 2011b). A northern fluvial source created hyperpycnal flows, which moved downslope and deposited sediment.

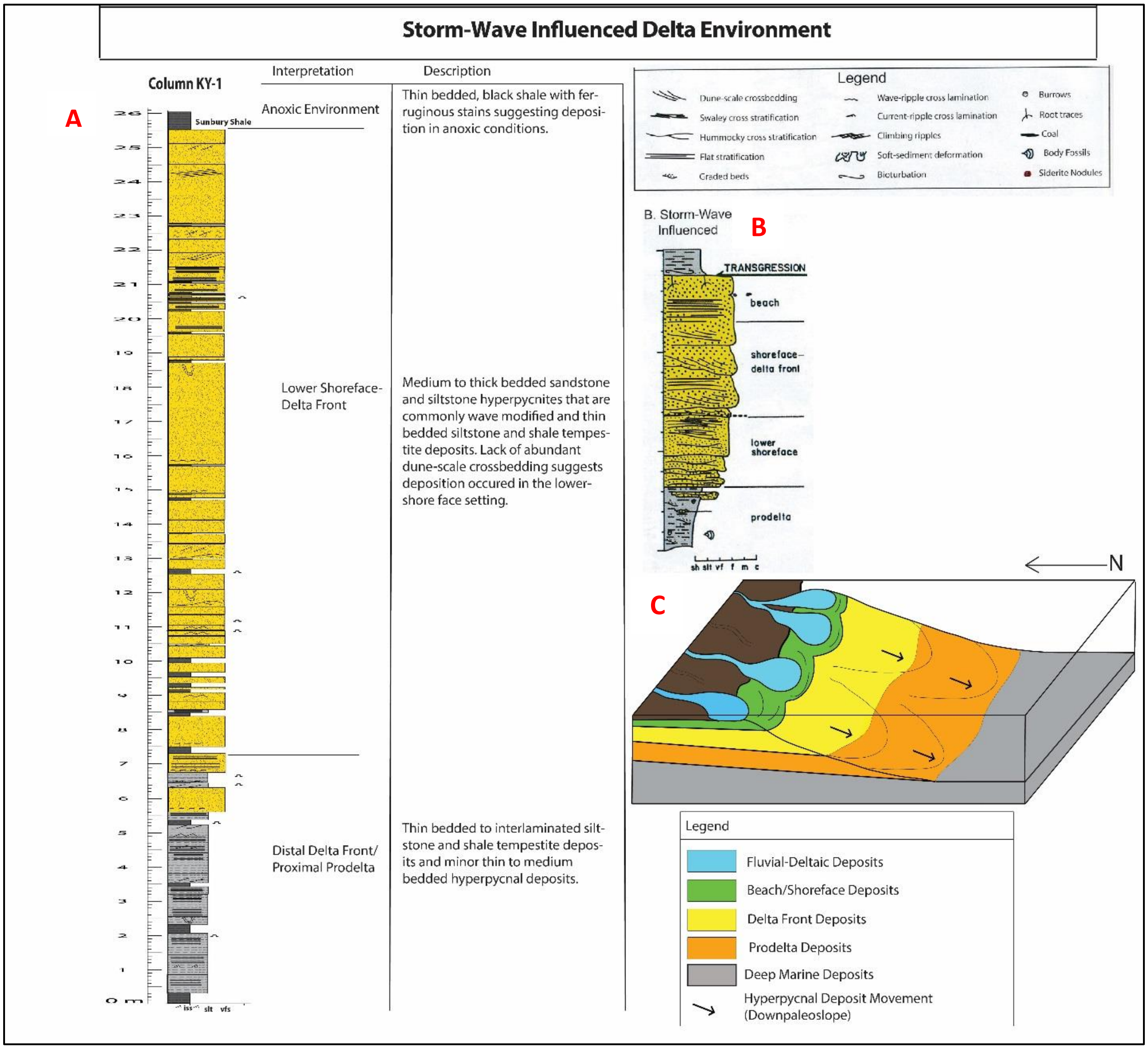

Figure 50. Typical Bedford-Berea stratigraphic column compared (A) compared to a general storm-wave influenced delta stratigraphic column (B) and a depositional model (C). A) Stratigraphic column for outcrop 1 with interpreted depositional environment and description of beds. The delta front and proximal prodelta environments contain sparse fauna due to salinity fluctuations and high turbidity rates, which inhibit burrowing, while prodelta deposits in normal deltaic environments have abundant fauna (Bhattacharya, 2011). B) Stratigraphic column B shows expected facies within a storm-wave influenced deltas in the Upper Cretaceous Dunvegan Formation (Bhattacharya, 2011). C) Simplified deltaic depositional model showing hyperpycnal flows moving down paleoslope.

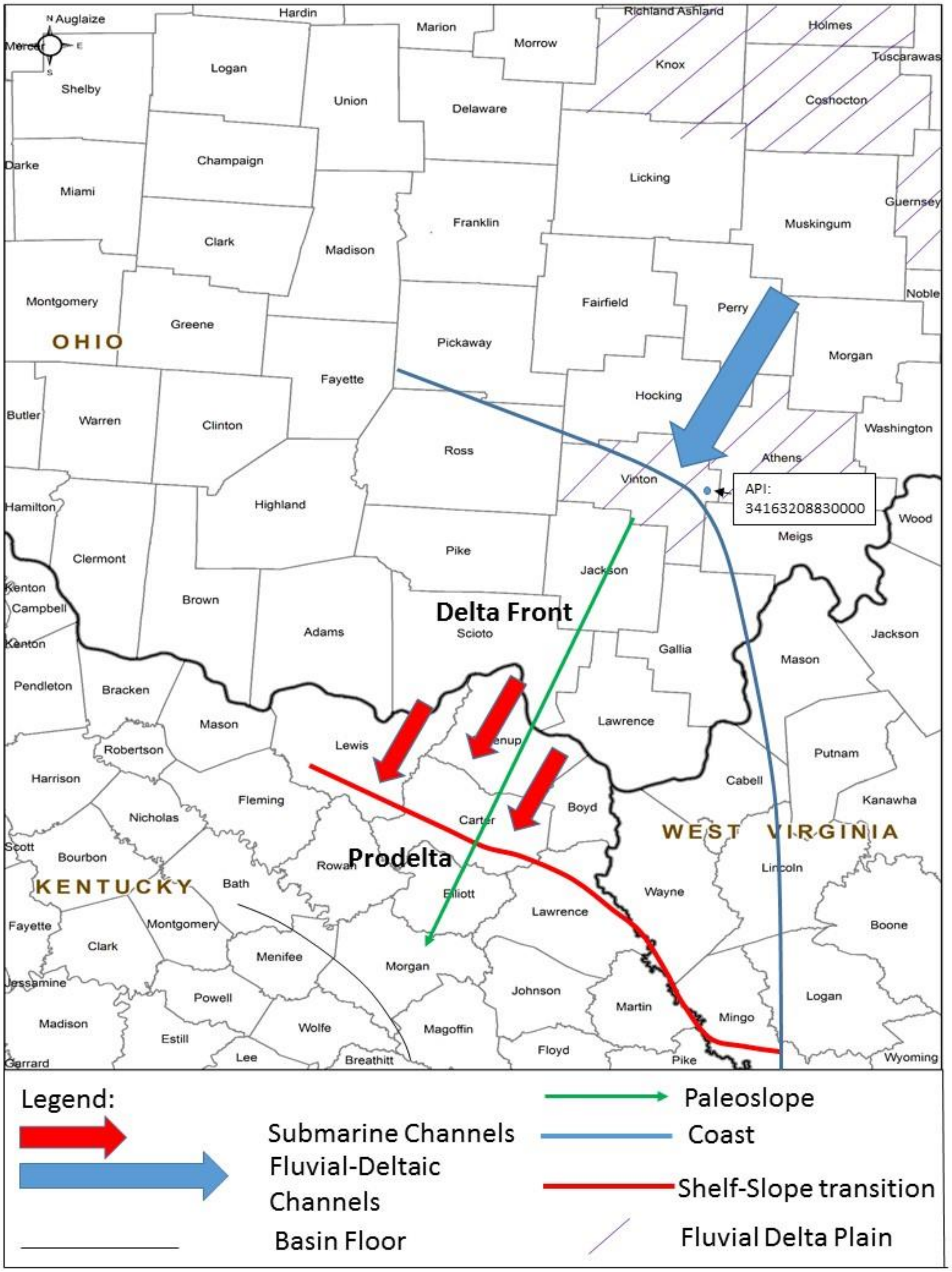

Figure 51. Depositional model during the lowstand system tract near the beginning of Bedford-Berea deposition. Delta front sediments dominate southeastern Ohio and northeastern Kentucky. Submarine channels formed near the shelf-slope transition in northeastern Kentucky, which are preserved in outcrop south of Vanceburg (Morris and Pierce, 1967) and in geophysical logs in northeastern Kentucky (Floyd, 2015). Fluvial and delta plain based on Tomastik (1996) report of fluvial and deltaic deposits.

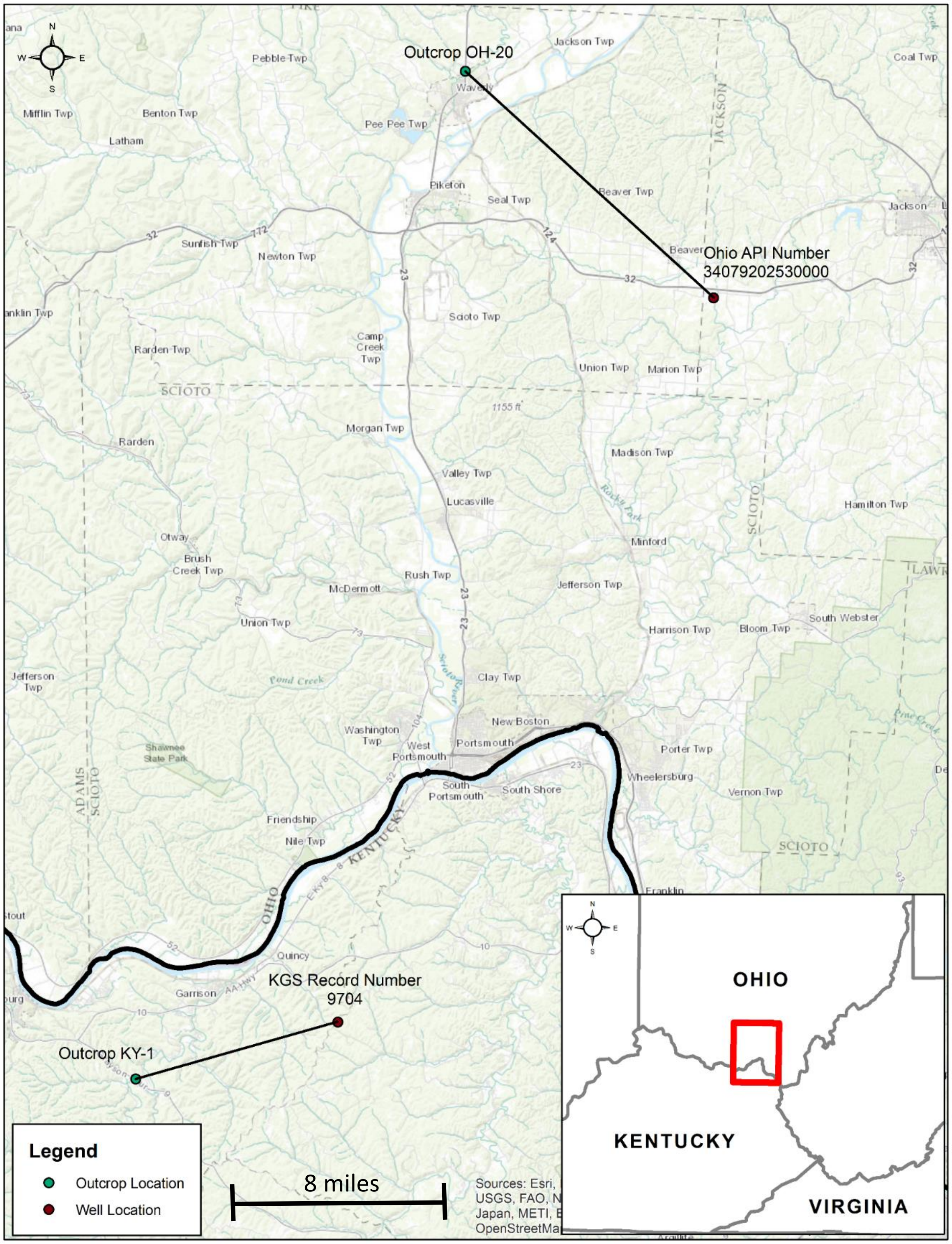

Figure 52. Map depicting the location of outcrops and nearby geophysical logs used in the correlation of outcrops to geophysical logs. A correlation was made in both Kentucky and Ohio to encompass the majority of the study area.

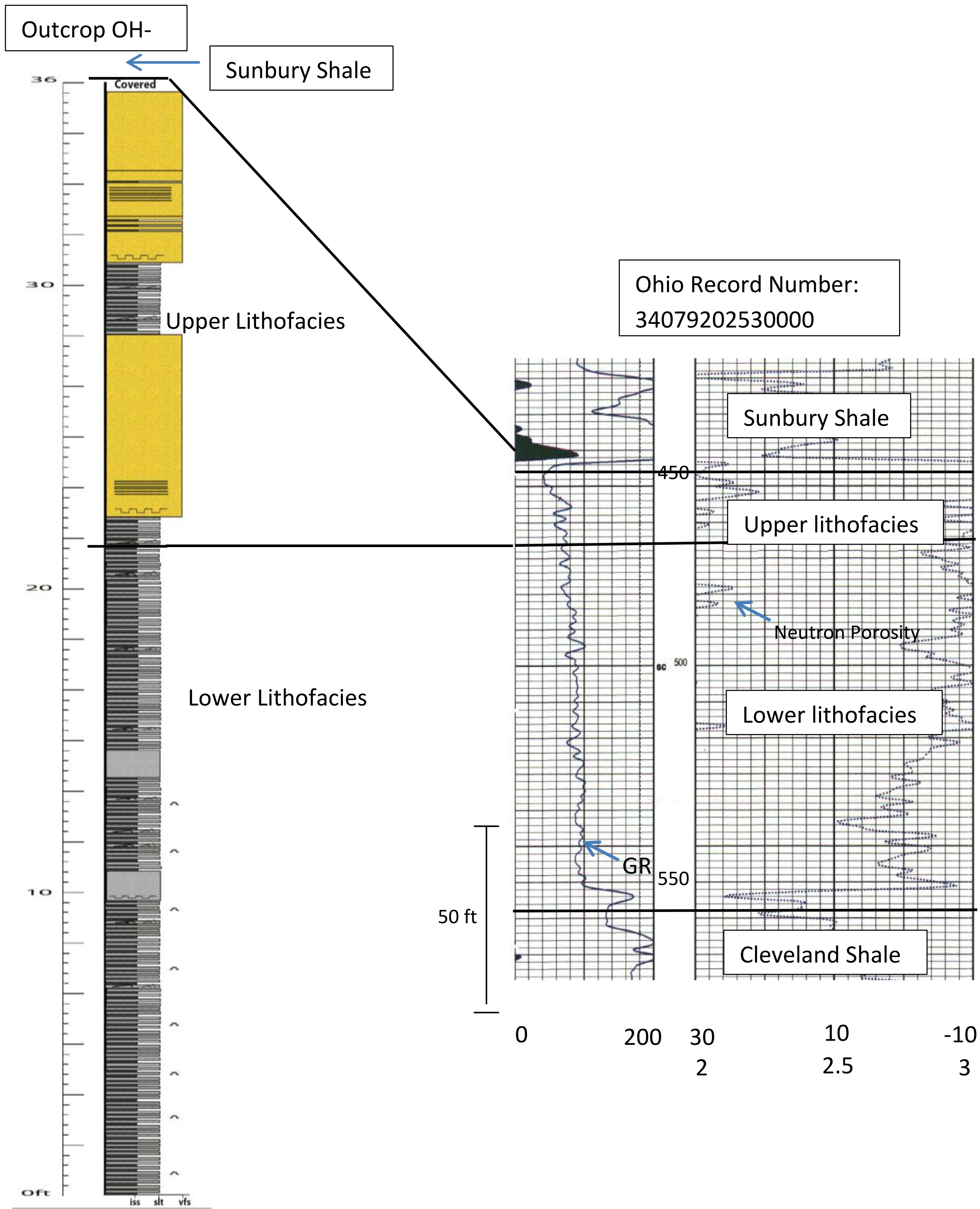

Figure 53. Stratigraphic column of outcrop 20 in southeastern Ohio correlated to a geophysical log (OH 34079202530000) illustrating how Bedford-Berea facies are represented in the subsurface (Figure 46 shows location).

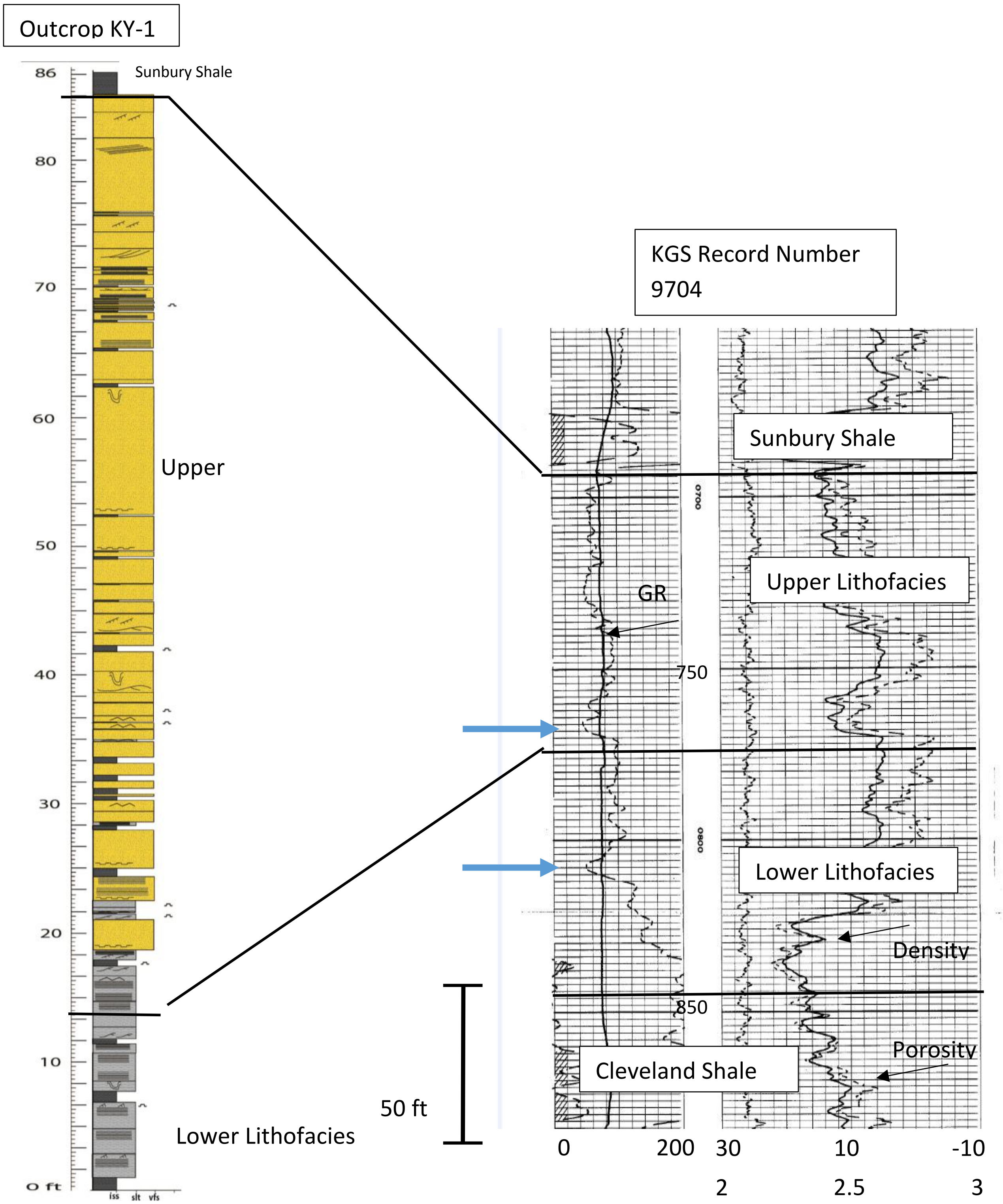

Figure 54. Stratigraphic column of outcrop 1 in northeastern Kentucky correlated to a nearby geophysical log (KGS 9704) illustrating how Bedford-Berea facies are represented in the subsurface. The location of KGS 9704 and the location of outcrop 1 is shown in Figure 46. Blue arrows indicate bell-shaped log patterns representing submarine channels, which are the best reservoir rock. First scale (on right) is a porosity scale and second scale is a density scale.

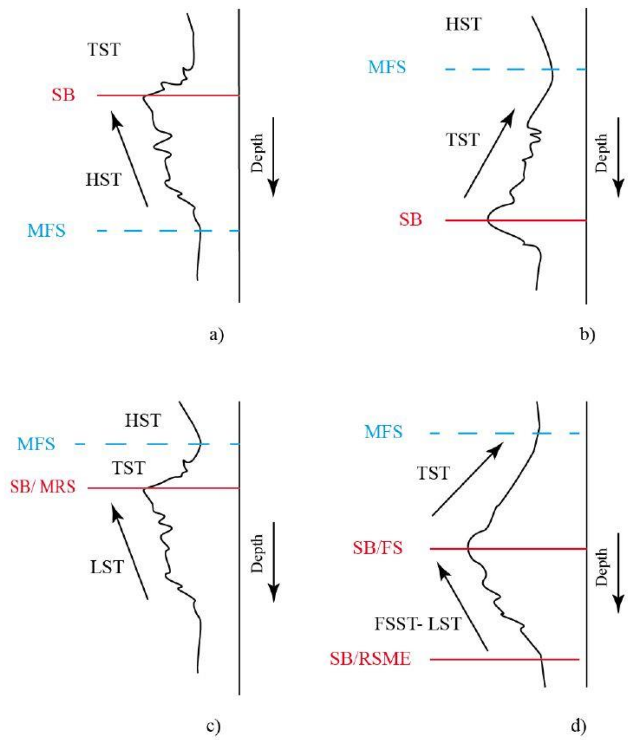

Figure 55. System tracts model within gamma-ray logs (Rider, 1996; Plint and Nummedal, 2000; Catuneanu, 2002).

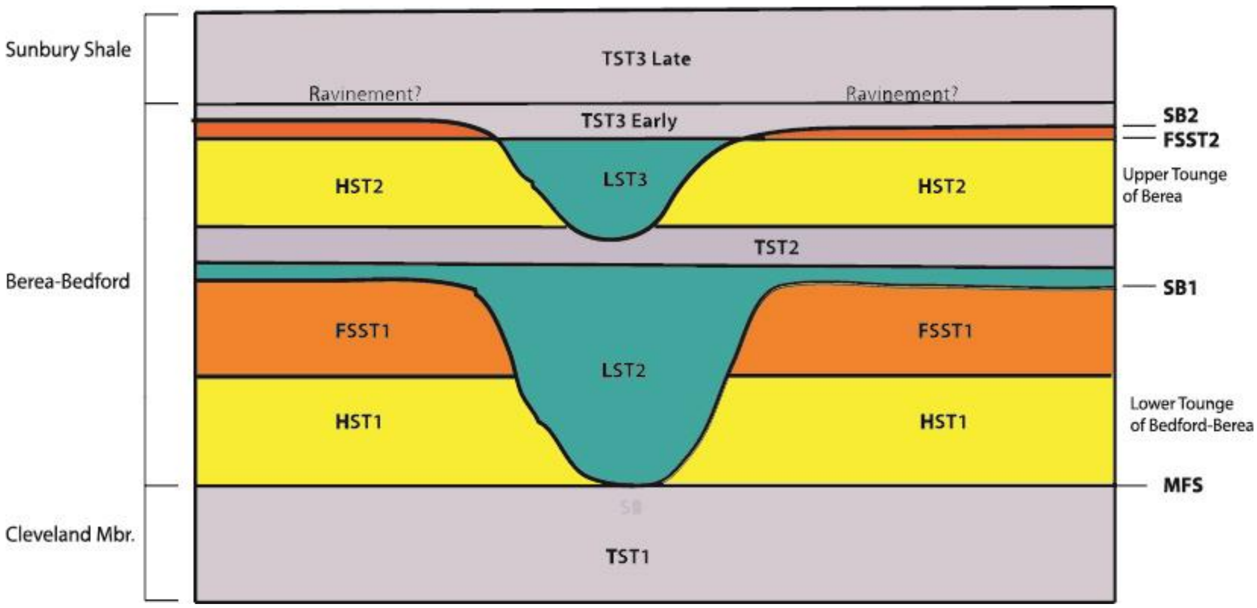

Figure 56. Sequence stratigraphy of the Bedford-Berea sequence in northeastern Kentucky and southern Ohio. Two sequences are present within the Bedford-Berea interval (SB1 and SB2). The first falling stage systems tract (FSST1) is suggested by submarine channels in northeastern Kentucky. The second Falling stage system tract (FSST2) indicated by Berea channel incision into the Red Bedford Shale in central Ohio (Pepper et al., 1954). Ettensohn (1994) reported a fossiliferous transgressive lag at the base of the Sunbury Shale, which has been interpreted to represent a major unconformity. The transgressive lag may be erosive and involve ravine development and be underlain by a firmground substrate.

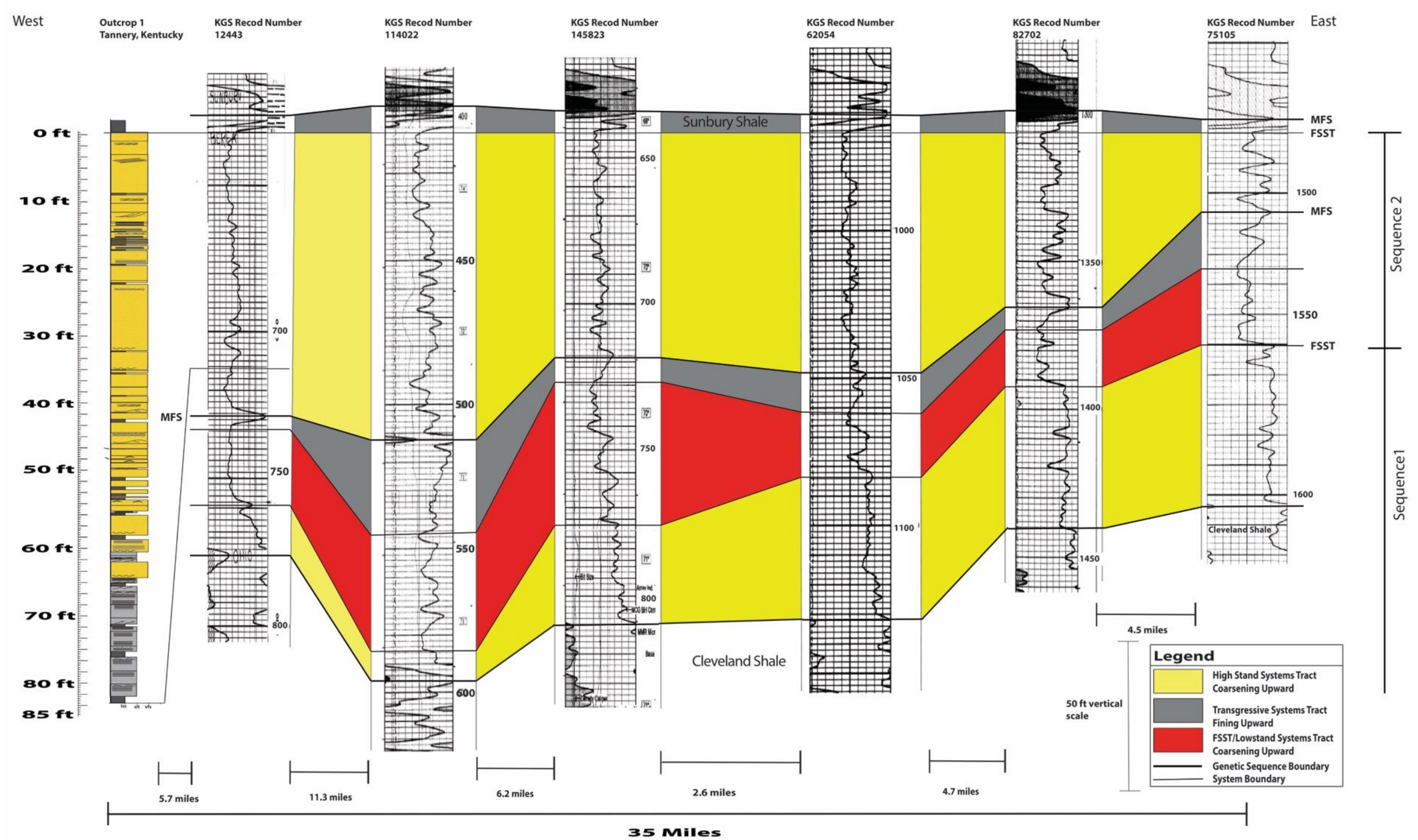

Figure 57. Outcrop to well log correlation of systems tracts within the Bedford-Berea sequence. The highstand systems tract in the Bedford Shale thins to west due to down cutting of submarine channels during the lowstand system tract. An obvious transgressive system tract is present throughout northeastern Kentucky, although it does thin due to down cutting of submarine channels during the following highstand system tract. All of outcrop 1 represents deposits deposited during a second highstand systems tract with a coarsening upward grain size pattern. Location of wells on figure 58.

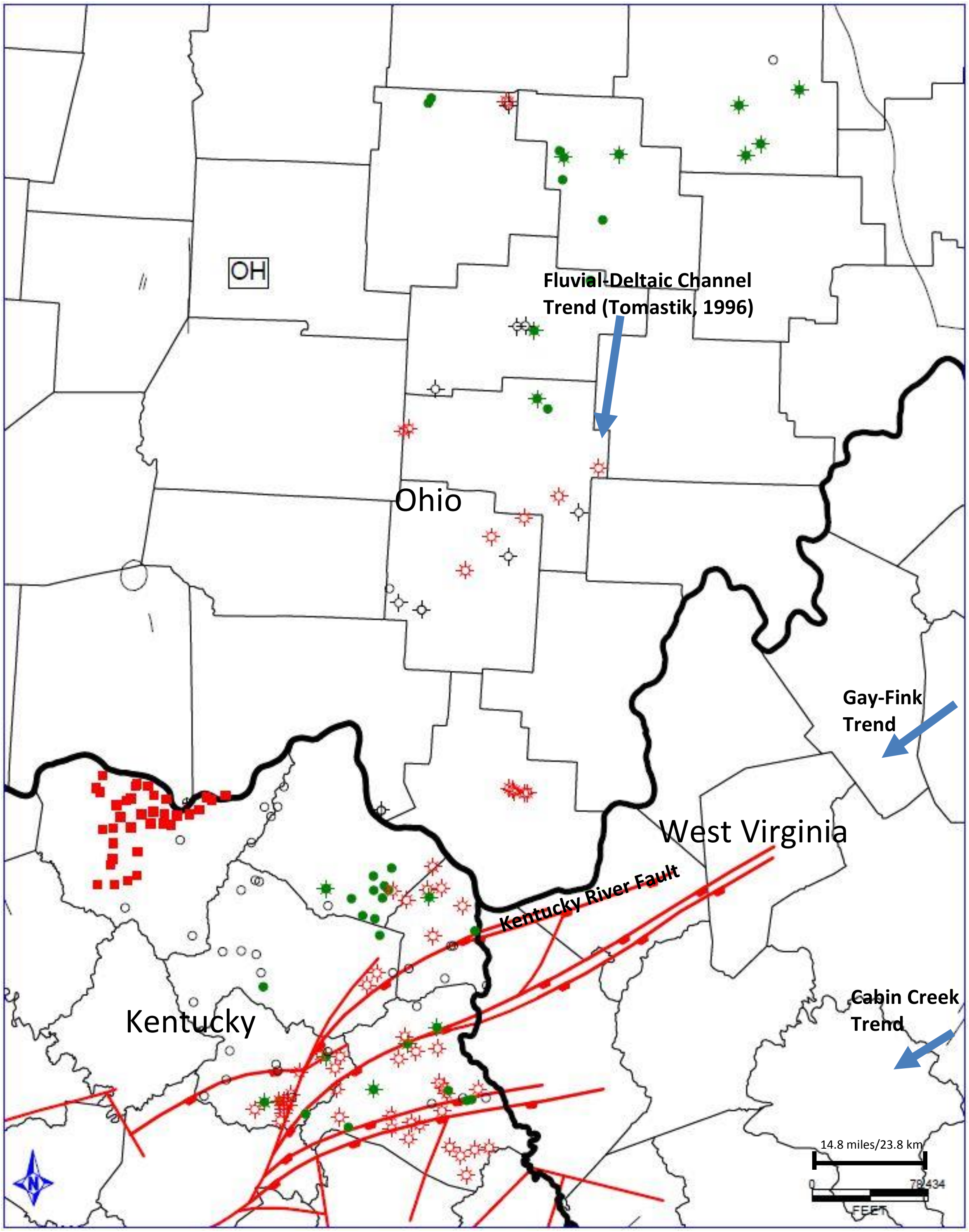

Figure 58. Location of geophysical logs and GQ map points (red squares) examined in this study. Geophysical logs in southeastern Ohio were analyzed for the presence of fluvial-delatic log signatures, while logs in northeastern Kentucky were examined for net sand thicknesses and submarine channel logs. The blue arrows represent the Gay-Fink and Cabin Creek fluvial trends in West Virginia and the fluvial-deltaic trend in central Ohio (Tomastik 1996).

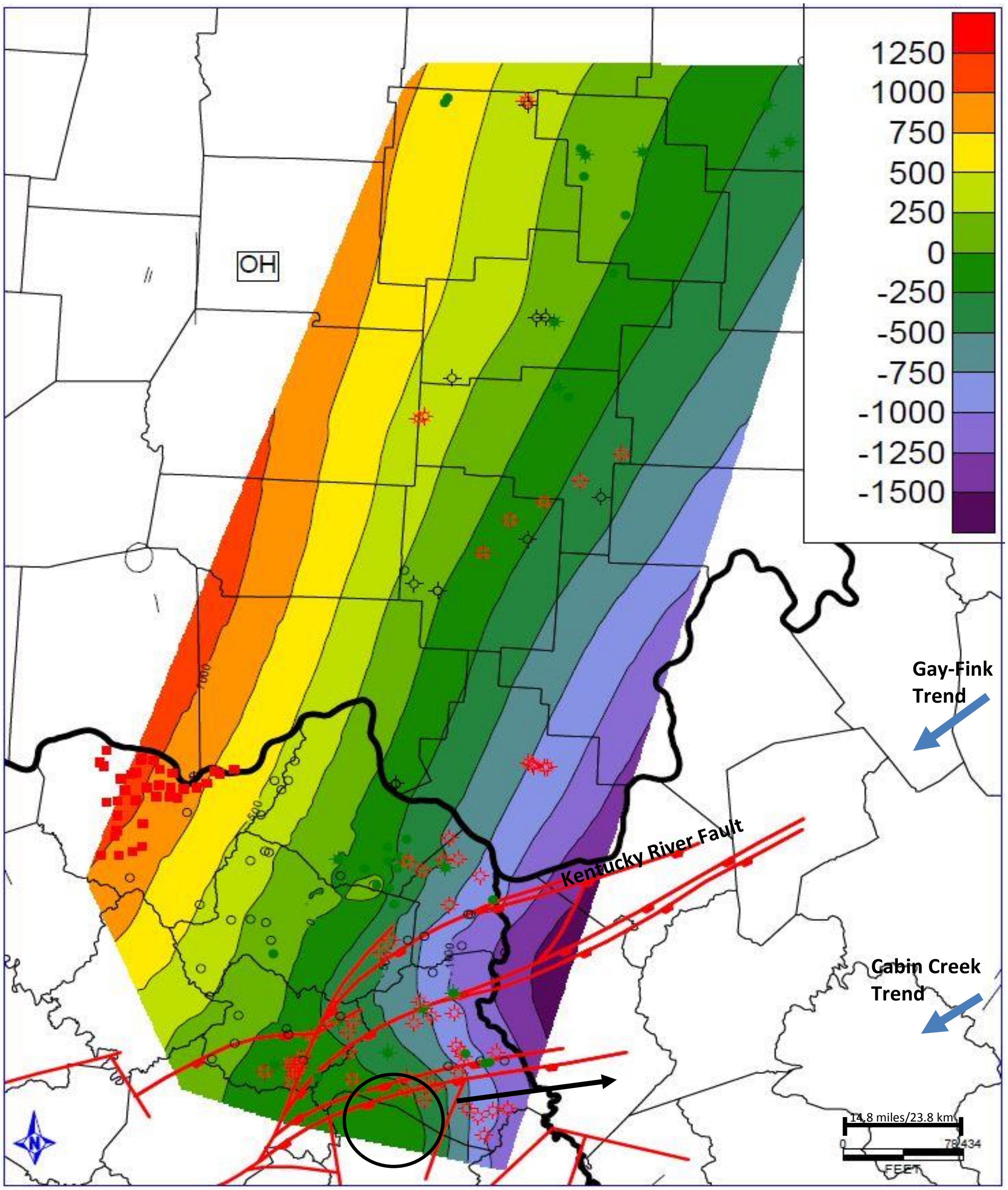

Figure 59. Structure contour map constructed for the top of the Berea sandstone in northeastern Kentucky and southeastern Ohio. The Berea Sandstone has a regional dip to the southeast. The black circle represents the Paint Creek Uplift and the black arrow indicates the plunge direction of the Hood Creek anticline.

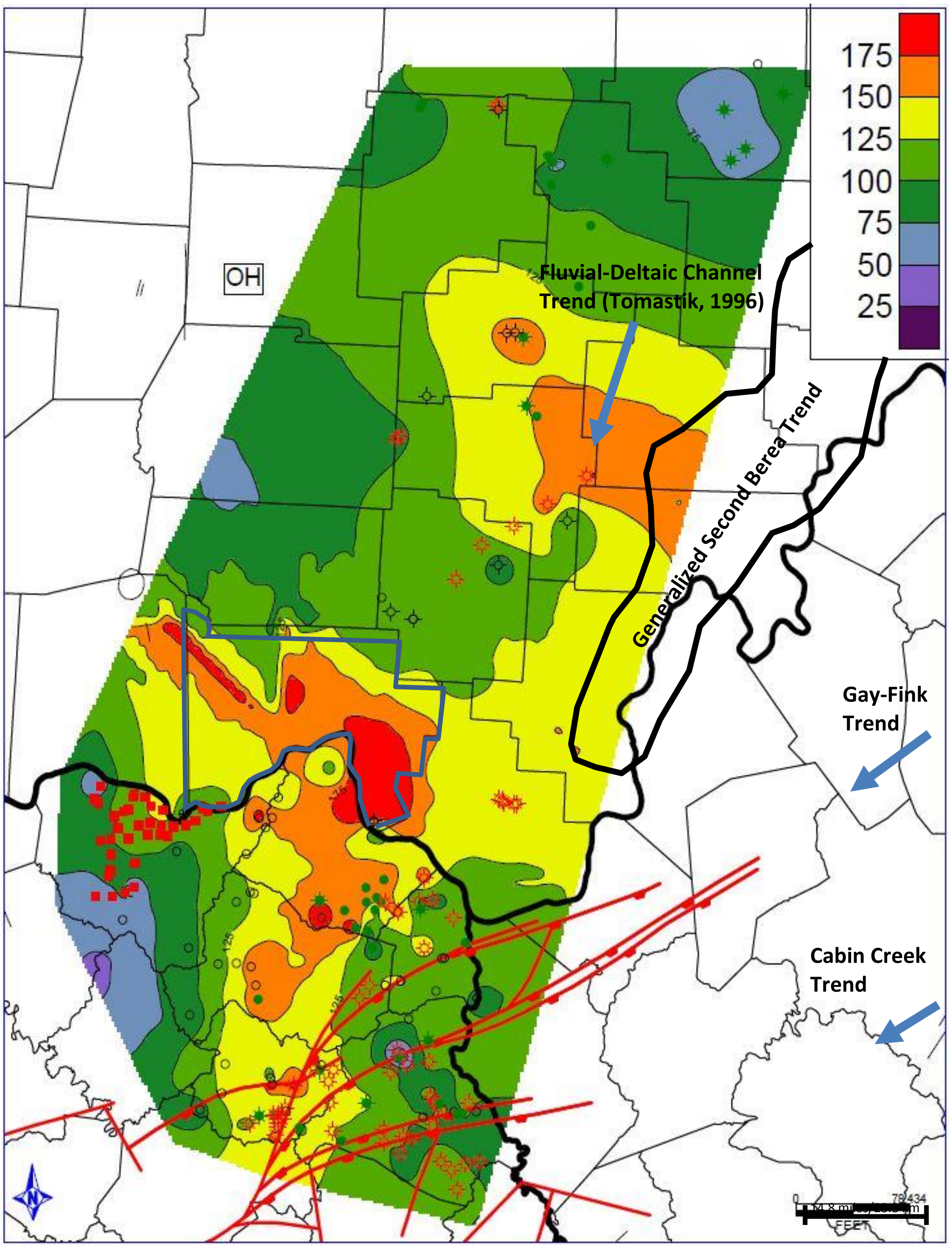

Figure 60. Bedford-Berea isopach map in northeastern Kentucky and southeastern Ohio. The isopach shows a thin north-south oriented thickness trend in northeastern Kentucky. In southeastern Ohio an east-west thickness trend is apparent; however, no gamma ray logs in Scioto County, Ohio were used due to lack of availability, which caused extrapolation to occur in Scioto County (outlined in blue). The barrier island deposited second Berea is outlined in black in Ohio. The south trending fluvial-deltaic channel in central Ohio sourced sediment to the study area.

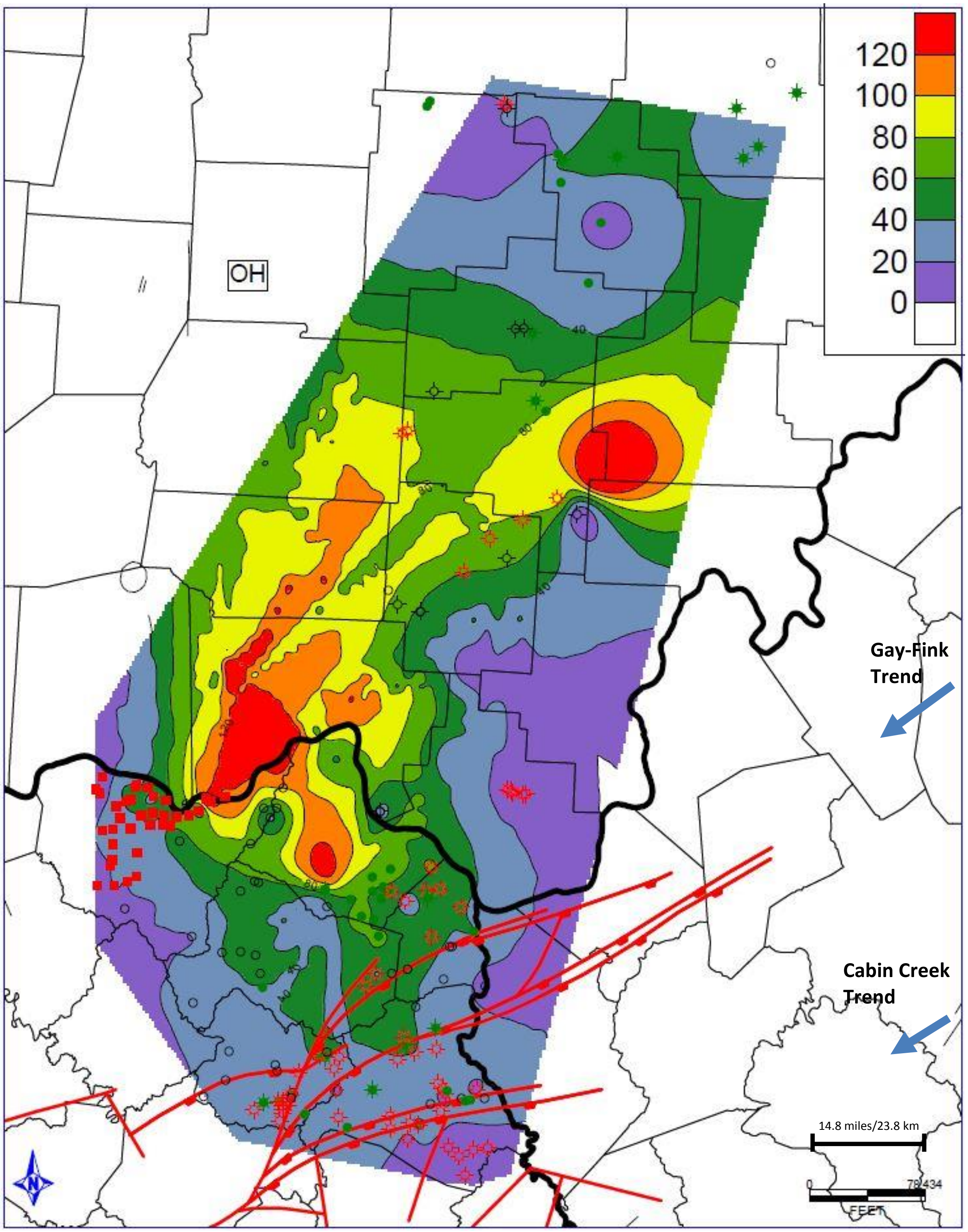

Figure 61. Net Berea isopach map using a gamma-ray cutoff of 101 API units which Floyd (2015) interpreted to be a best-fit signature for sand in log-to-core comparisons. Red lines represent Pre-Cambrian basement faults.

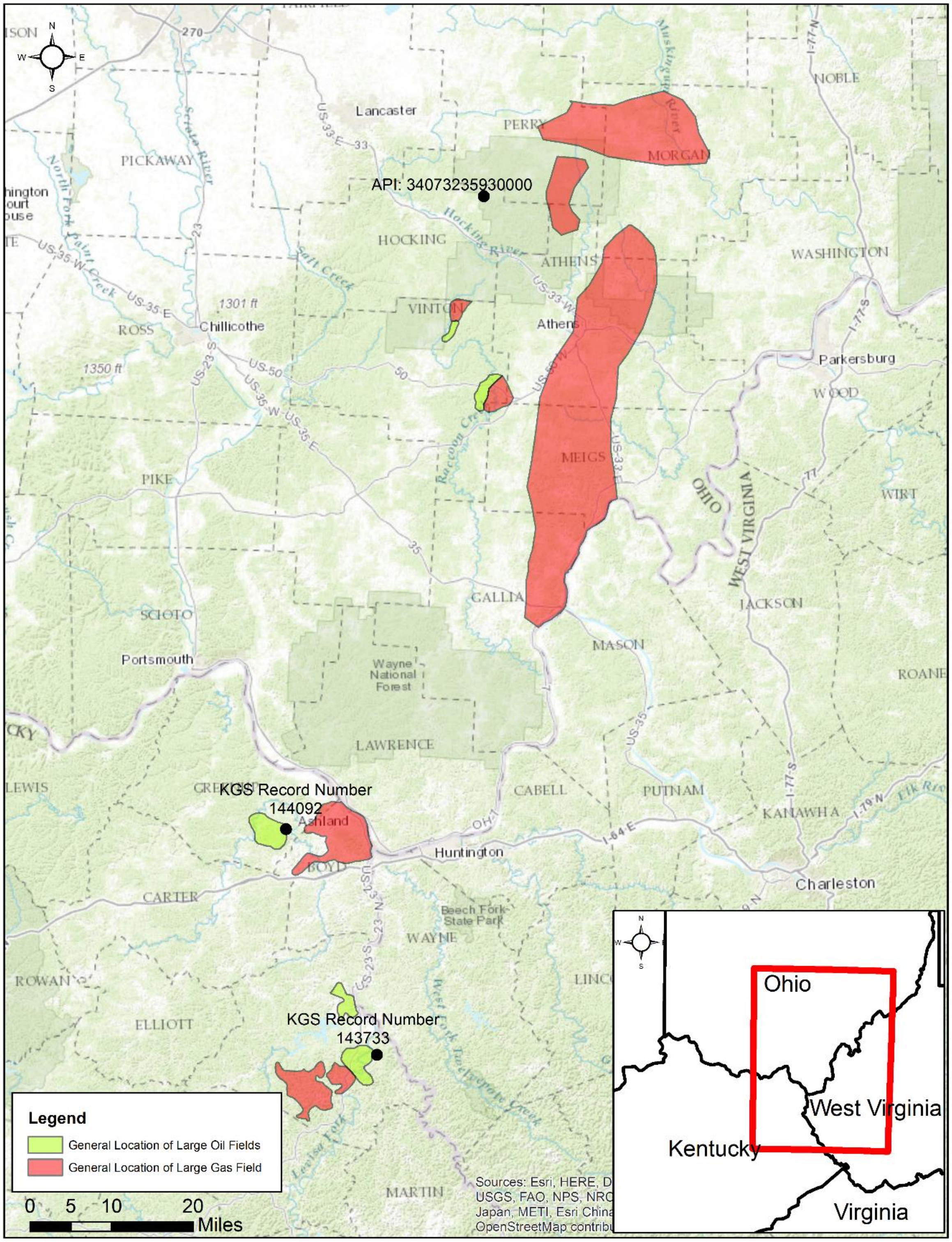

Figure 62. Location of large Bedford-Berea sequence oil and gas fields. Small oil and gas field are present throughout the study area.

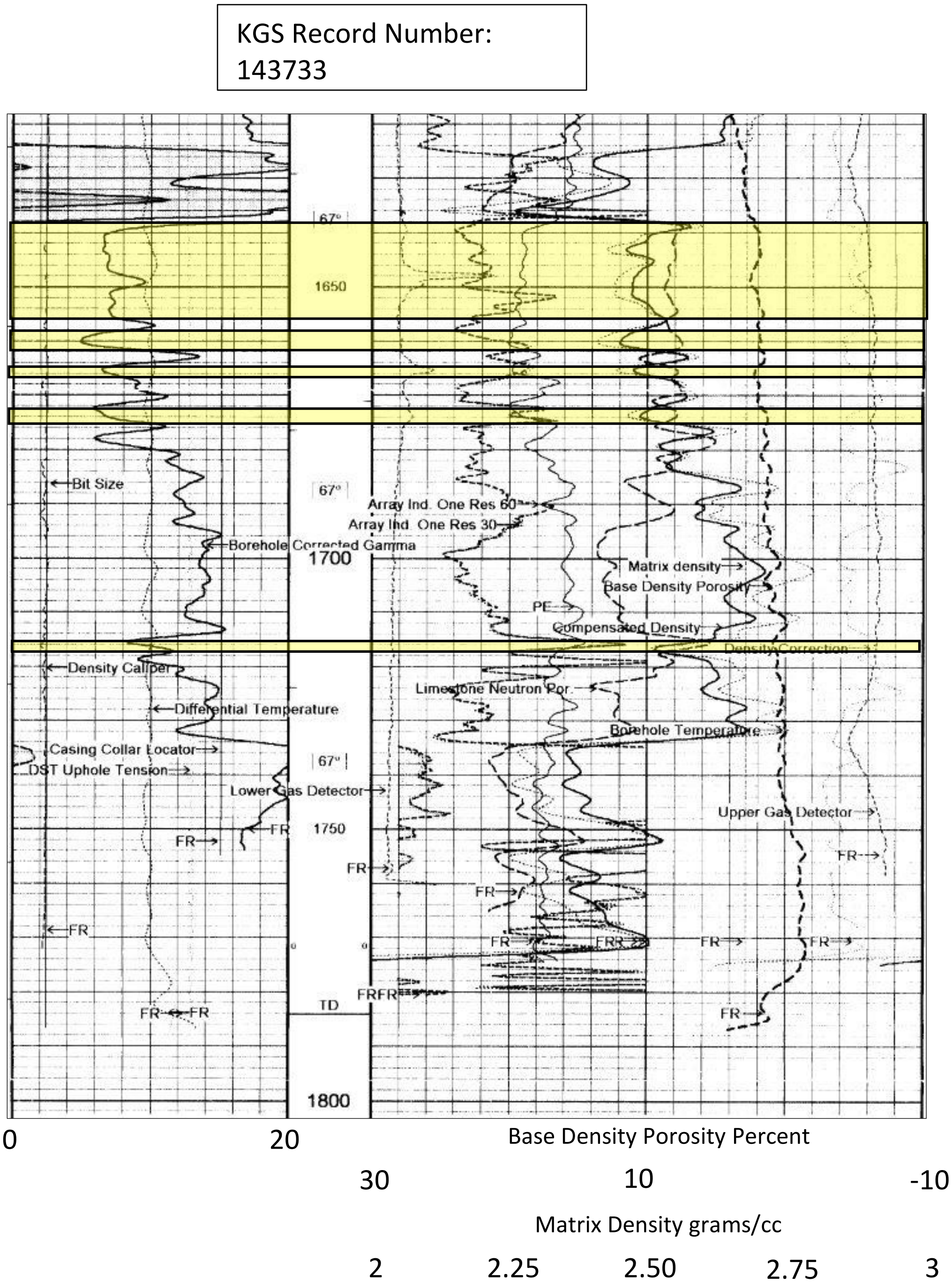

Figure 63. Geophysical log highlighting the Bedford-Berea reservoir in Lawrence County, Kentucky in the Beech Farm Consolidated Field. The thickest and most productive sands are near the top of the Bedford-Berea sequence, the thickest being 14 feet thick, whereas a thin pay sand is present near the bottom of the Bedford-Berea sequence. Location on figure 61.

KGS Record Number:
144092

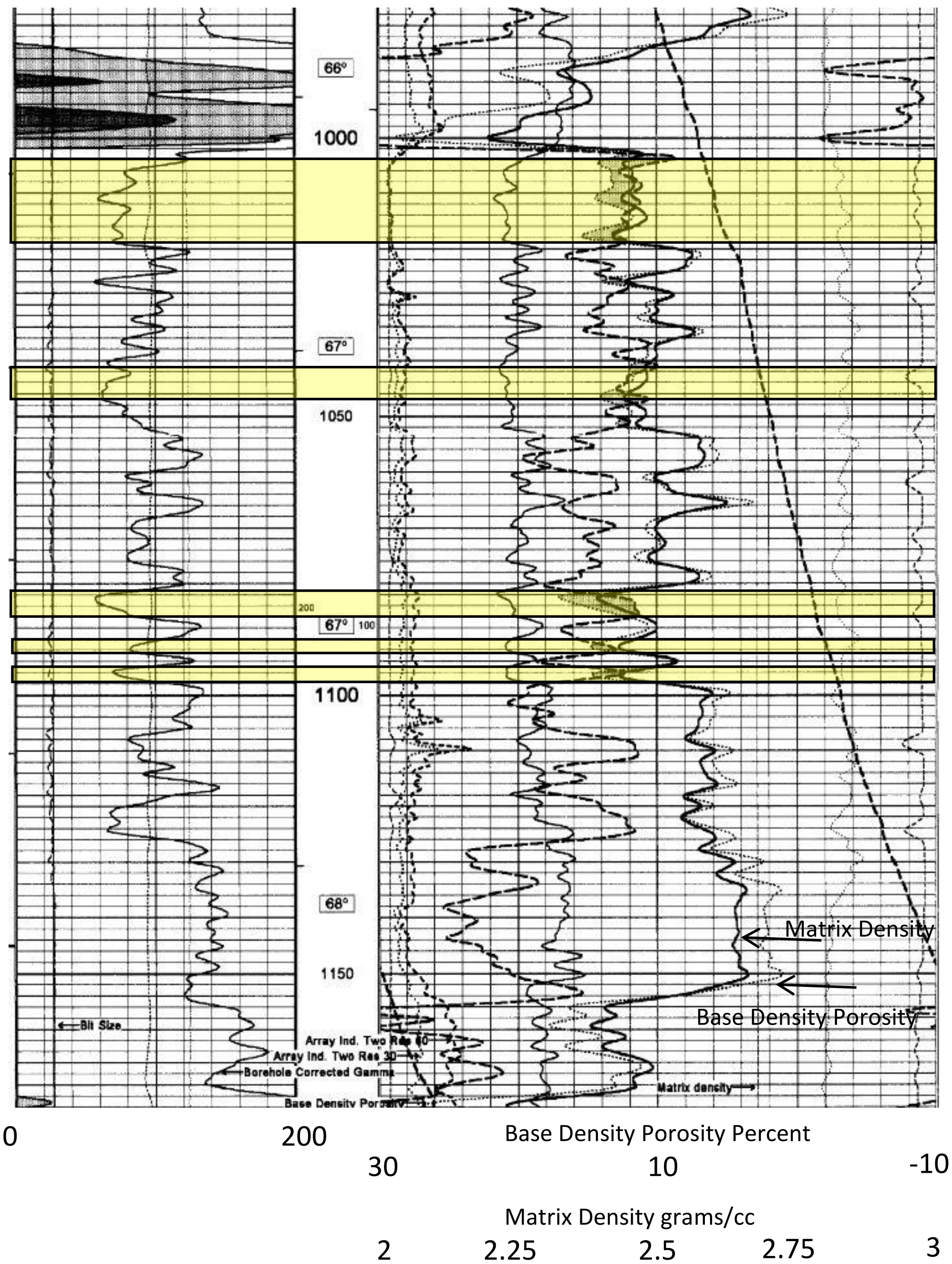

Figure 64. Geophysical log highlighting the Bedford-Berea reservoir in Greenup County, Kentucky in a new horizontal field. Similar to reservoirs in Lawrence County, Kentucky the thickest and most productive sands are at the top of the Bedford-Berea sequence, the thickest being 15 feet thick. Multiple pay sands are present near the bottom of the Bedford-Berea sequence and are much thicker than the lower pay sand found in Lawrence County, Kentucky.

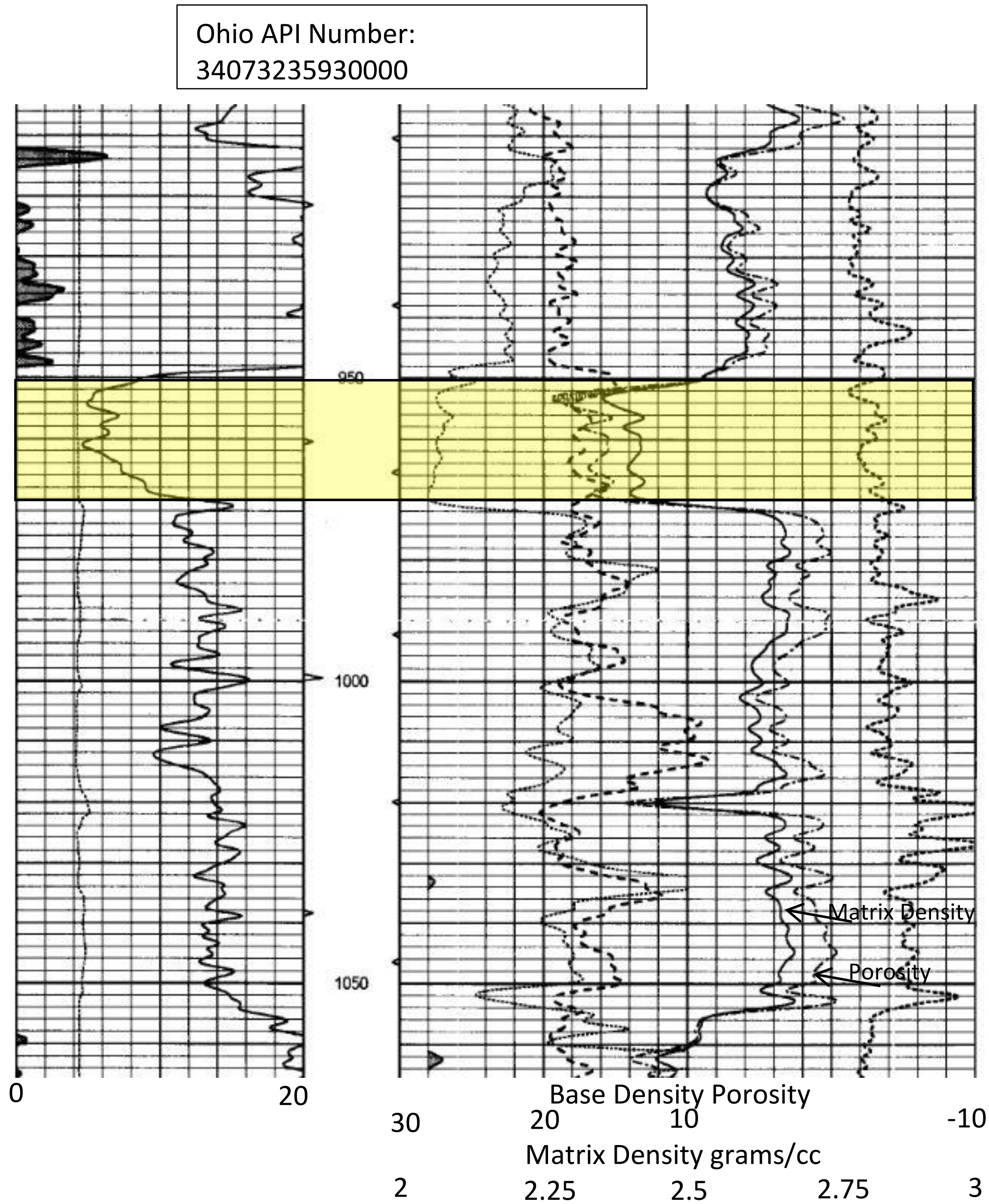

Figure 65. Geophysical log highlighting the Bedford-Berea reservoir in Hocking County, Ohio in the Old Gore gas field. The Bedford-Berea sequence in southeastern Ohio has one distinct pay sand, which occurs at the top of the Berea Sandstone and in this log is 19 feet thick with porosity values up to 18 percent.

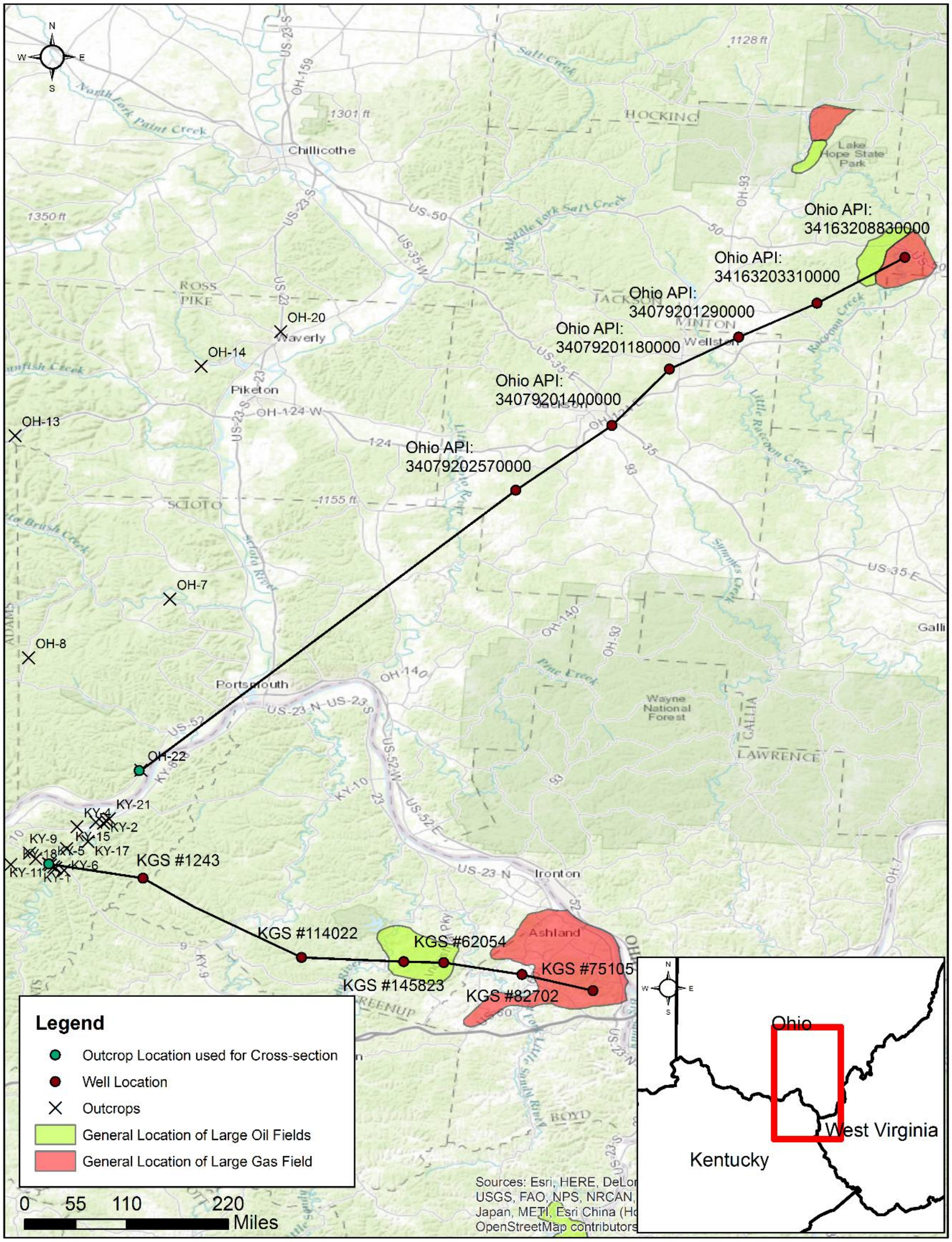

Figure 66. Locations of outcrops and wells used for the outcrop and geophsyical log correlations.

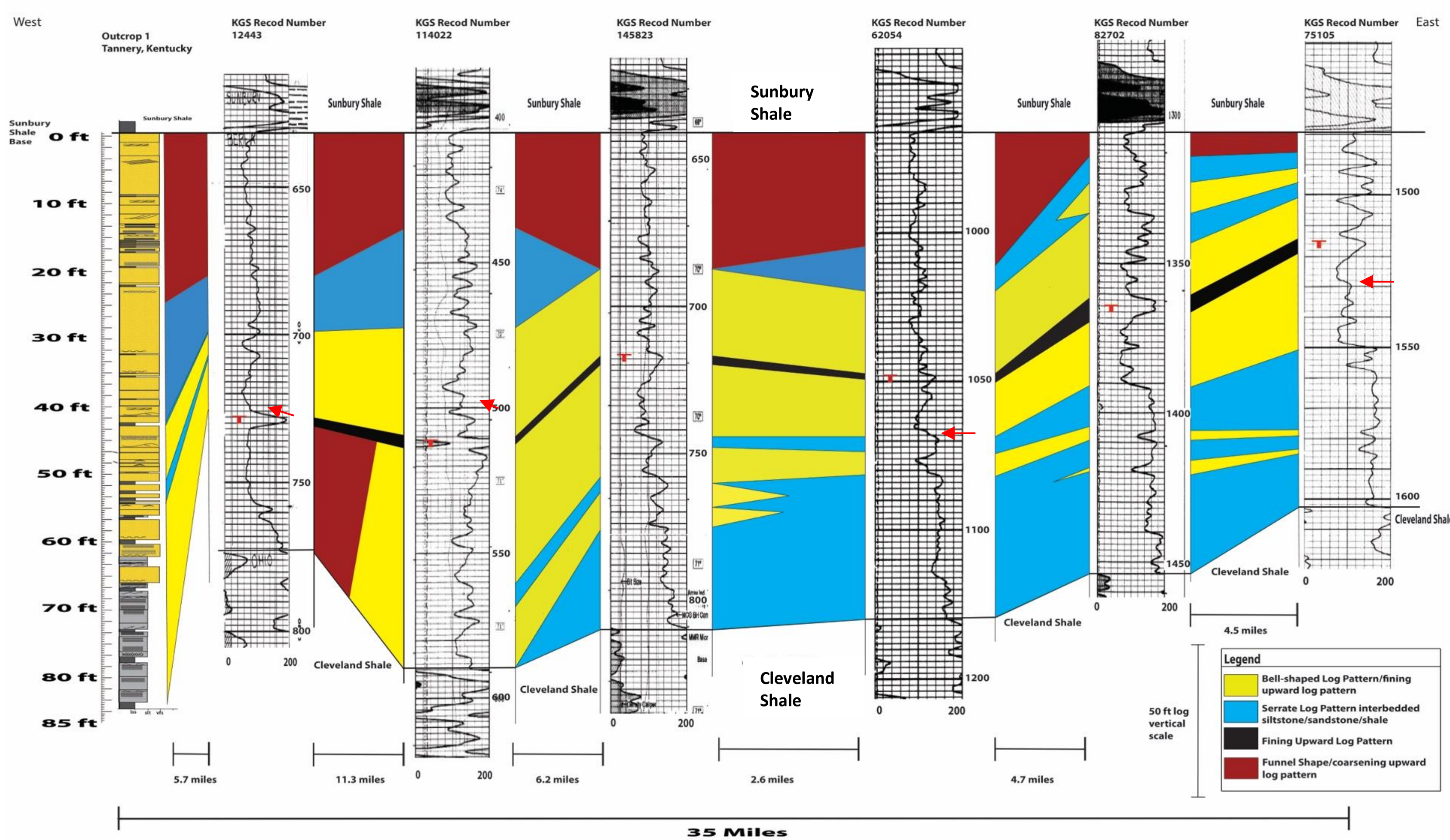

Figure 67. Correlation of KY-1 to nearby geophysical logs going from West-East. Note how the overall thickness of the Bedford-Berea thins towards the east. A transgressive event is present in all geophysical logs, although it becomes harder to differentiate at the eastern extent of the cross-section (marked by red T). Red arrows indicate distinct bell-shaped patterns within the Bedford-Berea sequence, which range from as small as six feet to upwards of 30 feet thick. These channel signatures were the result of the advance of submarine channels during the falling-stage and lowstand system tracts.

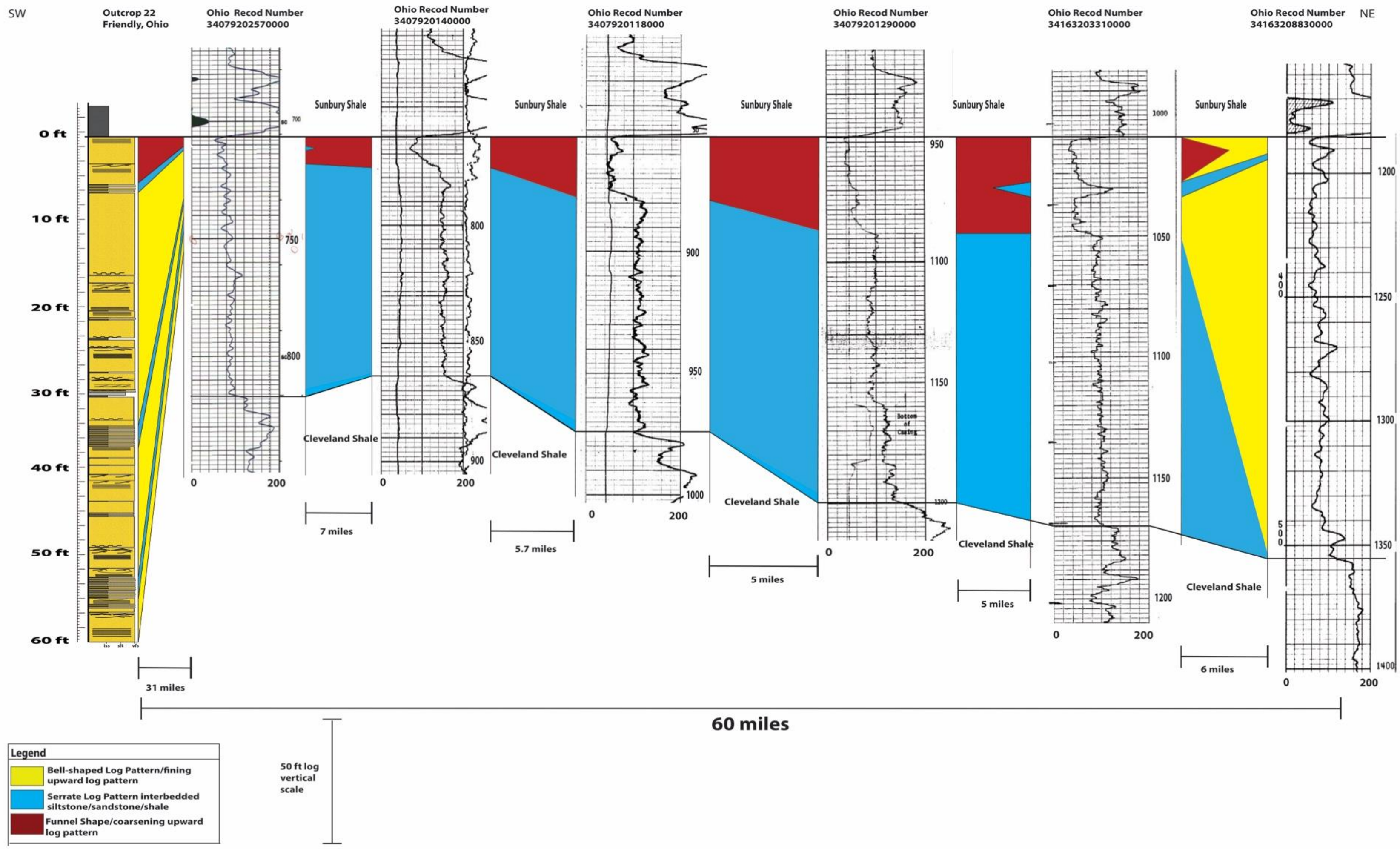

Figure 68. Illustrates the outcrop to subsurface correlation of outcrop OH-22 to nearby geophysical wells in southeastern Ohio. The upper 2 meters of Berea in outcrop correlates to funnel-shaped log pattern in the subsurface. Furthermore, moving northeast away from outcrop OH-22 this funnel-shaped pattern thickens. API number 34163208830000 is the last well in the cross section and has been interpreted to represent a fluvial-deltaic channel with a bell-shaped dominated log pattern in the Bedford-Berea sequence (Tomastik, 1996).

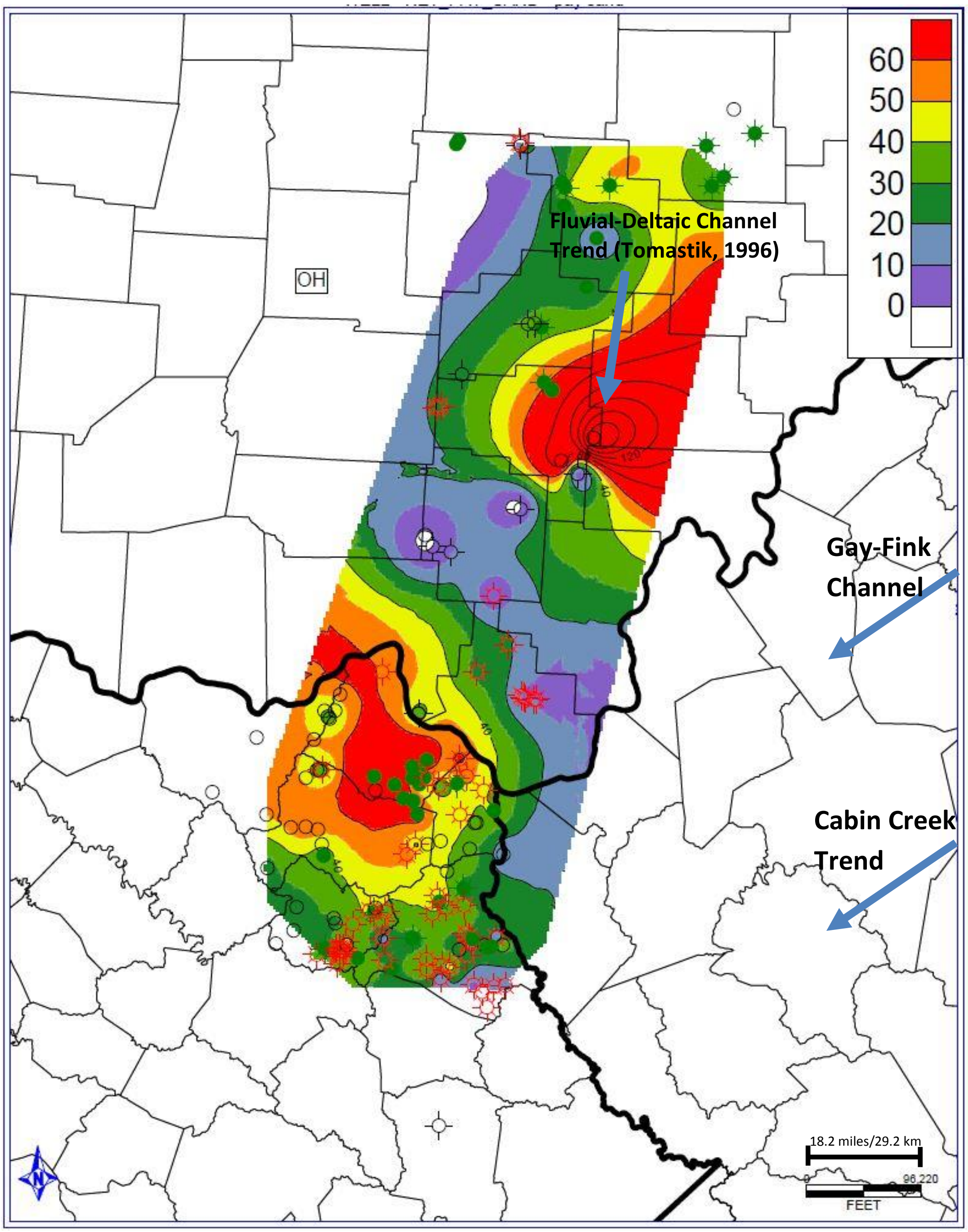

Figure 69. Net pay sand map within the Bedford-Berea sequence. The thickest pay sand occurs in Vinton County, Ohio (160 ft) due to the presence of a fluvial-deltaic channel and was less than ½ mile wide (Tomastik, 1996). The increased pay in eastern Vinton County, Ohio near the fluvial-deltaic channel may also contain the second Berea. In northeastern Kentucky, the thickest pay sand occurs in Greenup County, Kentucky and averages 60 feet thick.

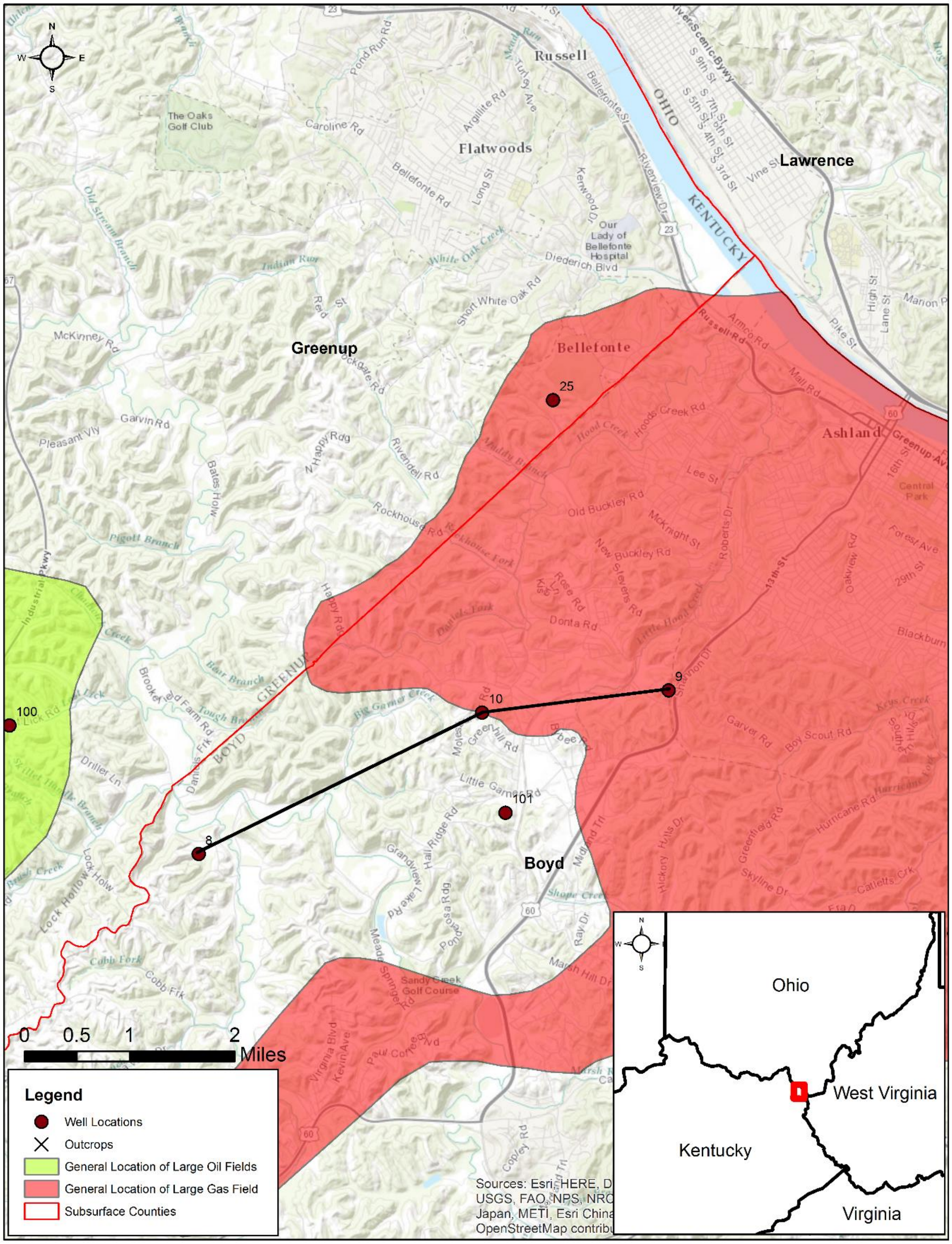

Figure 70. Location map of cross section through the Ashland Gas Field in Boyd County, Kentucky.

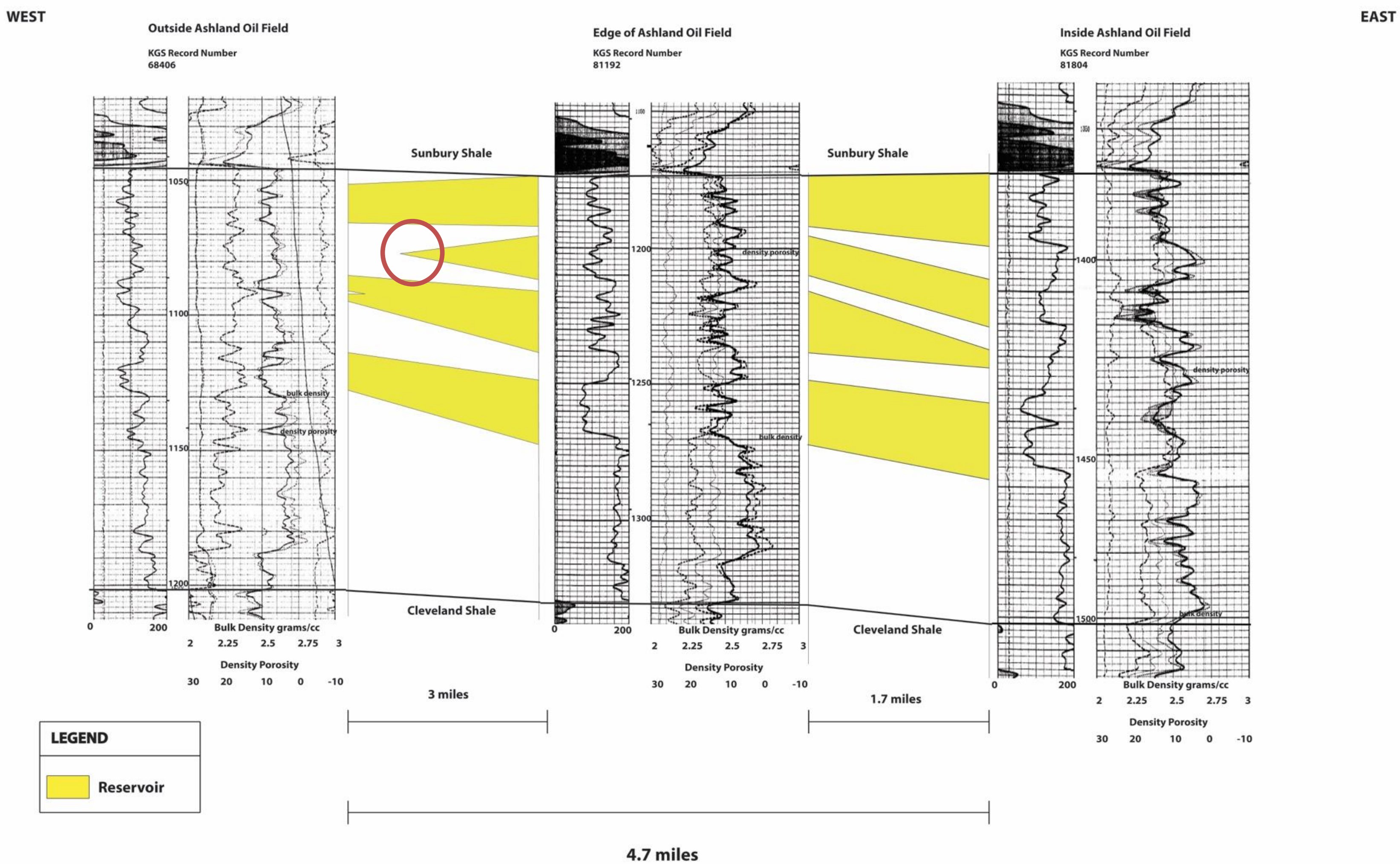

Figure 71. Cross section of the Ashland Gas Field in Boyd County, Kentucky. Facies changes and diagenetic changes control oil accumulation laterally, while thin shales act to compartmentalize pay zones within the field. Digaenetic changes (red circles) occur when the gamma ray signatures remain the same but porosity and permeability is lost. The red circle in this figure also corresponds to the most prolific producing zone in this field (1190-1210) according to driller logs and is based on how quickly it losses porosity outside of the field stopping gas from migrating further up dip

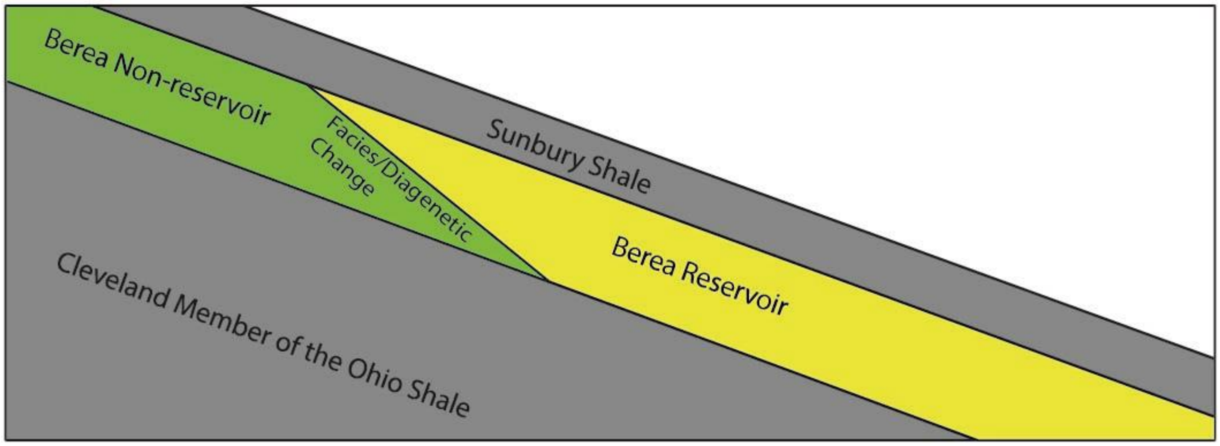

Figure 72. Schematic cross sectional illustration of facies and diagenetic changes cause the accumulation of hydrocarbons in the Ashland Gas Field. As hydrocarbons migrate up-dip they reach an impermeable/low porosity zone and can no longer migrate up dip causing pooling of oil and gas at the boundary.

CHARTS AND TABLES

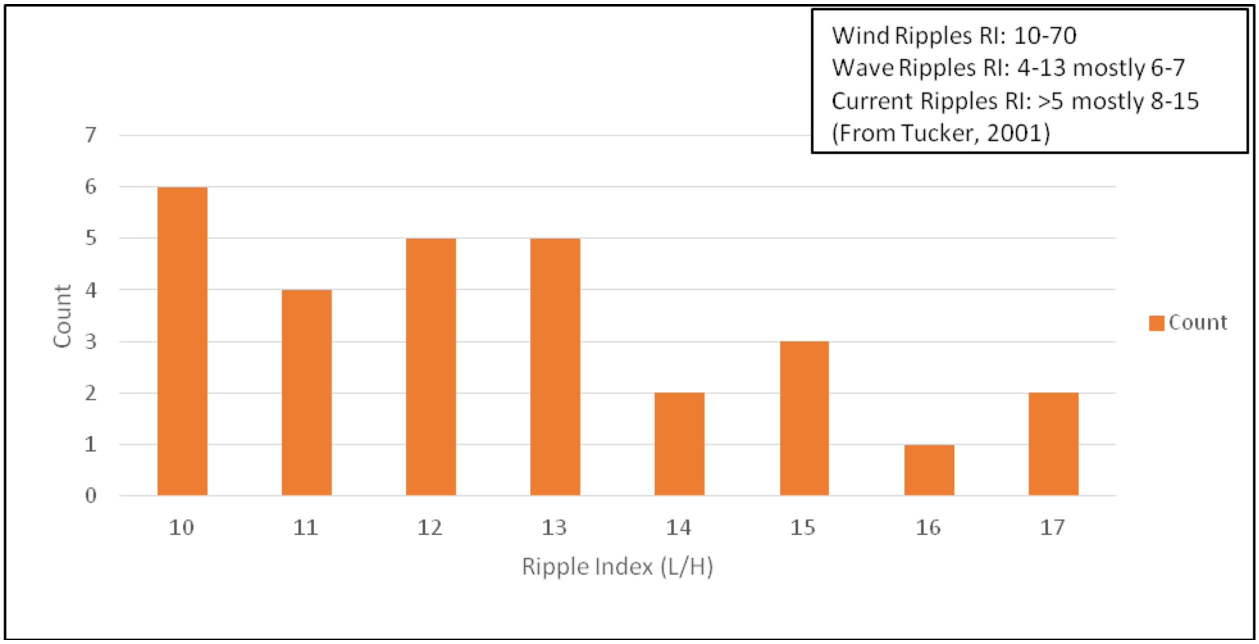

Chart 1. Ripple index values of oscillatory ripples in the Lower Bedford/Berea Lithofacies. The majority of the ripple indexes plot within the current ripple range. In outcrop, ripples are often associated with combined flow structures such as micro-hummocky cross-stratification indicating that ripples were produced under combined flow conditions and are combined flow ripples.

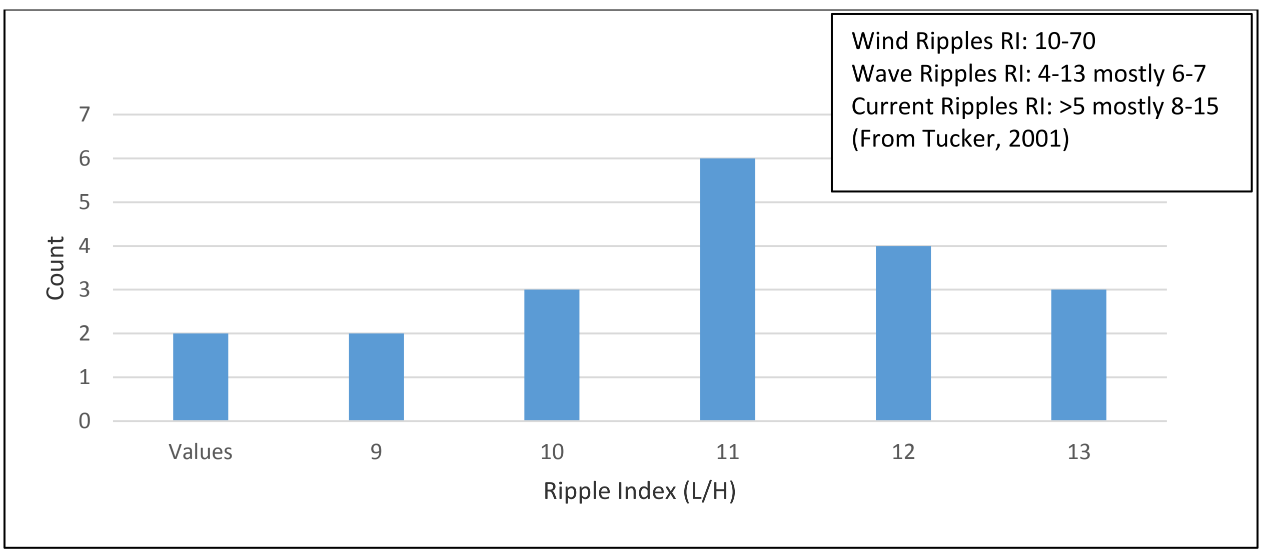

Chart 2. Ripple index values of oscillatory ripples in the Upper Berea Lithofacies. Ripple indices of the Upper Berea Lithofacies are similar to those within the Lower Berea Lithofacies and are associated with combined flow structures such as micro-hummocky cross-stratification indicating the presence of both unidirectional and oscillatory flows.

Table 1.

Facies Assemblage	Lower Lithof.	Description	Grain Size	Sedimentary Structures	Trace Fossils	Geometry
Assemblage A-B	A	Thin to medium bedded siltstone	Siltstone	Sparse current ripple cross-lamination, parallel lamination, hummocky cross-stratification	*Plan., Pal., Loph., Thal.,* (*Ner., Sca., Neo.)* and sparse *Chon.*	Tabular/ irregular
	B	Interlaminated siltstone/shale	Siltstone/ shale	Lenticular and wavy bedded, micro-hummocky cross-beds, ripple lamination, horizontal lamination	*Plan., Pal., Loph., Thal., Ner., Sca., Neo.* and sparse *Chon.*	Tabular/ disconti-nuous
Facies Assemblage	**Upper Lithof.**	**Description**	**Grain Size**	**Sedimentary Structures**	**Trace Fossils**	**Geometry**
Assemblage C-I	C	Medium to thick bedded tabular sandstone	Very fine sandstone and siltstone	Massive	*Plan., Pal., Loph., Thal.,* horizont al burrows (*Ner., Sca., Neo.)*	Tabular/ irregular
	D	Thin bedded, parallel laminated sandstone	Very fine sandstone and siltstone	Parallel lamination	None	Tabular

	E	Thin to medium bedded, rippled sandstone	Very fine sandstone and siltstone	Wave ripple/ combined flow ripple bedding and climbing ripple cross-lamination	None	Tabular
	F	Thin to medium bedded, hummocky cross-stratified sandstone	Very fine sandstone and siltstone	Hummocky cross-stratification	None	Tabular
	G	Thin to medium bedded, swaley cross-stratified sandstone	Very fine sandstone and siltstone	Swaley cross-stratification, micro-hummocky cross laminations	None	Tabular
	H	Thin to medium bedded, convolute sandstone	Very fine sandstone and siltstone	Convolute lamination	None	Tabular
	I	Thin interlaminated siltstone and carbonaceous detritus	Siltstone and shale	Thin couplets of siltstone and carbonaceous silt with parallel laminations	None	Tabular
	J	Thin interbedded siltstone and shale	Siltstone and silty shale	Wavy and lenticular ripple bedded, micro-hummocky cross-bedding, and parallel laminations	*Plan.*, *Pal.*, *Loph.*, *Thal.*, *Ner.*, *Sca.*, *Neo.* and sparse *Chon.*	Lenticular

	K	Large-scale channel siltstone	Siltstone	trough cross-bedding, large scale cross-bedding, convolute bedding, highly bioturbated	*Plan., and Pal.*	Channel form

Table 1. Identifies and describes sedimentary facies and facies assemblages present within the lower and upper lithofacies. *Planolites* (Plan.), *Palaeophycus* (Pal.), *Lophoctenium* (Loph.), *Thalassinoides* (Thal.), *Nereites?* (Ner.), *Scalarituba?* (Sca.) *Neonereites?* (Neo.) *Chondrites* (Chon.).

Ichnogenera	Toponomy				Ethologic Type					Stratigraphic Occurrence
	Epichnia (upper surface)	Endichina (witin bed)	Hypichnia (lower surface)	Exichia (between beds)	Repichnia (crawling trace)	Cubichnia (resting trace)	Domichnia (dwelling burrow)	Fodinichnia (feeding trace)	Pascichnia (grazing trace)	Bedford-Berea Sequence Late Devonian Age
Chondrites		✓						✓		R
Phycodes-like			✓					✓		R
Planolites		✓	✓		✓					R-C
Scalarituba	✓	✓	✓						✓	R-C
Thalassinoides		✓	✓				✓	✓		R
Neonereites/ Nereites	✓	✓	✓						✓	R-C

Table 2. Description of ethology, toponomy and ichnogenera of tracemakers within the lower lithofacies of the Bedford-Berea sequence using Chaplin (1980) classification techniques. R= Rare: found infrequently. C= Common: typically, but not present in every sample. A= Abundant: Present nearly all the time.

Ichnogenera	Toponomy				Ethologic Type					Stratigraphic Occurrence
	Epichnia (upper surface)	Endichina (witin bed)	Hypichnia (lower surface)	Exichia (between beds)	Repichnia (crawling trace)	Cubichnia (resting trace)	Domichnia (dwelling burrow)	Fodinichnia (feeding trace)	Pascichnia (grazing trace)	Bedford-Berea Sequence Late Devonian Age
Chondrites		✓						✓		R
Lophoctenium	✓	✓		✓				✓		R-C
Palaeophycus	✓									R-C
Phycodes-like			✓					✓		R
Planolites		✓	✓		✓					R-C
Scalarituba	✓	✓	✓						✓	R-C
Thalassinoides		✓	✓				✓	✓		R
Neonereites/ Nereites	✓	✓	✓						✓	R-C

Table 3. Description of ethology, toponomy and ichnogenera of tracemakers within the upper lithofacies of the Bedford-Berea sequence using Chaplin (1980) classification techniques. R= Rare: found infrequently. C= Common: typically, but not present in every sample. A= Abundant: Present nearly all the time. The upper lithofacies has a similar ichnogeneria as the lower lithofacies except for the presence of *Lophoctenium* in the upper lithofacies.

Ichnogenera	Toponomy				Ethologic Type					Stratigraphic Occurrence	
	Epichnia	Endichnia	Hypichnia	Exichia	Repichnia	Cubichnia	Domichnia	Fodinichnia	Pascichnia	Cowbell Member (Chaplin, 1980)	Bedford-Berea Sequence Late Devonian Age
Archaeichnium-like	✓	✓					✓			R-C	
Arthrophycus			✓					✓		C	
Asteriacites			✓			✓				R	
Bergaueria			✓		✓					C-A	
Calycraterion			✓				✓			R-C	
Chondrites		✓						✓		C-A	R
Cruziana	✓		✓		✓					C-A	
Cylindrichnus		✓				✓	✓			A	
Diplocraterion		✓				✓				R-C	
Gyrochorte	✓		✓		✓					R-C	
Helminthoida	✓	✓	✓						✓	A	
Helminthopsis		✓	✓						✓	R	
Lockiea			✓			✓				R-C	
Lophoctenium	✓	✓		✓				✓		R	R-C
Moncraterion		✓					✓			R-C	
Palaeophycus	✓									R-C	R-C
Phycodes-like			✓					✓		R	R
Phycosiphon	✓	✓	✓					✓		C	
Planolites		✓	✓		✓					C-A Av. 1 cm diameter	R-C 3.18 mm av. diameter
Radionereites-like			✓					✓		R	
Rusophycus		✓				✓				R-C	
Scalarituba	✓	✓	✓						✓	A	R-C
Thalassinoides		✓	✓				✓	✓			R
Neonereites/ Nereites	✓	✓	✓						✓		R-C
Teichichnus	✓	✓						✓		R	
Zoophycos I	✓	✓	✓	✓					✓	R-C	
Zoophycos II	✓	✓	✓	✓					✓	C-A	

Table 4: Description of ethology, toponomy and ichnogenera of tracemakers in the Bedford-Berea sequence compared to tracemakers of the Cowbell Member. Traces classified using Chaplin, (1980) classification techniques. R= Rare: found infrequently. C= Common: typically, but not present in every sample. A= Abundant: Present nearly all the time.

STRATIGRAPHIC COLUMNS

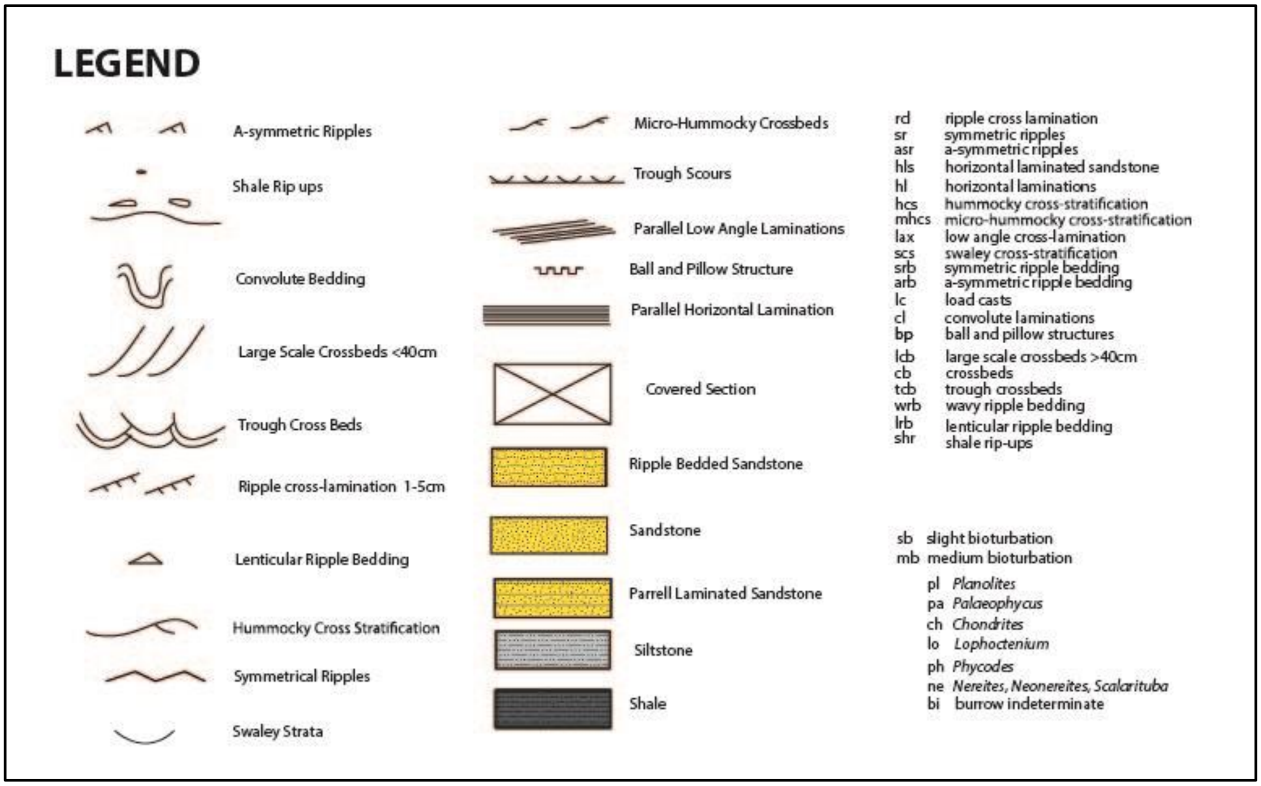

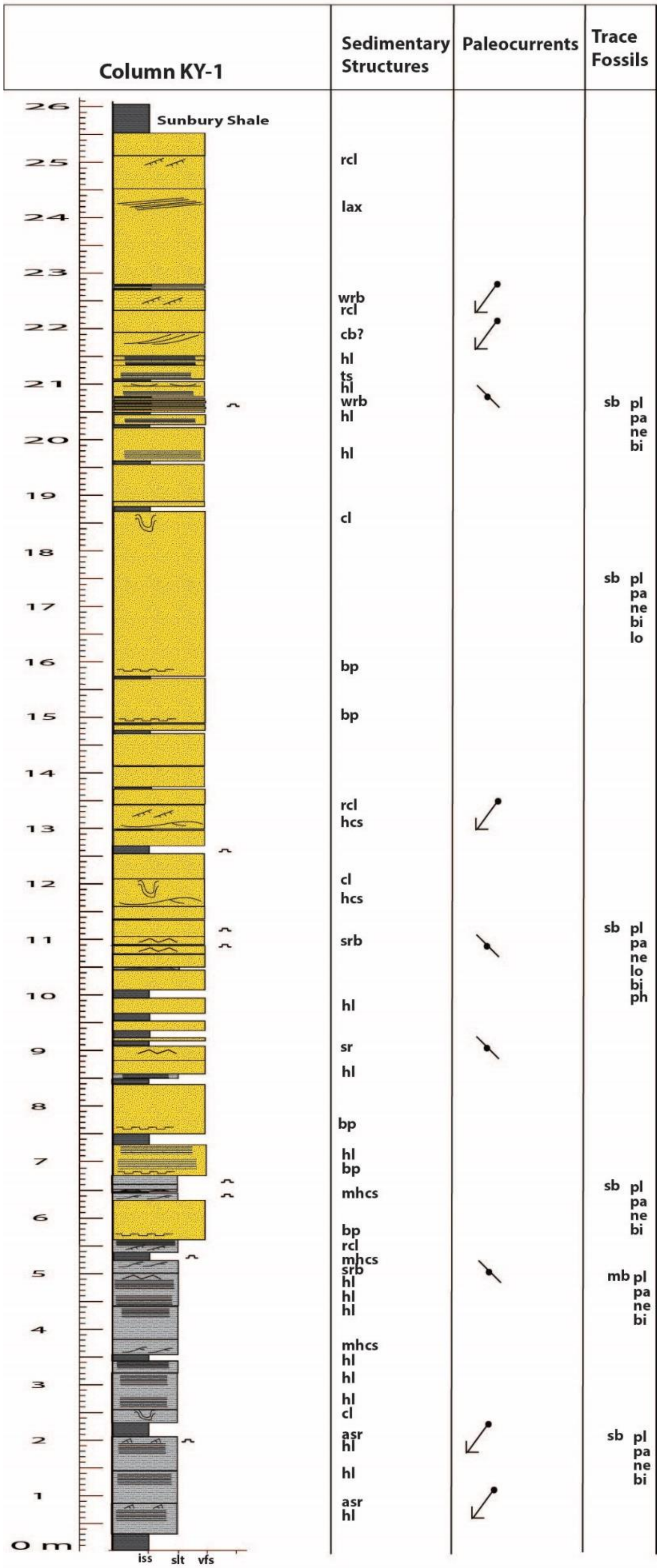

Column KY-1
Sedimentary Structures
Paleocurrents
Trace Fossils
Sunbury Shale
rcl
lax
wrb
rcl
cb?
hl
ts
hl
wrb
hl
hl
cl
bp
bp
rcl
hcs
cl
hcs
srb
hl
sr
hl
bp
hl
bp
mhcs
bp
rcl
mhcs
srb
hl
hl
hl
mhcs
hl
hl
hl
cl
asr
hl
hl
asr
hl
sb pl pa ne bi
sb pl pa ne bi lo
sb pl pa ne lo bi ph
sb pl pa ne bi
mb pl pa ne bi
sb pl pa ne bi
0 m
iss slt vfs

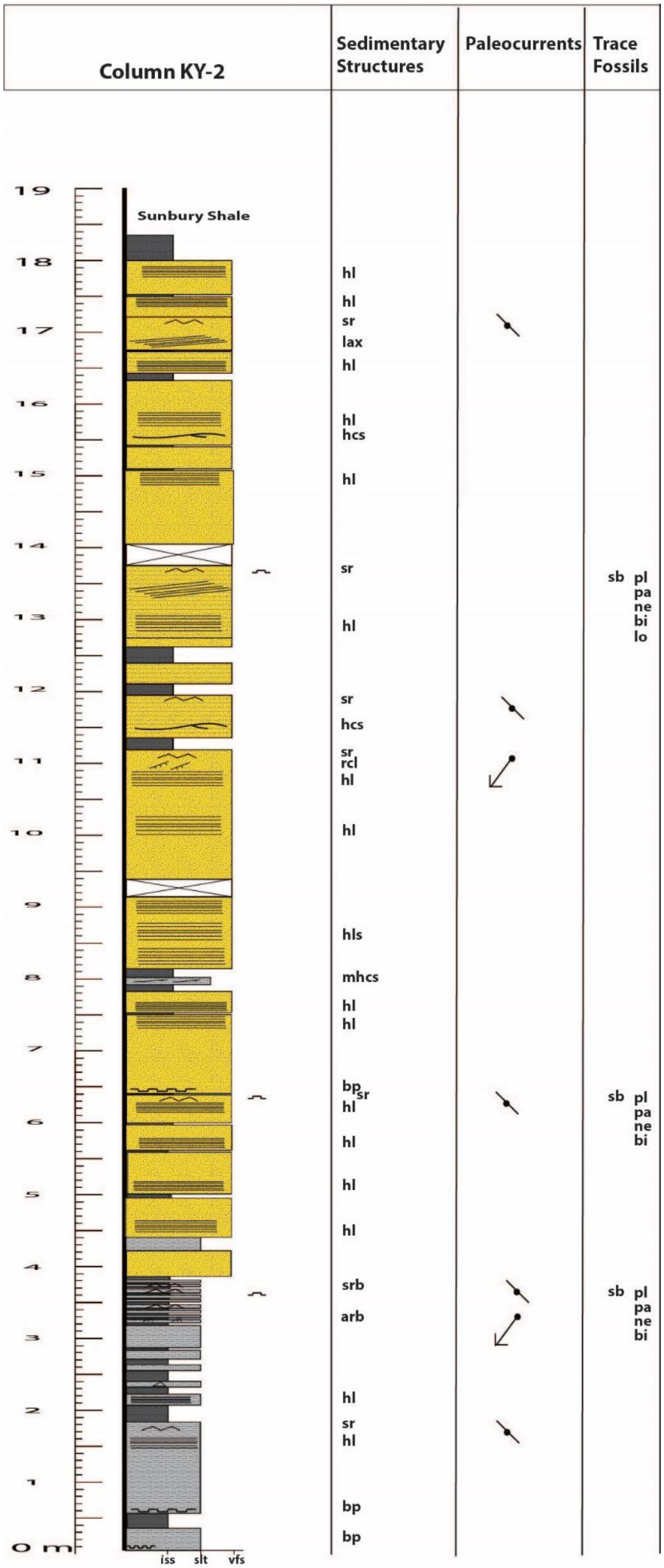
Column KY-2
Sedimentary Structures
Paleocurrents
Trace Fossils
Sunbury Shale
hl
hl
sr
lax
hl
hl
hcs
hl
sr
hl
sb pl pa ne bi lo
sr
hcs
sr
rcl
hl
hl
hls
mhcs
hl
hl
bp sr
hl
sb pl pa ne bi
hl
hl
hl
srb
arb
sb pl pa ne bi
hl
sr
hl
bp
bp
19
18
17
16
15
14
13
12
11
10
9
8
7
6
5
4
3
2
1
0 m
iss
slt
vfs

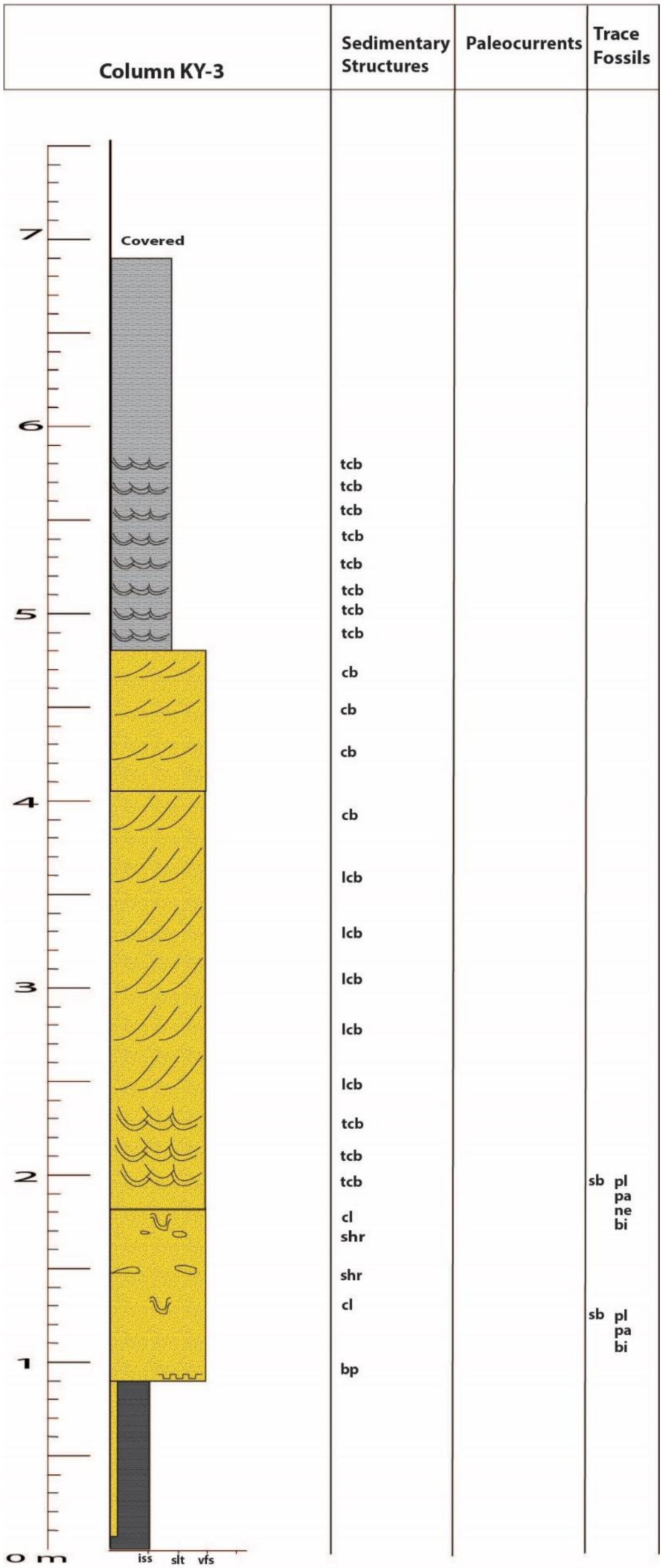
Column KY-3
Sedimentary Structures
Paleocurrents
Trace Fossils
Covered
7
6
5
4
3
2
1
0 m
iss
slt
vfs
tcb
tcb
tcb
tcb
tcb
tcb
tcb
tcb
cb
cb
cb
cb
lcb
lcb
lcb
lcb
lcb
tcb
tcb
tcb
cl
shr
shr
cl
bp
sb pl pa ne bi
sb pl pa bi

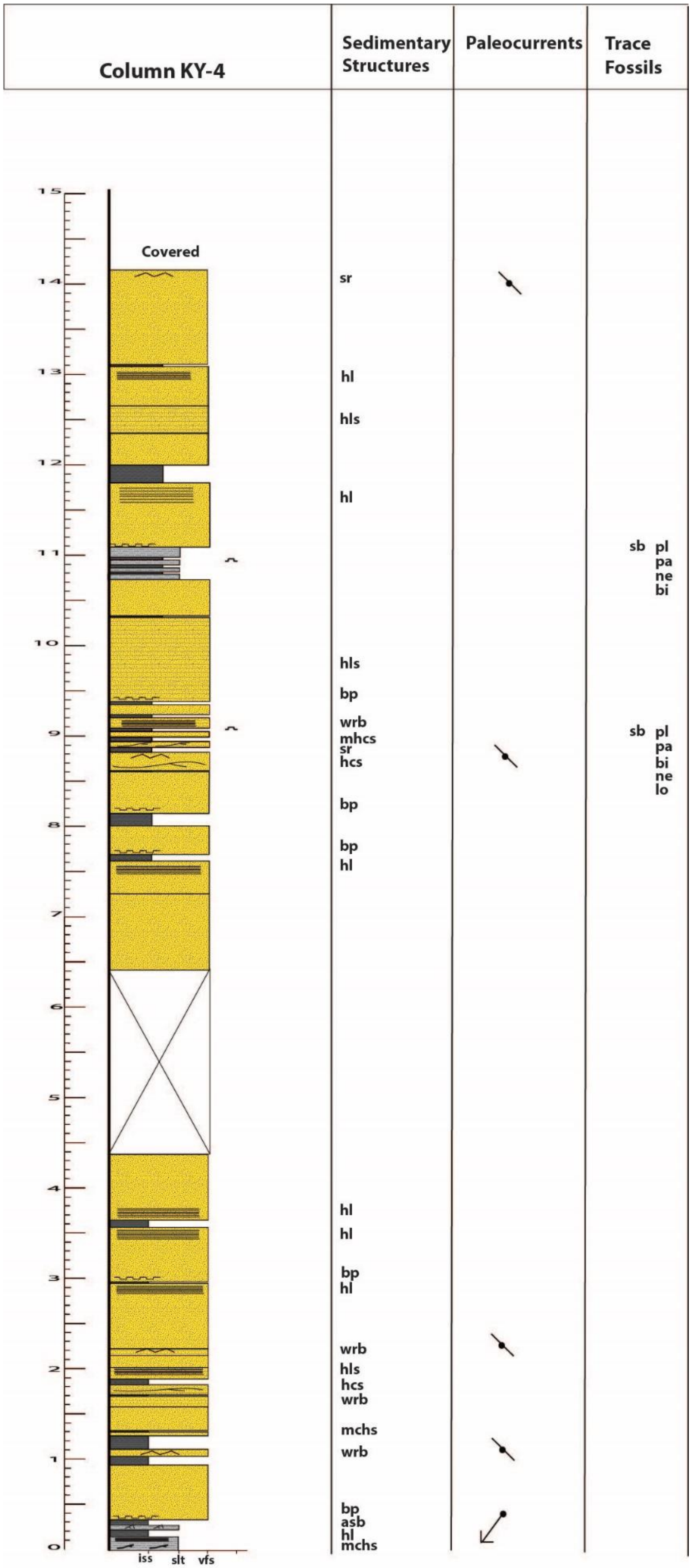
Column KY-4
Sedimentary Structures
Paleocurrents
Trace Fossils
Covered
15
14
13
12
11
10
9
8
7
6
5
4
3
2
1
0
iss
slt
vfs
sr
hl
hls
hl
sb pl
pa
ne
bi
hls
bp
wrb
mhcs
sr
hcs
sb pl
pa
bi
ne
lo
bp
bp
hl
hl
hl
bp
hl
wrb
hls
hcs
wrb
mchs
wrb
bp
asb
hl
mchs

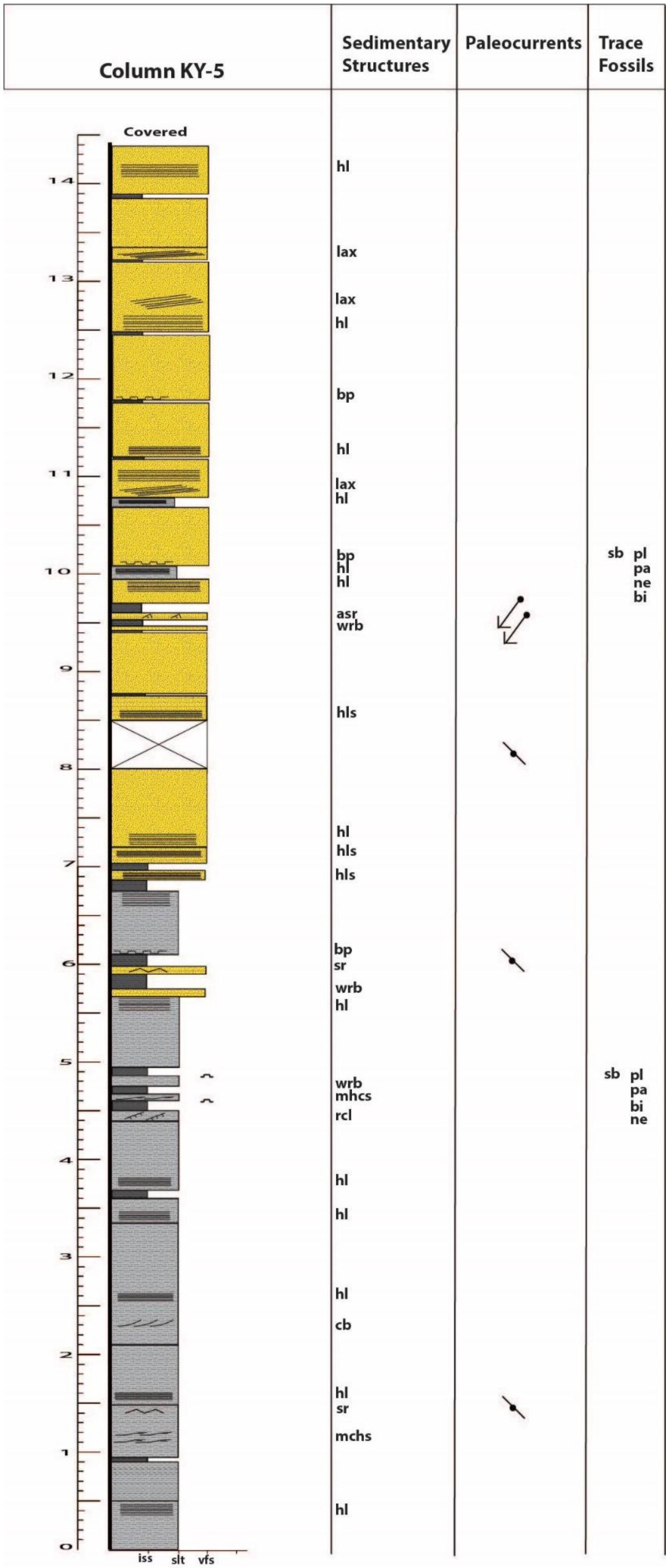
Column KY-5
Sedimentary Structures
Paleocurrents
Trace Fossils
Covered
14
13
12
11
10
9
8
7
6
5
4
3
2
1
0
iss
slt
vfs
hl
lax
lax
hl
bp
hl
lax
hl
bp
hl
hl
asr
wrb
hls
hl
hls
hls
bp
sr
wrb
hl
wrb
mhcs
rcl
hl
hl
hl
cb
hl
sr
mchs
hl
sb pl
pa
ne
bi
sb pl
pa
bi
ne

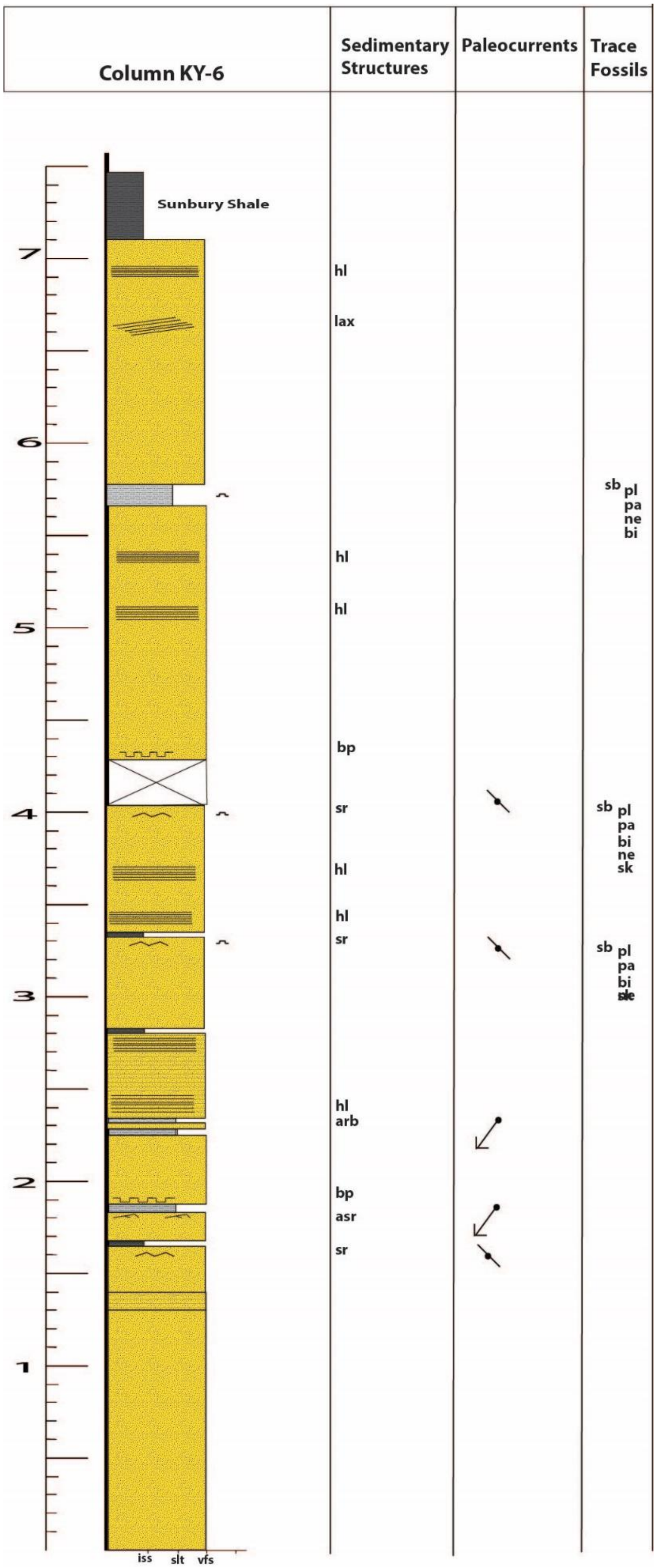
Column KY-6
Sedimentary Structures
Paleocurrents
Trace Fossils
Sunbury Shale
7
6
5
4
3
2
1
hl
lax
hl
hl
bp
sr
hl
hl
sr
hl
arb
bp
asr
sr
sb pl pa ne bi
sb pl pa bi ne sk
sb pl pa bi sk
iss slt vfs

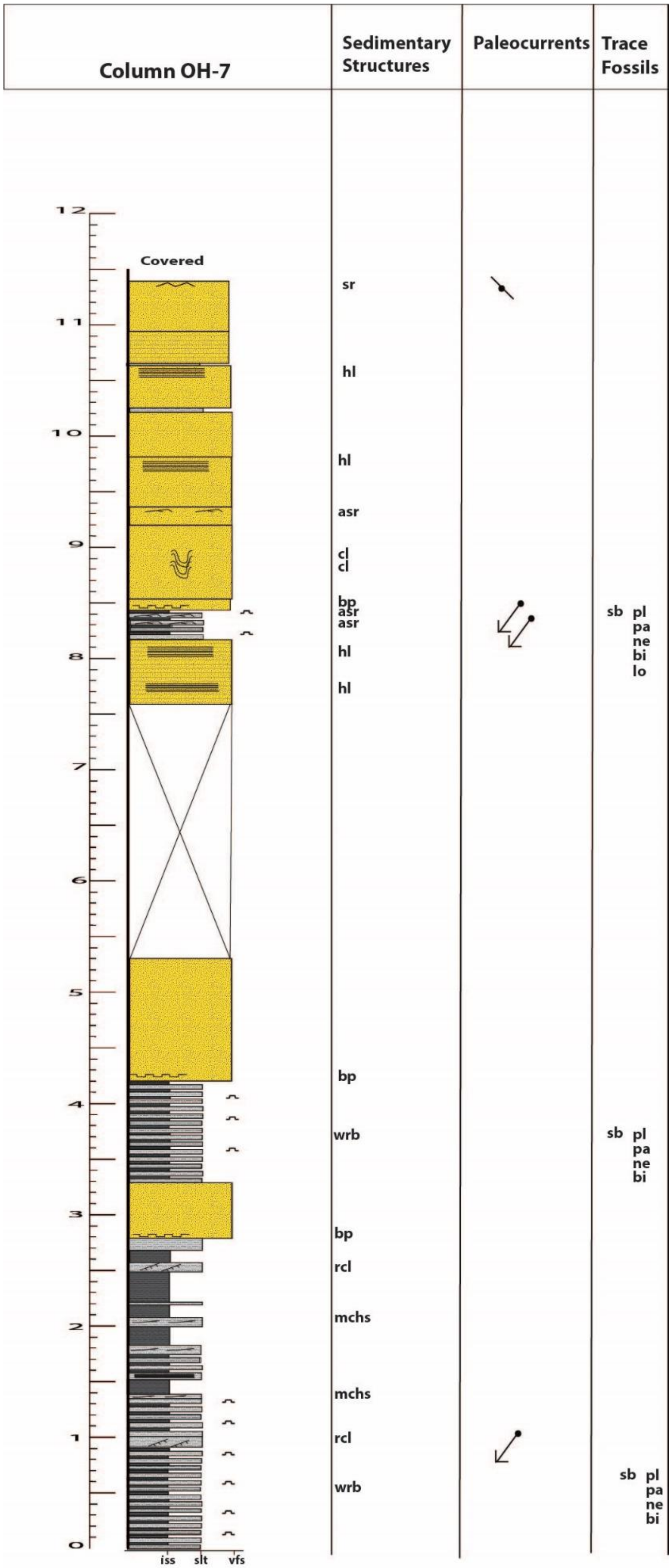
Column OH-7
Sedimentary Structures
Paleocurrents
Trace Fossils
12
11
10
9
8
7
6
5
4
3
2
1
0
Covered
sr
hl
hl
asr
cl
cl
bp
asr
asr
hl
hl
sb pl pa ne bi lo
bp
wrb
sb pl pa ne bi
bp
rcl
mchs
mchs
rcl
wrb
sb pl pa ne bi
iss
slt
vfs

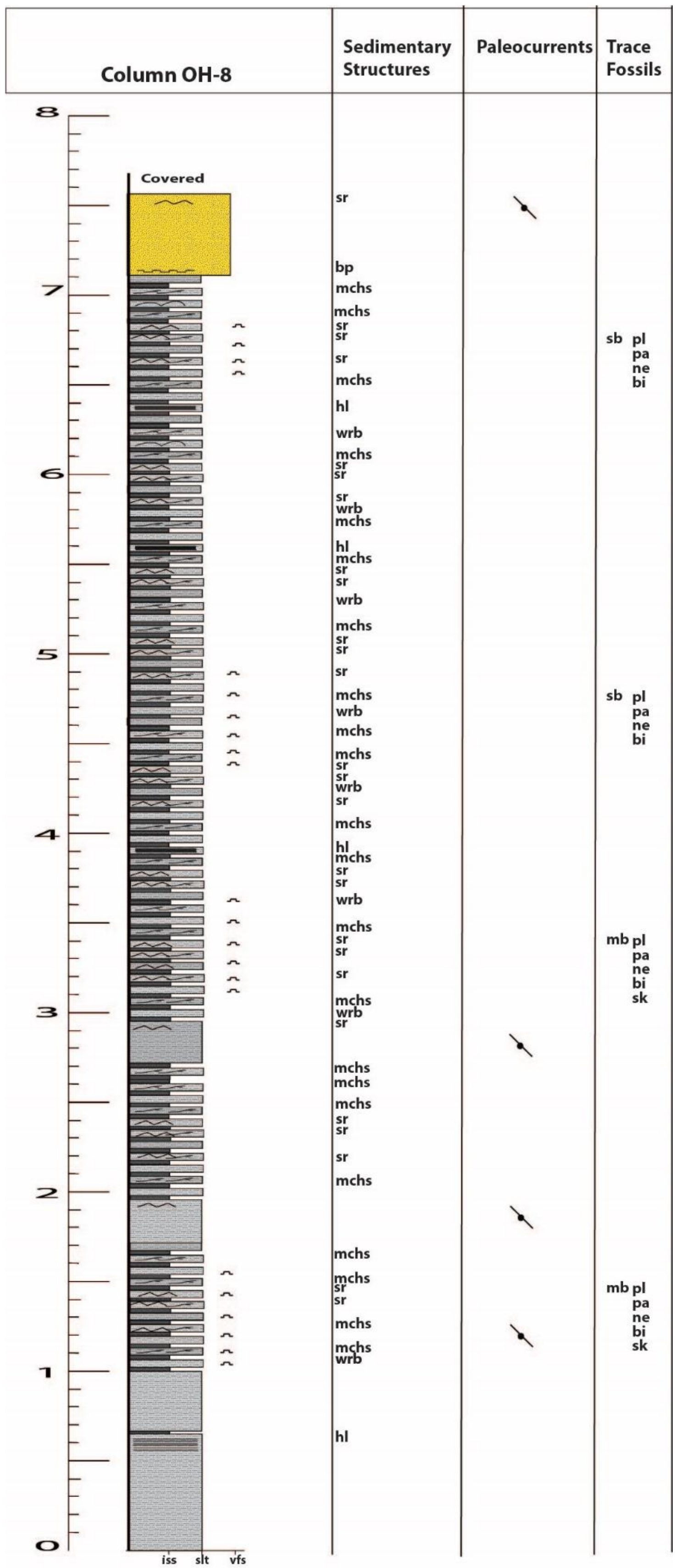
Column OH-8
Sedimentary Structures
Paleocurrents
Trace Fossils
8
Covered
sr
bp
7
mchs
mchs
sr
sr
sb pl pa ne bi
sr
mchs
hl
wrb
mchs
sr
sr
6
sr
wrb
mchs
hl
mchs
sr
sr
wrb
mchs
sr
sr
5
sr
mchs
sb pl pa ne bi
wrb
mchs
mchs
sr
sr
wrb
sr
mchs
4
hl
mchs
sr
sr
wrb
mchs
mb pl pa ne bi sk
sr
sr
sr
mchs
wrb
sr
3
mchs
mchs
mchs
sr
sr
sr
mchs
2
mchs
mchs
sr
mb pl pa ne bi sk
sr
mchs
mchs
wrb
1
hl
0
iss slt vfs

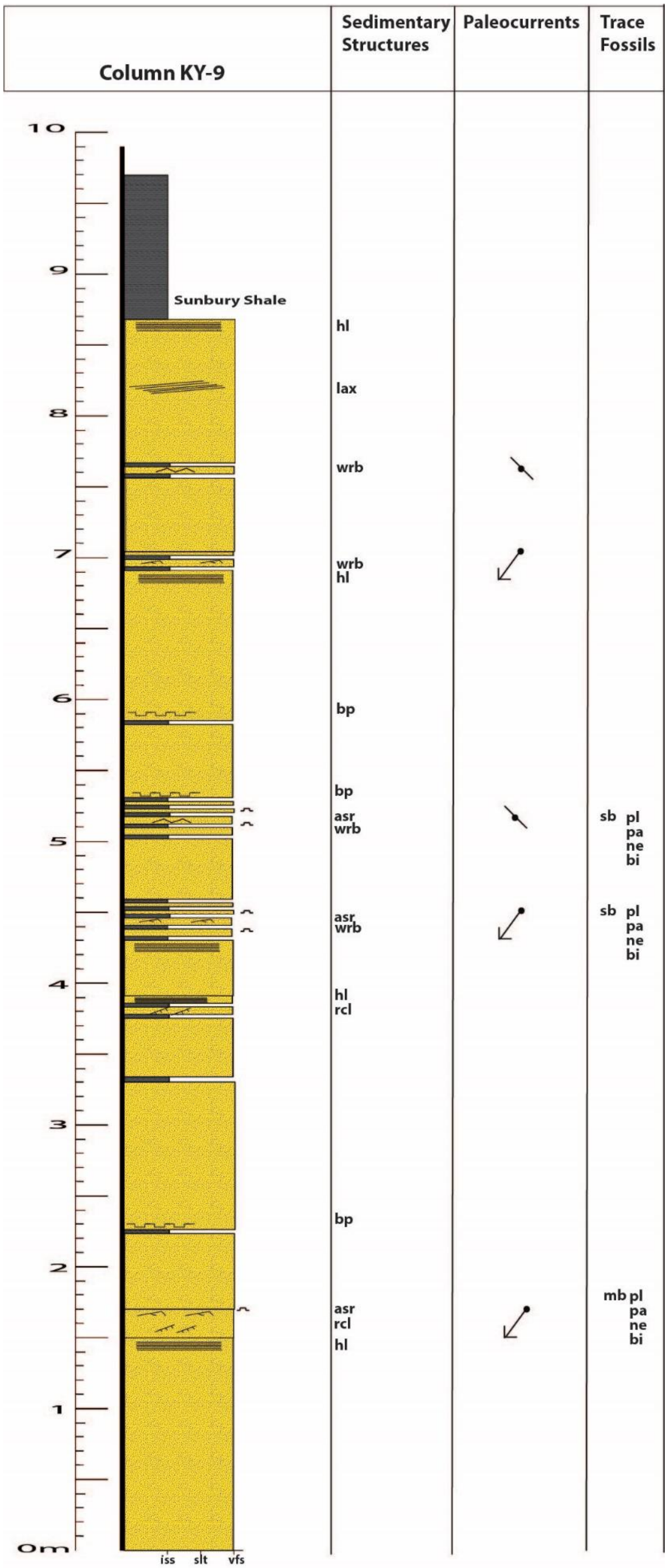
Column KY-9
Sedimentary Structures
Paleocurrents
Trace Fossils
10
9
8
7
6
5
4
3
2
1
0m
Sunbury Shale
hl
lax
wrb
wrb
hl
bp
bp
asr
wrb
sb pl
pa
ne
bi
asr
wrb
sb pl
pa
ne
bi
hl
rcl
bp
asr
rcl
hl
mb pl
pa
ne
bi
iss slt vfs

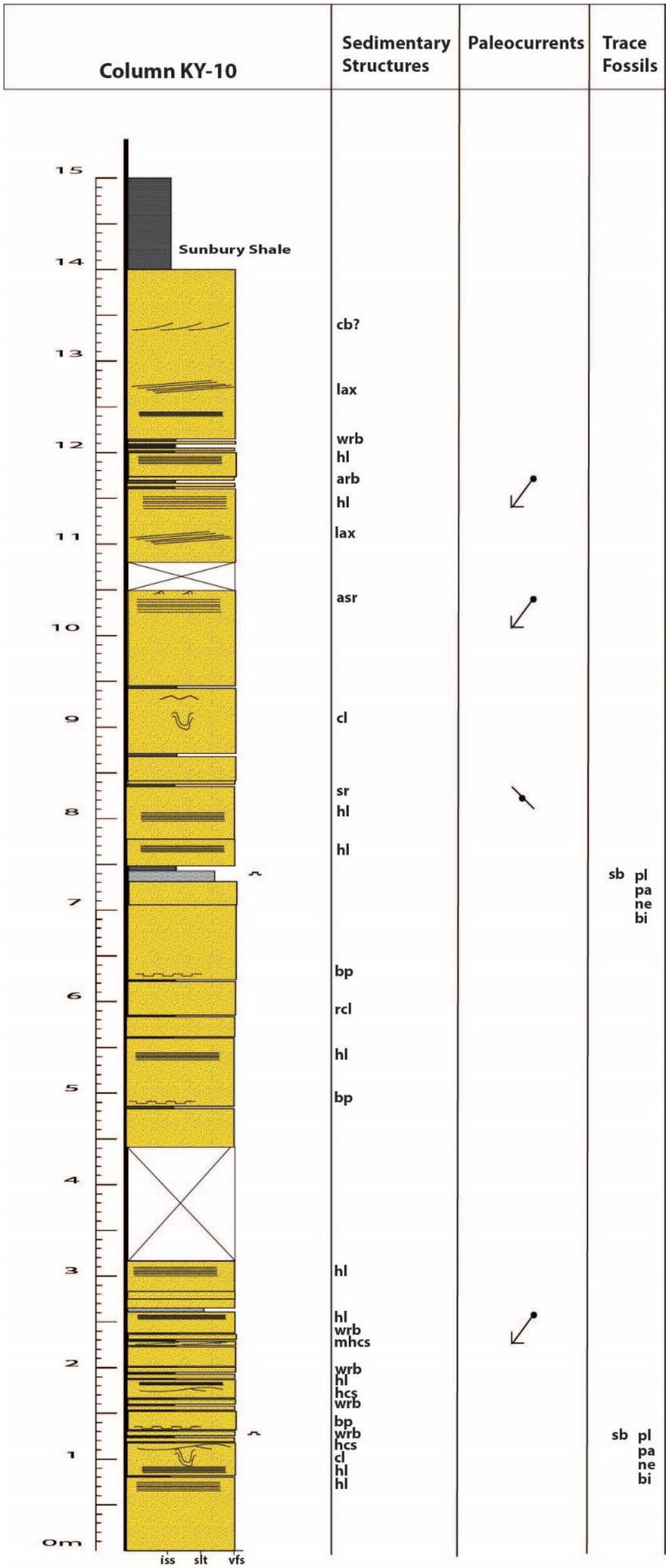
Column KY-10
Sedimentary Structures
Paleocurrents
Trace Fossils
15
14
13
12
11
10
9
8
7
6
5
4
3
2
1
0m
Sunbury Shale
cb?
lax
wrb
hl
arb
hl
lax
asr
cl
sr
hl
hl
sb pl pa ne bi
bp
rcl
hl
bp
hl
hl
wrb
mhcs
wrb
hl
hcs
wrb
bp
wrb
hcs
cl
hl
hl
sb pl pa ne bi
iss slt vfs

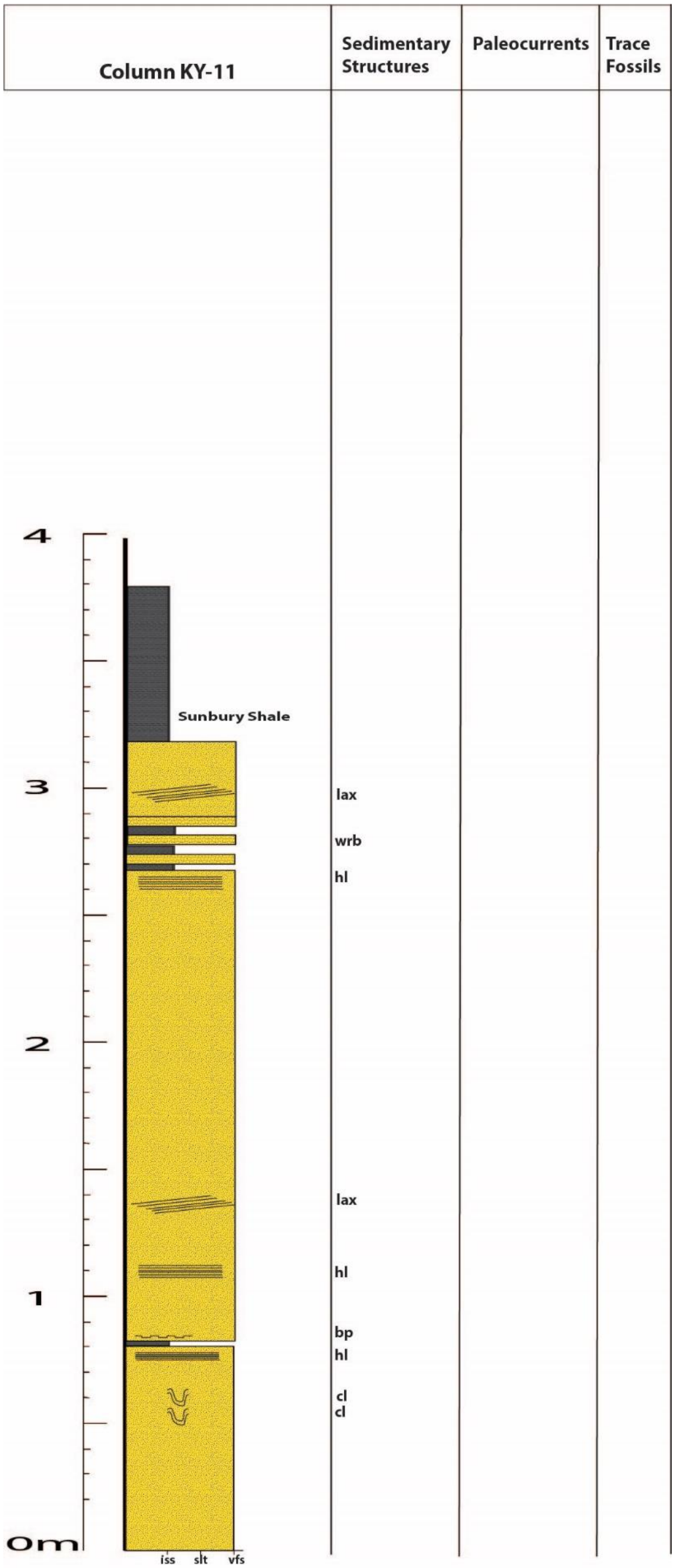
Column KY-11
Sedimentary Structures
Paleocurrents
Trace Fossils
4
3
2
1
0m
Sunbury Shale
lax
wrb
hl
lax
hl
bp
hl
cl
cl
iss
slt
vfs

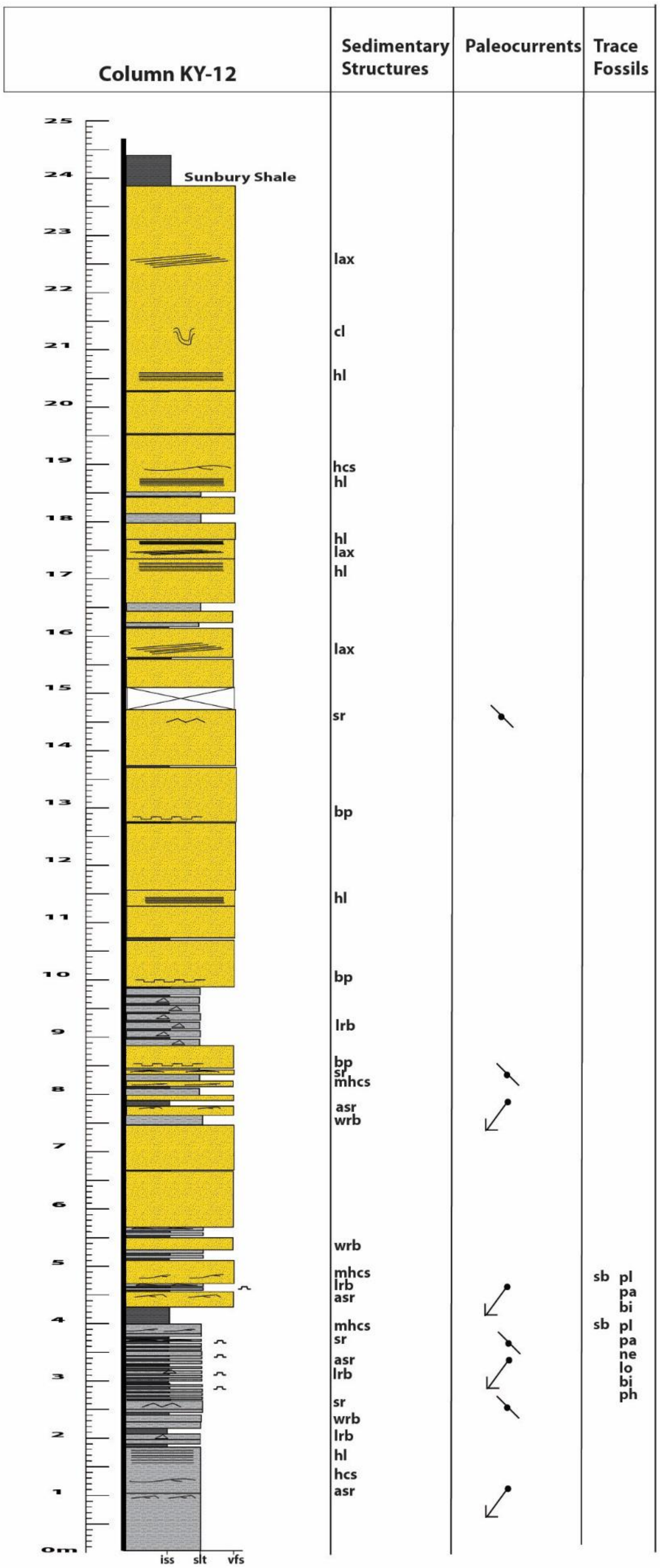
Column KY-12
Sedimentary Structures
Paleocurrents
Trace Fossils
Sunbury Shale
lax
cl
hl
hcs
hl
hl
lax
hl
lax
sr
bp
hl
bp
lrb
bp
sr
mhcs
asr
wrb
wrb
mhcs
lrb
asr
mhcs
sr
asr
lrb
sr
wrb
lrb
hl
hcs
asr
sb pl pa bi
sb pl pa ne lo bi ph
iss slt vfs
0m

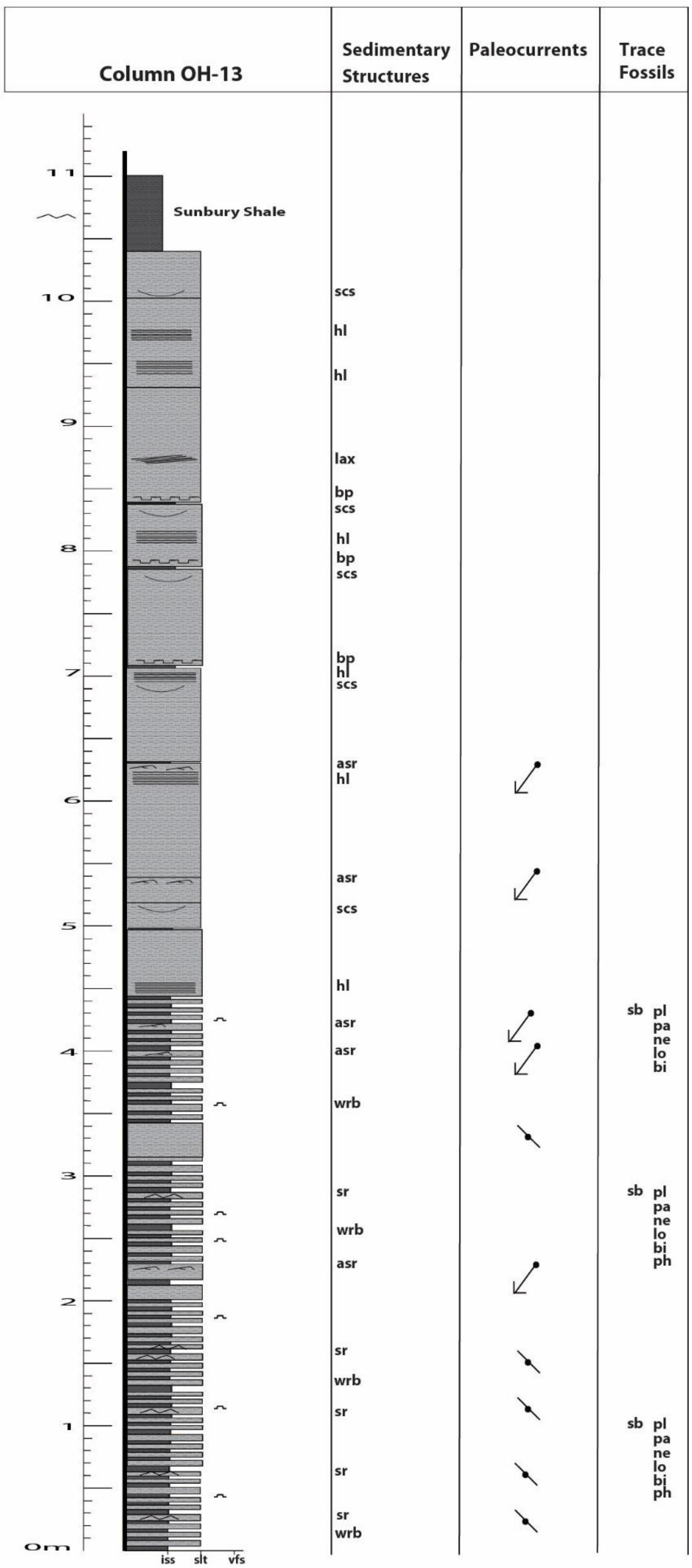

Column OH-13
Sedimentary Structures
Paleocurrents
Trace Fossils
Sunbury Shale
11
10
9
8
7
6
5
4
3
2
1
0m
iss
slt
vfs
scs
hl
hl
lax
bp
scs
hl
bp
scs
bp
hl
scs
asr
hl
asr
scs
hl
asr
asr
wrb
sr
wrb
asr
sr
wrb
sr
sr
sr
wrb
sb pl pa ne lo bi
sb pl pa ne lo bi ph
sb pl pa ne lo bi ph

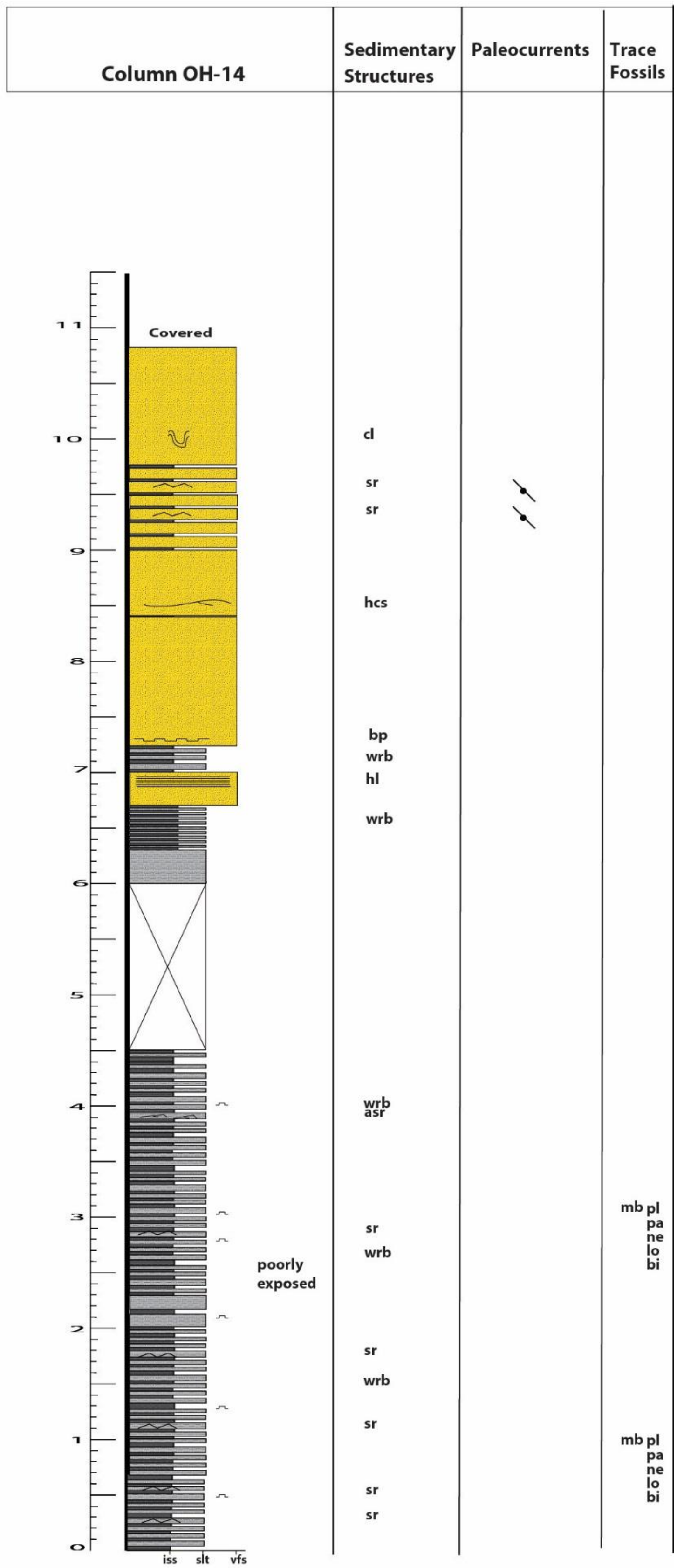
Column OH-14
Sedimentary Structures
Paleocurrents
Trace Fossils
Covered
11
10
9
8
7
6
5
4
3
2
1
0
cl
sr
sr
hcs
bp
wrb
hl
wrb
wrb
asr
sr
wrb
poorly exposed
sr
wrb
sr
sr
sr
mb pl pa ne lo bi
mb pl pa ne lo bi
iss
slt
vfs

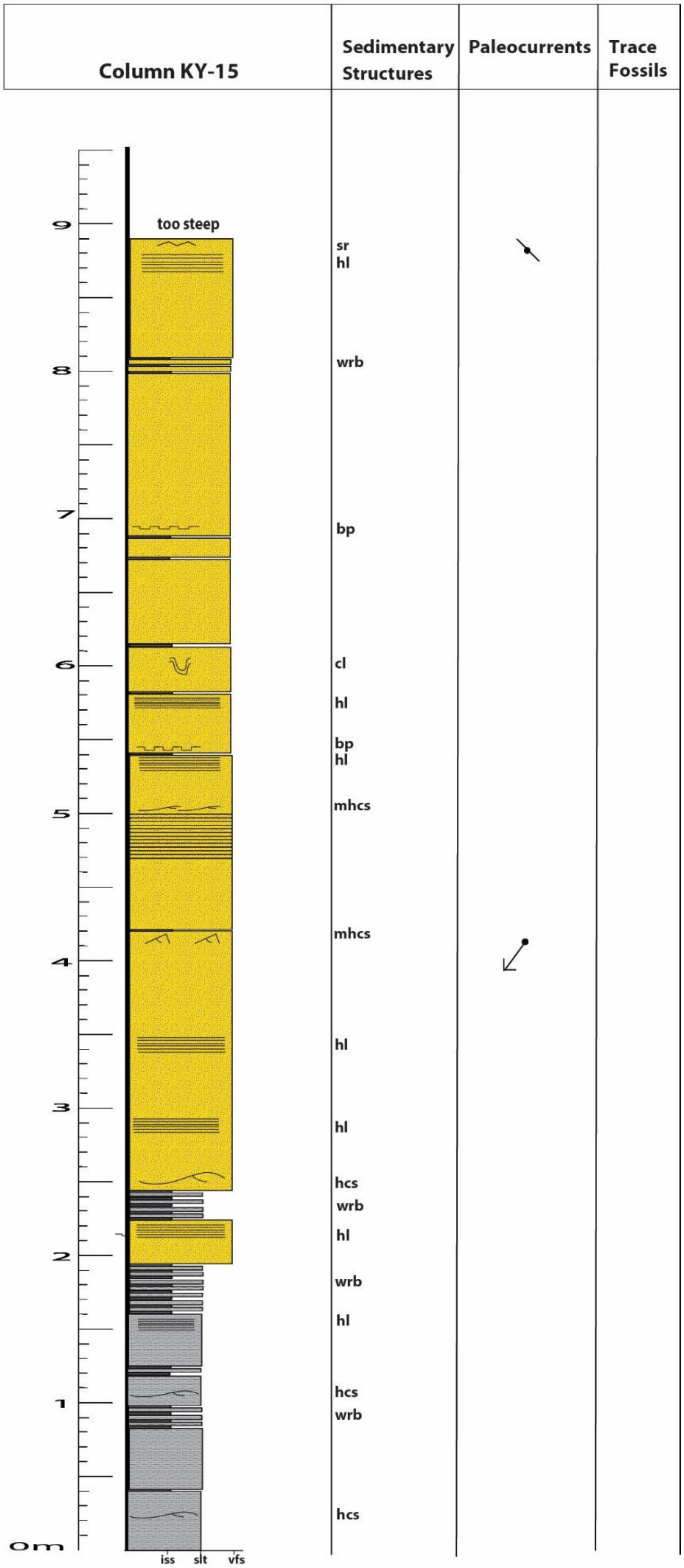
Column KY-15
Sedimentary Structures
Paleocurrents
Trace Fossils
too steep
9
8
7
6
5
4
3
2
1
0m
iss
slt
vfs
sr
hl
wrb
bp
cl
hl
bp
hl
mhcs
mhcs
hl
hl
hcs
wrb
hl
wrb
hl
hcs
wrb
hcs

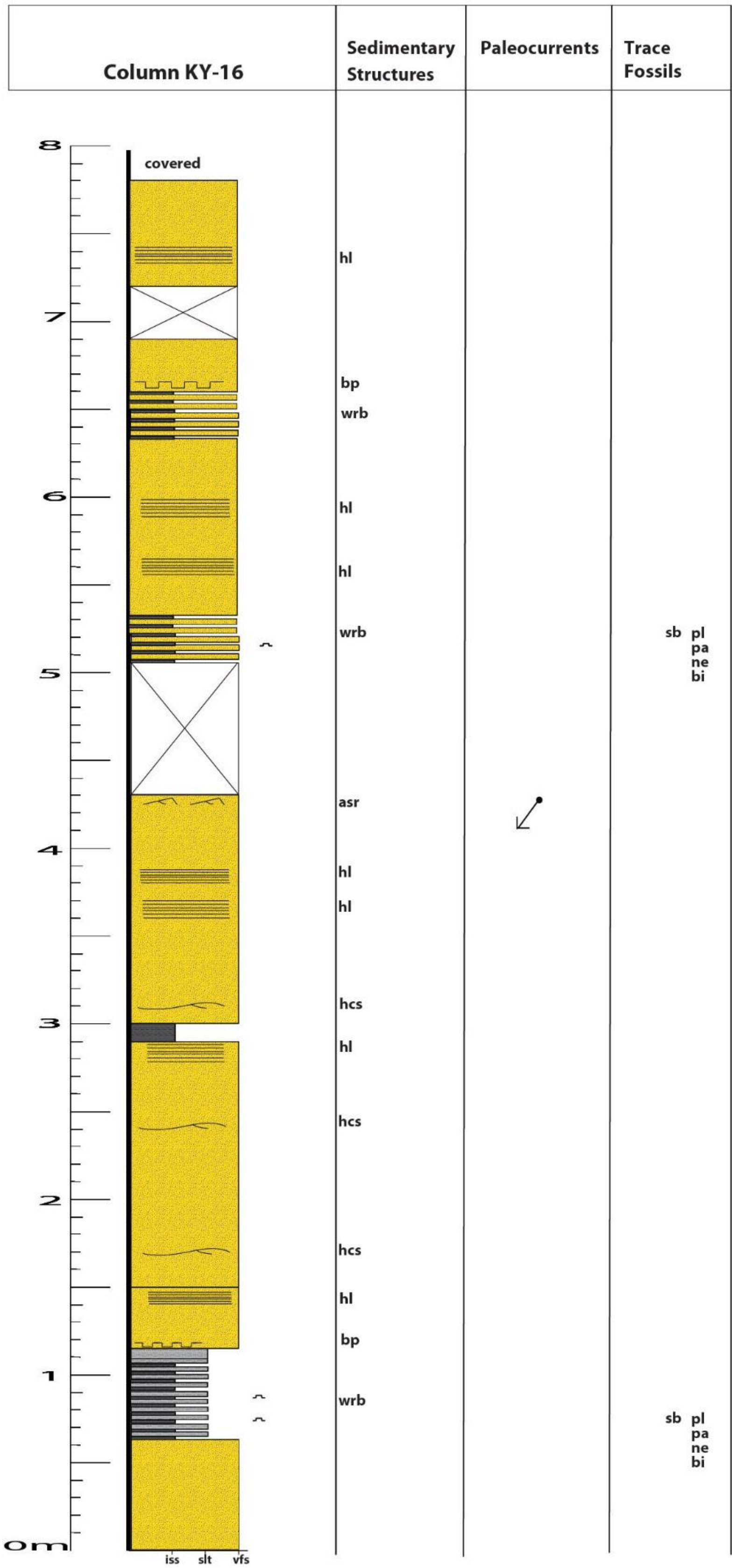
Column KY-16
Sedimentary Structures
Paleocurrents
Trace Fossils
covered
hl
bp
wrb
hl
hl
wrb
sb pl pa ne bi
asr
hl
hl
hcs
hl
hcs
hcs
hl
bp
wrb
sb pl pa ne bi
8
7
6
5
4
3
2
1
0m
iss
slt
vfs

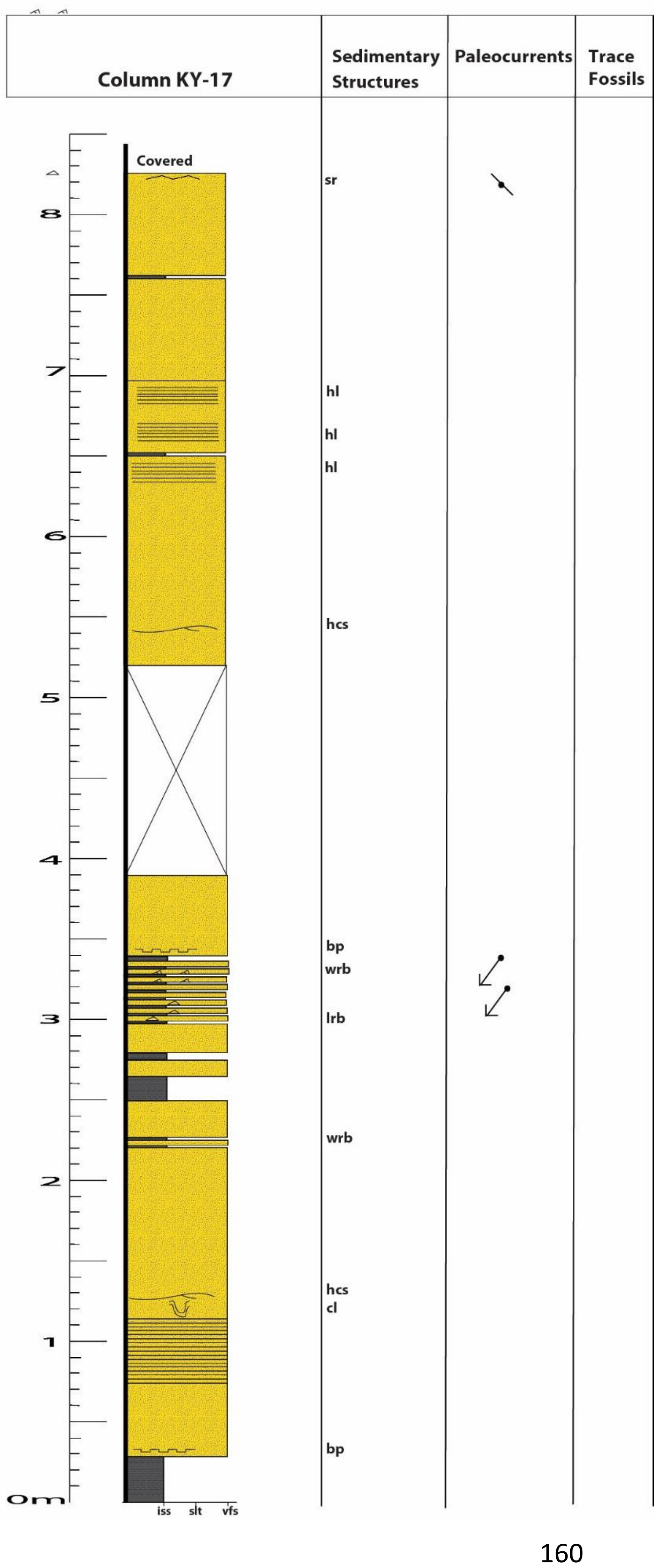
Column KY-17
Sedimentary Structures
Paleocurrents
Trace Fossils
Covered
sr
hl
hl
hl
hcs
bp
wrb
lrb
wrb
hcs
cl
bp
0m
1
2
3
4
5
6
7
8
iss
slt
vfs

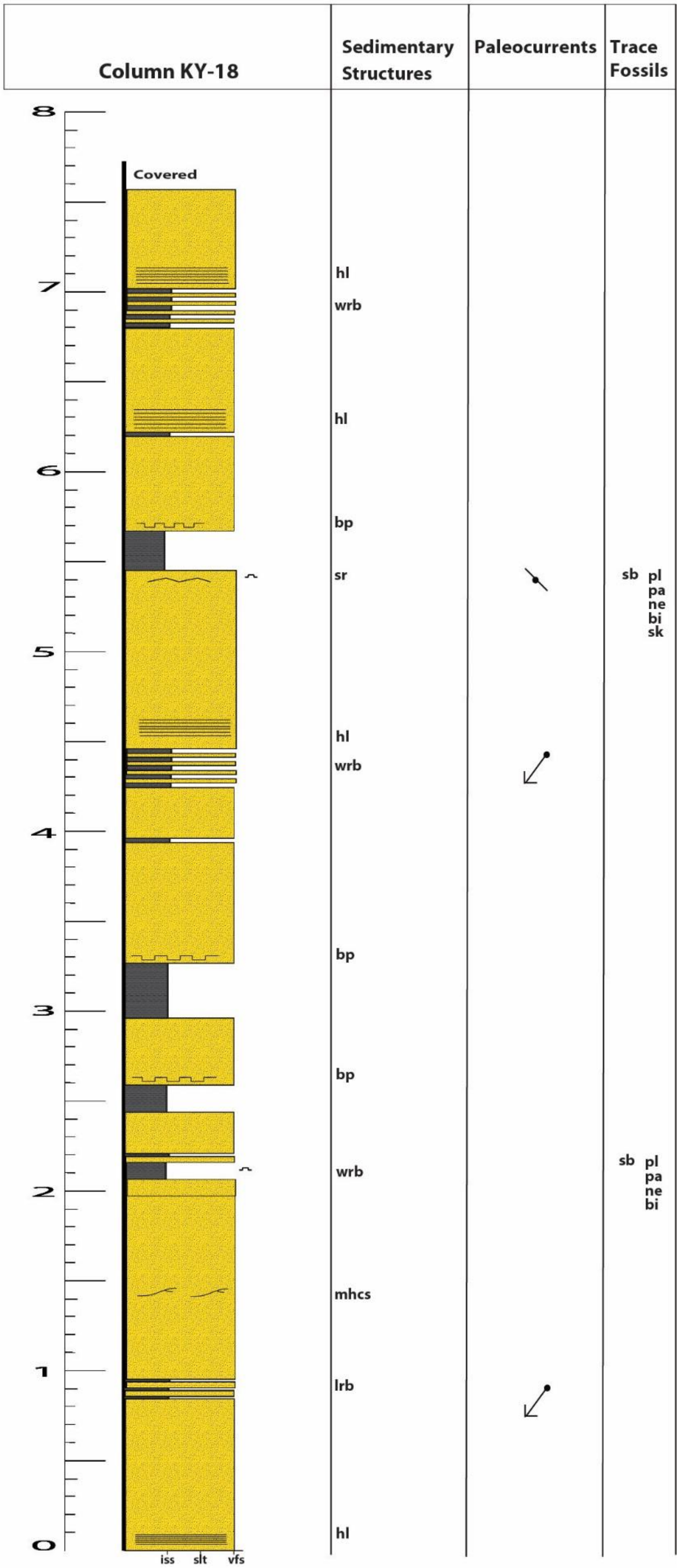
Column KY-18
Sedimentary Structures
Paleocurrents
Trace Fossils
Covered
8
7
6
5
4
3
2
1
0
hl
wrb
hl
bp
sr
hl
wrb
bp
bp
wrb
mhcs
lrb
hl
sb pl pa ne bi sk
sb pl pa ne bi
iss slt vfs

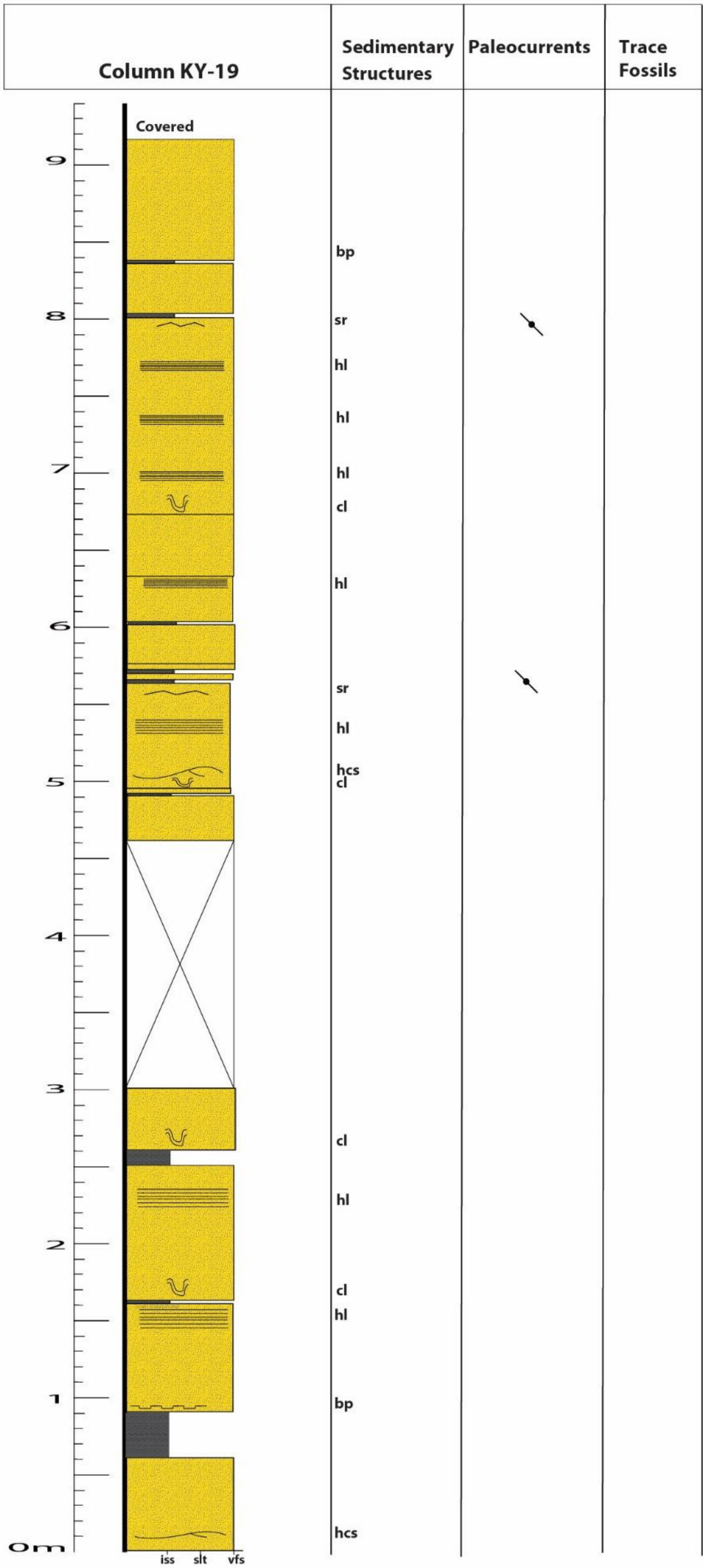

Column KY-19
Sedimentary Structures
Paleocurrents
Trace Fossils
Covered
9
8
7
6
5
4
3
2
1
0m
bp
sr
hl
hl
hl
cl
hl
sr
hl
hcs
cl
cl
hl
cl
hl
bp
hcs
iss
slt
vfs

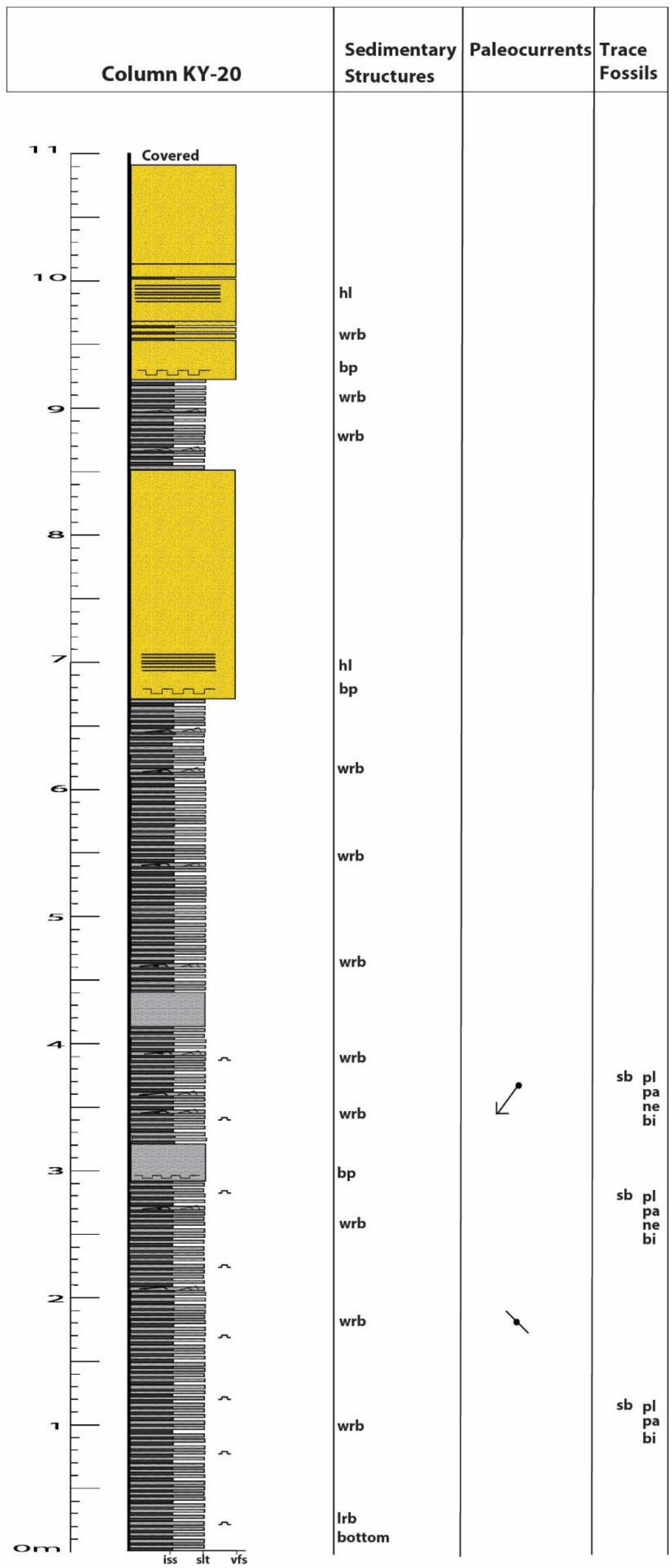

Column KY-20
Sedimentary Structures
Paleocurrents
Trace Fossils
11
10
9
8
7
6
5
4
3
2
1
0m
Covered
hl
wrb
bp
wrb
wrb
hl
bp
wrb
wrb
wrb
wrb
sb pl pa ne bi
wrb
bp
sb pl pa ne bi
wrb
wrb
sb pl pa bi
wrb
lrb
bottom
iss slt vfs

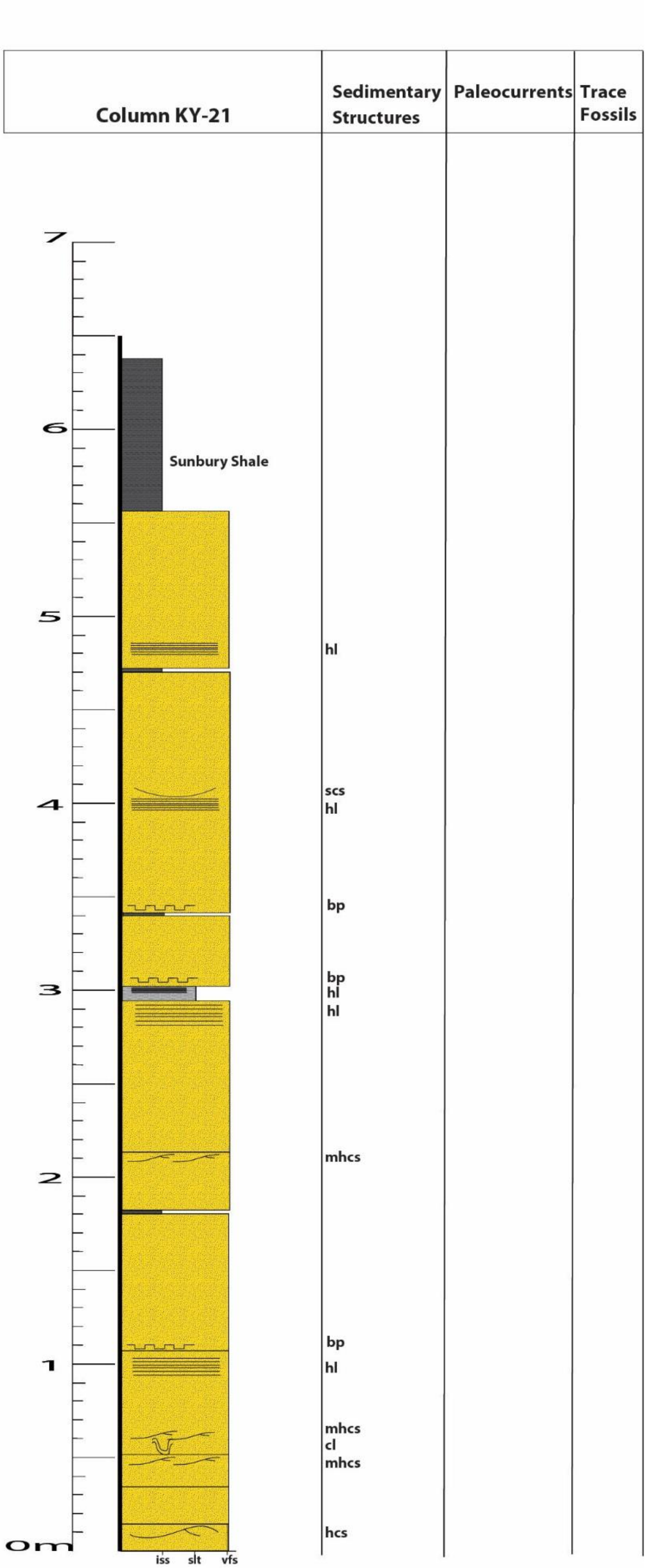
Column KY-21
Sedimentary Structures
Paleocurrents
Trace Fossils
7
6
Sunbury Shale
5
hl
4
scs
hl
bp
3
bp
hl
hl
2
mhcs
1
bp
hl
mhcs
cl
mhcs
hcs
0m
iss
slt
vfs

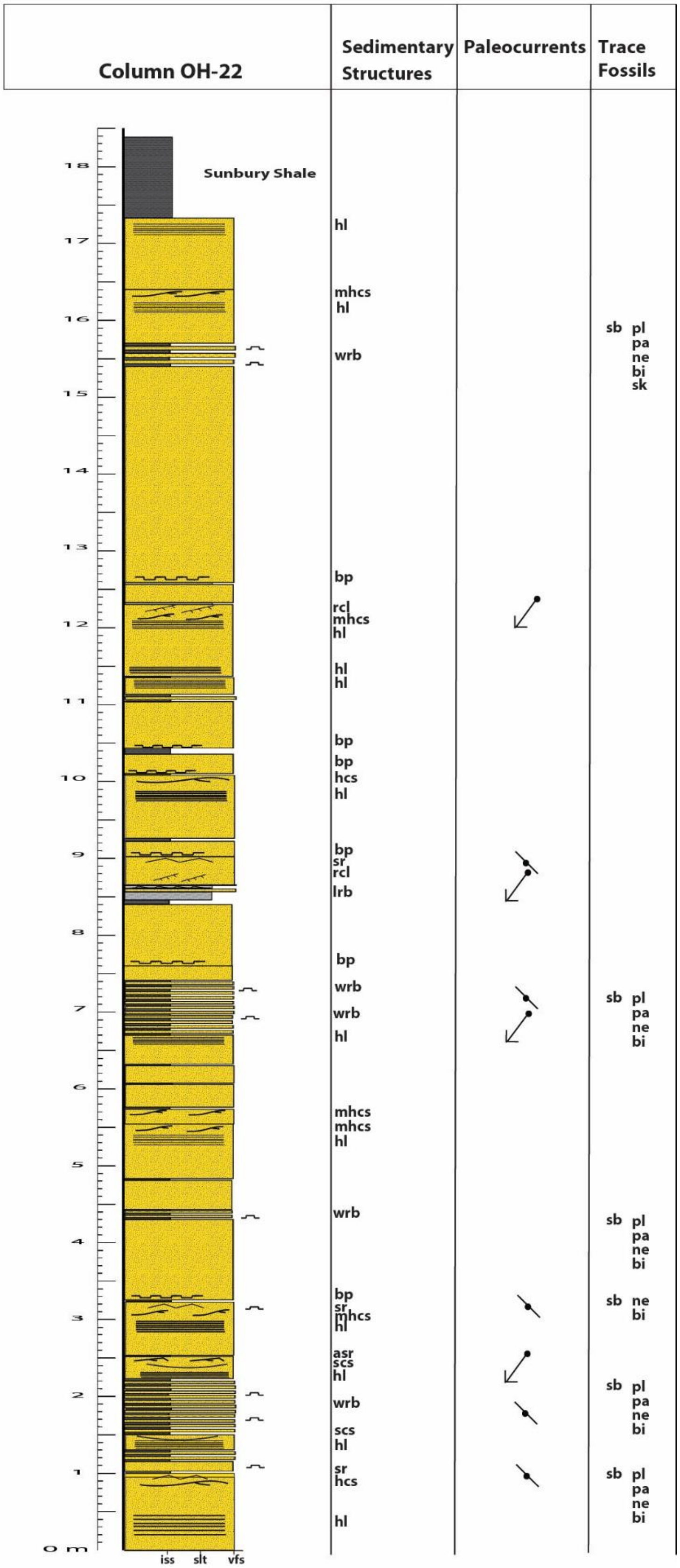
Column OH-22
Sedimentary Structures
Paleocurrents
Trace Fossils
Sunbury Shale
0 m
1
2
3
4
5
6
7
8
9
10
11
12
13
14
15
16
17
18
iss
slt
vfs
hl
mhcs
hl
wrb
bp
rcl
mhcs
hl
hl
hl
bp
bp
hcs
hl
bp
sr
rcl
lrb
bp
wrb
wrb
hl
mhcs
mhcs
hl
wrb
bp
sr
mhcs
hl
asr
scs
hl
wrb
scs
hl
sr
hcs
hl
sb pl pa ne bi sk
sb pl pa ne bi
sb pl pa ne bi
sb ne bi
sb pl pa ne bi
sb pl pa ne bi

REFERENCES

Ammerman, M.L., and Keller, G. R., 1979, *Delineation of Rome Trough in eastern Kentucky by gravity and deep drilling data*: American Association of Petroleum Geologists Bulletin, v. 63, no. 3, p. 341-353.

Angulo, S., and Buatois, A. L., 2011*, Ichnology of a Late Devonian-Early Carboniferous low-energy seaway: The Bakken Formation of subsurface Saskatchewan, Canada: Assessing paleoenvironmental controls and biotic responses*: Paleogeography, Paleoclimatology, Paleoecology, p. 46-60.

Arnott, R.W.C., 2010, *Deep-marine sediments and sedimentary systems*, *in* James, N.P., and Dalrymple, R.W., eds., Facies Models4: GEOtext 6, Geological Association of Canada, St. John's Newfoundland, p. 295-322.

Arnott, R.W.C., and Hand, B. M., 1989, *Bedforms, primary structures and grain fabric in the presence of suspended sediment rain*: Journal of Sedimentary Petrology, v. 69, p. 1062-1069.

Bai, S.L. and Ning, Z.S., 1989, *Faunal Change and Events across the Devonian-Carboniferous Boundary of Huangmao Section, Guangxi, South China*: Canadian Society of Petroleum Geologists, Calgary, Alberta, Memoir, v. 14, p. 147-157.

Bai, S.L., Bai, Z. Q., Ma, X.P., Wang, D.R., and Sun, Y.L., 1994, *Devonian Events and Biostratigraphy of South China*: Peking University Press, Beijing.

Bai, S.L., Ning, Z.S., and Orth, C.J., 1986, *Zonation and geochemical anomaly of the Devonian/Carboniferous boundary beds of Huangmao, Guangxi*: Acta Scientarum Naturalium Universitatis Pekinensis, p. 105-111.

Bhattacharya, J.P., 2006, *Deltas*, *In*: Walker, R.G., and Posamentier, H., eds., Facies Models revisited, SEPM Special Publication, v. 84, p.237-292.

Bhattacharya, J.P., 2011, *Deltas*, *In*: Noel, P.J., and Dalrymple, R.W., eds. Facies Models 4, Geological Association of Canada. Geotext, v. 6, p. 233-264.

Boggs, S., Jr., 2006, *Principles of Sedimentology and Stratigraphy*, 4th eds.: Prentice Hall, Upper Saddle River, NJ.

Bouma, A.H., 1962, Sedimentology of some flysch deposits: Amsterdam, Elsevier, 168p.

Bouma, A.H., 1997, *Comparison of fine grained, mud-rich and coarse grained, sand-rich submarine fans for exploration-development purposes*: Gulf Coast Association of Geological Societies Transactions, v. 47, p. 59-64.

Brenchley, P.J. and Newall, G., 1977, *The significance of contorted bedding in Upper Ordovician sediments of the Oslo Region Norway*: Journal Sedimentary Petrology, v. 47, n. 2, p. 819-833.

Camacho, H., Busby, C, J., and Kneeler, B., 2002, A new depositional model for the classical turbidite locality at San Clemente State Beach, California: AAPG Bulletin, v. 86, p. 1543-1560.

Cant, J.D., 1992, *Subsurface Facies Analysis*, *In*: Walker, R.G., eds., *Facies Models, Response to Sea Level Change*: Geological Association of Canada, pp. 27-45.

Caputo, M.V., de Melo, J.H.G., Streel, M., and Isbell, J.L., 2008, *Late Devonian and Early Carboniferous glacial records of South America*: Geological Society of America Bulletin Special Paper 441 pp. 161-173.

Catuneanu, O., 2002*, Sequence stratigraphy of clastic systems: concepts, merits, and pitfalls*: Journal of African Earth Sciences, v. 35, p. 1-43.

Chaplin, J.R., 1980, *Stratigraphy, trace fossil associations, and depositional environments in the Borden Formation (Mississippian*); *in* Geological Society of Kentucky Annual Field Conference Guidebook: Lexington, Kentucky Geological Survey, 114p.

Chaplin, J.R., and Mason, C.E., 1978, *Geologic map of the Garrison quadrangle, northeastern Kentucky*: U.S. Geological Survey Geological Quadrangle Map, GQ-401, scale: 1:24,000, one sheet.

Cheel, R. J., and Leckie, D. A., 1992, *Coarse-grained storm beds of the upper Cretaceous Chungo Member (Wapiabi Formation), southern Alberta, Canada*: Journal of Sedimentary Petrology, v. 62, p. 933-945.

Cole, G.A., Drozd, R.J., Sedivy, R., and Halpern, H.I., 1987, *Organic geochemistry and oil source correlations, Paleozoic of Ohio*: American Association of Petroleum Geologists Bulletin, v. 71, no. 7, p. 788-809.

Coogan, A.H., and Wells, N.A., 1992, *Northeastern Ohio's Berea Sandstone production [abs.], in Program and Abstracts*: The twenty-third Appalachian Petroleum Geology Symposium, "Exploration strategies in the Appalachian basin": West Virginia Geological and Economic Survey, Publication ICW-3, p. 19-20.

Cooper, P., 2002, *Reef development at the Frasnian/Famennian extinction boundary*: Paleogeography, Paleoclimatology, Coral Reef Symposium, 2, 1623-1630.

Cox, D.L., 1992, *Hydrocarbon accumulations of the Mississippian Berea Sandstone in west-central West Virginia* [abs.], in *Program and Abstracts*: The twenty-third Appalachian Petroleum Geology Symposium, "Mississippian plays in the Appalachian basin-Shallow targets for tough times": West Virginia Geological and Economic Survey, Publication ICW-4,p.10.

Darlymple, W. R., 2009, *Tidal Depositional Systems*, *In*: Walker, R.G., and Posamentier, H., eds., *Facies Models revisited*, SEPM Special Publication, v. 84, p. 201-236.

De Witt, W., Jr., 1951, *Stratigraphy of the Berea Sandstone and associated rocks in northeastern Ohio and northeastern Pennsylvania*: Geological Society of America Bulletin, v. 62, p. 1347-1370.

De Witt, W., Jr., 1970, *Age of the Bedford Shale, Berea Sandstone, and Sunbury Shale in the Appalachian and Michigan Basins, Pennsylvania, Ohio, and Michigan*: U.S. Geological Survey Bulletin 1294-G, 11 p.

De Witt, W., Jr., Roen, J.B., and Wallace, L.G., 1993, *Stratigraphy of Devonian black shales and associated rocks in the Appalachian Basin*, *in* Roen, J.B., and Kepferle, R.C., eds., *Petroleum Geology of the Devonian and Mississippian Black Shale of eastern North America*: U.S. Geological Survey, Bulletin 1909-B, 57p.

Dennison, J.M. (ed.), 1996*, Geologic Guide to Devonian Hydrocarbon Stratigraphy of Southeastern West Virginia and Adjacent Virginia*: American Association of Petroleum Geologists Eastern Section Meeting- 1996, 169p.

Dennison, J.M., 1985, *Catskill Delta shallow marine strata*, *in* Woodrow, D.L., and Sevon, W.D., *eds*., *The Catskill Delta*: Geological Society of America Special Paper 201, p. 91-106.

DeVay, J.C., Risch, D., Scott, E., Thomas, C., 2000, *Oroclinal bending of the Cape Ford Belt (CFB) and its effect on the formation and evolution of the Karoo basin, South Africa*: Terrane Processes at the Pacific Margin of Gondwana (TAPMOG), September 5-6, 2003.

Dickinson, W.R., Beard, L.Sl, Brakenridge, G.R., Erjavec, J.L., Ferguson, R.C., Inman, K.F., Knepp, R.A., Lindberg, F.A., Ryberg, P.T., 1983, *Provenance of North American Phanerozoic sandstones in relation to tectonic setting*: Geological Society of America Bulletin, v. 94, p. 222-235.

Duke, W.L., 1990, *Geostrophic circulation or shallow marine turbidity currents? The dilemma of paleoflow patterns in storm-influenced prograding shoreline systems*: Journal of Sedimentary Petrology, v. 60, p. 870-883.

Dumas, S. and Arnott R.W.C., 2006, Origin of hummocky and swaley cross-stratification-The controlling influence of unidirectional current strength and aggradation rate: Geologic Society of America, v. 34, n. 12, p. 1073-1076.

Drahovzal, J.A., and Noger, M.C., 1995, *Preliminary map of the structure of the Precambrian surface in eastern Kentucky*: Kentucky Geological Survey: Series XI, Map and Chart Series MCS8, scale 1:250,000.

Dyson, I. A., and Christopher, C. B., 1994, *Sequence Stratigraphy of an Incised Valley Fill: The Neoproterozoic Seacliff Sandstone, Adelaide Geosyncline, South Australia, in, Incised-valley systems*: Origin and Sedimentary Sequences, SEPM special publication, v. 51, p.

Ekdale, A. A., Bromley R. G., and Promberton, G. S., 1984, *Ichnology: The use of trace fossils in sedimentology and stratigraphy*: Society of Economic Paleontologists and Mineralogists, Short Course Notes Number 15, p. 317.

Elam, T.D., 1981, Stratigraphy and paleo-environmental aspects of the Bedford-Berea Sequence and the Sunbury Shale in Eastern and South-Central Kentucky MS thesis: University of Kentucky, 155 p.

Ettenshon, F.R., 1994, *Tectonic control on the formation and cyclicity of major Appalachian unconformities and associated stratigraphic sequences*, *in* Dennison, J.M., and Ettensohn, F. R., eds., *Tectonic and eustatic controls on sedimentary cycles*: SEPM Concepts in Sedimentology and Paleontology 4, p. 217-242.

Ettensohn, F.R., and Barron, L.S., 1981, *Depositional model for the Devonian-Mississippian black shales of North America: A paleogeographic-paleoclimatic approach*, *in* Roberts, T.G., ed., *Economic geology, structure* (Geological Society of America Cincinnati 1981 Field Trip Guide books, v. II): Falls Church, Virginia, American Geological Institute p. 344-357.

Ettensohn, F.R., and Elam, T.D., 1985, *Defining the nature and location of a Late Devonian-Early Mississippian pycnocline in eastern Kentucky*: Geological Society of America Bulletin, v. 96, p. 1313-1321.

Ettensohn, F.R., Lierman, R.T., and Mason, C.E., 2009, *Upper Devonian-Lower Mississippian clastic rocks in northeastern Kentucky: Evidence for Acadian alpine glaciation and models for source rock and reservoir-rock development in the eastern United States*: American Institute of Professional Geologists, Spring Field Trip Guide, April 18, 2009. 1-63p.

Ettensohn, F.R., Miller, M.L., Dillman, S.B., Elam, T.D., Geller, K.L., Swager, D.R., Markowitz, G., Woock, R.D., and Barron, L.S., 1988, *Characterization and implications of the Devonian-Mississippian black shale sequence, eastern and central Kentucky, U.S.A.: Pycnoclines, transgression, regression, and tectonism*, *in*: McMillan, N.J., Embry, A.F., and Glass, D.J., eds., *Devonian of the World: Proceedings of the 2nd International Symposium on the Devonian System*: Canadian Society of Petroleum Geologists, Memoir 14, v. 2, p. 323-345.

Floyd, J., 2015, Subsurface and Geological Analyses of the Berea Petroleum System in Eastern Kentucky, Earth and Environmental Sciences: MS thesis, University of Kentucky, 152 p.

Glikson, A.Y., Mory, A.J., Iasky, R.P., Pirajno, F., Golding, S.D., and Uysal, I.T., 2005, *Woodleigh Southern Carnavon Basin, Western Australia: history of discovery, Late Devonian age, and geophysical and morphometric evidence for a 120 km-diameter impact structure*: Australian Journal of Earth Sciences, 52, p. 545-553.

Gutschick, C., and Sandberg, A. C., 1991, *Upper Devonian biostratigraphy of the Michigan Basin*, Geologic Society of America, Special Publication, v. 256, p. 155-180.

Gutschick, R.C., and Rodriguez, J., 1977, *Late Devonian-Early Mississippian trace fossils and environments along the Cordilleran Miogeocline, western United States*. *In.* Crimes, T.P., and Harper, J.C., *eds*., International Symposium on Trace Fossils, Geological Journal, Special Issue, 9, 195-208.

Gutschick, R.C., and Rodriguez, J., 1979, Biostratigraphy of the Pilot Shale (Devonian-Mississippian) and contemporaneous strata in Utah, Nevada, and Montana, Brigham Young University Geology Studies, 26 (1), 37-62.

Harms J.C., Southard J.B., Spearing D.R. and Walker R.G., 1975, Depositional Environments as Interpreted from Primary and Sedimentary Structures and Stratification Sequences, 161 pp. Lecture Notes: Soc. Econ. Paleont. Miner. Course Notes, 2, Dallas.

Harris, D.C, 2014, Berea Sandstone Horizontal Oil Play, Appalachian Geological Society Meeting, Marshall University, March 12, 2014, http://www.uky.edu/KGS/emsweb/berea_ss/Upper_Devonian_Berea_SS.htm.

Harris, D.C., Drahovzal, J.A., Hickman, J.G., Nuttal, B.C., Baranoski, M.T., and Avary, K.L., 2004, *Rome Trough Consortium final report and data distribution (report submitted to industry partners and to the U.S. Department of Energy in fulfillment of U.S. Department of Energy contract DE-AF26-98FT02147*): Kentucky Geological Survey, Open-File Report 04-06, 1 CD-ROM.

Harris, D.L., 1975*, Oil and gas data from the Lower Ordovician and Cambrian rocks of the Appalachian Basin:* U.S. Geological Survey Miscellaneous Investigation Series Map I-917D, scale 1:2,500,000.

Harris, P. T., and Whiteway, T., 2011, *Global distribution of large submarine canyons, geomorphic differences between active and passive continental margins*: Marine Geology v. 285, p. 69-86.

Howard, J. D. and Lohrengel, C.F., II. (1969) *Large non-tectonic deformational structures from Upper Cretaceous Rock of Utah*: Journal Sedimentary Petrology, v. 39, p. 1032-1039.

Hudnall, J.S., and Browning, I.B., 1924, *Structural geologic map of the Paint Creek Uplift in Floyd, Johnson, Magoffin, Morgan, Lawrence, and Elliott counties, Kentucky*: Kentucky Geological Survey, ser. 6.

Hyde, J.E., 1911, *The ripples of the Bedford and Berea formations of central and southern Ohio*: Journal of Geology, v. 19, p. 257-269.

Jackson, D.S., 1985, Berea Sandstone (Mississippian) Perry Township, Ashland County, Ohio: MS Thesis, University of Cincinnati. 224 p.

Johnson, J. G., and Sandberg, C. A., 1989, *Devonian eustatic events in the western United States and their biostratigraphic responses*, *in* McMillan, N.J., Embry, A. F., and Glass, D. J., eds*. Devonian of the world*: Canadian Society of Petroleum Geologists Memoir 14, p. 171-178.

Johnson, J. G., Klapper, G., and Sandberg, C. A., 1985, *Devonian eustatic fluctuations in Euramerica*: Geological Society of America Bulletin, v. 96, p. 567-587.

Johnson, J. G., Klapper, G., Murphy, M. A., and Trojan, W. R., 1986, *Devonian series boundaries in central Nevada and neighboring regions, western North America*: Courier Forschungsintitut Senckenbery, v. 75, p. 177-196.

Kaiser, S.I, Aretz, M., and Becker, R.T., 2015*, The global Hangenberg Crisis (Devonian-Carboniferous transition): review of a first-order mass extinction*, *in*: Becker, R.T., Konigshof, P. and Brett, C.E. eds, *Devonian Climate, Sea Level and Evolutionary Events*, Geological Society, London, Special Publications, 423: 51 S., do.org/10.114/SP423.9.

Kaiser, S.I, Steuber, T., Becker, R.T., and Joachimski, M.M., 2006, *Geochemical evidence for major environmental change at the Devonian-Carboniferous*: Paleogeography, Paleocimatology, Paleoecology 240 p. 146-160.

Kearby, J.K., 1971, The Cowbell Member of the Borden Formation (Lower Mississippian) of northeastern Kentucky: A delta deposit (M.S. thesis): Lexington, University of Kentucky, 89p.

Kendall, G. St. C., 2012, Image viewed on 9/21/16 at http://www.sepmstrata.org/page.aspx?pagei39.

Kepferle, R.C., 1971, *Members of the Borden Formation (Mississippian) in north-central Kentucky*: U.S. Geol. Survey Bul. 1354-B, 18p.

Kneller, B., and Branney, M., 1995, *Sustained high-density turbidity currents and the deposition of thick massive sands*: Sedimentology, v. 42, p. 607-616.

Kuenen, P. H., 1965, *Values of experiments in geology*: Geol. En Mijnb., v. 44, p. 22-36.

Kuenen, P.H., 1958, *Experiments in Geology*: Trans. Glasgow, Geol. Soc., v. 23, p. 1-28.

Kuypers, M.M.M., Schouten, S., and Sinninghe Damste, J.S., 1998, *The Cenomanian/Touronian oceanic anoxic event: response of the atmospheric CO_2 level*, Mineralogical Magazine, 62A, 836-837.

Larese, R.E., 1974, Petrology and stratigraphy of the Berea Sandstone in the Cabin Creek and Gay-Fink trends, West Virginia [Ph.D. thesis]: Morgantown, West Virginia University. 245 p.

Lierman, R.T., Mason, C.E., Pashin, J.C., and Ettensohn, F.R., 1992, *Cowbell Member, Nancy Member, and Henley Bed of the Borden Formation, Sunbury Shale, and the Bedford-Berea sequence along State Route 546 in northeastern Kentucky*, *in* Ettensohn, F.R., eds., *Changing interpretations of Kentucky geology-Layer-cake, facies, flexure and eustacy*: Ohio Division of Geological Survey Miscellaneous Report No. 5, p. 142-145.

MacEachern, J.A., and Bann, K.L., 2008, *The role of ichnology in refining shallow marine facies models*, *in* Hampson, G., Steel, R., Burgess, P., and Dalrymple, R., eds*., Recent Advances in Models of Siliciclastic Shallow-Marine Stratigraphy*, SEPM Special Publication 90, p. 73-116.

Mason, C.E., and Chaplin, J.R., 1979, *Stop 2: Nancy and Cowbell members of the Borden Formation*, *in* Ettensohn, F.R., and Dever, G.R., Jr., eds., *Carboniferous geology from the Appalachian Basin to the Illinois Basin through eastern Ohio and Kentucky, Guidebook for Field*

Trip No. 4, IX International Congress of Carboniferous Stratigraphy and Geology: Lexington, University of Kentucky, p. 147-151.

Matchen, D.L., and Kammer, T.W., 2006*, Incised valley fill interpretation for Mississippian Black Hand Sandstone, Appalachian Basin, USA: Implications for glacial eustasy at the Kinderhookian-Osagean (Tn2-Tn3) boundary*: Sedimentary Geology, v. 191, p. 89-113, doi:10.1016/j.sedgeo.2006.02.002.

McBride, E.F., Weidie, A.E., and Wolleben, J.A., 1975, *Deltaic and associated deposits of the Difunta Group (Late Cretaceous to Paleocene), Parras and La Popa Basins, Northeastern Mexico, Deltas Models for Exploration*: Houston Geological Soc., p. 485-522.

McDowell, R.C., 1986, *The geology of Kentucky: a text to accompany the Geologic Map of Kentucky*: U.S. Geological Survey Professional Paper 1151-H, 68 p.

McGhee Jr., G.R., 1996, *The Late Devonian Mass Extinction: The Frasnian-Famennian Crisis*, Columbia University Press, New York, p. 303.

McGuire, W.H., and Howell, P., 1963, *Oil and gas possibilities of the Cambrian and Lower Ordovician in Kentucky*: Lexington, University of Kentucky, Spindletop Research Center, v. 1 p.

Mele, T.A., 1981, The occurrence of hydrocarbons in the Berea Sandstone in southeastern Ohio: Unpublished M.S. thesis, Ohio University, 82 p.

Miller, F.M., and Smail, S.E., 1997, *A Semiquantitative Field Method for Evaluating Bioturbation on Bedding Planes*: Society for Sedimentary Geology, v. 12. p. 391-396.

Morris, R.H., 1965a, *Geologic map of the Charters quadrangle, northeastern Kentucky*: U.S. Geological Survey Geological Quadrangle Map, GQ-293, scale: 1:24,000, one sheet.

Morris, R.H., 1965b, *Geologic map of the Stricklett quadrangle, northeastern Kentucky*: U.S. Geological Survey Geological Quadrangle Map, GQ-394, scale: 1:24,000, one sheet.

Morris, R.H., 1966, *Geologic map of the Buena Vista quadrangle, northeastern Kentucky*: U.S. Geological Survey Geological Quadrangle Map, GQ-525, scale: 1-24,000, one sheet.

Morris, R.H., and Pierce, K.L., 1967, *Geologic Map of the Vanceburg Quadrangle, Kentucky-Ohio*: U.S. Geological Survey Quandrangle Map, GQ-395, scale: 1:24,000, one sheet.

Morrow, J.R., and Hasiotis, S. T., 2007, *Endobenthic Response through Mass-Extinction Episodes: Predictive Models and Observed Patterns, Trace Fossils*: Concepts, Problem, Prespects, p. 573-595.

Morrow, J.R., and Sandberg, A. C., 2008, *Evolution of the Devonian Carbonate –shelf margin, Nevada*: Geosphere, v. 4, no. 2, p. 429-444.

Mutti, E., Tinterri, R., Benevelli, G., di Biase, D. and Cavanna, G., 2003, *Deltaic, mixed and turbidite sedimentation of ancient foreland basins*: Marine and Petroleum Geology, v. 20, p. 733-755.

Mutti, E., Tinterri, R., Remacha, E., Mavilla, N., Angella, S., and Fava, F., 1999, *An Introduction to the Analysis of Ancient Turbidite Basins fom an Outcrop Perspective*: American Association of Petroleum Geologists Course Note, 39, 93 p.

Myrow, P.M., Fischer, W., and Goodge, W.J., 2002, *Wave-Modified Turbidites: Combined-Flow Shoreline and Shelf Deposits, Cambrian, Antartica*: Journal of Sedimentary Research, v. 72, n. 5, p. 641-656.

Myrow, P.M., Lamb, M.P., Lukens, C., Houck, K, and Strauss, J., 2008, *Proximal to distal facies relationships in deposits of wave-influenced hyperpycnal flows*, *in* J.J. Ponce and E. B. Olivero, conveners, *Sediment transfer from shelf to deepwater-Revisiting the delivery mechanisms*: Conference Proceedings, AAPG Hedberg Conference, March 3-7, 2008, Ushuaia-Patagonia, Argentina, 5 p.

Myrow, P.M., Stauss, J.V., Creveling, J.R., Sicard, K.R., Ripperdan, R., Sandberg, C.A., and Hartenfels, S., 2011, *A carbon isotopic and sedimentological record of the latest Devonian (Famennian) from the Western U.S. and Germany*: Paleogeography, Paleoclimatology, Paleoecology, v. 306, p. 147-159.

Nittrouer, C.A., and Wright, L.D., 1994, *Transport of particles across continental shelves*: Reviews of Geophycis, 32, 85-113.

Nolde, J.E., and Milici, R.C., 1993, *Stratigraphic and structural controls of natural gas production from the Berea Sandstone (Mississippian), southwestern Virginia (abst*.): American Association of Petroleum Geologists Bulletin, v. 77, no. 8, p. 1471-1472.

Normark, W. R., 1970, *Growth patterns of deep sea fans*: AAPG Bulletin 54, p. 2170-2195.

Olariu, C., Steel, R. J., and Petter, A.L., 2010, *Delta-Front Hyperpycnal Bed Geometry and Implications for reservoir modeling*: Crataceous Panther Tongue Delta, Utah, *AAPG Bulletin,* v. 94, p. 819-845.

Pashin, J.C., 1985, Paleoenvironmental analysis of the Bedford-Berea sequence northeastern Kentucky and south-central Ohio [M.S. thesis]: Lexington, University of Kentucky, 105 p.

Pashin, J.C., 1990, *Reevaluation of the Bedford-Berea sequence in Ohio and adjacent states: New perspective on sedimentation and tectonics in foreland basins*: Lexington, University of Kentucky, Doctorate Dissertation, 411 p.

Pashin, J.C., and Ettensohn, F. R., 1987, *An epeiric shelf-to-basin transition: Bedford-Berea sequence, northeastern Kentucky and south-central Ohio*: American Journal of Science, v. 287, p. 893-926.

Pashin, J.C., and Ettensohn, F. R., 1992*, Paleoecology and sedimentology of the dysaerobic Bedford fauna (late Devonain), Ohio and Kentucky (USA)*: Paleogeography, Paleoclimatology, Paleoecology v. 91 p. 21-34.

Pashin, J.C., and Ettensohn, F. R., 1995, *Reevaluation of the Bedford-Berea Sequence in Ohio and Adjacent States: Forced Regression in a Foreland Basin*: Geological Society of America Special Publication 298, p. 1-62.

Pemberton, S.G., and Wightman, D.M., 1992*, Ichnological characteristics of brackish water deposits*, *in* Pemberton, S.G., eds., *Applications of Ichnology of Petroleum Exploration*: Society of Economic Paleontologists and Mineralogists, Core Workshop 17, p. 141-167.

Pepper, J.F., De Witt, W., Jr., and Demarest, D. F., 1954, *Geology of the Bedford Shale and Berea Sandstone in the Appalachian Basin*: U.S. Geological Survey Professional Paper 259, 111 p.

Pettijohn, F.J., 1975, Sedimentary Rocks, Harper and Row, 628 p.

Plint, A.G., 2010, *Wave- and storm-dominated shoreline and shallow marine systems*. *in*: *Facies Models*, 4th Edition, Dalrymple, R.W. and James, N.P., eds., Geological Association of Canada, p. 167-199.

Plint, A.G., and Nummedal, D., 2000, *The falling stage systems tract: recognition and importance in sequence stratigraphic analysis*, i*n*, D. Hunt and R.L. Gawthorpe, eds., *Sedimentary Responses to Forced Regressions*: Geological Society of London, Special Publication 172, p. 1-17.

Potter, P.E., DeReamer, J. H., Jackson, D. S., and Maynard, J. B., 1983*, Lithologic and paleoenvironmental atlas of Berea Sandstone in the Appalachian basin*: Appalachian Geological Society Special Publication 1, 157 p.

Prosser, C. S., 1912, *Disconformity between the Bedford and Berea in central Ohio*: Journal Geology v. 20, p. 585.

Rider, M., 1996, *The Geological Interpretation of Well Logs, 2nd Edition*: Whittles Publishing, Caithness, 280 p.

Riley, A.R., and Baranoski, T. M., 1988, *Analysis of stratigraphic and production relationships of Devonian Shale gas reservoirs in Lawrence County, Ohio*. Open-File Report 88-2, 30p.

Rothman, E.M., 1978, The Petrology of the Berea Sandstone (Early Mississippian) of South-central Ohio and a Portion of Northern Kentucky: M.S. Thesis, Miami University, Oxford, Oh., 105 p.

Sandberg, C.A., 1988, *Role of conodont biofacies in Late Devonian and Early Mississippian paleobiogeographic reconstructions of western United States*: Geological Society of America Abstracts with Programs, v. 20, p. 227.

Sandberg, C.A., Morrow, J. R., and Zieglar, W., 2002, *Late Devonian sea-level changes, catastrophic events, and mass extinctions*: Geological Society of America Special Publication 356, p. 356-473.

Sanders, J. E., 1965, *Primary sedimentary structures formed by turbidity currents and related sedimentation mechanisms*, *in* G. V. Middleton, eds., *Primary sedimentary structures and their hydrodynamic interpretation*: SEPM Special Publication 12, p. 192-219.

Selley, R.C., 1998, *Elements of Petroleum Geology*, 2nd ed., xvi 470 pp.

Shaler, N.S. 1877, *Notes on the investigations of the Kentucky Geological Survey during the years 1873, 1874 and 1875*: Kentucky Geological Survey Report Progam, v. 3, 129-282.

Single, E.L., 1956, Contorted Strata of the Lower Mississippian Rocks in Pick and Ross Counties, Ohio: M.S. Thesis, Univ. of Cincinnati, Cincinnati, Oh., 112 p.

Sorauf, J.E., 1965, *Flow rolls of Upper Devonian rock of south-central New York State*: Journal Sedimentary Petrology, v. 35, p. 553-563.

Spark, R. S. J., Bonnecaze, H. E. Huppert, J. R. Lister, M. A. Halloworth, J. Phillips, and H. Mader, 1993, *Sediment-laden gravity currents with reversing buoyancy*: Earth and Planetary Science Letters, v. 114, p. 243-257.

Streel, M., and Traverse, A., 1978, *Spores from the Devonian/Mississippian transition near the Horseshoe Curve section, Altoona, Pennsylvania, U.S.A*.: Review of Paleobotany and Palynology, v. 26, p. 21-39.

Sumner, E. J., Amy, L. A., and Talling, P. J., 2008, *Deposit structure and processes of sand deposition from decelerating sediment suspension*: Journal of Sedimentary Research, v. 78, p. 529-547.

Swift, D.J.P., Han, G. and Vincent, C.E., 1986, *Fluid processes and sea-floor response on a modern storm-dominated shelf: Middle Atlantic shelf of North America. Part I: the storm-current regime*, *in*: Knight, R.J. and McLean, J.R., eds., *Shelf Sands and Sandstones*: Canadian Society of Petroleum Geologists, Memoir 11, p. 99-119.

Tankard, A.J., 1986, *Depositional response to foreland deformation in the carboniferous of eastern Kentucky*: American Association of Petroleum Geologists Bulletin, v. 70, no. 7, p. 853-868.

Tomastik, E.T., 1996, *Lower Mississippian-Upper Devonian Berea and Equivalent Sandstones*, *in* Roen, J.B., and Walker, B.J., eds., *The atlas of major Appalachian gas plays*: West Virginia Geological and Economical Survey Publication V-25, p. 56-62.

Tucker, M.E., 2001, *Sedimentary Petrology, an Introduction to the Origin of Sedimentary Rocks*, 3rd edition, Blackwell, Oxford pp. 262.

Warner, C.J., 1978, Subsurface stratigraphy of the Berea and Cussewago sandstones in eastern Ohio: Unpublished M.S. thesis, Kent State University, 65p.

Wheatcroft, R.A., 2000, *Oceanic flood sedimentation, a new perspective*: Cont. Shelf Res., 20, 2059-2066.

Woodrow, D.L., Fletcher, F.W., and Ahrnsbrak, W.F., 1973, *Paleogeography and Paleoclimate at the deposition sites of the Devonian Catskill Delta and Old Red facies*: Geological Society of America Bulletin, v. 84, p. 3051-3063.

Zavala, C., Arcuri, M., Di Meglio, M., and Zorzano, A., 2016, *Intrabasinal and extrabasinal turbidites: Origin and distinctive characteristics*. International Conference and Exhibition, Barcelona, Spain, 3-6 April 2016: pp. 71-71.

Zavala, C., Carvajal, J., Marcano, J., and Delgado, M., 2008, *Sedimentological indices: A new tool for regional studies of hyperpycnal systems*, *in* J.J. Ponce and E.B. Olivero, conveners, *Sediment transfer from shelf to deepwater-Revisting the delivery mechanisms*: Conference Proceedings, AAPG Search and Discovery Article 50076, AAPG Hedberg Conference, March 3-7, 2008, Ushuaia-Patagonia, Argentina, 4 p.

Zavala, C., Marcano, J., Carvjal, J., and Delgado, M., 2011b, *Genetic indices in hyperpycnal systems; A case study in the late Oligocene-early Miocene Merecure Formation, Maturin Subbasin, Venezela*, *in* R. M. Slatt and C. Zavala, eds., *Sediment transfer from shelf to deep water –Revisiting the delivery system*: AAPG Studies in Geology 61, p. 53-73.

Zavala, C., Arcuri, M., Gamero Diaz, H., Contreras, C., and Di Meglio, M., 2011a, *A Genetic Facies Tract for the Analysis of Sustained Hyperpycnal Flow Deposits in* R. M. Slatt and C. Zavala, eds., *Sediment transfer from shelf to deep water –Revisiting the delivery system*: AAPG Studies in Geology 61, p. 31-52.

APPENDIX I IRB LETTER

MARSHALL UNIVERSITY

www.marshall.edu

Office of Research Integrity

December 16, 2016

Forrest Mattox
6687 Fishers Ridge Road
Liberty, WV 25124

Dear Mr. Mattox:

This letter is in response to the submitted thesis abstract entitled *"The Stratigraphy, Sedimentology and Reservoir Modeling of the Late Devonian Berea Sandstone/Siltstone in northeastern Kentucky and Southern Ohio."* After assessing the abstract it has been deemed not to be human subject research and therefore exempt from oversight of the Marshall University Institutional Review Board (IRB). The Code of Federal Regulations (45CFR46) has set forth the criteria utilized in making this determination. Since the information in this study does not involve human subjects as defined in the above referenced instruction it is not considered human subject research. If there are any changes to the abstract you provided then you would need to resubmit that information to the Office of Research Integrity for review and a determination.

I appreciate your willingness to submit the abstract for determination. Please feel free to contact the Office of Research Integrity if you have any questions regarding future protocols that may require IRB review.

Sincerely,

Bruce F. Day, ThD, CIP
Director

APPENDIX II RIPPLE INDEX

Bedford-Berea Ripple Index

Measurement	Wavelength (cm)	Ripple Height (cm)	Ripple Index
1	8.3	0.7	12
2	8.5	0.6	14
3	6.5	0.65	10
4	6.9	0.8	9
5	6.8	0.6	11
6	7.1	0.6	12
7	7	0.59	12
8	6.9	0.5	14
9	10	1	10
10	10.6	1	11
11	10.5	0.8	13
12	7.9	0.6	13
13	8.5	0.6	14
14	7	0.55	13
15	7.3	0.6	12
16	7	0.6	12
17	7	0.8	9
18	7.5	0.7	11
19	7	0.55	13
20	7.3	0.6	12
21	9.2	0.6	15
22	9	0.7	13
23	8.5	0.7	12
24	7.6	0.8	10
25	7.9	0.5	16
26	8	0.6	13
27	9	0.6	15
28	11	0.9	12
29	9.4	0.65	14
30	7.4	0.6	12
31	6.2	0.5	12
32	9	0.9	10
33	9	0.7	13
34	9	0.7	13
35	10	1	10
36	10.5	1.1	10
37	10	0.9	11

38	6	0.4	15
39	5	0.3	17
40	6	0.7	9
41	6.8	0.7	10
42	6.5	0.6	11
43	7	0.72	10
44	6.9	0.5	14
45	6.9	0.4	17
46	7	0.6	12
47	9	0.8	11
48	8	0.6	13
49	10	0.9	11
	Average	Average	
	7.98	0.675	
	Average Ripple Index:	11.82	

APPENDIX III PALEOCURRENTS

Wave Ripple Crest Measurements

Outcrop	Strike
1	305
1	299
1	309
1	306
1	300
1	312
1	317
1	315
1	305
1	302
2	312
2	310
2	311
2	309
2	318
4	302
4	301
4	297
5	297
5	305
6	299
7	309
8	305
8	309
8	316
8	315
8	305
9	299
9	307
9	310
9	304
10	304
10	298
12	299
12	301
12	315
12	313
12	309
13	315

13	309
13	309
13	314
13	315
13	310
13	309
13	310
15	309
17	305
17	309
17	302
17	310
18	310
18	312
19	307
19	308
20	312
20	315
22	315
22	311
22	316
22	305
22	309
23	320
23	318
23	320
23	319
23	315

Current Measurements

Outcrop	Type	Strike	Dip Azimuth	Inclination	Thickness
1	Asymmetric Ripple Bedding	194	284	10	
1	Asymmetrical Ripple	300	210		
1	Cross-bed??	200	290	20	30cm
1	Asymmetrical Ripple	303	213	11	
1	Ripple Bedding	200	290		
2	Asymmetrical Ripple	306	216		
2	Asymmetrical Ripple	303	213		
2	Asymmetrical Ripple	300	210		
2	Asymmetric Ripple Bed	145	235	13	2cm
2	Asymmetric Ripple Bed	170	260	11	3cm
4	Asymmetrical Ripple	306	216		
4	Ripple Bed	175	265		
5	Asymmetrical Ripple	310	220		
5	Asymmetrical Ripple	305	215		
6	Asymmetrical Ripple	309	219		3-4cm
6	Asymmetrical Ripple	310	220		
6	Asymmetrical Ripple	307	217		
6	Ripple Bedding	192	278		2cm
9	Asymmetrical Ripple	301	211		
9	Asymmetrical Ripple	297	207		
10	Asymmetrical Ripple	300	210		
10	Asymmetrical	297	207		

	Ripple				
10	Asymmetrical Ripple	310	220		
12	Asymmetrical Ripple	297	207		
12	Asymmetrical Ripple	292	202		
12	Asymmetrical Ripple	302	212		
13	Asymmetrical Ripple	320	230		2.4cm
13	Asymmetrical Ripple	319	229		2.7cm
13	Asymmetrical Ripple	328	238		3cm
13	Asymmetrical Ripple	303	213		4cm
14	Asymmetrical Ripple	310	220		2cm
16	Asymmetrical Ripple	302	212		2cm
18	Asymmetrical Ripple	310	220		
18	Asymmetrical Ripple	308	218		
20	Asymmetrical Ripple	307	217		
22	Asymmetric Ripple Lamination	310	220	16	5cm
22	Asymmetrical Ripple	310	220		
22	Asymmetrical Ripple	315	225		
22	Asymmetrical Ripple	311	221		
23	Asymmetrical Ripple	323	233		

Cross-beds Tener Mountain Location 13

Outcrop	Type	Strike	Dip Azimuth	Inclination	Thickness
13	Cross-bed??		63		10cm
13	Cross-bed??		52		16cm
13	Cross-bed??		46		18cm

APPENDIX IV MEASURED SECTIONS

Location:	1	Coordinates :	38 33' 07.84" N / 83 14' 05.04"W
Quad:	Garrison	Elevation:	579

Unit	Thickness	Color	Lithology	Sedimentary Structures	Contact	Fossils (Body, Trace)
KY-1-1	30 cm	Med. gray	Shale/silty shale	Thin bedded, parallel laminated		
KY-1-2	55cm	Light gray	Siltstone	Ripple bedding, horizontal lamination	Sharp	
	60cm	Light gray, WRS light brown	Siltstone	Parallel lamination, large hummocky cross-beds		
	60cm	Light gray, WRS light brown	Siltstone	Ripple bedding, parallel horizontal lamination	Sharp	
	52cm	Light gray, WRS light brown	Siltstone	Shale lens at bottom, convolute bedding directly above lens	Sharp	Burrows
	65cm	Light gray, WRS light brown	Siltstone	Parallel lamination		
	22cm	Light gray, WRS light brown	Siltstone	Parallel lamination		
	5cm	Dark gray	Shale	Fissile, parallel	Trans	
	25cm	Light gray, WRS light brown	Siltstone	Hummocky cross-stratification	Sharp	
	60cm	Light gray, WRS light brown	Siltstone	Parallel lamination		
	60cm	Light gray, WRS light brown	Siltstone	Ripple crests at top, parallel lamination, flame	Trans	

				structure towards bottom		
KY-1-3	60cm	SS: light gray. shale: dark gray	Siltstone/shale interbedded	Thin bedded, fissile, laminated, ripple cross laminations, micro-hummocky cross-stratification, lenticular ripple bedding	Trans	Burrows in float
KY-1-4	65cm	Light gray, WRS light brown	Very fine sandstone	Massive, crude low angle lamination, load casts on bottom		
	20cm	Light brown-light gray	Siltstone/shale interbedded	Wavy Ripple Bedding, with Symmetrical and Combined flow ripples	Trans	Burrow casts
	25cm	SS: light gray shale: dark gray	Shale/very fine sandstone	Ripple bedding in sandstone, load structures, burrowing on load structures on base		Small burrows in shale
	55cm	Light gray, WRS light brown	Very fine sandstone	Parallel laminations, ball and pillow structures on bottom	Sharp	
	20 cm	Med. gray	Shale	Fissile, parallel		
	85cm	Light gray	Very fine sandstone	Irregular load, massive	Sharp	
	8cm	Dark gray	Shale	Fissile, parallel		
	10cm	Light gray	Siltstone	Parallel lamination		
	18cm	Light gray	Very fine sandstone	Parallel lamination		
	25cm	Light gray	Very fine sandstone	Slightly asymmetric ripples on top		
KY-	8cm	Med. gray	Shale	Fissile, parallel	Trans	

1-5						
	4cm	Light gray	Siltstone		Trans	
	10cm	Med. gray	Shale	Fissile, parallel	Trans	
	18cm	Light gray	Very fine sandstone	Massive	Sharp	
	13cm	Med. gray	Shale	Fissile, parallel	Trans	
	28cm	Light gray	Very fine sandstone	Massive	Sharp	
	12cm	Dark gray	Shale	Fissile, parallel		
	38cm	Light gray	Very fine sandstone	Massive	Sharp	
	6cm	Med. gray	Siltstone/shale interbedded	Wavy ripple bedding, with symmetrical and combined flow ripples		
	22cm	Light gray	Very fine sandstone	Massive		
	70cm	SS: Light gray, shale: dark gray	Very fine sandstone, 3 shale	Thinly interbedded shales in 3 locations, shales 2cm thick, symmetric ripples below shales		
	40cm	Light gray	Very fine sandstone	Convolute bedding upper part, hummocky cross-bed lower part	Sharp	
	45cm	Light gray	Very fine sandstone	Massive		
	15cm	Med. gray	Shale	Fissile, parallel		Burrows
KY-1-6	27cm	Light gray	Very fine sandstone	Massive	Sharp	
	3cm	Med. gray	Shale	Fissile, parallel		
	45cm	Light gray	Very fine sandstone	2cm ripple lamination, hummocky cross lamination	Sharp	
	27cm	Light gray	Very fine sandstone	Massive		
	3cm	Med. gray	Shale	Fissile, parallel		

	33cm	Light gray	Very fine sandstone	Massive		
	2cm	Med. gray	Shale	Fissile, parallel		
	55cm	Light gray	Very fine sandstone	Massive	Sharp	
	5cm	Light gray	Sandstone/shale	Thin interbedded, wavy ripple bedding	Trans	
	11cm	Light gray	Very fine sandstone	Massive		
	2cm	Med. gray	Shale/very fine sandstone	Thin interbedded, wavy ripple bedding		
	75cm	Light gray	Very fine sandstone	Massive		
	2cm	Med. gray	Shale/ very fine sandstone	Thin interbedded, wavy ripple bedding		
	2.75m	Light gray, Light brown	Very fine sandstone	Poorly exposed thick bed, convolute bedding 20cm from top	Sharp	
KY-1-7	15cm	Light gray	Very fine sandstone/thin shale	Wave ripples at top		
	70cm	Light gray	Very fine sandstone	Thin bedded upper portion, massive lower portion	Sharp	
	3cm	Med. gray	Shale	Fissile, parallel		
	60cm	Light gray	Very fine sandstone	Thin bedded at top, parallel laminations at base		
	3cm	Med. gray	Sand/shale	Interlaminated	Trans	
	17cm	Light gray	Very fine sandstone	Parallel lamination		
	8cm	Med. gray	Sand/shale	Interlaminated	Trans	
	10cm	Med. gray	Very fine sandstone/shale	Lenticular ripple bedded	Trans	
	8cm	Med. gray	Shale	Fissile, parallel	Trans	
	32cm	Light gray	Very fine	Trough scours,	Sharp	

			sandstone	parallel lamination, massive		
	2cm	Med. gray	Sand/shale	Interlaminated	Trans	
	25cm	Light gray	Very fine sandstone	Parallel lamination, VFS grading to silt (Normal Grading)	Trans	
	8cm	Light gray	Very fine sandstone	Parallel lamination		
	7cm	Light gray	Very fine sandstone	Parallel lamination		
	40cm	Light gray	Very fine sandstone	Crossbed (30cm), large scour	Sharp	
	35cm	Light gray	Very fine sandstone	Solution cavities: vertical, massive	Sharp	
	35cm	Light gray	Very fine sandstone	Ripple bedded, thin bedded		
	10cm	Med. gray	Very fine sandstone/shale	Parallel lamination, VFS grading to shale	Trans	
	2.75m	Light gray	Very fine sandstone	Thick bedded bottom, parallel-low angle lamination, ripple bedded upper 20 cm	Trans	
KY-1-8		Dark gray	Shale	Sunbury Shale	Sharp	

Location:	2	Coordinates :	38 35' 48.62" N/ 83 10' 27.09" W
Quad:	Garrison	Elevation:	556

Unit	Thickness	Color	Lithology	Sedimentary Structures	Contact	Fossils (Body, Trace)
KY-2-1	30cm	Light gray, WRS light brown	Siltstone	Massive, ball and pillow structure		

	22cm	Med. gray	Silty shale	fissile, parallel laminated	Sharp	
KY-2-2	1.25m	Light gray, WRS Light brown	Siltstone	Ball and pillow, soft sediment deformation, ripple laminated that grades into thin bedded parallel lamination	Sharp	
	20cm	Med. gray	Shale	Thin bedded, parallel lamination		
	18cm	Light gray	Siltstone	Massive, parallel lamination on top	Sharp	
	13cm	Med. gray	Shale	Fissile, parallel laminated		
	10cm	Light gray	Siltstone	Massive		
	30cm	Med. gray	Shale, one siltstone bed	Ripple lamination, combined flow ripples, hummocky cross-stratification	Sharp	
	15cm	Light gray	Siltstone	Massive		
	4cm	Med. gray	Shale	Fissile, parallel laminated	Trans	
	30cm	Light gray	Siltstone	Massive		
	65cm	Light gray	Siltstone	Ripple lamination, asymmetric ripples	Sharp	
	35cm	Light gray, WRS light brown	Very fine sandstone	Massive	Trans	
	20cm	Light gray, med. gray	Siltstone/shale	Thin bedded, wavy ripple bedded, soft sed. Deformation		
KY-2-3	55cm	Light gray, WRS light brown	Very fine sandstone	Massive bottom, mud rip ups on bottom, parallel lamination	Sharp	

	5cm	Med. Gray	Shale	Parallel, fissile		
	60cm	Light gray, WRS light brown	Very fine sandstone	Parallel bedded at bottom, massive top	Sharp	
	2cm	Med. gray	Shale	Fissile, parallel laminated		
	35cm	Light gray, WRS light brown	Very fine sandstone	Parallel lamination on bottom, ripple lamination towards top, ripple marks on top??		
	2cm	Med. gray	Shale	Fissile, parallel laminated		
	38cm	Light gray, WRS light brown	Very fine sandstone	Massive bottom, parallel lamination middle, ripple marks on top	Sharp	
	2cm	Med. gray	Shale	Fissile, parallel laminated		
	1.3m	Light gray, WRS light brown	Very fine sandstone	Massive at bottom, parallel lamination towards top	Sharp	
	2cm	Med. gray	Shale	Fissile, parallel laminated		
	30cm	Light gray	Very fine sandstone	Parallel at base	Sharp	
	30cm	Med. gray/light gray	Shale/siltstone	Hummocky cross-stratification in thin siltstone, wavy ripple bedded	Trans	
	1.0m	Med. gray	Very fine sandstone	Parallel lamination in sandstone beneath two small shale layers, Shale layers less than 1cm		

	25cm	No exposure				
	1.8m	Light gray, WRS light brown	Very fine sandstone	0-60cm: massive, 65-80cm: parallel lamination, soft sediment deformation 80-175cm: massive, 175-180cm: ripple lamination, parallel	Sharp	
	18cm	Med. gray	Silty shale	Ripple lamination, thin bedded	Trans	
	60cm	Light gray	Very fine sandstone	Hummocky cross-stratification, ripple marks on top		
	15cm	Med. gray	Shale/Very fine sandstone	Thin interbedded, wavy/lenticular ripple bedded	Trans	
	30cm	Light gray	Very fine sandstone	Mud rip ups, parallel laminated	Sharp	
	25cm	Med. gray	Shale	Parallel, fissile		
	15cm	Light gray	Very fine sandstone	Massive		
KY-2-4	1m	Light gray, WRS light brown	Very fine sandstone	Parallel lamination, rib and furrows, ripple marks, crude low angle lamination	Sharp	
	30cm	Covered				
	1.2m	Light gray	Very fine sandstone	Massive, parallel lamination on top	Sharp	
	2cm	Med. gray	Shale	Fissile, parallel laminated		
	30cm	Light gray	Very fine sandstone	Massive		
	2cm	Med. gray	Shale	Fissile, parallel laminated		
	90cm	Light gray	Very fine	Cross-		

			sandstone	stratification with parallel lamination above, micro-hummocky cross-beds, massive at top		
	10cm	Med. gray	Very fine sandstone at top, shale at bottom	Shale is parallel laminated (inverse grading)	Trans	
	30cm	Light gray	Very fine sandstone	Parallel lamination, massive	Trans	
	2cm	Dark gray	Shale	Fissile, parallel laminated		
	45cm	Light gray	Very fine sandstone	Low angle lamination, ripple marks on top	Sharp	
	30cm	Light gray	Very fine sandstone	Massive at base, parallel at top	Sharp	
	1cm	Med. gray	Shale	Fissile, parallel laminated		
	45cm	Light gray	Very fine sandstone	Parallel lamination, ferruginous stains		Heavily burrowed
2-5		Dark gray	Shale	Sunbury Shale		

Location:	3	Coordinates :	38 32' 3.91"N/83 20' 31.29"W
Quad:	Garrison	Elevation:	556

Unit	Thickness	Color	Lithology	Sedimentary Structures	Contact	Fossils (Body, Trace)
KY-3-1	90cm	Dark gray	Shale	Fissile, parallel lamination, (Cleveland Shale)		
KY-3-2	8.2m	Light gray	Very Fine Sandstone and Siltstone	Ball and pillow, mud rip-ups, pyrite nodules,	Sharp	

				trough cross-beds, convolute bedding, pinch and swell scours, large scale cross-beds		

Location:	4	Coordinates	38 35' 34.53" N/ 83 12' 12.59" W
Quad:	Garrison	Elevation:	604

Unit	Thickness	Color	Lithology	Sedimentary Structures	Contact	Fossils (Body, Trace)
KY-4-1	15cm	Light gray	Siltstone	Micro-hummocky cross-beds on bottom, parallel lamination above and on top		Bedding plane bioturbation in float
	20cm	Light gray to med. gray	Shale and siltstone	Thin interbedded, wavy ripple bedded, combined flow ripples	Trans	Small amount bedding plane bioturbation
	60cm	Light gray	Very fine sandstone	Ball and pillow on bottom, massive		
	10cm	Med. gray	Shale	Fissile, parallel lamination		
	8cm	Light gray	Very fine sandstone	Ripple lamination, micro-hummocky cross-beds	Sharp	
	15cm	Light gray	Shale	Fissile, parallel lamination	Trans	Bedding plane bioturbation in float
	5cm	Light gray	Very fine sandstone	Micro-hummocky cross-beds, ripples		Horizontal burrows
	1cm	Med. gray	Shale	Fissile, parallel lamination		

	28cm	Light gray	Very fine sandstone	Massive		
	40cm	Light gray to med. gray	Very fine sandstone and shale	Ripple lamination (wavy), micro-hummocky cross-beds, parallel fissile top	Trans	
	15cm	Light gray	Very fine sandstone	Massive	Sharp	
	9cm	Light gray	Very fine sandstone and shale	Ripple lamination (wavy), ripple marks (appear symmetric)		
KY-4-2	75cm	Light gray	Very fine sandstone	Massive, parallel bedding at top	Sharp	
	2cm	Med. gray	Shale	Fissile, parallel lamination		
	60cm	Light gray	Very fine sandstone	Massive, parallel at top		
	10cm	Light gray	Very fine sandstone and shale	Parallel at top in shale/poorly exposed	Trans	
	70cm	Light gray	Very fine sandstone	Parallel at bottom, massive	Sharp	
	2m	CLIFF				
	80cm	CLIFF				
	35cm	Light gray	Very fine sandstone	Massive at bottom, parallel at top		
	7cm	Med. gray	Shale	Fissile, parallel lamination		
	30cm	Light gray	Very fine sandstone	Massive		
	12cm	Med. gray to light gray	Shale/thin very fine sandstone	Lenticular ripple lamination (possible bundling)	Trans	
	45cm	Light gray	Very fine sandstone	Massive		
KY-4-3	2cm	Med. gray	Shale	Fissile, parallel lamination		
	20cm	Light gray	Very fine sandstone	Hummocky cross-stratification,		Bedding plane

				symmetrical ripples on top (combined flow ripples?)		bioturbation on top
	25cm	Med. gray to light gray	Very fine sandstone-Thin shale	Hummocky cross-stratification, ripple lamination, parallel lamination at bottom	Trans	
	14cm	Light gray	Very fine sandstone	Massive		
	4cm	Med. gray	Shale	Fissile, parallel lamination		
KY-4-4	85cm	Light gray, WRS light brown	Very fine sandstone	Ball and pillow on bottom, parallel bedding throughout (bundling?) convolute soft sediment deformation laterally	Sharp	
	1cm	Med. gray	Shale	Fissile, parallel lamination		
	35cm	Light gray	Very fine sandstone	Ripple lamination on top, massive	Sharp	
	30cm	Light gray to med. gray	Shale/very fine sandstone	Thin bedded shale, wavy ripple bedded	Trans	Bedding plane bioturbation 1-3
	79cm	Light gray	Very fine sandstone	Soft sediment deformation, parallel lamination on top		
	20cm	Med. gray	Shale/very fine sandstone	Ripple lamination, parallel lamination	Trans	Bedding plane bioturbation 1-2
	35cm	Light gray	Very fine sandstone	Massive	Trans	
	30cm	Light gray	Very fine sandstone	Parallel bedded		Bedding plane

						bioturbation 1-3
	45cm	Light gray	Very fine sandstone	Massive, parallel at top		
	1cm	Med. gray	Shale	Fissile, parallel lamination		
	1.05m	Light gray	Very fine sandstone	Massive, slightly asymmetrical ripples on top (combined flow?)		Horizontal burrows

Location:	5	Coordinates	38 33.05' 6.85" W/ 83 14' 3.08"N
Quad:	Garrison	Elevation:	583

Unit	Thickness	Color	Lithology	Sedimentary Structures	Contact	Fossils (Body, Trace)
KY-5-1	50cm	Light gray, WRS light brown	Siltstone	Massive, parallel lamination at top		
	40cm	Light gray, WRS light brown	Siltstone	Massive	Sharp	Bedding plane bioturbation bottom
	2cm	Med. gray	Shale	Fissile, parallel lamination		
	54cm	Light gray	Siltstone	Massive at bottom, swaley cross-stratification, micro-hummocky, rippled top	Sharp	Limited burrowing on top
	60cm	Light gray	Siltstone	Parallel Lamination on bottom, massive	Sharp	
	1.2m	Light gray	Siltstone	Soft sediment deformation, large scale cross-bed, massive, top has	??	

				thin parallel lamination		
	25cm	Light gray	Siltstone	Parallel lamination on bottom, massive	Sharp	
	3cm	Med. gray	Shale	Fissile, parallel lamination		
	75cm	Light gray	Siltstone	0-23cm: massive, thin parallel lamination, massive	Sharp	
KY-5-2	55cm	Med. gray	Interbedded siltstone and shale	Micro-hummocky cross-stratification, ripple cross lamination, wavy ripple bedded	Trans	Horizontal burrows
	65cm	Light brown	Siltstone	Massive, parallel lamination at top	Sharp	
KY-5-3	45cm	Med. gray	Interbedded siltstone and shale	Massive siltstone at bottom, wavy ripple bedded, current ripples, lenticular ripple bedded at top	Trans	1-2 Bedding plane bioturbation
KY-5-4	63cm	Light gray	Very fine sandstone	Ball and pillow bottom, massive, parallel at top	Sharp	
	27cm	Light gray	Shale and siltstone	Thin bedded, lenticular ripple bedded, ripple lamination		
	15cm	Light brown	Very fine sandstone	Massive, parallel bedded	Sharp	
	80cm	Light gray to brown	Very fine sandstone	Thin parallel bed at bottom (2cm thick),	Sharp	
	50cm		COVERED			
	25cm	Light gray to brown	Very fine sandstone	Massive at bottom, parallel lamination top	Sharp	
	1cm	Med. gray	Shale	Fissile, parallel lamination		
	65cm	Light gray	Very fine sandstone	Massive	Sharp	
	30cm	Med.	Interbedded	Current ripples,		Sparse

		Gray to grown	Siltstone and shale	Micro-hummocky cross-stratification, wavy ripple bedding at bottom, lenticular at top		Burrowing
	24cm	Light gray	Very fine sandstone	Massive, thin parallel lamination at top	Trans	
	11cm	Light gray	Siltstone	Parallel lamination throughout	Trans	
	62cm	Light gray to brown	Very fine sandstone	Ball and pillow bottom, massive	Trans	
	10cm	Med. gray	Siltstone	Massive, parallel lamination at top		
	38cm	Light gray	Very fine sandstone	Low angle lamination at bottom, parallel lamination middle, massive top	Sharp	
	2cm	Med. gray	Shale	Fissile, parallel lamination		
	54cm	Light gray	Very fine sandstone	Parallel lamination bottom, massive	Sharp	
	2cm	Med. gray	Shale	Fissile, parallel lamination		
	65cm	Light gray	Very fine sandstone	Ball and pillow bottom, intense soft sediment deformation, massive	Sharp	
	2cm	Med. gray	Shale	Fissile, parallel lamination		
	65cm	Light gray	Very fine sandstone	Bottom 20cm parallel lamination, 2cm low angle lamination?, massive	Sharp	
	4cm	Med. gray	Shale	Fissile, parallel lamination		
	15cm	Light gray	Very fine sandstone	Low angle lamination, thin bedded parallel		

				lamination at top		
	4cm	Med. gray	Shale	Fissile, parallel lamination		
	50cm	Light gray	Very fine sandstone	Massive bottom, parallel lamination middle	Sharp	
	COVERED					

Location	6	Coordinates	38 32' 42.23" W/ 83 13' 02.94" N
Quad:	Garrison	Elevation:	625

Unit	Thickness	Color	Lithology	Sedimentary Structures	Contact	Fossils (Body, Trace)
KY-6-1	1.3m	Light gray	Very fine sandstone	Parallel lamination bottom, massive	Trans	
KY-6-2	13cm	Light gray	Very fine sandstone	Thin bedded, parallel lamination		
	25cm	Light gray	Very fine sandstone	Massive, slightly asymmetric ripple marks on top	Sharp	Slightly burrowed top
	1cm	Med. gray	Shale	Fissile, parallel lamination		
	18cm	Light gray	Very fine sandstone	Ripple lamination, asymmetric ripple top?	Sharp	Slightly burrowed top
	4cm	Med. gray	Siltstone	Thin bedded, parallel lamination	Trans	
	40cm	Light gray	Very fine sandstone	Ball and pillow bottom, massive	Trans	
	10cm	Light gray	Siltstone and very fine sandstone	Ripple lamination in siltstone, thin bedded		
	45cm	Light gray	Very fine sandstone	Parallel lamination bottom, massive	Trans	
	2cm	Med. gray	Shale	Fissile, parallel lamination		
	50cm	Light gray to grown	Very fine sandstone	Rib and furrows on bottom?, symmetric ripples	Sharp	Slightly burrowed top

				on top, micro-hummocky cross-stratification		
	1cm	Med. gray	Shale	Fissile, parallel lamination		
	72cm	Light gray	Very Fine Sandstone	Massive, parallel lamination, symmetrical rippled top (poorly preserved)	Sharp	Slightly burrowed top
	20cm		COVERED			
KY-6-3	1.45m	Light gray to brown	Very Fine Sandstone	Soft sediment deformation, parallel lamination, 80-110cm: massive, 110-115cm: thin parallel beds, 115-145cm: massive	Sharp	
	14cm	Light gray to med. gray	Siltstone and Shale	Ripple lamination in siltstone, thin bedded, wavy ripple bedded	Trans	
	1.3m	Light gray	Very Fine Sandstone	Massive, low angle lamination, parallel lamination upper 20cm		
KY-6-4		Dark gray	Shale	Sunbury Shale	Sharp	

Location	OH-7	Coordinates	38 50' 41.84"W/83 06' 01.64"N
Quad:		Elevation:	590

Unit	Thickness	Color	Lithology	Sedimentary Structures	Contact	Fossils (Body, Trace)
OH-7-1	88cm	Dark gray to med brown	Interbedded siltstone and shale	Shale: fissile, parallel laminated; siltstone: wavy ripple bedded, ripple lamination		1-3 bedding plane bioturbation
OH-	10cm	Light	Very fine	Massive, ripple	Trans	

7-2		gray	sandstone	lamination at top		
	29cm	Med. gray	Interbedded siltstone and shale	Thin bedded, fissile, wavy ripple bedded	Trans	
	4cm	Light gray	Siltstone	Micro-hummocky cross-stratification	Sharp	
	11cm	Dark gray	Shale	Fissile, parallel lamination		
	7cm	Light gray	Very fine sandstone	Massive, parallel lamination at top	Sharp	
	13cm	Med. gray	Shale and very fine sandstone	Fissile, thin bedded, wavy ripple bedded		
	10cm	Light gray	Siltstone and very fine sandstone	Micro-hummocky cross-stratification	Trans	
	20cm	Med. gray	Silty shale	Thin bedded, fissile		1-2 beddding plane bioturbation
	10cm	Light gray	Very fine sandstone	Micro-hummocky cross-stratification, ripple lamination at top		
	15cm	Med. gray	Shale	Thin bedded, fissile	Trans	
	6cm	Light gray	Very fine sandstone	Micro-hummocky cross-stratification		
	25cm	Med. gray	Silty shale	Fissile, thin bedded		
	10cm	Light gray	Siltstone and very fine sandstone	Massive, ripple lamination at top	Sharp	
	20cm	Light gray	Very fine sandstone	Ungulatory bedding, ripple lamination	Trans	
	50cm	Light gray	Very fine sandstone	Ball and pillow bottom from very thin shale layer, massive	Sharp	
	90cm	Med. gray	Interbedded siltstone	Shale: fissile, parallel laminated;	Trans	1-2 bedding plane

			and shale	siltstone: wavy ripple bedded, micro-hummocky cross-stratification		Bioturbation
OH-7-3	1.1m	Light gray	Very fine sandstone	Massive	Sharp	
	12cm	Med. gray	Silty Shale	Fissile, parallel lamination, poorly exposed		
	70cm	Light gray	Very fine sandstone	Poorly exposed	Sharp	
	40cm	Med. gray	Shale	Fissile, parallel lamination, poorly exposed		
	60cm	Light gray	Very fine sandstone	Poorly exposed	Sharp	
	50cm	Med. gray	Shale	Fissile, parallel lamination, poorly exposed		
	65cm	Light gray	Very fine sandstone	Massive bottom, parallel lamination top	Sharp	
	22cm	Med. gray	Siltstone and shale	Slightly asymmetric ripples, thin bedded	Trans	
	7cm	Light gray	Very fine sandstone	Massive	Trans	
	65cm	Light gray	Very fine sandstone	Soft sediment deformation, convolute bedding		
	15cm	Light gray	Very fine sandstone	Symmetrical ripples (slightly asymmetric) thin bedded	Trans	
	45cm	Light gray	Very fine sandstone	Massive bottom, parallel lamination top		
	40cm	Light gray	Very fine sandstone	Massive		
	3cm	Med. gray	Siltstone	Ripple lamination		
	38cm	Light gray	Very fine sandstone	Massive, parallel lamination at top		

	2cm	Med. gray	Shale	Fissile, parallel lamination		
	32cm	Light gray	Very fine sandstone	Massive, parallel lamination	Sharp	
	45cm	Light gray	Very fine sandstone	Symmetrical ripples (slightly asymmetric) on top, parallel lamination		

Location:	OH-8	Coordinates	38 46' 48.34" W/ 83 15' 23.35" N
Quad:		Elevation:	809

Unit	Thickness	Color	Lithology	Sedimentary Structures	Contact	Fossils (Body, Trace)
OH-8-1	65cm	Light gray	Very fine sandstone	Massive, parallel lamination at top		
	2cm	Med. gray	Shale	Fissile, parallel lamination		
	35cm	Light gray	Very fine sandstone	Massive, parallel lamination at top	Sharp	
OH-8-2	70cm	Light gray	Interbedded siltstone and shale	Wavy bedded, micro-hummocky cross-stratification, ripple lamination	Trans	
	35cm	Light gray	Very fine sandstone	Massive, symmetrical ripples on top	Trans	Sparse burrows on top
	80cm	Light gray to med. gray	Interbedded siltstone and shale	Wavy bedded, ripple laminations in siltstone, minor wavy beds		Sparse burrowing
	25cm	Light gray	Very fine sandstone	Massive, ripples on top	Sharp	
	95cm	Light gray to med. gray	Interbedded siltstone and shale	Wavy bedded towards bottom, lenticular bedded towards top, symmetrical ripples		

	3cm	Light fray	Very fine sandstone	Parallel bedded, very thin		
	72cm	Light fray to med. gray	Interbedded siltstone and shale	Symmetrical ripples, wavy and lenticular bedding		1-2 bedding plane bioturbation
OH-8-3	2.35m	Light gray to med. gray	Interbedded shale and siltstone	Wavy and lenticular ripple bedding, ripple lamination in silt, beds are typically 3-5cm thick		1-2 bedding plane bioturbation
OH-8-4	40cm	Light gray	Very fine sandstone	Massive, ripples on top	Sharp	
	COVERED					

Location	KY-9	Coordinates	38 33' 49.71" W/ 83 15' 21.20" N
Quad:	Garrison	Elevation:	691

Unit	Thickness	Color	Lithology	Sedimentary Structures	Contact	Fossils (Body, Trace)
KY-9-1	1.5m	Light gray to brown	Very fine sandstone	Parallel lamination toward top, massive		
	20cm	Light gray	Very fine sandstone	Slightly asymmetric ripple marks, ripple lamination	Trans	
	53cm	Light gray	Very fine sandstone	Massive		
	1cm	Med. gray	Shale	Fissile, parallel lamination		
	1.05m	Light gray	Very fine sandstone	Massive	Sharp	
	1cm	Med. gray	Shale	Fissile, parallel lamination		
	40cm	Light gray	Very fine sandstone	Massive	Sharp	
	15cm	Med.	Interbedded	Wavy ripple	Trans	

		Gray to light gray	Shale and siltstone	bedded, ripple lamination in siltstone, parallel lamination in top siltstone beds		
	38cm	Light gray	Very fine sandstone	Massive, parallel at top	Sharp	
	30cm	Light gray	Interbedded shale and siltstone	Ripple lamination, symmetric ripples		1-3 bedding plane bioturbation
	42cm	Light gray	Very fine sandstone	Massive	Sharp	
	30cm	Med. gray	Interbedded shale and siltstone	Ripple lamination, thin bedded, wavy ripple		
	53cm	Light gray	Very fine sandstone	Ball and pillow, massive	Sharp	
	2cm	Med. gray	Shale	Soft sediment deformation		
	1.1m	Light gray	Very fine sandstone	Massive, parallel at top	Sharp	
	12cm	Med. gray	Interbedded shale and siltstone	Ripple lamination, rippled top		
	58cm	light gray	Very fine sandstone	Massive, parallel at top	Sharp	
	10cm	Med. gray	Interbedded shale and siltstone	Ripple bedded siltstone (wavy), thin bedded		
	1.1m	Light gray	Very fine sandstone	Ferruginous stains, parallel at top, climbing ripples one location	Sharp	
KY-9-2		Dark gray	Shale	Sunbury Shale		

Location:	KY-10	Coordinates	38 32' 55.00" W/ 83 14' 44.48"N
Quad:	Garrison	Elevation:	614

Unit	Thickness	Color	Lithology	Sedimentary Structures	Contact	Fossils (Body, Trace)
KY-10-1	70cm	Light gray	Very fine sandstone	Massive, parallel lamination at top		
KY-10-2	1cm	Med. gray	Shale	Fissile, parallel lamination		
	33cm	Light gray	Very fine sandstone	Parallel lamination, convolute bedding, Hummocky cross-stratification at top	Sharp	
	15cm	Light gray	Very fine sandsonte	Convolute bedding, wavy ripple Beds where shale is present	Trans	
	22cm	Light gray	Very fine sandstone	Massive, soft sediment deformation	Trans	
	15cm	Med. gray	Shale and siltstone	Wavy ripple bedded, ripple lamination in some locations		1-2 bedding plane bioturbation
	24cm	Light gray	Very fine sandstone	Massive at bottom, small scale hummocky cross-stratification, parallel beds at top, ripple marks on top	Sharp	Burrowing on top (1)
	18cm	Med. gray	Interbedded very fine sandstone and shale	Wavy ripple bedded		
	35cm	Light gray	Very fine sandstone	Massive, soft sediment deformation		
	20cm	Med. gray	Interbedded very fine sandstone and shale	Wavy ripple bedded, micro-hummocky cross-stratification at bottom	Trans	

	22cm	Light gray	Very fine sandstone	Massive, parallel lamination at top		
	4cm	Med. gray	Siltstone	Wavy bedded		
	10cm	Light gray	Very fine sandstone	Massive	Trans	
	13cm	Med. gray	Siltstone	Wavy bedded, micro-hummocky cross-stratification	Trans	
	28cm	Light gray	Very fine sandstone	Massive, parallel lamination at top	Trans	
	1.1m		COVERED			
KY-10-3	42cm	Light gray	Very fine sandstone	Massive		
	1cm	Med. gray	Shale	Fissile, parallel lamination		
	75cm	Light gray	Very fine sandstone	0-52cm: massive, 52-57cm: parallel lamination, 57-75cm: massive	Sharp	
	2cm	Med. gray	Shale	Fissile, parallel lamination		
	24cm	Light gray	Very fine sandstone	Massive, soft sediment deformation	Sharp	Small burrows on top
	1cm	Med. gray	Shale	Fissile,parallel lamination		
	38cm	Light gray	Very fine sandstone	Massive		
	2cm	Med. gray	Shale	Fissile, parallel lamination		
	80cm	Light gray	Very fine sandstone	Massive, soft sediment deformation	Sharp	
	40cm	Light gray	Very fine sandstone and siltstone	Climbing ripples in places, very fine sandstone transitions to silt upward	Trans	
	10cm	Med. gray	Shale	Fissile, parallel lamination		
	30cm	Light gray	Very fine sandstone	Parallel lamination, symmetrical ripples	Sharp	

				in float		
	58cm	Light gray	Very fine sandstone	Ripples on bottom persevered in finer grained section, parallel lamination		
	3cm	Med. gray	Shale	Fissile, parallel lamination		
	4cm	Light gray	Siltstone	Wavy ripple bedded		
	28cm	Light gray	Very fine sandstone	Massive, soft sediment seformation		
	4cm	Med. gray	Shale	Fissile, parallel lamination	Trans	
	72cm	Light gray	very fine sandstone	Massive, convolute beds, parallel lamination top	Sharp	
	3cm	Med. gray	Shale	Fissile, parallel lamination		
	1.2m	Light gray	Very fine sandstone	Parallel lamination, symmetrical ripples, massive, scours on top?	Sharp	
	70cm	Float				
	80cm	Light gray	Very fine sandstone	Massive, low angle lamination, parallel at top		
	20cm	Light gray	Interbedded siltstone and shale	Wavy bedded, micro-hummocky cross-stratification		
	25cm	Light gray	Very fine sandstone	Parallel lamination		
	8cm	Med. gray	Interbedded siltstone and shale	Wavy bedded, micro-hummocky cross-stratification		
	1.7m	Light gray	Very fine sandstone	Ripple laminations top, cross-bedding, small scour, thick bedded	Sharp	
KY-10-4	1m	Dark gray	Shale	Sunbury Shale		

Location:	KY-11	Coordinates :	38 33' 27.16" W/ 83 14' 55.63" N
Quad:	Garrison	Elevation:	720

Unit	Thickness	Color	Lithology	Sedimentary Structures	Contact	Fossils (Body, Trace)
KY-11-1	70cm	Light gray	Very fine sandstone	0-55cm: massive, 55-70cm: convolute (soft sediment deformation)		
	2cm	Med. gray	Shale	Fissile, parallel lamination		
	1.8m	Light gray	Very fine sandstone	Low angle laminations, parallel lamination, parallel lamination at top	Sharp	
	20cm	Light gray	Interbedded very fine sandstone shale	Wavy ripple bedded, micro-hummocky cross-stratification		
	40cm	Light gray	Very fine sandstone	Massive, crude low angle lamination		
KY-11-2	1.2m	Dark gray	Shale	Sunbury Shale	Sharp	

Location	KY-12	Coordinates :	38 35' 59.56" W/ 83 10' 15.05" N
Quad:	Garrison	Elevation:	559

Unit	Thickness	Color	Lithology	Sedimentary Structures	Contact	Fossils (Body, Trace)
KY-12-1	1m	light gray, WRS light brown	Siltstone	symmetrical ripples, massive, parallel lamination		
	85cm	Light	Siltstone	Massive, faint		

		gray, WRS light brown		hummocky cross-stratification, top has parallel lamination		
	15cm	Light gray to med. gray	Siltstone/shale	Lenticular ripple bedded	Trans	
	12cm	Light gray	Siltstone	Scours at top	Sharp	
	20cm	Light gray to med. gray	Siltstone/shale	Wavy ripple bedded, micro-hummocky cross-stratification		
	10cm	Light gray	Siltstone	Asymmetrical ripples on top, massive	Sharp	
	12cm	Light gray to med. gray	Siltstone and shale	Thin bedded, wavy ripple bedded		
	15cm	Light gray	Siltstone	Massive, symmetrical ripples on top	Sharp	
KY-12-2	72cm	Med. gray	Shale and siltstone	Lenticular ripple bedding		1-3 Bedding plane bioturbation
KY-12-3	10cm	Light gray	Siltstone	Massive	Sharp	
	30cm	Light gray	Shale and siltstone	Lenticular ripple bedding, both symmetrical and asymmetrical ripples (combined flow ripples?)	Trans	
	20cm	Light gray	Siltstone	Massive, micro-hummocky cross-stratification		
	25cm	Med. gray	Silty shale	Fissile, parallel lamination		
	28cm	Light gray	Very fine sandstone	Massive, slightly asymmetric ripples on top	Sharp	Burrows on top (2)

	21cm	Light gray	Shale and siltstone	Ripple bedding (lenticular)		
	42cm	Light gray	Very fine sandstone	Massive, micro-hummocky cross-stratification, flame structures, massive	Sharp	
	20cm	Light gray	Siltstone and shale	Ball and pillow, wavy ripple bedded		
	21cm	Light gray	Very fine sandstone	Massive		
	21cm	Light gray	Siltstone and shale	Ball and pillow, lenticular ripple bedded		
KY-12-4	1m	Light gray, WRS light brown	Very fine sandstone	Massive	Sharp	
	1cm	Med. gray	Shale	Fissile, parallel lamination		
	78cm	Light gray, WRS light brown	Very fine sandstone	Soft sediment deformation, massive	Sharp	
	15cm	Light gray	Siltstone	Ripple bedding		
	15cm	Light gray	Very fine sandstone	Massive, symmetrical ripples on top		Burrows on top (2)
	10cm	Med. gray	Siltstone	Parallel lamination		
	15cm	Light gray	Very fine sandstone	Massive, slightly asymmetric ripples on top		
	65cm	Light gray	Siltstone/very fine sandstone/ shale	Wavy ripple bedded, symmetrical ripples, micro-hummocky cross-stratification		

	40cm	Light gray	Very fine sandstone	Ball and pillow, massive	Sharp	
	72cm	Med. gray	Interbedded siltstone and shale	Soft sediment deformation, lenticular ripple bedding towards top		
	80cm	Light gray	Very fine sandstone	Massive	Sharp	
	5cm	Med. gray	Shale	Poorly exposed		
KY-12-5	55cm	Light gray	Very fine sandstone	Soft sediment deformation, massive	Sharp	
	30cm	Light gray	Very fine sandstone	Thin bedded, parallel laminations		
	1.2m	Light gray	Very fine sandstone	Massive		
	2cm	Med. gray	Shale	Fissile, parallel lamination		
	2m	Light gray	Very fine sandstone	Rippled top, poorly exposed (cliff), massive, parallel laminations middle	Sharp	
	40cm	LARGE FLOAT				
	50cm	Light gray	Very fine sandstone	Massive		
	5cm	Med. gray	Shale	Fissile, parallel lamination		
	70cm	Light gray	Very fine sandstone	Massive, low angle lamination	Sharp	
	10cm	Med. gray	Shale and siltstone	Thin bedded (wavy ripple bedded), micro-hummocky cross-stratification		
	20cm	Light gray	Very fine sandstone	Massive		
	15cm	Med.	Siltstone	Thin bedded,		

		gray		unrippled, massive		
	78cm	Light gray	Very fine sandstone	Massive, parallel at top	Sharp	
	35cm	Light gray	Very fine sandstone	Low angle lamination, parallel lamination and micro-hummocky cross-stratification		
	30cm	Light gray, WRS light brown	Very fine sandstone	Massive		
	15cm	Light gray to med. gray	Siltstone	Micro-hummocky cross-stratification		
	30cm	Light gray, WRS light brown	Very fine sandstone	Massive	Sharp	
	9cm	Med. gray	Shale	Fissile, parallel lamination		
KY-12-6	1m	Light gray	Very fine sandstone	Massive	Sharp	
	1cm	Med. gray	Shale	Fissile, parallel lamination		
	1m	Light gray	Very fine sandstone	Massive	Sharp	
	3cm	Med. gray	Shale	Fissile, parallel lamination		
	70cm	Light gray	Very fine sandstone	Massive, large amounts of soft sediment deformation	Sharp	
	2cm	Med. gray	Shale	Fissile, parallel lamination		
	4.0m	Light gray	Very fine sandstone	Massive, ferruginous	Sharp	

				stains, low angle laminations, soft sediment deformation		
KY-12-7	30cm	Dark gray	Shale	Sunbury Shale		

Location:	OH-13	Coordinates	39 1' 31.64"N/3 16' 19.20"W
Quad:		Elevation:	1061

Unit	Thickness	Color	Lithology	Sedimentary Structures	Contact	Fossils (Body, Trace)
OH-13-1	2 m	Med. gray	Interbedded siltstone and shale	Micro-hummocky cross-stratification, symmetrical and asymmetric ripples, thin bedded		1-3 bioturbation in silt
OH-13-2	30cm	Light gray	Siltstone and shale	Wavy ripple bedded, slightly asymmetric ripples		
	80cm	Light gray	Interbedded siltstone and shale	65% covered, wavy ripple bedded	Trans	1-2 bedding plane bioturbation in silt
	30cm	Light gray	Siltstone	Massive, ripple marks on top		
	1m	Light gray	Interbedded siltstone and shale	Micro-hummocky cross-stratification, symmetrical ripple marks, wavy ripple bedding		1-2 bedding plane bioturbation in silt
OH-13-3	55cm	Light gray	Siltstone	Parallel lamination at base, massive	Sharp	
	1cm	Med. gray	Shale	Fissile, parallel lamination		
	20cm	Light gray	Siltstone	Massive	Sharp	
	20cm	Light gray	Siltstone	Massive, thick bedded, faint ripple crests on top		

	90cm	Light gray	Very fine sandstone	Massive, very small ripple crests, parallel lamination at top		
	1cm	Med. gray	Shale	Fissile, parallel lamination		
	75cm	Light gray	Very fine sandstone	Swaley bedding, rippled upper surface, massive, parallel lamination at top	Sharp	
	1cm	Med. gray	Shale	Fissile, parallel lamination		
	80cm	Light gray	Very fine sandstone	Ball and pillow structures, massive	Sharp	
	1cm	Med. gray	Shale	Fissile, parallel lamination		
	60cm	Light gray	Very fine sandstone	Poorly exposed, ball and pillow, parallel lamination, massive, scour fill 30cm axis 327	Sharp	
	1.1m	Light gray	Very fine sandstone	50cm scour fill axis 320, faint Low angle lamination above scour fill, massive, ball and pillow	Sharp	
	75cm	Light gray	Very fine sandstone	Parallel lamination at base, massive		
	40cm	Light gray	Very fine sandstone	Massive, ferruginous strains		
OH-13-4		Dark gray	Shale	Sunbury Shale	Sharp	

Location:	OH-14	Coordinates	39 6' 8.74"N/ 83 3' 56.79"W
Quad:		Elevation:	713

Unit	Thickness	Color	Lithology	Sedimentary Structures	Contact	Fossils (Body, Trace)
OH-14-1	4.5m	Med. gray, WRS light brown	Interbedded shale and siltstone	Mainly covered, around 35% Siltstone, commonly rippled, wavy-lenticular rippled		2-3 bedding plane bioturbation
	2m	LARGE FLOAT				
OH-14-2	40cm	Light gray	Siltstone	Massive		
	30cm	Light gray	Siltstone and shale	Low angle cross-beds, beds appear scoured (3m wide, 35cm deep)		
	30cm	Light gray	Very fine sandstone	Parallel lamination	Sharp	
	1.2m	Light gray	Very fine sandstone	Massive		
	1cm	Med. gray	Shale	Fissile, parallel lamination		
	1m	Light gray	Very fine sandstone	Two sections thin laterally, hummocky cross-beds at bottom, massive, structures occur in 10cm spacing	Sharp	
	1.3m	Light gray	Very fine sandstone	Convolute beds, clay clasts present in hummocky cross-beds, ripple crest on top, massive bedding bottom		
	COVERED					

Location	KY-15	Coordinates	38 35' 52.12" N/ 83 10' 56.81"W
Quad:	Garrison	Elevation:	560

Unit	Thickness	Color	Lithology	Sedimentary Structures	Contact	Fossils (Body, Trace)
KY-15-1	40cm	Light gray	Siltstone	Hummocky cross-beds, massive		
	1cm	Med. gray	Shale	Fissile		
	42cm	Light gray	Siltstone	Massive	Sharp	
	15cm	Light gray	Interbedded shale/silts	Lenticular ripple bedding		
	20cm	Light gray	Siltstone	Hummocky bedding	Sharp	
	7cm	Light gray	Silt/shale	Lenticular ripple bedding, slightly ripple bedded		
	35cm	Light gray	Siltstone	Massive, parallel beds 5-15cm		
	32cm	Light gray	Siltstone and shale	Wavy ripple bedded, micro-hummocky cross-stratification		
	47cm	Light gray	Very fine sandstone	Massive, parallel beds 5cm		
	20cm	Light gray	Shale and siltstone	Wavy ripple bedded, micro-hummocky cross-stratification		
	1.45m	Light gray	Very fine sandstone	0-10cm: hummocky, 10-30cm: massive, 30-35cm: parallel lamination, 35-55cm: massive, 55-65cm: parallel laminations, 65-1.4cm: massive, ripple marks	Sharp	
	1cm	Med.	Shale	Fissile		

		gray				
	50cm	Light gray	Very fine sandstone	Massive		
	30cm	Light gray	Very fine sandstone	Thin bedded, parallel lamination		
	40cm	Light gray	Very fine sandstone	Micro-hummocky cross-stratification, parallel lamination		
	40cm	Light gray	Very fine sandstone	Soft sediment deformation, parallel lamination		
	2cm	Med. gray	Shale	Fissile		
	30cm	Light gray	Very fine sandstone	Convolute bedding, soft sediment deformation	Sharp	
	1cm	Med. gray	Shale	Fissile		
	60cm	Light gray	Very fine sandstone	Massive, thick bedded, parallel lamination top 7 cm	Sharp	
	2cm	Med. gray	Shale	Fissile		
	15cm	Light gray	Very fine sandstone	Massive	Sharp	
	2cm	Med. gray	Shale	Fissile		
	1.1m	Light gray	Very fine sandstone	Massive, thick bedded, parallel lamination top 10 cm	Sharp	
	10cm	Light gray	Shale and siltstone	Wavy ripple bedded, micro-hummocky cross-stratification		
	80cm	Light gray	Very fine sandstone	0-25cm: massive 25-35cm: parallel lamination, ripple marks on top		
	TOO STEEP					

Location:	KY-16	Coordinates	38 34' 07.09" N/ 83 12' 52.88"W
Quad:	Garrison	Elevation:	552

Unit	Thickness	Color	Lithology	Sedimentary Structures	Contact	Fossils (Body, Trace)
KY-16-1	64cm	Light gray	Very fine sandstone	Massive (poorly exposed)		
	50cm	Med. gray to light gray	Interbedded shale and siltstone	Bottom 20cm parallel lamination, upper 30cm wavy ripple bedded, ripple migration, ripple lamination		1-2 bedding plane bioturbation
	40cm	Light gray	Siltstone and very fine sandstone	Ball and pillow, massive, parallel lamination upper portion	Sharp	
	1.4m	Light gray, WRS light brown	Very fine sandstone	Large crude hummocky cross-beds, then massive, followed by large crude hummocky cross-beds, top 10cm parallel lamination		
	10cm	Med. gray	Shale and very fine sandstone	Wavy ripple bedded		
	1.3m	Light gray, WRS light brown	Very fine sandstone	Small hummocky cross-beds at bottom, massive, parallel lamination in middle, ripple bedded top	Sharp	Vertical burrows on top
	90cm		COVERED			
	30cm	Med. gray	Shale and very fine sandstone	Wavy ripple bedded		1-2 bedding plane bioturbation
	70cm	Light gray	Very fine sandstone	Crude parallel lamination, massive	Sharp	

	30cm	Light gray	Shale and siltstone	Wavy ripple bedded		
	35cm	Light gray	Very fine sandstone	Ball and pillow, massive	Sharp	
	45cm		COVERED			
	60cm	Light gray	Very fine sandstone	15cm massive, 5cm parallel lamination, 40cm massive	Sharp	
	COVERED		COVERED			

Location:	KY-17	Coordinates :	38 34' 07.09" N/ 83 12' 52.88"W
Quad:	Garrison	Elevation:	552

Unit	Thickness	Color	Lithology	Sedimentary Structures	Contact	Fossils (Body, Trace)
KY-17-1	30cm	Med. gray	Silty shale	Thin bedded, fissile		Small amount bedding plane bioturbation
	45cm	Light gray	Very fine sandstone	Massive	Sharp	
	1.05m	Light gray	Very fine sandstone	Bottom 20cm convolute bedding, 20-35cm: faint hummocky cross-bed, massive		
	5cm	Light gray	Shale and siltstone	Wavy ripple bedded, ripple lamination locally		
	20cm	Light gray	Very fine sandstone	Massive	Sharp	
	15cm	Med. gray	Silty shale	Thin bedded, fissile		
	10cm	Light gray	Very fine sandstone	Massive		
	5cm	Med. gray	Silty shale	Thin bedded, fissile		
	20cm	Light	Very fine	Massive		

		gray	sandstone			
	40cm	Med. gray	Interbedded shale and siltstone	Lenticular and Wavy ripple bedding, current ripple and symmetric ripples present		1-2 Bedding plane bioturbation
	50cm	Light gray	Very fine sandstone	Massive	Sharp	
	1.3m		COVERED			
	1.4m	Light gray	Very fine sandstone	Poorly exposed, faint hummocky cross-beds, parallel lamination		
	1cm	Med. gray	Shale	Thin bedded, fissile		
	40cm	Light gray	Very fine sandstone	Parallel lamination on bottom grades into massive	Sharp	
	5cm	Med. gray	Shale	Fissile, poorly exposed		
	55cm	Light gray	Very fine sandstone	Massive, rippled top, symmetrical ripples	Sharp	Burrows on top
	COVERED		COVERED			

Location	KY-18	Coordinates	38 32' 50.86" N/ 83 13' 36.57"W
Quad:	Garrison	Elevation:	625

Unit	Thickness	Color	Lithology	Sedimentary Structures	Contact	Fossils (Body, Trace)
KY-18-1	80cm	Light Gray	Very Fine Sandstone	Bottom: 5cm parallel lamination, massive, convolute lamination		
	15cm	Med. Gray	Interbedded siltstone	Wavy ripple bedded, lenticular		

			and very fine sandstone	ripple bedding at top with more Shale		
	1m	Light gray	Very fine sandstone	0-30cm: massive, 35-40cm: thin bedded (climbing ripples), 40cm-1m: massive	Sharp	
	20cm	Med. gray	Shale and siltstone	Bottom 10cm ripple bedded, then grades into shale		1-2 bedding plane bioturbation
	90cm	Light gray	Very fine sandstone	Ball and pillow, massive, scoured top		
	30cm	Light gray	Shale and very fine sandstone	Scour fills, thin bedded	Sharp	
	70cm	Light gray	Very fine sandstone	Massive, parallel lamination		
	1cm	Med. gray	Shale	Fissile, parallel lamination		
	30cm	Light gray	Very fine sandstone	Massive	Sharp	
	20cm	Med. gray	Very fine sandstone and siltstone	Wavy ripple bedded		
	1m	Light gray	Very fine sandstone	0-20cm: parallel lamination, massive, ripple marks on top (slight a-sym.?)		Burrows on top
	20cm	Light gray	Shale	Fissile, parallel lamination		
	50cm	Light gray	Very fine sandstone	Ball and pillow, massive	Sharp	
	3cm	Med. gray	Shale	Fissile, parallel lamination		
	55cm	Light gray	Very fine sandstone	0-5cm: parallel lamination, 5-55cm: massive		
	COVERED					

Location:	KY-19	Coordinates	38 33' 05.12" N/ 83 16' 34.88"W
Quad:	Garrison	Elevation:	689

Unit	Thickness	Color	Lithology	Sedimentary Structures	Contact	Fossils (Body, Trace)
KY-19-1	60cm	Light gray	Very fine sandstone	Ball and pillow, large hummocky cross-Bed		
	30cm	Light gray	Shale and siltstone	Fissile, wavy bedded		
	70cm	Light gray	Very fine sandstone	Ball and pillow, parallel lamination throughout bed	Sharp	
	1cm	Med. gray	Shale	Fissile, parallel lamination		
	80cm	Light gray	Very fine sandstone	Bottom 20cm: convolute, 20-80cm: parallel beds/lamination	Sharp	
	10cm	Med. gray	Shale	Fissile, parallel lamination		
	40cm	Light gray	Very fine sandstone	Convolute bottom 10cm, massive		
	1.6m		COVERED			
	30cm	Light gray	Very fine sandstone	Massive		
	5cm	Med. gray	Shale and siltstone	Wavy ripple bedding		Sparse bedding plane bioturbation
	1m	Light gray	Very fine sandstone (silty)	Convolute bedding, hummocky cross-bed, parallel lamination, rippled on top symmetrical		Burrows on top
	25cm	Light gray	2 very fine sandstone beds and 2 shale beds	Ripple migration, ripple lamination, parallel lamination middle		
	25cm	Light gray	Very fine sandstone	Massive, top 5cm: parallel lamination	Sharp	
	2cm	Med.	Shale	Fissile, parallel		

		gray		lamination		
	30cm	Light gray	Very fine sandstone	Massive, top 6cm parallel lamination		
	40cm	Light gray	Very fine sandstone	Massive		
	1.3m	Light gray	Very fine sandstone	Convolute bedding 5-10cm, parallel lamination 15-1.25m (throughout), top 5cm ripple lamination		
	1cm	Med. gray	Shale	Fissile		
	30cm	Light gray	Very fine sandstone	Massive		
	2cm	Med. gray	Shale	Fissile		
	80cm	Light gray	Very fine sandstone	Poorly exposed, massive		
	COVERED					

Location:	KY-20	Coordinates	39 08' 25.59" N/ 82 58' 39.16"W
Quad:	Garrison	Elevation:	633

Unit	Thickness	Color	Lithology	Sedimentary Structures	Contact	Fossils (Body, Trace)
KY-20-1	2.9m	Med. gray	Interbedded silt/shale	Ripple bedded, lenticular ripple bedding, wavy ripple bedding in location, bedford		Planolites?
	30cm	Light gray	Siltstone	Ball and pillow, massive		
	95cm	Med. gray	Interbedded silt/shale	Wavy/lenticular bedding, common ripples		1-2 bedding plane bioturbation
	25cm	Light gray	Siltstone	Massive, parallel lamination top		

	2.3m	Med. gray	Interbedded silt/shale	more wavy ripple bedded, lenticular bedding still present, common ripples		1-2 bedding plane bioturbation
	1.8m	Light gray	Very fine sandstone	Ball and pillow, soft sediment deformation, parallel lamination, massive	Sharp	
	75cm	Med. gray	Interbedded silt/shale	Wavy ripple bedded, 2cm thick beds		Bedding plane bioturbation
	32cm	Light gray	Very fine sandstone	Massive		
	17cm	Light gray	Shale and siltstone	Wavy ripple bedded, ripple lamination?		
	22cm	Light gray	Very fine sandstone	Massive, parallel lamination top		
	12cm	Light gray	Very fine sandstone	Massive		
	70cm	Light gray	Very fine sandstone	Poorly exposed, massive		
	COVERED					

Location:	KY-21	Coordinates :	38 36' 24.76"N/ 83 09' 14.75"W
Quad:	Garrison	Elevation:	614

Unit	Thickness	Color	Lithology	Sedimentary Structures	Contact	Fossils (Body, Trace)
KY-21-1	15cm	Med. gray	Very fine sandstone	0-10cm: massive, 10-15cm: hummocky cross-bed		
	20cm	Light gray	Very fine sandstone	Massive		

	18cm	Light gray	Very fine sandstone	thin bedded, hummocky cross-bed		
	55cm	Light gray	Very fine sandstone	0-40cm: parallel lamination, 40-55cm: massive	Sharp	
	70cm	Light gray	Very fine sandstone	Ball and pillow, massive	Sharp	
	1cm	Med. gray	Shale	Fissile		
	30cm	Light gray	Very fine sandstone	0-20cm: massive, 20-30cm: hummocky cross-beds		
	80cm	Light gray	Very fine sandstone	0-70cm: massive, 70-80cm: parallel lamination		
	8cm	Med. gray	Siltstone	Parallel lamination		
	40cm	Light gray	Very fine sandstone	Massive, ball and pillow structure		
	1cm	Med. gray	Shale	Fissile		
	1.2m	Light gray	Very fine sandstone	Ball and pillow bottom, 0-60cm: massive, 60-80cm: parallel lamination-swaley, 80-1.2m: massive, top 5cm thin bedded parallel lam.		
	2cm	Med. gray	Shale	Fissile		
	80cm	Light gray	Very fine sandstone	0-10cm: parallel lamination, 10-70cm: massive, 70-80cm: ferruginous stains		

		Dark gray	Shale	Sunbury Shale	Sharp	

Location:	OH-22	Coordinates :	38 39' 17.70"N/ 83 07' 56.52"W
Quad:	Garrison	Elevation:	534

Unit	Thickness	Color	Lithology	Sedimentary Structures	Contact	Fossils (Body, Trace)
OH-22-1	1m	Light gray	Very fine sandstone	0-15cm: massive, 15-20cm: parallel, 20-90cm: massive, 90-1m: hummocky cross-bed, rippled top, scours on top of bed	Sharp	
	1cm	Med. gray	Shale	Fissile, parallel laminations		
	50cm	Light gray	Very fine sandstone and shale	0-15cm: massive, 15-30cm: wavy bedded, 30-35cm: massive, 35-42cm: parallel lamination, 42-50cm: swaley beds, rippled top		Top has bedding plane bioturbation
	70cm	Light gray	Very fine sandstone and shale	Wavy ripple bedded, interlaminated silt, sand and shale		Float has bedding plane bioturbation
	30cm	Light gray	Very fine sandstone	0-20cm: massive, mud flasers, 20-23cm: parallel lamination, 23-		Top has bedding plane bioturbation

				30cm: climbing ripples, rippled Top		
	1cm	Med. gray	Shale	Fissile, parallel lamination		
	70cm	Light gray	Very fine sandstone	0-65cm: massive grades to parallel lamination, 65-70cm: mico-hummocky cross-beds, rippled top		Top has bedding plane bioturbation
	1cm	Med. gray	Shale	Fissile, parallel laminatinon		
	1m	Light gray	Very Fine sandstone	Ball and pillow, soft sediment deformation		
	10cm	Light gray	Very fine sandstone and shale	Wavy ripple bedded	Trans	
	37cm	Light gray	Very fine sandstone	Massive		
	3cm	Med. gray	Shale	Fissile, parallel lamination		
	60cm	Light gray	Very fine sandstone	0-55cm: massive, 55-57cm: parallel lamination, 57-60cm: micro-hummocky cross-beds	Sharp	
	20cm	Light gray	Very fine sandstone	0-15cm: massive, 15-20cm: micro-hummocky (ungulatory Beds)		
	2cm	Med. gray	Shale	Fissile, parallel lamination		
	30cm	Light gray	Very fine sandstone	Massive		
	1cm	Med.	Shale	Fissile, parallel		

		gray		lamination		
	25cm	Light gray	Very fine sandstone	Massive		
	1cm	Med. gray	Shale	Fissile, parallel lamination		
	40cm	Light gray	Very fine sandstone	0-35cm: massive, 35-40cm: parallel lamination	Trans	
	60cm	Light gray	Very fine sandstone and shale	Interbedded, wavy ripple bedded	Trans	1-2 bedding plane bioturbation
	20cm	Light gray	Very fine sandstone	Massive		
	80cm	Light gray	Very fine sandstone	Ball and pillow, massive		
	18cm	Med. gray	Shale to siltstone	Lenticular ripple bedding	Trans	
	5cm	Light gray	Very fine sandstone	Massive	Trans	
	3cm	Med. gray	Shale to siltstone	Lenticular Rripple Bedding		
	35cm	Light gray	Very fine sandstone	0-30cm: massive, 30-35cm: ripple lamination, rippled top		Top has bedding plane bioturbation
	23cm	Med. gray	Very fine sandstone and shale	Ball and pillow between shale and very fine sand, top 3cm shale		
	75cm	Light gray	Very fine sandstone	0-55cm: massive, 55-65cm: parallel lamination, 65-75cm: micro-hummocky	Sharp	
	23cm	Light gray	Very fine sandstone	Poorly exposed		
	7cm	Med. gray	Shale	Fissile, parallel lamination		
	60cm	Light	Very fine	Ball and pillow	Sharp	

		gray	sandstone	Massive		
	10cm	Med. gray	Very fine sandstone and shale	Wavy ripple bedded		
	1m	Light gray	Very fine sandstone	0-10cm: parallel lamination, massive, 10-20cm: parallel lamination, 20-45cm: massive, 45cm-65m: parallel lamination, 70cm: micro-hummocky cross-stratification, ripple		
	2cm	Med. gray	Shale	Fissile, parallel lamination		
	25cm	Light gray	Very fine sandstone	Massive		
	1cm	Med. gray	Shale	Fissile, parallel lamination		
	2.8m	Light gray	Very fine sandstone	Ball and pillow, large soft sediment deformation (flow rolls)		
	30cm	Med. gray	Very fine sandsonte and shale	0-10cm: shale, 10-30cm: wavy ripple bedded		1-2 bedding plane bioturbation
	70cm	Light gray	Very fine sandstone	0-50cm: massive, 50-70cm: micro-hummocky	Sharp	
	85cm	Light gray	Very fine sandstone	0-50cm: massive, 50-80cm: parallel lamination, 85cm: Scours		
OH-22-1	2m	Dark gray	Shale	Sunbury Shale	Sharp	

Location	KY-23	Coordinates :	38 34' 31.01"N/ 83 18' 31.06"W
Quad:	Garrison	Elevation:	788

Unit	Thickness	Color	Lithology	Sedimentary Structures	Contact	Fossils (Body, Trace)
	4m	COVERED				
KY-23-1	2m	Med. gray	Siltstone/shale	Lenticular/ wavy ripple bedded, 55-65% shale, silty is poorly exposed due to float, ripples		2-3 bedding plane bioturbation
	3.8m	Med. gray	Siltstone/shale	55-65% shale, silt is commonly rippled, fissile shale that is interbedded with silt		2-3 bedding plane bioturbation
	1m	COVERED				
KY-23-2	40cm	Light gray	Shale/siltstone	70% siltstone, wavy ripple bedded, common ripple marks		1-2 bedding plane bioturbation
	30cm	Light gray	Very fine sandstone	Massive - parallel lamination		
	10cm	Light gray	Shale and very fine sandstone	1cm Shale, 9cm very fine sandstone, wavy ripple bedded		
	35cm	Light gray	Very fine sandstone	Massive, scoured top locally	Sharp	
	30cm	Med. gray	Shale/siltstone	Wavy ripple bedded, common ripple marks		
	80cm	Light gray	Very fine	Scoured top	Sharp	

			sandstone	1.3m in size with a 168 and 180 trough axis, un-scoured location massive beds, parallel Lamination		
	2cm	Med. gray	Shale	Fissile		
	40cm	Light gray	Very fine sandstone	0-35cm: massive, 35-40cm: ungulatory beds, rippled top		
	2cm	Med. gray	Shale	Fissile		
	37cm	Light gray	Very fine sandstone	0-10cm: massive, 10-37cm: parallel lamination		
	15cm	Med. gray	Shale/siltstone /shale	Siltstone has faint ripple marks		
	1.2m	Light gray	Very fine sandstone	0-60cm: massive, 60-90cm: parallel lamination, 90-1.2m: massive, ferruginous stains	Sharp	
KY-23-3	2m	Dark gray	Shale	Sunbury Shale	Sharp	

APPENDIX V TRACE FOSSILS

Epirelief Traces

Sample	Orientation	Length	Diameter	Occurrence	Name
1	Horizontal	3 cm	3 mm	Abundant	*Scalarituba/Nereites/Neonereites*
1	Horizontal	2.7cm	2 mm	Abundant	*Scalarituba/Nereites/Neonereites*
1	Vertical		3 mm	Abundant	*Skolithos*
1	Horizontal	2.5cm	1.5cm	Sparse	Resembles *Cruziana*
1	Horizontal	1cm	1cm	Abundant	*Phycosiphon?*
1	Horizontal	1.2cm	1 cm	Sparse	*Chondrites*
2	Horizontal	8 cm	1.5 cm	Sparse	*Lophoctenium*
3	Horizontal	7 mm	4 mm	Abundant	*Phycosiphon*
4	Horizontal	2 cm	3 mm	Sparse	??
4	Horizontal	4 cm	3 mm	Abundant	*Scalarituba/Nereites/Neonereites*
4	Horizontal	1.5cm	1cm	Sparse	Resembles *Cruziana*
4	Vertical		3mm	Sparse	*Skolithos*
5	Horizontal	3.5 cm	2 cm	Sparse	*Phycosiphon?*
5	Horizontal	3 cm	4 mm	Sparse	*Phycosiphon?*
5	Horizontal	3 cm	2 mm	Abundant	*Scalarituba/Nereites*
5	Vertical		4 mm	Abundant	*Skolithos*
6	Horizontal	1cm	3 mm	Abundant	*Scalarituba/Nereites*
6	Horizontal	6 cm	5 mm	Abundant	*Scalarituba/Nereites*
6	Horizontal	2.7 cm	3 cm	Abundant	*Lophoctenium*
6	Horizontal	4 cm	2.6 cm	Abundant	*Lophoctenium*
6	Horizontal	2.4 cm	2.5 cm	Abundant	*Lophoctenium*
6	Horizontal	2.5cm	2 mm	Abundant	*Nereites*
9	Horizontal	2cm	3 mm	Sparse	*Scalarituba*
10	Vertical		1 mm	Abundant	*Skilithos*
10	Horizontal	2 cm	2 mm	Sparse	*Scalarituba/Nereites*
12	Horizontal	2 cm	3 mm	Abundant	*Aulichnites*
12	Horizontal	3.5cm	1cm	Sparse	*Lophoctenium*
12	Horizontal	1 cm	4 mm	Abundant	*Phycosiphon?*
12	Vertical		2 mm	Abundant	*Skolithos*
12	Horizontal	4 mm	2 mm	Sparse	*Chondrites*
13	Horizontal	1.0cm	3mm	Sparse	*Scalarituba*
13	Horizontal	4cm	8 mm	Sparse	*Lophoctenium*
13	Horizontal	7 mm	2 mm	Abundant	*Phycosiphon?*
13	Horizontal	3 cm	1 mm	Sparse	??
14	Horizontal	7.3cm	.3cm	Sparse	*Scalarituba/Nereites*
14	Vertical		1 mm	Abundant	*Skolithos*
15	Vertical		1.2 mm	Sparse	*Skolithos*
16	Vertical		1 mm	Sparse	*Arenicolites*

16	Vertical		1mm	Abundant	*Skolithos*
17	Horizontal	3cm	2 mm	Abundant	*Scalarituba/Nereites*
17	Horizontal	6 mm	2.3 mm	Sparse	*Phycosiphon?*
17	Vertical		2 mm	Sparse	*Skolithos*
18	Horizontal	4cm	3 mm	Abundant	*Nereites/Neonereites*
18	Horizontal	3.3cm	3 mm	Abundant	*Scalarituba/Neonereites*
18	Horizontal	1.4 cm	1 cm	Abundant	*Phycosiphon?*
18	Vertical		.8 mm	Sparse	*Skolithos*
20	Vertical		1 mm	Sparse	*Skolithos*

Hyporelief Traces

Sample	Length	Diameter	Occurrence	Name
2	6 cm	2 mm	Abundant	*Planolites*
2	1 cm	3 mm	Sparse	*Thalassinoides*
5	2.4 cm	3 mm	Abundant	*Planolites*
5	1 cm	1 mm	Abundant	*Planolites*
6	1.6 cm	8 mm	Abundant	*Planolites*
6	.7 cm	4 mm	Abundant	*Palaeophycus*
6	3.6 cm	5 mm	Sparse	*Thalassinoides*
7	3 cm	5 mm	Sparse	*Palaeophycus*
7	2.8 cm	4 mm	Abundant	*Thalassinoides*
8	1.2 cm	4.4 cm	Sparse	*??????*
8	1.3 cm	2mm	Abundant	*Planolites*
8	1.2 cm	2mm	Sparse	*Palaeophycus*
9	3.5 cm	4mm	Abundant	*Planolites*
9	2 cm	2mm	Abundant	*Planolites*
10	3.4 cm	5mm	Sparse	*Planolites*
16	5 mm	3 mm	Sparse	*Palaeophycus*
16	1cm	2 mm	Abundant	*Planolites*
19	1cm	3 mm	Sparse	*Thalassinoides*
19	1.3cm	4 mm	Abundant	*Planolites*
20	5.5cm	2 mm	Sparse	*Palaeophycus*
20	2.6cm	2 mm	Abundant	*Planolites*
20	1.5 cm	3 mm	Sparse	*Thalassinoides*

Appendix VI Log List

Kentucky Well List

Number	Kentucky Record Number	X- Location (KY North 1983 projection)	Y- Location (KY North 1983 projection)
1	75200	2112230	319332.1
2	75228	2120259	282374.4
3	2350	2091948	287045.7
4	2357	2095948	309125.8
5	2356	2097647	309245.1
6	2348	2067440	293778.7
7	75178	2083871	315910.7
8	55882	2065882	340125.6
9	81804	2089469	348347.1
10	81192	2080110	347228.9
11	143358	2047656	316352
12	134672	2045677	290744
13	3030	1953770	346994.7
14	3028	1963334	353730.1
15	2909	1967232	290929
16	2977	1941225	305209.9
17	2836	1921476	270993.7
18	2983	1953813	305756.1
19	2958	2056595	290996
20	2908	1963954	303428.5
21	108674	1965945	352812.4
22	60413	1968770	281428.5
23	22791	2028612	341230.4
24	9703	1978486	403555.9
25	74873	2083670	362909.7
26	9696	2012605	336419.7
27	9704	1974032	396904
28	9702	1982777	417197
29	140457	2050864	349928.3
30	141810	2049552	341625.6
31	142277	2044447	327597.6
32	143258	2036075	329721.2
33	143364	2055782	361987.7
34	143532	2053789	347065.3
35	144092	2043449	356548.9
36	144221	2043676	346800.9

37	73048	1875076	334987.5
38	12435	1920685	316073.4
39	12443	1960672	379278
40	12441	1912356	381004.3
41	12445	1969556	403417.9
42	8424	2011222	234006.3
43	8423	2007608	235361
44	8326	1979915	204102.9
45	8310	1962979	198161.7
46	8304	1969588	203162.3
47	87598	1978713	224506.1
48	109648	1985337	201045.6
49	112140	2020908	234208.6
50	63477	1928646	207255
51	8421	1977414	228739.5
52	8406	1943566	218360.6
53	52437	2012569	237414.7
54	8403	1945986	237997.3
55	78289	1997371	195092.2
56	37252	2017398	226218.3
57	113876	1985090	203775.6
58	114092	1982440	195983.5
59	114376	1982664	198536.4
60	114444	1987467	208574.2
61	115001	1993289	223576.8
62	115132	1985439	200945.7
63	116011	1988290	206351.8
64	116062	1980410	190795.5
65	120424	1979641	203982.4
66	120436	1982397	200858.6
67	120435	1982430	203785.2
68	11624	2026414	186119.9
69	11647	2066532	242673.2
70	27130	2112215	170897.4
71	11649	2060680	232570
72	28543	2043577	211754.8
73	30124	2114333	212055.6
74	87908	2095207	172569.8
75	88739	2102476	166675.4
76	37586	2069090	189154.9
77	49720	2067391	178203
78	62480	2106412	153628.7

79	90998	2086587	253809.2
80	83175	2086977	239575.4
81	50748	2091183	213021.9
82	101940	2072230	237455.9
83	37301	2055420	194027.3
84	50717	2088245	216266.7
85	106746	2055821	185254
86	11665	2072880	268141.7
87	83097	2119783	205953.3
88	115164	2074851	187689.5
89	115280	2020485	192997.9
90	51023	2083056	202189.5
91	51404	2104162	205975.6
92	35086	2018337	211922.8
93	133869	2089890	197085.5
94	134427	2093073	209056.7
95	143733	2110121	204984.6
96	143735	2106788	204260.7
97	143936	2094212	211044.6
98	114022	2011281	347833.8
99	145823	2011340	348049.1
100	62054	2056379	346584.1
101	82702	2081288	342198.6
102	75105	2103816	336144.5
103	29491	2112002	181763.4
104	140197	2113366	186542.7
105	140198	2114455	187549.2
106	132257	2116298	192105.3

Ohio Well List

Number	UWI/API	X	Y
107	34163209070000	2161668	673514.8
108	34163209110000	2154406	680479.3
109	34163209160000	2067251	660103.9
110	34163209230000	2063806	658716.9
111	34163209240000	2182869	603195.4
112	34079202520000	2060664	541936.7
113	34079202530000	2054356	551618.7
114	34079202540000	2065959	53912.22
115	34079202570000	2076108	537205.2
116	34079202680000	2134892	573378.3
117	34145202120000	2048727	400914.8
118	34145600330000	2048722	401184.7
119	34087205070000	2147746	413121.4
120	34087205100000	2139011	413992.6
121	34087205110000	2145821	412669.9
122	34087205130000	2135586	416246.7
123	34087205160000	2137666	415160
124	34073235450000	2085492	686975.3
125	34073235930000	2190625	760696.1
126	34073235950000	2152448	726671.2
127	34073236010000	2140935	729492.5
128	34073236030000	2146526	729884.9
129	34127272350000	2209996	846268.5
130	34127273160000	2172484	844209.1
131	34127273270000	2198896	801730.3
132	34127273310000	2169588	848636.2
133	34127273420000	2171719	829066.7
134	34045213200000	2133390	882323.7
135	34045213210000	2135053	881700
136	34045213220000	2134965	879452.2
137	34045214940000	2082712	884413.2
138	34045214970000	2080652	880975.2
139	34119287800000	2314518	910267.6
140	34119287890000	2332262	890063.2
141	34119287900000	2306009	853428.8
142	34119287910000	2296028	845576.6
143	34119287980000	2291364	879564.8
144	34163203310000	2169160	614265.4

145	34163208830000	2196261	633409.4
146	34079201290000	2145623	599591.2
147	34079201180000	2123445	586785.4
148	34079201400000	2105686	563877.2